TECHNICAL REPORT

RESEARCH TO DETERMINE FAILURE MODES FOR TRANSISTORS

CONTRACT NAS8-11059

Editor: B. Bair

Contributors: A. Fox, E. A. Herr,
A. Poe, R. Quick, L. Smith

General Electric Company
Semiconductor Products Department
Syracuse, New York

ABSTRACT

This report presents the results obtained from an investigation of the reliability of 1,500 diffused planar transistors of the 2N718A type, manufactured by three separate processes. The transistors were subjected to a series of stress conditions in a number of screens and a matrix life test plan. The stresses included temperature, temperature and bias, power dissipation and centrifuge step stressing of sufficient magnitude to produce failures. The failures were analyzed to assign failure modes and determine whether they were a function of material, process or design. In analyzing this data, an evaluation was made of the performance of devices during the stress screens and under power operating conditions for three thousand hours. A number of charts, graphs and tables were prepared to show population trends, effectiveness of stress screens, burn-in, truncation and noise screening. The failure analysis procedure, failure mode chart and the relation of the failure mechanisms and stress conditions were shown. A number of detailed failure analysis investigations and reports were made to show the relationship of stress, manufacturing process and performance of the devices. Failure rate comparisons were made of the three processes before and after screening. Several recommendations are developed for screening techniques to remove failure modes as they are related to the manufacturing process.

This report shows that it is possible to develop effective and economical reliability screens related to the manufacturing process used for this diffused planar transistor. Some areas for manufacturing process improvement are also indicated.

TABLE OF CONTENTS

TABLE OF CONTENTS

Page

SECTION V. NOISE STUDY

SECTION VI. PROCESS DETAILS

LIST OF ILLUSTRATIONS

DEFINITIONS OF SYMBOLS

FAILURE RESPONSE CATEGORIES

Symbol	Definition
1	**Parameter within original spectification limit**
2	Parameter within an end-of-life limit
3	Parameter within a catastrophic limit
4	Parameter beyond a catastrophic limit

Electrical Definition of Symbol Limits

Parameter	1	2	3	4
I_{CBO}	10 nA	10-100 nA	100-1000 nA	>1 uA
I_{EBO}	10 nA	10-100 nA	100-1000 nA	>1 uA
BV_{CEO}	40 V	30-40 V	20-30 V	<20 V
BV_{CEO} % Shift	15 %	25 %	50 %	>50 %
h_{FE}	40-120	35-40 & 120-150	28-35 & 150-180	<28 or > 180
h_{FE} % Shift	15 %	15-25 %	25-50 %	>50 %
$V_{CE(sat)}$ % Shift	15 %	15-25 %	25-50 %	>50 %
$V_{BE(sat)}$ % Shift	15 %	15-25 %	25-50 %	>50 %

TECHNICAL REPORT

RESEARCH TO DETERMINE FAILURE MODES FOR TRANSISTORS

CONTRACT NAS8-11059

SUMMARY

A detailed investigation for determining the reliability of a total of 1500 diffused planar transistors of the 2N718A type manufactured by three different processes was conducted. Each process lot was divided into several sub-lots which were subjected to several levels of stress screening followed by a number of accelerated life tests. The matrix of screens included: High Stress Screen, Moderate Stress Screen, Centrifuge Stress Screen, Burn-In Screen and Control Lot. The stress levels and time durations were selected to produce failures according to four defined failure criteria levels. An analysis of the failures produced was made and a failure mode was assigned.

A test of the electrical parameters listed on the 2N718A specification sheet was the criterion used for selecting the devices stressed on this program. The High Stress Screen consisted of 168 hours of stress at an ambient temperature of 250°C with a reverse bias of 30 volts. This was followed by 168 hours of storage at 300°C and then 20,000G centrifuge. The Moderate Stress Screen consisted of 168 hours of stress at an ambient temperature of 200°C with a reverse bias of 30 volts, followed by 168 hours of storage at 200°C and then 20,000G centrifuge. A Centrifuge Screen was also used which consisted of a single 20,000G centrifuge stress. A Control Lot was formed which was not screened with any of the above screens.

Following these stresses, the sub-lots were further divided and placed on a 3,000 hour life test at several levels. The operating life test levels were 800mW at T_A of 25°C, 700mW at T_A of 25°C, 500mW at T_A of 25°C, 400mW at T_A of 150°C and 200mW at T_A of 150°C. Data readouts were taken at 0, 168, 340, 680, 1000, 1500, 2000 and 3000 hours.

The four defined failure criteria levels are listed in the definitions and symbols and correspond to devices which pass the specification limit, end of life limit, catastrophic limit and that are beyond the catastrophic limit.

The failures that were produced were examined in sufficient detail to determine whether they were a function of material, process or design. The dominant failure mode found in all three processes was surface inversion. Devices from all the processes were subject to an increase in I_{CBO} when they were placed on a reverse voltage and temperature stress. The devices from Process B withstood this stress better than devices from the other processes indicating that the guard ring was stopping the inversion layer in the collector region. Devices from Process C also suffered from microcracks indicating that the process of bonding leads to the pellet had not been optimized and was not in good enough control to prevent strains during bonding. Detailed Failure Analysis Reports are included for other less dominant failure modes for suggested process improvements.

The large amount of data from the matrix test plan was assembled and summarized in a series of tables and figures. The tables permit a direct comparison of the several processes for response to stress, parameter distribution and distribution shifts with stress time as well as other significant functions. Analysis based on the test results of this program indicate the advantages of a stress screen for reliability improvement of these devices. A recommended stress screen is given in this report. Comparisons of the failure rates obtained on operating life tests for about three thousand hours of test time are also shown. Several distribution graphs are included to show the stability of the primary parameters I_{CBO} and h_{FE} of the population of devices under several levels of operating power.

SECTION I - PROGRAM RESULTS

A. REVIEW OF PROGRAM

This program consisted of a detailed study for determining the reliability of a total of 1,500 diffused planar transistors of the 2N718A type, manufactured by three different processes. A review of the electrical specification for the transistor type, photographs of the internal construction of the three devices, and details of the differences of the devices are in Section VI of this report. Tests were designed to determine modes of failure, process capabilities and to investigate stress screening techniques for detecting the presence of each mode of failure. Each process lot was divided into several sub lots which were then subjected to a testing matrix.

As an initial step in the program all of the devices were tested for hermetic seal by using the Radiflo test method. The test was conducted to a sensitivity of 1 X 10^{-10} standard cc/sec. leak rate. The electrical parameters of all of the devices according to the specification test conditions were also measured. The Noise Figure measurement for each transistor was also taken on the Quan-Tech Noise Figure Analyzer. One Noise Figure measurement is included as a part of the specification, but three more were added to aid in the determination of the applicability of Noise Figure screening as a reliability screen.

The next step involved a determination of the dominant failure mechanisms for devices manufactured by each of the three processes. It was also desired to determine the stresses to which each process would respond most readily. The population of units was sampled and placed in a step-stress matrix. The stresses involved temperature only, temperature and reverse voltage, power, centrifuge and shock and vibration. The initial step-stress matrix was continued at levels high enough to produce failures in the devices.

The detailed analysis of the failures produced in the step-stress matrix was included in a previous Quarterly Report. It was determined that Process A units had surface related failures as the most dominant failure mechanism. There were also a few instances of failure due to gold in the base lead migrating and alloying into the pellet so that the collector was shorted to the base. The Process B units also had surface related failures and were found to have lead separation from the post of the header as the dominant failure mechanism. Many of these leads appeared to be almost cut through due to the bonding pressure when the lead was applied. There were also two instances of the pellet separating from the header. The Process C units showed bulk degradation as the most dominant failure mechanism. When analyzed most of these units showed micro-cracks under the lead bond connections. This may have been due to excessive lead bonding pressure. The Process C units also had failure mechanisms related to surface degradation.

From an analysis of the data, three screening stresses were then derived. A High Stress Screen consisted of 168 hours of stress at an ambient temperature of 250°C with a reverse bias of 30 Volts. This was followed by 168 hours of storage at 300°C, which was then followed by a 20,000G centrifuge stress. A Moderate Stress Screen was designed which consisted of 168 hours of stress at an ambient temperature of 200°C with a reverse bias of 30 Volts, followed by 168 hours of storage at 200°C and then a 20,000G centrifuge stress. A Centrifuge Screen was also used which consisted of a single 20,000G centrifuge stress. A Control Lot was formed which was not screened with any of the above stress screens.

The units which had not been used on the step-stress matrix were then divided into four parts. Each of these parts was placed on one of five levels of a 3,000 hour life test. The life test levels were 800 milliwatts at an ambient temperature (T_A) of 25°C, 700 milliwatts at a T_A of 25°C, 500 milliwatts at a T_A of 25°C, 400 milliwatts at a T_A of 150°C and 200 milliwatts at T_A of 150°C. Data were read out on critical parameters at 0, 168, 340, 680, 1,000, 1,500, 2,000 and 3,000 hours. Four failure response categories were derived so that the electrically defined failures could be located at each readout time in the life test. In general, the units were not actually removed from life test, but were left on test to determine if further degradation occurred. These failure response categories are identified as 1, 2, 3 and 4 and correspond to units that met the original specifications, units that would have met normal high reliability end-of-life requirements, units that met catastrophic limits, and units that shifted beyond catastrophic limits. Thus, each response category identified a further degree of shift of the critical parameters.

This form of the test matrix resulted in 20 individual test cells for each of the processes. Since less than 500 units of each type were available, the total number of devices in each life test cell was necessarily reduced to a small number. This meant that the overall statistical confidence that could be placed in the results of any one of the life test cells was comparatively low. However, the trend of the response to the life test could be determined and when the data from the cells were suitably combined, reasonably confident estimates could be made of the response of each of the three processes.

The failures that were produced were examined in sufficient detail to determine whether the failure was a function of material, process, or design. The data accumulated from the matrix test plan was assembled and summarized in a series of tables and figures. The tables follow the text of this report and are reviewed in detail in the appropriate sections of the report. In general, the organization is such that each of the three processes may be compared for the same life test cell.

When the life tests were all completed the survivors were run through another centrifuge stress test. This gave information about any apparent hardening of the bonds, however, it also masked some of the results that might have been found from failure analysis, since some of the units were catastrophically destroyed in this second centrifuge stress.

B. TEST RESULTS

1. General. Table 1 shows the calculated failure rates for all of the life test conditions and for the various stress screens. The several life test conditions were also summarized to show an overall failure rate following a stress screen and a life test.

The failure rate calculations are all based on the Poisson distribution with a consequent assumption of a constant failure rate in time. The calculations were all made for a 60% confidence level. It should be pointed out that only trends may be derived from this information since some of the total unit hours of test were quite small. The Poisson distribution type of calculation is supposed to be independent of the number of test hours or the number of units involved. However, it is known that semiconductor devices are subject to certain random failures, and this type of failure mode reduces confidence in some of the life test results. It is certain that this accounts for some of the high failure rates which appear in the table. It is anticipated that these failure rates would not be as high if a larger sample size were used.

Tables 2 through 5 show the number of units submitted to the several screens, the number that fell out according to each response category during the screen, and the number of devices that failed in each of the response categories during the life test.

Tables 6 through 10 show the results of the centrifuge stress test that followed the life test. Again, the tables are organized according to the process and the life test conditions showing the number of units submitted to the centrifuge test and the number that failed after 20,000 G's and 150,000 G's.

It was decided to assess the effect of considering the first 168 hours of each life test as an additional burn-in screen. Therefore, the number of units that failed during the burn-in period is also included in Tables 2 through 5. The second failure rate calculation in Table 1 shows the reduction in the failure rate that would be observed if the failed units had been removed at the end of the 168 hours of burn-in.

2. Failure Rates. The failure rates calculated and shown in Table 1 are based on the data which is contained in Tables 2, 3, 4 and 5. For example, Table 2 contains the number of units and the number of failures that occurred on the 3,000 hour life test. These units had previously been subjected to the High Stress Screen. Process A units were divided in the five life test conditions as shown in Table 2. Under the 200 milliwatt life test condition, 28 units were submitted to the High Stress Screen. At the end of the screen, 6 of these units were rejected. Thus, 22 units were started on the 3,000 hour life test. At the end of 168 hours of burn-in, one unit was detected as a failure. At the end of the 3,000 hour life test one additional failure was found. A total of 66,000 unit test hours were accumulated. With the two failures, the expected failure rate calculated was 4.7% per 1,000 hours at a 60% confidence level. This is the first failure rate (FR1). When using the burn-in as a screen, one failure would have been removed from the lot before the life test. Therefore, only one failure would have occurred during the life test. However, the total number of test hours must also be reduced to 21X(3000-168) or 59,472 unit hours. Using the one failure produced, the second expected failure rate (FR2) would be 3.4% per 1,000 hours at the 60% confidence level. This procedure was repeated for each of the other processes and life test cells and for each of the stress screens. In several of the cells the burn-in screen would not have eliminated any units and thus the two failure rates are the same.

a. High Stress Screen. The High Stress Screen was damaging for Process B and C Units, since the life test results show higher failure rates for units that survive the screen than for those which were not subjected to the screen. The Process A units which survived the screen showed a slight reduction in failure rate but when the data associated with the stress screen responses were analyzed, it was seen that the Process A units showed more significant movements when subjected to the High Stress Screen than for the other screens. Therefore, it was concluded that the High Stress Screen actually resulted in destructive degradation of the units. The table below shows the summary of results of the High Stress Screen. The tabulation was obtained by adding together the unit hours and the number of failures for each of the life test conditions.

LIFE TEST FAILURES AFTER HIGH STRESS SCREEN

	Process A	Process B	Process C
Test, K-hours	375	360	24
Total Failures	11	42	5
Failure Rate 1	3.3	12	26
Test, K-hours	368	278	17.5
Post Burn-in Failures	10	20	4
Failure Rate 2	3.1	7.8	30

b. Moderate Stress Screen. The Moderate Stress Screen appeared to be quite successful in reducing the failure rate observed for Process A and Process B devices. In most of the life test matrix cells a substantial reduction in the failure rate was observed.

For the Process C units, the moderate stress screen did not show the same precise pattern. On the two higher power life test conditions, a reduction was observed in the failure rate of those units which survived the screen compared to those units which were not subjected to the screen. However, the other life test conditions showed that the screen actually appeared to increase the failure rate; thus, indicating some potential damage to the units. When the response pattern of the devices which were subjected to the screen (Table 3) is compared to the response pattern of the devices which were not screened (Table 5) it is seen that approximately the same failure pattern occurs. Thus, it seems reasonable to conclude that Process C devices will have a certain number of failures on these kinds of life tests and that these failures will occur in screened or non-screened devices.

The general response pattern, and the apparent lack of damage leads to the conclusion that the Moderate Stress Screen could be used on these devices without degrading them. The following table provides a summary of the failure rates for the Moderate Stress Screen:

LIFE TEST FAILURES AFTER MODERATE STRESS SCREEN

	Process A	Process B	Process C
Test, K-hours	486	438	321
Total Failures	7	19	33
Failure Rate 1	1.7	4.7	11
Test, K-hours	481	395	271
Post Burn-in Failures	6	10	22
Failure Rate 2	1.5	2.9	8.8

c. Centrifuge Screen. The Centrifuge Screen did not appear to have any significant effect upon Process A Transistors. The failure rate observed was slightly reduced in some of the life test cells, but was also slightly increased in the 200 milliwatt cell. It is not felt that much significance can be placed on these results because of the small magnitudes.

For the Process B transistors, the Centrifuge Screen appears to be destructive for all but two of the life test cells. For the 500 milliwatt and 400 milliwatt life test cells a reduction in the observed failure rate is seen when centrifuge screening is used.

For Process C transistors the Centrifuge Screen seemed to be destructive for all life test cells except at the 700 milliwatt level, which showed a reduction in the failure rate over the devices in the control lot. These results will be discussed more thoroughly in the next section of this report. The following table provides a summary of the life test results for the Centrifuge Screen:

LIFE TEST FAILURES AFTER CENTRIFUGE SCREEN

	Process A	Process B	Process C
Test, K-hours	255	240	273
Total Failures	8	20	29
Failure Rate 1	3.7	9.0	11
Test, K-hours	255	194	205
Post Burn-in Failures	8	9	13
Failure Rate 2	3.7	5.4	7.1

d. Control Lot. The units which were not subjected to any stress screen were regarded as the Control Lot for the matrix of life test cells. The failure rates are shown in a similar manner as for the other stress screen devices. The data in Table 5 indicated that a substantial number of units for Process C transistors failed when they were screened to the initial specification parameters. Of the failures that were found in this electrical parameter screening test, approximately half exceeded the maximum limit for I_{CBO} and the other half exceeded the maximum limit for h_{FE}. The h_{FE} failures were probably due to instrumentation differences. The I_{CBO} failures could well have been due to the storage time between the manufacturer's initial screening and the time of the program screen. There was a slight tendency observed for the I_{CBO} to increase on some units during the time of storage for the Process C devices. The observed failure rates are summarized for the control Lot devices below:

LIFE TEST RESULTS - CONTROL LOT

	Process A	Process B	Process C
Test, K-hours	234	213	306
Total Failures	8	14	32
Failure Rate 1	4.0	6.6	11
Test, K-hours	228	202	227
Post Burn-in Failures	7	8	11
Failure Rate 2	3.7	4.6	5.6

e. <u>Burn-in.</u> The use of the first 168 hours of life test as an additional burn-in screen has been discussed previously. When the failure rate data was analyzed, it was found that burn-in had almost no effect on the devices made by Process A. For the Process B devices, the failure rates observed could be reduced by using the first 168 hours of the life test as an additional screen in almost all cases. This indicated that the movement of the distribution of the parameters which had been started by the stress screen was not complete and that the first 168 hours of life test could be used to screen out units that changed. The Process C devices also showed a reduction in the observed failure rate by using the first 168 hours of life test as an additional screen.

3. <u>Centrifuge Failures After Life Test.</u> After the completion of the life tests, all of the surviving devices were subjected to a two level centrifuge test. The test was designed to stress units in the Y_1 axis, the axis which would tend to pull the lead bond away from the

pellet. The devices were first stressed at 20,000G and then were stressed at 150,000G. After each stress, the devices were measured and considered to have failed if they exhibited an electrical open following the test. Tables 6 through 9 contain the data for all stresses combined, as well as the summary of the combined life test results. It was felt that this type of test following the 3,000 hour life test would reveal any tendency of devices from the several processes to show the formation of intermetallic compounds, generally called purple plague. The junction temperatures of the devices were high enough in several of the life tests so that any tendency to produce the intermetallic compounds should have occurred on the life tests. The results in the centrifuge tables do not show any such pattern of failure. Some of the devices do indeed fail, however, others survive even the 150,000G centrifuge test quite successfully. The Centrifuge Screen before the life test was not effective in removing devices which failed centrifuge following the life test.

There was no observable basic difference in the performance of devices made by the three processes when subjected to this kind of test. Approximately 90% of the devices for any of the three processes were capable of surviving a 20,000G centrifuge test after a 3,000 hour life test. When the stress was raised to 150,000G's, approximately half of the units were still able to survive.

C. RECOMMENDED SCREENS

1. General. The purpose of any screen is to remove those devices which may fail at some point in time. It is also required that the devices that pass the screen are not degraded. A recommended screen is not normally developed by a direct comparison of arbitrarily defined failure rates observed on some set of life tests. It is more important to observe the general population response trends to the screen and to factor in the results of failure

analysis so that it may be determined whether or not the occurrence of a failure mechanism has been reduced by the proposed screening procedure. The recommended screening procedures developed are based upon an analysis of the failures produced and the population response trends noted in the appropriate tables and graphs in this report.

2. Process A. The High Stress Screen results showed a reduction in the failure rate for Process A devices; however, when the observed population shifts were examined, it was found that this screen produced the largest amount of shift. It was therefore, concluded, that the High Stress Screen was moderately damaging to Process A devices. The Moderate Stress Screen resulted in a reduction of the failure rate. The Centrifuge Stress Screen showed little real effect on the failure rate. It did not seem to be damaging to the units. It was also found that the burn-in test following the stress screen resulted in a small reduction of the failure rate.

3. Process B. The High Stress Screen was found to be definitely damaging for Process B devices. The Moderate Stress Screen resulted in a reduction in the failure rate with no apparent damage. The Centrifuge Screen showed an apparent decrease in the failure rate for the 400 and 500 milliwatt life tests, but this reduction was small and the population shift data indicated that the test should be considered at least moderately destructive for these devices. The use of an additional 168 hours of the life test as a burn-in following the stress screening resulted in a reduction of the failure rate for these devices.

4. Process C. Once again, the High Stress Screen proved to be damaging for the devices subjected to it. The Moderate Stress Screen resulted in a somewhat indeterminate answer since the failure rate was improved for some of the test cells and was not significantly improved for others. When the population response pattern was analyzed, it appeared that this screen would result in general improvement in the performance of devices during a life test. The Centrifuge Screen

appeared to be destructive in all cases. Once again, adding 168 hours of burn-in following the stress screen resulted in a reduction of the observed failure rate.

5. <u>All Processes Combined.</u> When the observed life test failures and the observed response of the population parameters were examined in combination, the test data indicated that the Moderate Stress Screen was successful in reducing the potential failure rate of the devices surviving the screen. It was successful for all of the processes to some degree and did not appear to induce any failures. The performance of the lot subjected to this screen may be further improved by operating the devices for 168 hours as an additional burn-in. Therefore, the most effective screen found in the test program for devices made by these three processes was:

a) Reverse bias of 30 volts at an ambient temperature of 200°C for 168 hours.
b) Storage at 200°C for 168 hours.
c) Centrifuge stress at 20,000G's in Y_1 plane.
d) Operating life tests at rated power to obtain the maximum device junction temperature for 168 hours.

Since the devices showed evidence of channel formation and then cure, it is felt that the recommended stress screen above can be improved. The information obtained from many other physics of failure studies also tends to support this argument. It should also be noted that centrifuge testing, particularly as a 100% screen, is a slow and comparatively expensive process. Centrifuge screening tends to be relatively inefficient unless there is a manufacturing defect in the devices. Centrifuge stressing should be done as a sample test to prove the device performance and not be used as a screening test on this type of small geometry pellet.

When all of the Failure Analysis data were examined, the dominant failure mechanism for all three processes was surface related degradation. This was often evidenced by the formation of surface channels. The screening technique should include some test for the identification and removal of devices which exhibit channeling. Such a test would require stressing the units for a period of 168 hours at an ambient temperature of 200°C with a reverse bias of 30 volts. At the end of this time period, the heater in the oven should be turned off, but the voltage stress should be left on the units until they have cooled to room temperature. This procedure will assure that any channels that have been formed will remain. The units should be read out for the leakage current, at the rated voltage, and those showing any significant shift should be screened from the lot. The specification limit for the collector cutoff current, I_{CBO}, is 10 nanoamperes at a collector to base voltage of 60 volts. The recommended screening limit should be based on the individual device shift in leakage current. A recommended limit is to allow an increase in leakage current of 5 to 10 times the initial reading. This leakage current measurement must be made within a maximum period of 12 hours after the devices have been cooled to room temperature.

It could be possible to apply the truncation screening technique discussed in Section II.G. to an inspection lot. Truncation screening is most applicable to parameter distributions which are highly tailed or which exhibit a definite bi-modal distribution. The technique is difficult to specify since it is dependent on the shape of the parameter distributions rather than the parameter values. The dependence of truncation screening on the distribution shape means that individual data must be taken and the distribution characteristics must be determined. The resultant characteristic must be analyzed and a decision made to determine the truncation point. All of these steps add cost to the devices and the lot processing could become very expensive, particularly if the lot contains a large number of devices.

If it was determined that a pattern existed which was susceptible to truncation screening, and if this pattern was representative of the production, then it might be possible to translate the truncation point into a specification limit. The truncation point would be a function of the manufacturing process and would almost certainly be different for each process, which would make it difficult to apply.

Therefore, a practical and efficient screening procedure would include the following steps:

(a) Serialize, or otherwise identify the devices, and measure I_{CBO}.

(b) Stress the devices for 168 hours at an ambient temperature of $200^{o}C$ with a reverse bias of 30 volts. Allow the devices to return to room temperature leaving the reverse bias on.

(c) Measure I_{CBO} and reject all devices which show an increase greater than 10 times the initial reading. This measurement must be completed within 12 hours after the time the devices have cooled to room temperature.

(d) Place the devices on an operating life test for 168 hours. The life test conditions should assure that the junction temperature is close to the maximum rating.

(e) Measure the devices, reject and remove any devices which exceed the specification limits.

(f) The lot may now be tested in accordance with normal lot inspection and acceptance procedures.

SECTION II - STRESS SCREEN RESULTS

A. INTRODUCTION

This section discusses the response of the devices to the several screens used before the life tests were started. The data associated with this section appear in Tables 11 through and including 61. The tables were organized to show comparisons of the three processes for a given parameter for each step of the various screens. Comparisons are shown of the stability of the population of devices as each step of the stress screen was performed.

Tables	Subject
11-24	High Stress Screen
25-37	Moderate Stress Screen
38-51	Centrifuge Screen
52-61	Control Lot

The tables are arranged so that information is shown in the order of Process A, B, and C for the following order of parameters I_{CBO}, h_{FE}, BV_{CEO}, I_{EBO}, $V_{CE(sat)}$, and $V_{BE(sat)}$. The values of I_{CBO} and h_{FE} are shown for the processes in all screens. The other electrical parameters are shown only for Process B and C. This format was chosen based on the results of the initial evaluation, which indicated that some parameter movement might be seen in the tests in these combinations.

Each of the tables shows the process involved, the screen, the parameters, the details of the stress, and a graph of the percentile shift at the end of each step in the screen, as well as a set of tabulated values for these shifts.

B. HIGH STRESS SCREEN

The High Stress Screen consisted of three steps. The first step subjected the units to a reverse bias of 30 volts for a period of 168 hours at an ambient temperature of 250°C. The second step subjected the units to a 168 hour bake at 300°C. The final step subjected the units to a 25,000G centrifuge test in the Y_1 plane.

1. Process A. The I_{CBO} response of the Process A units to the High Stress Screen is shown in Table II. Examination of the graph shows that Process A units increased in leakage current significantly after the first portion of the stress, recovered to essentially initial values after the bake portion and then increased slightly after the centrifuge test. The device response followed the pattern that would be expected for units that exhibited a surface inversion type of failure mechanism.

The h_{FE} shift, in Table 14, supports this analysis. The h_{FE} was measured at a relatively high collector current and, hence, would not reflect small changes in I_{CBO}.

2. Process B. The I_{CBO} shift (Table 12) and the h_{FE} shift (Table 15) again indicated surface inversion as the dominant failure mechanism. The BV_{CEO} (Table 17), I_{EBO} (Table 19), and the saturation voltage data (Tables 21, 23) all tended to confirm the assignment of a surface inversion failure mechanism. It should be noted that the Process B units showed the response pattern to a lesser degree than the Process A units.

3. Process C. The Process C units showed a steadily increasing leakage current (Table 13) as a result of the several

stress steps. The leakage current increased so rapidly after the second stress that the screening was discontinued at that point since it was not desired to destroy all of the units. The Process C units appeared to be increasing in leakage current with stress because of the presence of microcracks under the lead bonds. The presence of these cracks is discussed in more detail in the failure analysis section of the report.

The failure mechanisms for Process C units seemed to be a combination of surface inversion and microcracks. This was confirmed by the shift in I_{CBO} shown in Table 13, h_{FE} in Table 16, BV_{CEO} in Table 18, I_{EBO} in Table 20, $V_{CE(sat)}$ in Table 22 and $V_{BE(sat)}$ in Table 24.

4. All Processes Combined. The High Stress Screen showed the presence of surface inversion for all three processes, and microcracks for Process C. The I_{CBO} response was the most significant. When the data was analyzed in detail, it was seen that the screen degraded the devices. This analysis was generally confirmed when the failure rates were calculated for the devices after they had been on life test.

C. MODERATE STRESS SCREEN

Like the High Stress Screen, the Moderate Stress Screen was composed of three steps. The first step subjected the units to a reverse bias of 30 volts for 168 hours at an ambient temperature of 200°C. The second step was a high temperature bake for 168 hours at 200°C. The last step was a 25,000G centrifuge stress in the Y_1 plane.

1. Process A. The I_{CBO} distribution shift for the Process A units is shown in Table 25. As in the High Stress Screen, the

population shifted upward after the reverse bias and temperature stress, recovered during the bake stress and then increased slightly following the centrifuge stress. The device response was again typical of the pattern expected for a surface inversion failure mechanism.

The h_{FE} shift (Table 28) supports this analysis. Again, the measurement was performed at a relatively high collector current and did not reflect small changes in I_{CBO}.

2. Process B. The previous response pattern was again repeated. The I_{CBO} (Table 26), h_{FE} (Table 29), BV_{CEO} (Table 31), and saturation voltages (Tables 34 and 36) data all reinforced the conclusion that the dominant failure mechanism was related to surface inversion. For this screen, the response was approximately equal to the response of the Process A units.

3. Process C. The I_{CBO} response for the Process C units (Table 27) showed a definite pattern of shift and cure for the Moderate Stress Screen. The pattern was still typical of a surface inversion. However, the Process C units were not subjected to the Centrifuge Stress since 16% of the units were removed after the bake and it was not desired to risk losing more units in this third step of the Moderate Stress Screen. The h_{FE} distribution (Table 30) did not change significantly throughout the several steps of the stress screen.

The BV_{CEO} response to the Moderate Stress Screen is shown in Table 32. The significant change was in the lower 10% of the distribution, which showed a rather large decrease in BV_{CEO} following the first stress. However, these units generally recovered during the second stress. This represented another confirmation of surface inversion. The I_{EBO} distribution (Table 33), the $V_{CE(sat)}$ distribution (Table 35) and the $V_{BE(sat)}$ distribution (Table 37) showed shifts following the stresses which continued to support surface inversion as the dominant failure mechanism.

4. All Processes Combined. As in the High Stress Screen, the Moderate Stress Screen showed the presence of surface inversion for all three processes. There was also a possibility of microcracks being present in the Process C devices. The most significant response was seen in I_{CBO} again. The screen did not appear to have damaged the devices and this analysis was generally confirmed by the life test results.

D. CENTRIFUGE SCREEN

The Centrifuge Screen consisted of one single step in which the devices were subjected to a 25,000G centrifuge stress in the Y_1 plane.

The I_{CBO} response to the stress is shown in Tables 38, 39, and 40. In each case the value increased after the stress, but this increase was in the order of a nanoampere and, hence, is not regarded as being significant.

The h_{FE} distributions shown in Tables 41, 42, and 43 also showed some small movement of the population. The total movement was not significantly above normal measurement accuracy and was regarded as insignificant.

The distribution of BV_{CEO} in Tables 44, and 45, I_{EBO} in Tables 46 and 47, $V_{CE(sat)}$ in Tables 48 and 49, and $V_{BE(sat)}$ in Tables 50 and 51, all showed very slight population movement after the centrifuge stress. The movement was small, and there was no significant pattern. Some evidence was noted that the devices responded differently after being subjected to a life test. Thus, in comparison with the Control Lot, some degradation was introduced, but the degree and the precise degradation was difficult to assess from the sample sizes available.

E. CONTROL LOT

The Control Lot was held in an unscreened condition. It was read three times corresponding approximately to the reading times that were used for the devices being subjected to the other screens. Thus, there was an initial reading, a second reading approximately seven weeks later and a third reading approximately ten weeks after the initial reading. It was expected that no significant distribution shifts would show during this time span since the devices were stored at a room temperature ambient.

The I_{CBO} distribution shown in Tables 52, 53, and 54 indicated shifts but these were generally less than one nanoampere and are insignificant.

The h_{FE} distributions are shown in Tables 55, 56, and 57. Once again some small amount of shift seemed to be taking place, but the magnitude was not significant.

The other parameters were read out only for the Process C devices. Since rejects had been found in this lot during the initial testing, it was decided to check to determine if any shift was taking place. The BV_{CEO} in Table 58, the I_{EBO} in Table 59, the $V_{CE(sat)}$ in Table 60 and $V_{BE(sat)}$ in Table 61 did not show any significant amount of change through the ten week period.

F. STRESS SCREEN YIELDS

An assessment was made of the number of devices that could have been screened out by applying the various stress screens. The data in Table 86 shows the number of devices that were started into the screen and the number that were rejected according to the various response categories after the screen. It will be noted that some of the devices that could have been rejected by the screen were placed on life tests. This was done to determine whether or not these devices would continue to shift throughout the life test.

G. TRUNCATION SCREEN

Truncation screening has been discussed in Quarterly Reports #2, #3, and #4 and in the report Non-Destructive Reliability Screening of Electronic Parts, reference 19, pp. 4-29.

One form of truncation screening employs a "pulled-in" limit rather than the usual specification limit. Thus, initial limits would be selected so that units outside a normal distribution pattern would be removed from the lot by means of the initial screening. This form of reliability screening has many desirable characteristics if techniques can be developed for its application. Some of the complications of truncation screening, as applied to noise measurements, are shown in Section V of this report.

If the same reasoning is applied to units which failed during a test, an evaluation of the effects of truncation screening can be provided. In the evaluation process, application of the initial limits plus a 25% shift limit was used to truncate the distribution after the various steps of the stress.

It may also be hypothesized that any out of normal condition within a device will cause one or more of the parameters to have a bi-modal distribution. When this correlation is established, elimination of the upper (or lower) percentiles of the distribution can remove one part of the bi-modal distribution and would be expected to result in performance improvement on life test.

This study uses the term truncation screening to apply to the removal of units in the outer limits of the distribution rather than units in the outer limits of the 2N718A specification values. The essential difference can be illustrated by reference to $V_{CE(sat)}$. The 2N718A specification gives a limit of 1.5 volts. The full distribution of all three processes was enclosed in the range of 85 to 450 millivolts with Process A ranging from 150 to 409 millivolts and Processes B and C ranging from 80 to 165 millivolts. The use of 1.5 volts as a test limit for screening is not useful since all devices would have easily met this limit.

This means that a particular lot of devices could have a distribution which was generally quite narrow and also have one or two devices that were significantly separated from the rest of the distribution. All of these devices could meet the specification limit. In general, the devices separated from the balance of the distribution would be regarded as unusual, and truncation could screen out these devices. This technique is applicable to the lot being examined at any one time.

Normal lot-to-lot variations of a single process can cause a small shift in the distribution due to small variations in diffusion time or temperature, resistivity of the original crystal, or many other reasons which have no relation to reliability.

The units listed in Table 88 passed the Moderate Stress Screen and then failed on life test. The tabulated values are the percentiles of the parameter distribution of the devices. The table can be used to estimate the reduction in the total lot that would result from screening out more of these failures. For example, if it had been decided to screen out the upper and lower ten percent of devices for each of the parameters listed, fifteen out of nineteen of the devices would have been screened out.

An assessment was made of the capability of using a Truncation Screen as a substitute for stress screening. Table 89 was prepared similar to Table 88 to demonstrate this technique. The table shows that all of the units which later failed the I_{EBO} limits could have been screened out initially by screening out the upper ten percent of the distribution. If this had been done, all of the I_{CBO} failures would also have been removed. The high frequency noise test could also have been effective. However, the units that could have been removed by a Noise Figure screen could also have been removed more easily and economically by the I_{EBO} screen.

The results of applying truncation screening to all failures believed to be free from damage due to stress screen or life test power levels are shown in Table 90. All three processes show evidence of damage at the 500 milliwatt levels due to the transient triggered thermal runaway condition. The 500 milliwatt life test circuits did not have the diode protection against transients and thermal runaway which is normally used in life tests. All three processes also showed evidence of damage due to the High Stress Screen. In addition, Process C devices showed evidence of damage due to high temperatures on life test. When the data was analyzed in detail, it was found that screening out the upper and lower 3% of the h_{FE} distribution would have removed 15% of the later failures at a cost of 6% of the units in the lot.

Successive truncation of this lot could detect 37% of all the failures. The truncation screening would be performed at the following points:

I_{EBO}	@ 97th percentile	3 units eliminated
BV_{CEO}	@ 95th percentile	5 units eliminated
h_{FE}	@ 95th percentile	4 units eliminated
h_{FE}	@ 5th percentile	3 units eliminated
$V_{CE(sat)}$	@ 95th percentile	4 units eliminated
		19 units or 37% of Failures

If the percentages are multiplied, a yield of 79% is indicated. However, some duplication of failures does exist and the actual screening yield would be closer to 90%. This means that 19 of 51 failures could be eliminated by screening out about 58 of 578 units. The screen would be expensive since about 39 good units would be screened out to remove the 19 units which failed.

Table 91 summarizes the results that could be obtained by truncation screening for h_{FE} and several noise parameters. Screening at the 95th percentile of the h_{FE} distribution would be very effective for Process A units, effective for Process B units and ineffective for Process C units. Screening to the 5th percentile of the h_{FE} distribution would be effective for Process A and C. Other individual and combined screens can be assessed in a similar fashion.

Devices which had been placed on the 500 milliwatt life test, or the High Stress Screen, did not have the same response to truncation screening. That is, devices stressed in the tests that were damaging responded differently to truncation screening than the devices stressed in non-damaging tests. When the data were analyzed, it was found that there was little difference between the failed units and the entire population. If the upper and lower 15th percentiles of the I_{CBO} distribution for the Control Lot were screened, no significant results would be produced. There is some evidence that successive truncation could be effective but the main conclusion drawn is that a separate failure mode was induced in the damaging tests which reduced the effectiveness of the Truncation Screen.

From the foregoing analysis, it may be seen that the application of truncation screening is limited. Comparatively elaborate data analysis techniques must be employed, and the resultant parameter characteristics must be shown to be bi-modal or highly tailed. In addition, the Truncation Screen would have to be separately established for each manufacturing process to achieve maximum effectiveness. The last requirement would result in a cumbersome and confusing specification. It is concluded, therefore, that the potential advantages of truncation screening are overcome by the disadvantages. It is felt that any attempt to make use of general truncation techniques would result in inefficient screens, as well as limited specifications.

SECTION III - LIFE TEST RESULTS

A. INTRODUCTION

It was realized that an important factor influencing the results to be obtained on the life tests was the actual junction temperature of the devices under the operating life test conditions. To assess the variation of the junction temperature, measurements were made of the thermal resistance of a sample of the devices which would be put on life tests. The thermal resistance was measured in accordance with standard JEDEC measurement methods. Although the thermal resistance of the samples was found to vary, the range was small. In fact, there was a small enough variation to make the assumption that all of the devices would be operating at about the same junction temperature under the same stress conditions.

The life test tables and graphs show parameter response data for I_{CBO} and h_{FE} for each stress screen and process. The High Stress Screen life test data are shown first, followed by the data for the Moderate Stress Screen, the Centrifuge Stress Screen and the Control Lot. For each screen, the I_{CBO} data for each life test measurement are presented first and are followed by a graph of these responses. The h_{FE} data and graph are next. With this organization, the parameter response to one of the screens and life tests can be readily compared for the three manufacturing processes.

As discussed in Section I, the statistical confidence that could be placed in the results of any one of the life test cells was comparatively low. The trend of the response to the life test could be determined, and reasonably confident estimates could be made of the response of each of the three processes, when the data from the cells were suitably combined.

The failures that were produced were examined in sufficient detail to determine whether the failure was a function of material, process, or design. However, when the life tests were all completed, the survivors were subjected to another centrifuge test. Information was obtained about any apparent hardening of the bonds but the failed units were catastrophically destroyed. Thus, some of the results that might have been found from failure analysis were masked. The failure analysis procedures and some representative, detailed failure analysis reports are contained in Section IV of this report.

The life tests for this program were 3000 hours in length at the following conditions:

1. Power = 800mW, V_{CB} = 20V, T_A = 25°C
2. Power = 700mW, V_{CB} = 20V, T_A = 25°C
3. Power = 500mW, V_{CB} = 20V, T_A = 25°C
4. Power = 400mW, V_{CB} = 20V, T_A = 150°C
5. Power = 200mW, V_{CB} = 20V, T_A = 150°C

B. HIGH STRESS SCREEN

The High Stress Screen consisted of 168 hours of stress at an ambient temperature of 250°C with a reverse bias of 30 volts. This was followed by 168 hours of storage at 300°C, which was then followed by a 20,000G centrifuge stress. A portion of the devices from each of the three processes were stressed through this screen, and were then divided into sublots and placed on life test. Devices from Process A and B were placed on each of the five life test conditions. The devices from Process C were represented only in the room temperature life tests since the High Stress Screen had proved damaging, and comparatively few Process C units were subjected to it. Eliminating two of the life test cells was more practical than a further reduction of the number of units in each cell. The life test data and graphs are contained in Tables 62 through 67.

The I_{CBO} distribution for Process A and B devices shifted during the life test in a fashion that indicated surface related, or channeling, failures. The magnitude of the shifts also tended to indicate that the screen had resulted in some degradation of the devices. The Process C units showed over an order of magnitude greater shifts. The response pattern for Process C tended to confirm the previous analysis which indicated the presence of microcracks and that the High Stress Screen degraded these devices. The h_{FE} distributions remained comparatively stable throughout the life tests, a pattern that was in agreement with the presence of surface inversion as the dominant failure mechanism.

The estimated failure rates calculated for the devices are shown in Table 1, and have been discussed in detail in Section I.B.

C. MODERATE STRESS SCREEN

The Moderate Stress Screen consisted of 168 hours of stress at an ambient temperature of 200°C with a reverse bias of 30 volts, followed by 168 hours of storage at 200°C and then a 20,000G centrifuge stress. Once again, a portion of the devices from each of the three processes were stressed through the screen, and were then divided into sub-lots and placed on life test. The life test data and graphs are contained in Table 68 through 73.

The I_{CBO} distribution shift for Process A and B devices was less than the shift for the High Stress Screen, but still indicated a surface related failure mechanism. There did not appear to be any destructive degradation of the devices. The Process C units showed significantly less shift than had been shown for the High Stress Screen, but the shift was greater than that for the Process A and B units. Thus, the Process C units still exhibited the presence of microcracks as well as a surface related failure mechanism. For this set of life tests, the Process B units were the most stable. The h_{FE} distributions again remained comparatively stable throughout the life tests.

The estimated failure rates calculated for the devices are also in Table 1 and have been discussed in Section I.B. The Moderate Stress Screen and life test resulted in lower estimated failure rates than those calculated for the High Stress Screen and life test.

D. CENTRIFUGE SCREEN

The Centrifuge Screen consisted of a single, 20,000G centrifuge stress. A portion of the devices from each of the three processes were stressed through the screen, and were then divided into sub-lots and placed on life test. The life test data and graphs are contained in Tables 74 through 79.

The I_{CBO} distribution for all three processes did not show a large shift on life test. The shift pattern indicates that some degradation may have resulted from the screen, but the amount of degradation is difficult to assess from the sample sizes used. The Process C units showed the greatest shift, and the response to the Centrifuge Screen tended to confirm the presence of microcracks. The amount of shift on h_{FE} tended to confirm the analysis.

The estimated failure rates calculated for the units are in Table 1, again, and were discussed in Section I.B. The Centrifuge Screen and life test resulted in higher failure rates than those calculated for the Moderate Stress Screen and life test.

E. CONTROL LOT

The Control Lot was held in an unscreened condition. This portion of the devices was measured electrically three times, corresponding to the measurement times of the screened devices. The lot was then divided into sub-lots and placed on life test. The life test data and graphs are contained in Tables 80 through 85.

The I_{CBO} distribution for all three processes responded in a fashion which indicated the presence of channeling, a surface related failure mechanism. The Process C units continued to show the largest shift. The h_{FE} distribution generally showed more shift than had been observed for the screened devices, which was in accord with the expected results.

The estimated failure rates, in Table 1, were discussed in Section I.B. and were generally higher than those calculated for the Moderate Stress Screen and life test.

F. ALL PROCESSES COMBINED

Throughout the stress screens and life tests, the dominant failure mechanism found in all three processes was related to surface degradation, or channeling. The Process C devices also were found to have microcracks under the lead bonds. The failure rates which were estimated from the life test results were considered to be reasonable when the failure criteria, sample sizes and stress levels of the tests were all considered.

The process strengths that were demonstrated in the program were the good process control evident in the Process A units and the guard ring structure of the Process B units. The potential process improvements would add the guard ring to the Process A and B units and tighten the process control for the Process B and C units.

SECTION IV - FAILURE MECHANISMS AND ANALYSIS

A. PHYSICAL NATURE OF FAILURE MECHANISMS

1. Type A - Surface Defects. Most failures of this type are attributed to inversion layers or accumulated surface charges on the collector-base junction. Reverse bias voltages, such as those applied in power dissipation tests, will set up surface fringe fields across the junction similar to those in a parallel plate capacitor. The fringe field can then line up dipole atoms or ions on the dielectric SiO_2 surface or within the passivation layer so that (-) charges face the collector surface and (+) charges are aligned facing the base.

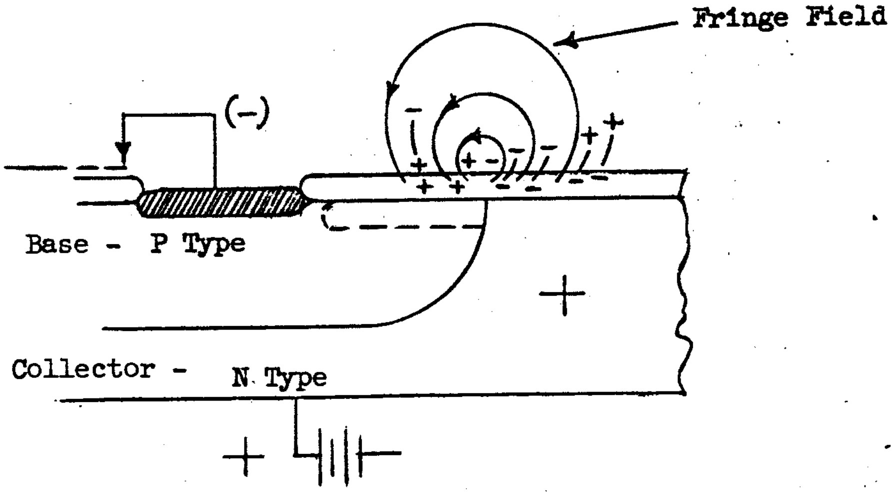

As the sketch shows, the + charges lined up on the base side of the surface will electrostatically attract electrons from the bulk. The accumulated charge may build up sufficiently at the surface to cause inversion of the "P" material to "N". A similar effect of opposite polarity can take place on the collector surface. Note that when the inversion layer grows to meet the base ring, a direct path from the collector to the base exists. Under reverse bias, this narrow surface channel effectively becomes thinner and eventually pinches off as the space charge region gets wider with voltage. This effect gives the I_{CBO} characteristic a high saturating type of slope.

Since the mobility of the charges under the electric field will increase with temperature, the Type A failure mechanism is accelerated when voltage is applied under high temperature conditions.

Units with Type A behavior can usually be completely recovered by heating without bias. The heat apparently serves to redistribute and disperse the aligned charges so that the unit recovers to the original characteristics.

If the oxide condition, or internal ambient, is such that the surface potential under thermal equilibrium conditions is extremely on the "N" side, a device may have low leakage before a high temperature test but will develop a Type A leakage characteristic as charges align to their equilibrium "N" condition under high temperature. In this case, both the base and collector surface potentials will have shifted toward "N". Thus, an "N" inversion on the base and an N+ accumulation on the collector will lead to Type A leakage, together with a reduced or degraded BV_{CBO} (now determined by the collector N+ resistivity). Measurement of BV_{CBO} after power tests or other tests applying reverse bias to the collector-base junction have maximum values determined by the bulk resistivity or junction defect spots. This occurs because the collector tends to be pushed toward "P" or high resistivity "N" by the reverse bias.

Emitter-base surfaces influenced by a positive field grid bias (N type) have been shown to result in an h_{FE} degradation. Thus, it may be assumed that an "N" type inversion on the base, reaching into the emitter-base junction area will degrade h_{FE}. Temperature-induced surface failures, which may have uniformly influenced oxides toward "N", will have degraded h_{FE} levels along with Type A collector-base characteristics. The observed I_{EBO} may rise to fairly high levels if the emitter-base inversion is severe. The h_{FE} response is an especially sensitive indicator at low current levels, where the recombination at the emitter-base surface produces a higher proportion of the total current.

Devices which show an h_{FE} degradation can frequently be recovered by heating in ambients such as air, oxygen, or nitrogen under conditions which reverse the mobile surface condition.

2. Type B-Bulk Degradation. Type B degradation is usually characterized by a relatively high leakage current at high collector-base voltages. At voltages of 1V or less, leakages may be low (0.5nA or less) as compared to Type A rejects, which run from 10nA to 10uA at low voltages. It has also been found that these units are relatively unrecoverable by heating. A small improvement may often be seen, but this improvement is insignificant when compared with the 3 - 5 order of magnitude improvement for the Type A degradation.

Visual examination of Type B units may reveal the location of a bulk defect or failure. For example, visible "hot spots" in the aluminum contacts often can be found, indicating that high current concentrations developed during the test period.

Collector-base junction irregularities associated with microcracks, and characterized by sharp breaks in the normally smooth junction profile, have been made visible on units (by sectioning and staining) which have never been placed on any electrical stress. This further supports the theory that Type B rejects can be initiated at weak junction points produced by some processing fault. The fact that random sectioning can find these defects indicates that, in some cases, the numerical density of these defects can be high.

An interesting point is that the deep dips or spikes in the junctions of some rejects seem to be located under the aluminum base ring. Microcracks or defects in other locations produce only slight irregularities. Deep collector-base junction irregularities have never been spotted under the aluminum contact area of the emitter. This suggests that surface deposited aluminum can penetrate the full length of a relatively long microcrack and then diffuse out as a "P" cylinder into the lightly-doped "N" collector material surrounding the microcrack.

The thermal conditions of the aluminum alloying process are apparently sufficient to cause this defect. The sketch shows an example of the defect.

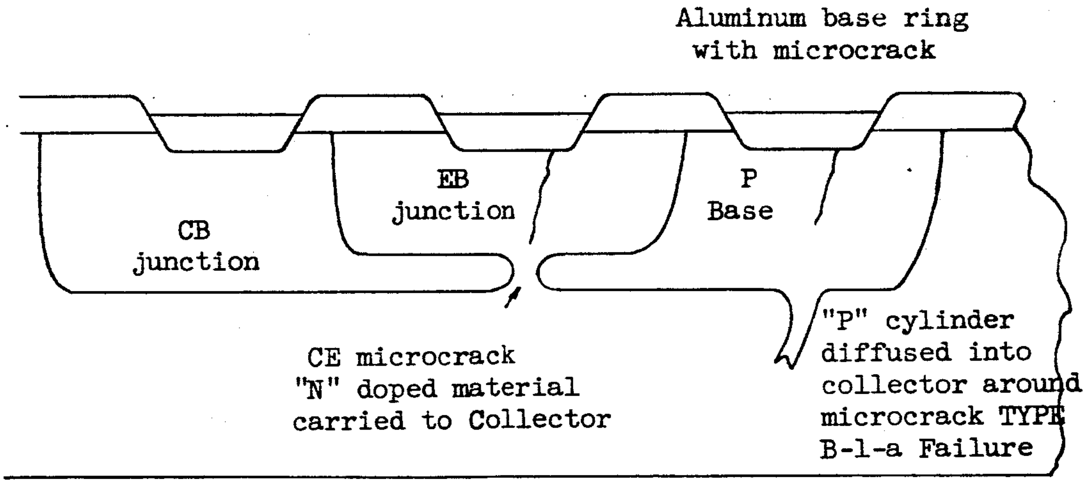

Ball bonding may also contribute to this failure mode by introducing additional cracks at the pressure areas. The thermal and electrical stresses present in high power life tests may then be sufficient to cause further metallic migrations with time, until the runaway conditions result.

The absence of visible deep spikes in the emitter areas may be explained by examining the behavior of the emitter dopant. The dopant is present in very heavy concentrations at the emitter and may be carried along with the aluminum migration processes previously described. The presence of this compensating impurity prevents inversion of the "N" type collector. In fact, if the concentration of the dopant exceeds that of the aluminum at the collector-base junction, the collector-base junction should slope upward towards the surface. A large or heavily-doped concentration penetrating to the collector may be expected to create an "N" type pipe coupling the emitter to the collector. These conditions should result in a failure mode which would appear as collector-to-emitter shorts or as low voltage breakdown types limited by punch-through into the emitter, Type B-3-b.

Type B failures which show evidence of having been through a severe runaway condition, can sometimes be traced to defective life test circuitry, high voltage spikes and transients, in which case the failure would be reclassified as Type F.

Cracked pellets lead to another form of Type B-2 failure, evidenced by an I_{CBO} increase. Damaged junctions which may be caused during scribing and separating operations, are especially sensitive to electrical stresses. Cracks may propagate from any rough broken edges into junction areas, usually following the natural (111) cleavage planes. Cracks and chips may also be caused by rough handling during pellet mount or wire bonding operations.

3. Type C - Opens. Type C-1 failures are opens where the aluminum has peeled away following the stress. The basic cause of failure in this case is poor alloying of the aluminum to the silicon. When tensile stresses cause localized separation of the aluminum from the silicon surfaces, the resulting flexing of the brittle intermetallic phases causes these areas to fail in the vicinity of the bond area. The gold bond to the aluminum may remain

relatively intact and a bare silicon surface is exposed.

Type C-6 failures result from intermetallic deterioration. It has been found that opens formed on high temperature tests almost always occur at the point of contact between the gold wires and the aluminum contacts. Gold interdiffuses rapidly with aluminum at temperatures as low as 200°C. A gold-aluminum phase diagram shows that a series of intermetallic compounds and alloys are formed, ranging through the entire percent composition range. Some of these intermetallic compounds are brittle and have crystalline volumes considerably different than the elements that compose them. This contributes to deterioration of the interface and weakening of the bond.

It must be emphasized, however, that intermetallics are universally present on all devices and do not by themselves cause failure. Failures will be observed only if certain defects are present which exaggerate the effect of the intermetallic compounds. Prolonged aging of devices at 300°C does not necessarily produce severe loss of mechanical strength under normal use conditions, with properly made bonds.

Type C-6-b failures are demonstrated by increases in $V_{CE(sat)}$ which occur as contact resistances change. If high temperature storage results in severe metallurgical degradation of the emitter bond, both $V_{CE(sat)}$ and $V_{BE(sat)}$ will increase proportionally to the voltages developed in these bonds. This degradation can sometimes be seen before a complete open of the Type C-6-a occurs. A deterioration of the pellet mount due to the effects of severe oxidizing conditions (water vapor at high temperatures) will result in $V_{CE(sat)}$ increase and little change in $V_{BE(sat)}$.

The Type C-5-a failure may leave the same type of metallurgical trace characteristic of a C-6 intermetallic deterioration. A grey or black patch may be left on the aluminum pattern and the gold bond may be separated cleanly from the aluminum at the gold aluminum interface. In this type of failure, however, the original gold-aluminum contact area is considered to have been insufficient to withstand subsequent stresses. This may happen with offside base bonding, in which the gold ball bond does not uniformly contact the full width of the base ring. The contact area will also be reduced if the bonding temperature or pressure is low, if surfaces are dirty or oxidized, or if the reducing gas coverage is poor.

4. Type D - Faulty Post Bond Assembly. The wire bond to the gold post may separate if the post surface is contaminated or very thin, or if bonding pressure is low or the gas cover is inadequate. This is categorized as a Type D-1 failure.

An internal short, Type D-3 failure, can occur when the package construction requires internal wires to be in close proximity to the posts, pellet edges or metal walls. Large mechanical stresses such as centrifuge or vibration, or wire sagging effects after long thermal exposure may cause the internal components to short.

5. Type E - Humidity & Hermeticity. Type E leakage increases may be summarized as package hermeticity defects not affected by pellet quality. These leakage increases are divided in several categories and represent conductivity increases due to the permeation of water (or any other conductive fluid) into the inner air space of the device. Permeation can occur through pinholes left by defective hermetic welding (Type E-1). When condensation occurs in the device, rather than being confined to external surfaces, relatively long bake times are usually required to out-diffuse the moisture and to recover the original leakage characteristics.

Type E-5 leakage differs from other Type E's in the retention of water (or another conductive material) between external electrical contacts rather than on internal surfaces. Exposure to salt spray atmospheres may cause corrosion products, such as iron or kovar rust paths to bridge across contacts. These salts are relatively insoluble and cannot be removed by the water rinse that follows salt spray testing.

These external leakage effects increase with higher humidity conditions. Thus, measurements made in a hot humid room may have a considerably higher leakage level than if the test was performed in a dry atmosphere. Type E-5-a leakage can be eliminated by chemical washing and drying without resorting to extensive bakeouts. Thus, Type E-5-a leakage can be detected by elimination of humidity response after an acid dip, hot water wash and dry gas blow-off.

6. Type F - Improper Measurement Techniques. Type F failures are frequently identifiable from visual evidence of unusual situations such as melted open wires. This class of failure generally results from an error in handling, an error in test equipment accuracy or calibration, or transients in the test equipment. An analysis of the circuitry involved generally reveals that the visually evident failure would have been impossible to obtain if the device had been properly connected to a circuit in good operating condition.

B. FAILURE MODE CHART

The next several pages contain Failure Mode Charts which have been developed to define and illustrate failure mode categories, failure mechanisms and failure causes. The charts also show the most likely failure indicator and the stress which generally causes the failure. The failure code shown in the charts is used in all the Failure Analysis Reports.

The Failure Mode Charts were originally developed to cover all the possible failures of silicon planar transistors and thus contain some failure codes which were not observed in the failures produced in this program.

FAILURE MODE CHART. SILICON PLANAR TRANSISTOR.

FAILURE MODE CATEGORY	FAILURE INDICATOR & STRESS CAUSING FAILURE	FAILURE MODE	FAILURE MECHANISM	FAILURE CAUSES
$\boxed{A}$ Pellet Surface Degradation	I_{CO} increase with high BV_{CBO} Degradation in h_{FE} (at low I_C levels) I_{CO} increases BV_{CBO} degrading Induced by Reverse Bias with high temperature Power stresses with reverse bias High temperature alone	$\boxed{1}$ Inherently unstable oxide passivation	$\boxed{a}$ Ionizable states built into oxide structure causes the following to occur: p inversion of collector or n inversion of base Surface recombination velocity increase at EB junction. Base usually going toward n potential Accumulation layer' - collector surface going n	$\boxed{1}$ Non-optimum diffusion and oxide growth baking
				$\boxed{2}$ Inadequate cleaning steps prior to oxide growth operations
		$\boxed{2}$ Surface contamination	$\boxed{a}$ Material on SiO_2 surface initiates oxide ionization	$\boxed{1}$ Organic and KPR residues
				$\boxed{2}$ Inorganic ionizable salts
			$\boxed{b}$ Gas ambient contamination	$\boxed{1}$ Insufficient outgassing
				$\boxed{2}$ Poor hermetic seal
				$\boxed{3}$ Contamination of cap weld flush
		$\boxed{3}$ Surface oxide defects	$\boxed{a}$ Damaged passivation susceptible to ionization degradation	$\boxed{1}$ Etch processes pitting of Si and SiO_2
				$\boxed{2}$ Non-uniform oxides

FAILURE MODE CHART SILICON PLANAR TRANSISTOR.

FAILURE MODE CATEGORY	FAILURE INDICATOR & STRESS CAUSING FAILURE	FAILURE MODE	FAILURE MECHANISM	FAILURE CAUSES
A Pellet Surface Degradation (Continued)				3 Etch undercutting from contact process KPR failure
		4 Improper diffusion	a Junction surface damaged	1 Excess deposition of doping impurities
			b Junctions irregular	1 KPR processing out of control
			c Junctions misaligned	
	Irregular BV_{CBO} characteristic	5 Presence of current concentration centers	a Microplasma and defect sites dissipate excess power	1 Sharp junction irregularities
				2 n+ points in junction
				3 Bulk defect site propagating to surface

FAILURE MODE CHART — SILICON PLANAR TRANSISTOR

FAILURE MODE CATEGORY	FAILURE INDICATOR & STRESS CAUSING FAILURE	FAILURE MODE	FAILURE MECHANISM	FAILURE CAUSES
$\boxed{B}$ Pellet Material degradation	I_{CO} increase - usually catastrophic & essentially irreversible	$\boxed{1}$ Defects in substrate or epitaxy	$\boxed{a}$ Defect site acts as current concentration point inducing localized overheating, "hot spots" progressive deterioration	$\boxed{1}$ Substrate not sufficiently clean prior to epitaxial deposition
				$\boxed{2}$ Stacking fault crystalline irregularities
	I_{CO} increase having reversible surface-like properties Frequently very mobile with voltage Sometimes irreversible h_{FE} degradation	$\boxed{2}$ Cracks or chips in critical areas	$\boxed{a}$ Microcracks in surface	$\boxed{1}$ Wafer preparation defects prior to diffusion or aluminizing
			$\boxed{b}$ Severe cracks in pellet	$\boxed{1}$ Rough scribing edges propagating cracks
				$\boxed{2}$ Pellet too thin (easily cracked)
				$\boxed{3}$ Rough handling at pellet mount
				$\boxed{4}$ Rough handling or excessive pressure at bonding
			$\boxed{c}$ Microcracks or cracks in pellet after mechanical or thermal shock	$\boxed{1}$ Cracks not originally in pellet but induced by severe mechanical or thermal shocking due to strains built into pellet

FAILURE MODE CHART. SILICON PLANAR TRANSISTOR.

FAILURE MODE CATEGORY	FAILURE INDICATOR & STRESS CAUSING FAILURE	FAILURE MODE	FAILURE MECHANISM	FAILURE CAUSES
$\boxed{B}$ Pellet Material Degradation (Continued)	Irreversible h_{FE} degradation or Leakage increase	$\boxed{3}$ Contact metal penetration into junctions	$\boxed{a}$ Metal migration into junctions creates high leakage points or areas with high recombination velocities. The effect is irreversible unless the metal is gettered out or neutralized	$\boxed{1}$ Metal diffused into junctions due to high localized temperatures at high stress levels of power
				$\boxed{2}$ Metal source such as a gold bond is in very close proximity to junction. Diffusion is easier under these conditions
			$\boxed{b}$ Metal migration runs away to create a dead short	$\boxed{3}$ A unit with poor thermal dissipation (due to pellet bond voids) will operate hotter and run away or degrade sooner

FAILURE MODE CHART SILICON PLANAR TRANSISTOR.

FAILURE MODE CATEGORY	FAILURE INDICATOR & STRESS CAUSING FAILURE	FAILURE MODE	FAILURE MECHANISM	FAILURE CAUSES
C Faulty bond to pellet	Mechanical stresses Vibration Shock Centrifuge Leading to open base or emitter	1 Faulty deposition of contacts	a Aluminum bond to silicon substrate is inadequate Aluminum peels off with open bond	1 Vacuum deposition out of control
				2 Deposition or alloy furnace gas contaminated
				3 Alloy temperature-time cycle inadequate
				4 Silicon substrate insufficiently etched
				5 Silicon substrate contaminated
		2 Cracks in silicon - metal bond	a Open occurs with silicon chips adhering to pulled-off wire	1 Bond pressure too high
				2 Bond temperature too low
				3 Wire material - wrong composition (too hard)
				4 Processing accidents with bonding tools
		3 Voids in bond	a Aluminum or silicon missing in open bond area	1 Aluminum accidentally scratched away in processing
				2 Silicon chipped out by processing accidents
	Mechanical stresses and/or very long high temperature storage Leading to open base or emitter	4 Separation of bond from wire	a Ball bond still adhering to pellet - wire broken off above it	1 Accidental processing damage to wire section
				2 Metallurgical weakness in the wire section resulting from intermetallic diffusion of aluminum into wire

FAILURE MODE CHART SILICON PLANAR TRANSISTOR

FAILURE MODE CATEGORY	FAILURE INDICATOR & STRESS CAUSING FAILURE	FAILURE MODE	FAILURE MECHANISM	FAILURE CAUSES
C Faulty bond to Pellet (Continued)	Open base or emitter due to mechanical stresses	5 Separation of ball bond from metallized surface	a Bond area is insufficient - or poor adhesion over adequate bond area	1 Bond placed off center
				2 Metallizing too thin
				3 Bonding operation out of control causing oxidizing gas cover or
				4 Insufficient temperature - time cycle
				5 Contact metallizing surface is oxidized or
				6 Contaminated (Organic material especially)
			b Defects causing overstress condition of bond	1 Oversize wire used
				2 Ball size and weight too large
	Open base or emitter - or $V_{(SAT)}$ parameters increasing due to long high temperature storage, mechanical shock, very high power operation & mechanical stress	6 "Purple Plague" deterioration	a Bond initially strong deteriorating to open at bond to aluminum interface	1 Intermetallic diffusion causing Au - Al brittle compound formation
			b Ohmic contact resistance develops in Au - Al bond interface	

FAILURE MODE CHART SILICON PLANAR TRANSISTOR

FAILURE MODE CATEGORY	FAILURE INDICATOR & STRESS CAUSING FAILURE	FAILURE MODE	FAILURE MECHANISM	FAILURE CAUSES
C Faulty bond to Pellet (Continued)	High $V_{CE(SAT)}$ develops or collector opens due to mechanical shock	7 Faulty preform pellet bond	a Preform bond made initially weak	1 Pellet collector surface oxidized
				2 Pellet collector surface contaminated
				3 Cover gas in bond operation oxidizing or contaminated
				4 Alloy temperature - time cycle insufficient
				5 Preforms contaminated
				6 Preforms - wrong composition
			b Bond deteriorated with time	1 High temperature storage in ambient containing H_2O gas
				2 Inorganic salt contamination in bond is at high level
		8 Faulty Preform to Header bond	a Preform bonded to silicon not adhering properly to header	1 Header contaminated
				2 Preform contaminated
	Short-primarily E-B short after electrical, thermal or mechanical stress	9 Faulty placement of bond on pellet	a Wire bond shorting to contact area across junction	1 Wire placed off center on contact areas, i.e. base bond overlapping E-B junction toward emitter or emitter bond toward base

FAILURE MODE CHART SILICON PLANAR TRANSISTOR

FAILURE MODE CATEGORY	FAILURE INDICATOR & STRESS CAUSING FAILURE	FAILURE MODE	FAILURE MECHANISM	FAILURE CAUSES
D Faulty bond to post assembly	Open base or emitter due to mechanical stresses	1 Faulty wire to post connection	a Separation at bond-post interface	1 Post surface contaminated 2 Bond made on post area having insufficient gold 3 Bond wire contaminated 4 Bond wire - wrong composition 5 Bond operation out of control (time - temperature) 6 Bond damaged in process
	Parameters - non-functioning	2 Improper lead routing	a Base bond placed on emitter post or vice versa	1 Bond operator error
	Internal shorts - intermittence due to mechanical stresses or long term temperature exposure	3 Lead wires internally shorting	a Wires touching collector post or pellet edge	1 Wires placed too close to collector edge 2 Wires excessively long 3 Header design does not allow sufficient room for movement
	Open base or emitter due to mechanical stresses or very long high temperature exposure	4 Broken wire	a Wire broken in round section	1 Usually due to accidental damage to wire section 2 Crystal growth and plane slippage in wire
			b Bond adhering to post - wire is broken in or just above bond	1 Bonding pressure - temperature too high - overly thin wire section squeezed out

FAILURE MODE CHART.   SILICON PLANAR TRANSISTORS.

FAILURE MODE CATEGORY	FAILURE INDICATOR & STRESS CAUSING FAILURE	FAILURE MODE	FAILURE MECHANISM	FAILURE CAUSES
$\boxed{E}$ Improper Packaging	Tests involving liquids or H_2O cause high I_{CBO}, I_{EBO}, h_{FE} or Result in chemical and physical deterioration to internal components	$\boxed{1}$ Faulty cap to header seal	$\boxed{a}$ Leak in header - cap seal	1 Welder out of control
				2 Cap or header plating not uniform
				3 Damaged package or cap
			$\boxed{b}$ Hermeticity failure at cap weld due to mechanical or thermal shocks	1 Hermetic seal OK after fabrication but opens up after mechanical or thermal shocks due to welding under marginal or less than optimum conditions
		$\boxed{2}$ Faulty terminal to insulator seal	$\boxed{a}$ Glass to metal oxide seal leaks	1 Defective header
				2 Metal oxide seal damaged by processing steps
			$\boxed{b}$ Glass or ceramic insulator cracked & leaking	3 Seal broken by handling
		$\boxed{3}$ Faulty header to insulator seal	$\boxed{a}$ Glass to metal oxide seal leaks	1 Defective header
				2 Metal oxide seal damaged by processing steps
				3 Seal broken by handling
		$\boxed{4}$ Terminal fatigue	$\boxed{a}$ External terminal broken off	1 Defective headers
	High humidity ambient or tests involving liquids cause high I_{CBO}, I_{EBO}	$\boxed{5}$ External surface contamination	$\boxed{a}$ Conductive external surface paths on device	1 Rust and other salts across external contacts
				2 Excessive porosity and H_2O retention in ceramic
				3 Plating on terminals inadequate
		$\boxed{6}$ Marking deterioration	$\boxed{a}$ Markings illegible	
		$\boxed{7}$ Finish	$\boxed{a}$ Plating inadequate	1 Defective plating

FAILURE MODE CHART. SILICON PLANAR TRANSISTORS.

FAILURE MODE CATEGORY	FAILURE INDICATOR & STRESS CAUSING FAILURE	FAILURE MODE	FAILURE MECHANISM	FAILURE CAUSES
E Improper Packaging (Continued)	Shorts, deterioration of parameters, intermittent readings	8 Foreign material inside package	a Process material fragment loose in package	1 Fragments introduced at process steps
			b Airborne particles in package	2 Improper process room control
	Loss of hermeticity or I_{CO} or h_{FE} degradation if pellet is damaged	9 Ceramic cracked will fail hermeticitytests pellet may also crack due to header failure	a Header ceramic cracks during mechanical or thermal stresses	1 Mechanical shocks or stresses exceed the breaking strength of the relatively brittle header components
		10 Package cracks and pellet damage results from fixturing	a Header ceramic cracked due to poor fit in fixturing	1 Header failure is due to a warped ceramic condition or other geometric defect which causes incompatibility between package & fixturing
	Open contacts indicated after mechanical stress, centrifuging	11 Header construction is inadequate - tears open under stress, usually between plated layers	a Collector islands break open from header during mechanical stresses	1 Header plating interface bond strengths are inadequate
				2 Collector island glass - metal seals are insufficiently strong to withstand forces
	Header broken open after mechanical or thermal shock	12 Metallizing bond between flange and ceramic base is inadequate	a Header failure takes place between the cylindrical metal flange and the ceramic base	1 Metallizing bond is not made strong enough

FAILURE MODE CHART SILICON PLANAR TRANSISTOR

FAILURE MODE CATEGORY	FAILURE INDICATOR & STRESS CAUSING FAILURE	FAILURE MODE	FAILURE MECHANISM	FAILURE CAUSES
$\boxed{F}$ Improper measurement technique	Incorrect data supplied	$\boxed{1}$ Inadequate accuracy	$\boxed{a}$ Measurement errors	1 Faulty instrumentation
		$\boxed{2}$ Inadequate calibration		2 Defective external contacts to device from test equipment
	Shorted and high leakage units, not recoverable and opens and otherwise damaged devices	$\boxed{3}$ Transients in equipment	$\boxed{a}$ Internal alloy spots in device	1 Faulty switching, power supply problem, etc.
			$\boxed{b}$ Wires melted open by current surge	
		$\boxed{4}$ Improper handling	$\boxed{a}$ Package physically damaged	1 Operator error
			$\boxed{b}$ Device connected into test circuit incorrectly	

C. FAILURE ANALYSIS PROCEDURE

Six general basic categories of failures have been defined in the failure mode charts. Preliminary analysis procedures have been developed to determine these categories within about 48 hours of log-in of rejects in the Reject Analysis Laboratory. The detailed analysis procedures required to determine the cause of failure then can be efficiently scheduled for groups of units and completion of analysis effected as rapidly as possible.

The basic categories or Preliminary Analysis Codes are defined as:

Type A. Surface degradation - a reversible effect due to the influence of relatively mobile charges and ions in the surface.

Type B. Pellet degraded permanently and irreversibly - damage may be a crack or internal alloy.

Type C. Pellet bond problems - usually open or defective wire or pellet mount.

Type D. Faulty bond to post assembly - opens or wires mechanically contacting internal components.

Type E. Package problems - hermeticity of header construction failure.

Type F. Failure due to improper handling.

The flow charts presented as Figures 1 and 2 follow the handling of failures through preliminary analysis and through final analysis procedures. The initial electrical measurements made in the laboratory on all D.C. parameters shown in the verification measurements are usually enough to assign a Preliminary Analysis Code.

Type A failures are further identified and characterized by the response to bake-out, and treatment in chemicals. A dew point apparatus is used for cold temperature measurements and for identification of hermeticity failures. This apparatus has been specifically developed for the detection of small quantities of water. A special test procedure for the determination of susceptibility of devices to collector or base inversion has also been worked out. In addition, a mass spectrometer facility has been utilized to confirm the presence of water when it is indicated by electrical measurements, and to detect gas impurities. For example, carbon dioxide, hydrogen, oxygen and argon have been identified.

The initial characterization of Type E failures is often similar to varieties of surface degradation initiated by contaminants, since contaminants entering through hermeticity defects will affect pellet behavior in the same manner as contaminants trapped in a hermetic device. Radiflo, dew point, floating emitter potential and fluorescent penetrant dye (Zyglo) tests are used to make a positive identification of this type of defect.

Type B and D failures are classed together since the electrical characteristics are often (not always) catastrophic in nature. Thus, initial analysis identifications are not always possible until the units are decapped and visually examined. Sectioning procedures have been developed for alloy shorts and electrochemical methods have been developed for removal of bonded wires without physical damage to the brittle semiconductor beneath the wire. Special etches are also used to show up dislocation and crystalline defect lines.

Devices which show Type C, D, E and F failures may be open electrically and therefore are not identifiable until units are decapped and examined. F type shorts are frequently identifiable from visual evidence of unusual situations such as shorts across the emitter-base junction, or melted open wires, or even by examination of test data before and after verification.

D. FAILURE ANALYSIS SUMMARY

The test data for all the failures produced in the test program were analyzed to determine the general failure mechanism. Representative samples of each type of failure mechanism were then analyzed in detail. These detailed analyses are summarized in this paragraph.

1. Process A. Three of the failures that were analyzed showed failure mechanisms related to impurities introduced in different areas of fabrication.

Unit A155 showed a tendancy toward surface inversion. The surface inversion tendancy is related to the method of oxide growth, the density of oxide vacancies and gettering impurities from diffusion and oxidation steps and the number of mobile ions introduced into the oxide by processing. Complete elimination of this type of failure would require considerable experimentation with basic processes.

The failure in Unit A353 may be related to impurities introduced into the gold plating by the vendor supplying headers and can be controlled to some extent by rigid vendor control, QC vigilance, and process control. This failure occurred after a relatively long period under high temperature stress.

The failure in Unit A419 indicated a process defect in degassing or decontaminating of parts. The presence of water in this device was detected by dew point testing and electrical analysis.

SUMMARY OF FAILURE ANALYSES FOR PROCESS A UNITS

Unit	Primary Parameter Failed	Test Causing Failure	Failure Description	Failure Code
A353	V_{SAT}	400mW, 150°C 1500 hr	The collector contact resistance increased by about 13 ohms due to separation between the silicon and the eutectic bond.	C-7-b
A528	I_{EBO}	300°C bake 168 hr	High I_{EBO} leakage due to a bridge of aluminum running from base ring to the emitter-base junction. Conductive leakage developed from ring through emitter oxide - faulty deposition processing.	Faulty Processing
A419	I_{CBO}	400mW, 150°C 1500 hr	Leakage found to be due to a high humidity inside the device, as much as 90 mm pressure under heat. The source of H_2O was faulty outgassing of parts in manufacturing - not a hermeticity leak.	A-2-b
A155	I_{CBO}	500mW, 25°C 1000 hr	A collector inversion layer formed under reverse bias power. No defect noted in passivation.	A-1-a

SUMMARY OF FAILURE ANALYSES FOR PROCESS A UNITS

Unit	Primary Parameter Failed	Test Causing Failure	Failure Description	Failure Code
A557	h_{FE} I_{EBO}	500mW, 25°C 1000 hr	A runaway condition had resulted in a metal bridge across the emitter-base junction. Oxide chips and strains were found in this same area and are believed to have made device more sensitive to this type of runaway.	B-2-a
A74	--	700mW, 25°C 340 hr.	Analysis indicated the data at 340 hours was erroneous. Unit had not degraded. All readings subsequent to 340 hours were valid.	Not Legitimate

2. Process B. The detailed analysis of the Process B devices showed h_{FE} degradation and lead bond problems.

a. h_{FE} Degradation. The first four devices in the summary showed that high power stressing resulted in considerable changes in the emitter-base surface potentials of the devices.

Large changes in h_{FE} and BV_{CEO} result from these shifts in base surface potentials. BV_{CEO} is inversely related to h_{FE}

$$BV_{CEO} \approx BV_{CBO} / \sqrt[n]{h_{FE}}$$ (See Bibliography, Ref.20).

A change of the P base surface toward intrinsic or N potential will usually result in h_{FE} degradation and BV_{CEO} increase (Units B-305, 359, 543) while a shift of the base surface potential toward P will usually raise gain and decrease BV_{CEO} (Unit B-541).

Several factors contributed to make this device sensitive to h_{FE} shifts under power tests.

(1) The geometry of the Process B device was considerably smaller than either the Process A or C, resulting in emitter areas of 46 and 176 mil^2. Thus, for the same power levels, current densities and localized emitter junction temperatures were considerably higher for Process B devices, even though the long emitter perimeter allowed more efficient current distribution than the circular geometries of the Process A and C devices. Unit B-305 is a device in which the emitter ran exceptionally hot. The appearance indicated that localized temperatures > 550°C had been reached, causing the silicon to begin alloying into the aluminum and resulting in an emitter-base short. The 700mW life test circuit was in the common base configuration with the base protected against runaway by a diode. An emitter current of 35 mA was designed in by the $R_E = 286\Omega$. As the device heated up in test, the h_{fb} could have $= 1$ ($I_B = 0$) and the unit went into an I_{CEO} mode at a voltage $= (V_{CB} + V_E) = 30$ volts.

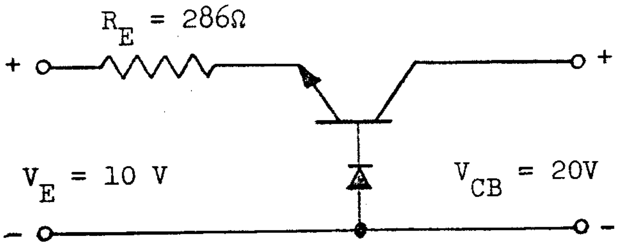

Simplified
700mW
Life Test
Circuit

I_{CEO} could then have risen to any level determined only by the device and resistor in series. Calculations showed that at an $I_E = 52.5$ mA, a maximum possible power of 788 mW ($V_{CB} = 15V \times 52.5$ mA) was dissipated by the collector-base junction. The emitter current may have increased even further, with less total runaway dissipation by the device. However, at some point, the safe current handling capacity of the emitter was exceeded, especially if current hogging at a secondary breakdown spot served to concentrate the emitter current even further.

(2) The basic oxide growth process of the Process B devices may have left an excessively high positive space charge (N potential) at the SiO_2 - Si interface. Many factors could have contributed to this condition, such as the method of growth (O_2 or H_2O) and the temperature of oxidation.

(3) The changes in base surface potential noted also indicated the presence of sufficient numbers of ions which could have moved under bias fields or by thermal diffusion to the SiO_2 - Si interface to change surface potentials toward N. Sodium is an ion noted most frequently in the literature with this capability.

Unit B-541 was of interest because it illustrated an h_{FE} instability in which the N oxide potential was moving steadily toward P with a resulting improvement in gain. An oxygen ambient has been noted to have this affect, both in the literature and in our labs. Mobile plus ions or plus oxide vacancy sites in the oxide apparently are tied up by the oxygen ambient. For this device, the cause was defective hermeticity.

The Process B devices above are free from any surface effects causing degradation at the collector-base junction. There appeared to be insufficient densities of mobile plus ions to cause complete inversion of the P surface (required for large increases of I_{CBO}) and the guard ring design may have been effective toward stopping any collector inversion from reaching the high recombination centers at the pellet edge.

b. Bond Problems. A second pattern of failures was seen in the analysis for the two open gold-aluminum post bonds (B-446 and 515). The use of aluminum wires, while relieving any intermetallic problems in high temperature storage or operation at the pellet, transfers these problems to the posts.

Aluminum wires are much more difficult to bond consistently than gold wires. The oxide problem results in occasional weak initial contacts (Unit B-446). Also, the bonding pressures required for aluminum are higher and result in bond sections which are much more flattened and thinned out than corresponding gold wire TCB sections. The thin sections are then especially susceptible to gold intermetallic diffusion penetration from the gold post and break off readily under shock (Unit B-515). The advantages of aluminum bonding, with good process control, may overcome any of these disadvantages.

SUMMARY OF FAILURE ANALYSES FOR PROCESS B UNITS

Unit	Primary Parameter Failed	Tests Causing Failure	Failure Description	Failure Code
B-305	h_{FE} I_{EBO}	700mW, 25°C 168 hr	An emitter-base high resistance short developed by migration of metal down into the emitter-base junction. Emitter area showed very hot running. The circuit allowed up to 788 mW dissipation if h_{fb} goes to 1.0 during life test.	B-3-a
B-359	h_{FE}	700mW, 25°C 680 hr.	h_{FE} degradation due to relatively unstable surface at emitter-base junction under bias fields. Related to mobile ions in oxide (Surface potential changes).	A-1-a

SUMMARY OF FAILURE ANALYSES FOR PROCESS B UNITS

Unit	Primary Parameter Failed	Tests Causing Failure	Failure Description	Failure Code
B-541	h_{FE}	800mW, 25°C 168 hr	h_{FE} increasing during test due to hermeticity leak in glass bead. Emitter-base surface potential is unstable and recombination velocity decreases in oxygen ambient.	A-1-a, E-2-a
B-543	h_{FE}	700mW, 25°C 2000 hr.	h_{FE} degradation-unstable emitter-base surface potential under power biases.	A-1-a
B-354	I_{CBO}	500mW, 25°C 168 hr.	A 3 Megohm short developed during life test due to a filament connecting intermittently from the aluminum base ring to the pellet edge.	E-8-b
B-446	Open Base	800mW, 25°C 2000 hr	The gold-aluminum contact at the post opened up. Analysis (lack of intermetallic compounds) indicated a poor initial bond had been made which fatigued open under repeated stress cycles.	D-1-a
B-515	Open Emitter	700mW, 25°C 680 hr.	Gold-aluminum post bond over squeezed on edge of post. Intermetallic formations caused intermittent open.	D-1-a

SUMMARY OF FAILURE ANALYSES FOR PROCESS B UNITS

Unit	Primary Parameter Failed	Tests Causing Failure	Failure Description	Failure Code
B-450	Open external lead	700mW, 25°C 2000 hr	Fatigue of terminal finally broke off emitter.	E-4-a

3. Process C. The Process C device was subject to a failure mechanism not seen in the Process A and B devices. Microcracks were found penetrating the junctions surrounding the ball bond intermetallic formations in these units.

The following is a description of the techniques which were used to identify and document this unique failure type, coded as B-2-a, in units C-98 through C-576.

a. Electrical Identification. The electrical behavior of devices having cracks through the junctions usually has the behavior characteristics given in the table below. These characteristics are also symptoms of the various other effects listed.

Defect in Device	I_{CBO}-(near Breakdown)	I_{CES}@V_{CB}=0 to Punch - thru or Avalanche	Floating E Potential (E_F)	I_{CBO}, I_{CES}, E_F in dry gas ambient	BV_{CBO}	Low Current (I_C=100ua) h_{FE}
1. Crack in CB junction	Unstable-drifts up	= I_{CBO}	None	Same	Noisy	Normal
2. Crack in CB & EB junction.	Unstable-drifts up	>I_{CBO}	Responds	Same	Noisy Unstable	Degraded

Defect in Device	I_{CBO}-(near Breakdown)	I_{CES}@V_{CB}=0 to Punch - thru or Avalanche	Floating E Potential (E_F)	I_{CBO}, I_{CES}, E_F in dry gas ambient	BV_{CBO}	Low Current (I_C=100ua) h_{FE}
3. External bead conduction.	Ohmic I_{CBO} drifts down	$>I_{CBO}$	Responds drift down	Recovers	Normal	Normal
4. Internal bead conduction & high H_2O ambient.	Unstable up or down	$>I_{CBO}$	Responds unstable down	Same	Walkout or Loop	Normal
5. Pellet Contamination.	Drift up or down	$= I_{CBO}$	None	Same	Walkout	Normal or Degraded
6. Low Reach - Through Voltage	Stable	$>I_{CBO}$	Responds stable	Same	Soft	Normal

b. Decapping - and Electrical Tests. The Process C devices, when decapped, had a very significant response to ambients: I_{CBO} and E_F drifting to high levels in lab or high humidity air and recovering under dry ambients, a behavior which can again be interpreted as being due to cracks or to the presence of hygroscopic conductive salts across the header beads. Emitter cracks (2 in Table) could be definitely identified at this stage by disconnecting the emitter wire to post bond. Complete recovery of any E_F response at this point confirms an emitter crack in the pellet. This is shown in the diagram below, where R_{CE}, R_E and R_S are all in parallel with the E_F meter.

R_{CE} - the effective resistance of the crack penetrating both junctions.

R_E - resistance of glass bead.- emitter post

R_S - due to conduction across the face of the pellet.

R_B - resistance of glass bead - base post

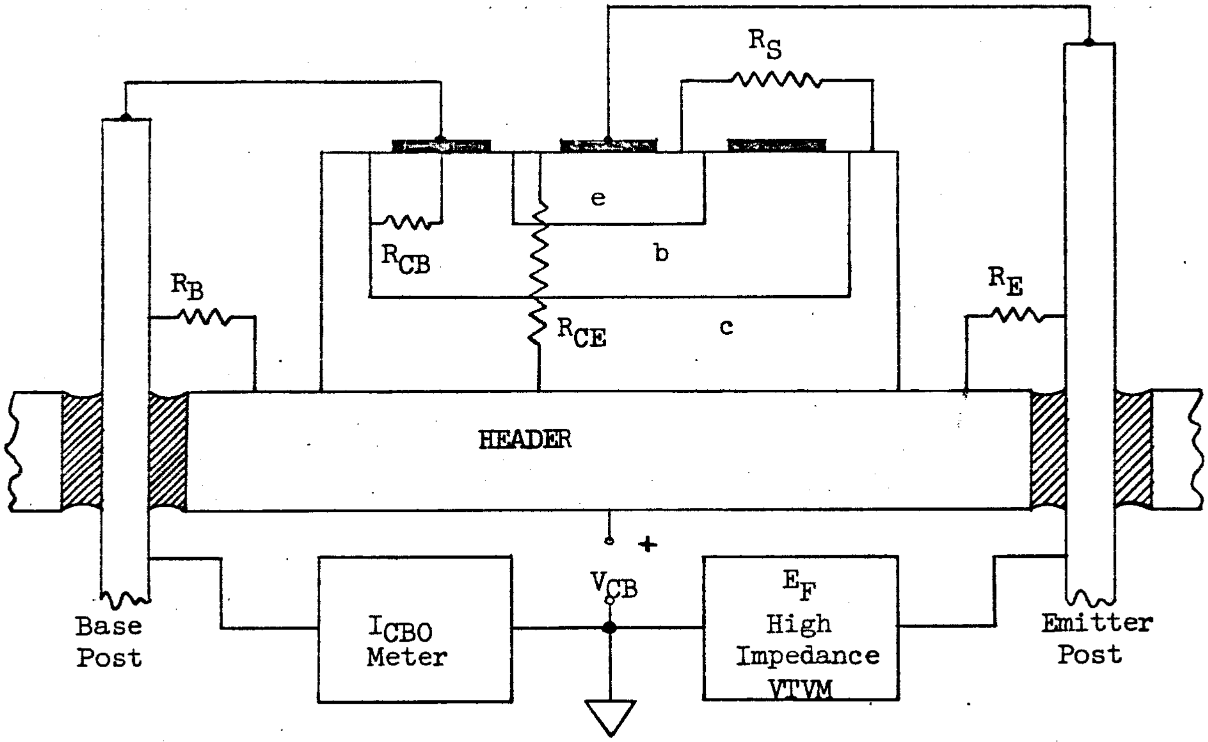

When the base is grounded, R_S (due to contamination or even inversion conduction across the entire pellet surface) is completely shunted out to ground.

Disconnecting the emitter-post contact eliminates the R_{CE} path so that R_E is then measured alone. In Units C-98, C-400 and C-505, this procedure identified the existence of R_{CE}, the unstable component due to cracks through both junctions. R_{CB} may also be isolated from

R_B (the base bead leakage) by breaking the post bond.

Devices C-147, C-293 and C-576 did not fail any parameters on test. They are included here because in lab tests on "good" Process C devices, severe crack characteristics usually appeared after a 300°C overnight bake on decapped devices, indicating failure under this relatively mild thermal shock. It must be emphasized at this point that the dry nitrogen ambient inside the device stabilizes the characteristics considerably. Exposure to air brings out the unstable high leakage drift.

Cracks were not seen in any of the devices by pellet examination, even under high power microscopy.

c. Etching. Chemical and electro-chemical removal of the contacts was then used to identify cracks under the contacts.

(1) A 10% NaOH etch was used to remove the aluminum contacts. Patterns remaining in the silicon beneath the aluminum indicated that a relatively heavy coat, probably at least 1 micron thick, of aluminum is alloyed into the silicon at temperatures over 550°C. See the deep patterns left in the failure analysis photographs for C-147, C-293, and C-301. The cracks were still not visible.

(2) The bonds and gold-aluminum intermetallics were removed electrolytically in a KOH-KCN solution at +3 volts, which selectively etched off wires (either base or emitter). A non-selective gold etch, such as aqua regia, will usually destroy the header mount making further handling of the pellet difficult. The photographs in the failure analysis report for Unit A-557 show the progressive removal of metal by this technique. The mechanical removal of wires would introduce cracks and defeat the purpose of this investigation.

This etch technique finally revealed cracks growing peripherally around the bonds and just under the black outer edge of the intermetallic growth areas surrounding the bonds. See the photographs in the failure analyses for Units C-363 (base and emitter), C-147 (base) and C-293 (base). In the last two cases, the cracks penetrated the silicon outside of the aluminum contact areas and were unmistakable.

d. Sections. Sections were made to further study the penetration of the cracks and to reveal the construction details of these devices.

The photographs for Unit C-576 showed cracks and pertinent details most clearly. The section through an electrically indicated cracked emitter shows cracks penetrating diagonally inward and ending less than 0.9 mil from the top surface. The photos also show the collector diffusion depth to have been very shallow for a large area device (about 0.2 mil), and a relatively deep penetration (1 mil) of intermetallic compound - most probably Au_5Al_2 under the bond and Au_2Al in the sides (See Bibliography-21). Two photos of ball bonds made to Process A units aged for equivalent time periods are shown for comparison.

Section studies were also made for Units C-400 and C-293.

e. Oxide Thickness. Oxide thicknesses were studied to see if there was any relation to this mechanism. A thick oxide structure, for example, would be expected to put more strain on the thermally mismatched silicon beneath it than the thin 10-15,000 Å films used in the Process A and B devices.

Photographs of Unit C-301 show the technique used to measure oxide thickness. Half the pellet was masked against an HF etch and then the interference fringes of the undercut mask boundary were counted and the top surface colors noted.

The thickness was then estimated from a set of standards or calculated from the formula:

$$d = \frac{n\lambda}{4\mu}$$

where λ is the wave length of light used - estimated with good accuracy in white light at 5400 Å (green band)

$\mu = 1.5$, the index of refraction of SiO_2

$n = 1, 3, 5, 7$ for each fringe counted

d = thickness of oxide in Å.

The Process C device oxide proved to be generally thinner than the Process A and B which had been measured previously (in the First Quarterly Report). An interesting difference between Process A and C devices was that the Process C device emitter oxide is thicker than the uniform thickness base-collector oxide. By comparison, Process A devices were fabricated with the collector oxide thicker than the base oxide which was thicker than the emitter oxide.

Comparable oxide thicknesses are:

	Process A	Process C (Unit C-301)
Collector	12000Å	6300Å
Base	8500	6300
Emitter	5000	7100

Measurements of other Process C devices gave even thinner oxide values. From these measurements of Process C units, a process of oxidation can be assumed. Following diffusion of the base and emitter, all masking oxides were stripped off and the full thicknesses of the passivation oxide were grown onto the clean silicon. Heavily doped silicon (emitters) will grow a thicker oxide skin under the same oxidizing conditions as can be estimated from work reported by Deal and Sklar (Ref. 22), showing plots of oxide growth on phosphorous doped silicon at the low temperature of 920°C in wet oxygen to give about 7100 Å on $1.5 \times 10^{20}/cm^3$ (comparable to emitter concentration) to about 6000 Å for 10^{16} to $10^{18}/cm^3$ material (collector-base doping).

Thus, there is no evidence to believe the oxide growth technique contributed to abnormal strains in the silicon surface.

f. Theory Developed - B-2-a Failures. The investigations described above have led to the development of the following theory:

The gold-aluminum intermetallics found in the bond sections were as much as 1 mil thick probably due to the availability of aluminum from the heavily deposited contacts which were alloyed deeply to the silicon. Like other gold intermetallics, the physical properties of these compounds are hard and strong. Thermal expansion coefficients of one of the intermetallics, Au_2Al, which is likely to be present in the bond can be calculated from a paper by Bernstein (Ref. 23), as $14.8 \times 10^{-6}/°C$, this being extremely mismatched from Si at $4.2 \times 10^{-6}/°C$.

During contraction from 300°C, the massive, hard intermetallic section which was well bonded into the underlying silicon, in an area extending 5 to 9 mils, puts the silicon surface into severe tension and produces the fractures as shown.

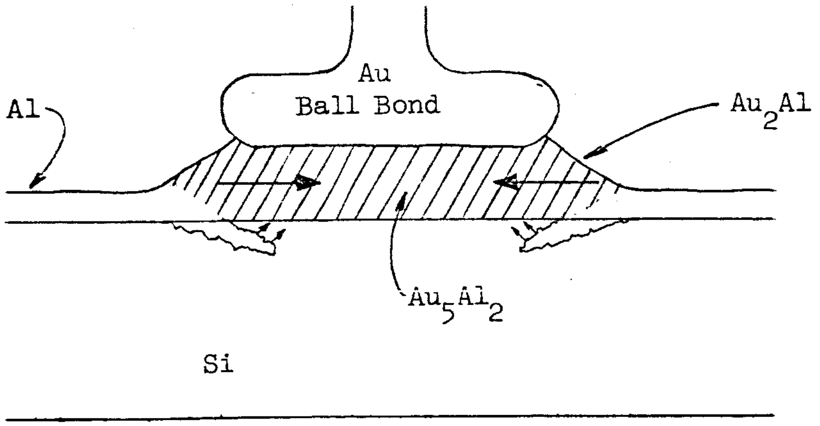

This type of failure was not able to be demonstrated when a small sample of experimental ball bonded devices were fabricated.

g. Defects. Three more of the failures which were analyzed showed characteristics related to bulk defects. Unit C-233, called a B-2-a failure, is not like those discussed previously. In this case, microcracks appeared in the junction area some distance from the bonds.

SUMMARY OF ANALYSES FOR PROCESS C UNITS

Unit	Primary Parameters Failed	Test Causing Failure	Failure Description	Failure Code
C-98	I_{CBO} 680 hr, h_{FE} 2000 hr	200°C & 400mW, 150°C	I_{CBO}, I_{CES} parameters very unstable, h_{FE} degraded. Analysis indicated emitter and collector junctions were cracked. Cracks were not made visible.	B-2-a
C-363	I_{CBO} 2000 hr	700mW, 25°C	Behavior of device indicated cracks in collector-base junction. Etching off contacts revealed microcracks under bonds.	B-2-a
C-400	I_{CBO} 1000 hr	200°C & 500mW, 25°C	Analysis indicated probability of crack in junctions. A small crack located by sectioning through the emitter bond.	B-2-a
C-505	I_{CBO} 3000 hr & h_{FE} degraded 25%	200°C and 500mW, 25°C.	Analysis indicated a probable crack through the emitter bond. The crack was not made visible in tests.	B-2-a

SUMMARY OF ANALYSES FOR PROCESS C UNITS

Unit	Primary Parameter Failed	Test Causing Failure	Failure Description	Failure Code
C-182	ΔBV_{CEO} increase > 40%	500mW, 25°C	ΔBV_{CEO} is not due to shift in h_{FE}. A collector-base junction defect had resulted in a sharp microplasma-type I_{CBO} increase near a V_{CB} of 60 Volts originally. The life test pushed this voltage out to 90 Volts, due to "P" inversion of the collector, and carried the BV_{CEO} along with it.	A-5-a
C-288	I_{CBO} 168 hr	700mW, 25°C	A defect site was found in the aluminum ring during analysis. It is assumed this spot ran hot during test causing an inversion layer.	A-5-a
C-233	I_{CBO} 680 hr	500mW, 25°C	Defect sites, microcracks, were found in the collector-base junction crossing the aluminum ring. Surface inversion formed easily in this area. These cracks are not the same as those previously described for Units C-98-C-576.	B-2-a

SUMMARY OF ANALYSES FOR PROCESS C UNITS

Unit	Primary Parameter Failed	Test Causing Failure	Failure Description	Failure Code
C-406	I_{CBO} 340 hrs	700mW, 25°C	Header found severely contaminated. Impurity gases contributed to the formation of an inversion layer.	A-2-b
C-275	Collector base short 340 hrs	400mW, 150°C	A collector-base short of 14Ω was caused by faulty processing and the placement of the base wire against the pellet edge.	D-3-a
C-61	I_{CBO} 680 hr	400mW, 150°C	Analysis indicated the 680 hr readout was faulty. Unit had not degraded.	Not Legitimate

Unit	Life Tests Device Passed Without Failure	Analysis & Behavior in Lab	Failure Code
C-147	200°C and 500mW, 3000 hrs	A bake at 300°C in lab and decapping severely degraded I_{CBO} and BV_{CBO} breakdown. Etching off of contacts showed a micro-crack had developed just outside of the junction under the base intermetallic.	Not degraded on test. Degraded in Lab.

Unit	Life Tests Device Passed Without Failure	Analysis & Behavior in Lab	Failure Code
C-293	250°C, 300°C and 500mW, 3000 hrs.	After lab bake and decap, severe degradation of I_{CBO} was noted. Photos and sections of contact areas showed a considerable crack around the intermetallic growth of the base bond, penetrating collector-base junction.	Not degraded on test.
C-576	250°C, 300°C 500mW, 3000 hrs.	After lab bake and decap operations, h_{FE}, I_{CBO}, E_F badly degraded and acted "cracked". Section made through the emitter bond clearly defined a fracture under the emitter bond intermetallic, passing through the junctions.	Not degraded on test. Degraded in lab.
C-301	250°C, 300°C and 500mW 3000 hrs.	Unit did not degrade in lab bakeouts. Device used for study of oxide thickness.	Not degraded on test or in Lab.

E. FAILURE ANALYSIS REPORTS

The Failure Analysis Reports included in this report are representative of the failure analyses conducted for the program.

Each report contains:

1. The device and process identification.
2. The Test Cell number.
3. The Failure Mode Category.
4. A summary of the Failure Analysis.
5. A detailed description of the analysis which includes graphs, tables and device photographs, as applicable.

FAILURE ANALYSIS REPORT

Sheet 1 of Final

Unit No. A 74	Test Cell No. 419-202	Process A	Failure Mode Category Not a Failure

Summary of Analysis:

The device was determined to be good and the failure indication on life test was in error.

h_{FE} shift at the 250°C @ 30V and 300°C may be calibration error. Unit stable throughout 700mW test. h_{FE} and V_{SAT} reading at 340 hours indicating a short, appears to be equipment error.

Unit was very stable upon receipt for failure analysis. The unit has been determined to be 'no failure'.

Prepared by: Alfred Poe
Failure Analysis Engineer

Date: 9/8/65

FAILURE ANALYSIS REPORT

Sheet 1 of 2

Unit No.	Test Cell No.	Process	Failure Mode Category
A 155	419-218	A	A-1-a

Summary of Analysis: Device failed I_{CBO} at the 168 hour readout of the life test. Failure was caused by mobile ions in the oxide.

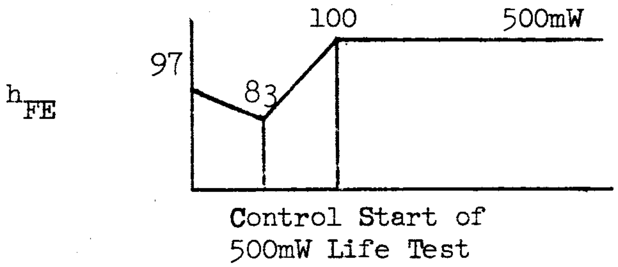

h_{FE} Behavior - Stable. Control reading (83) is probably faulty, probably a calibration error. BV_{CEO} remains stable.

Laboratory Measurements:

I_{CBO} failing at 168 hour

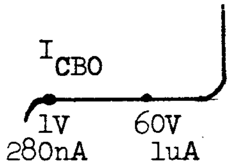

120V after tests

Collector breakdown high due to surface inversion.

After bake @ 300°C

102V

Inversion layer gone. Collector resistivity back to low resistivity N with resulting dec.in breakdown.

Prepared by: Alfred Poe
Failure Analysis Engineer

Date: 10/4/65

FAILURE ANALYSIS REPORT

Sheet 2 of Final

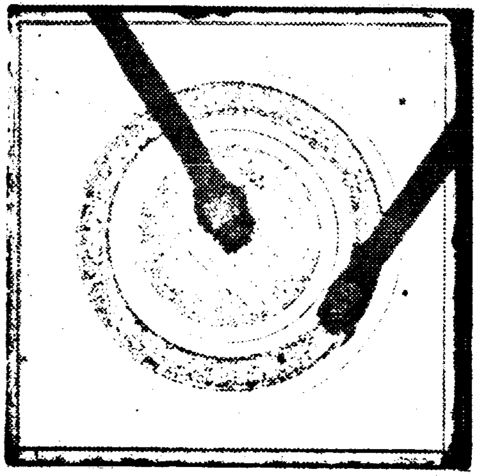

Visual inspection of pellet does not show any defect spot at or near the collector-base junction (see photo).

This unit failed due to presence of mobile ions in the oxide which could move in the 20V field of the life test.

FAILURE ANALYSIS REPORT

Sheet 1 of 3

Unit No.	Test Cell No.	Process	Failure Mode Category
A 353	419-204	A	C-7-b

Summary of Analysis: The cause of failure of this unit had been determined to be a degraded collector contact causing an increase in collector contact resistance. Unit failed for $V_{CE(SAT)}$ at the end of the 3000 hour life test.

$V_{CE(SAT)}$ increase is usually due to an increase in contact resistances, emitter or collector. Stability of $V_{BE(SAT)}$ indicates the collector contact is probably degraded.

Laboratory Measurements:

A series of measurements were made in which resistances of contacts are measured directly. Circuit for this measurement:

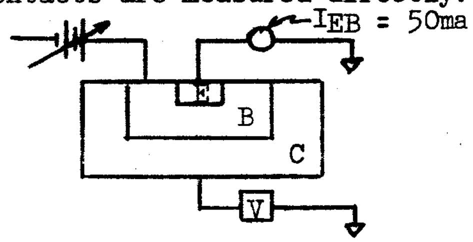

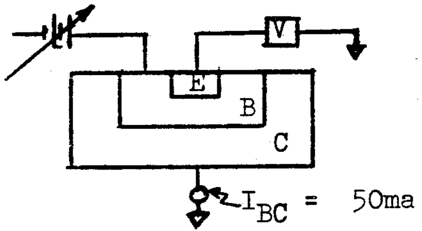

	$V_{CE(SAT)}$	R_{coll}	R_{emit}	$(I_E R_E + I_C R_C)$	Resistive Component to $V_{CE(SAT)}$
Receipt	1.2V	14.4 ohm	1.8 ohm	55(1.8) + 50(14.4)= .819 V	
After 300°C Bake	0.57V	2.1 ohm	1.5 ohm	55(1.5) + 50(2.1) = 113mV	

The resistive component results in a drop greater than 800mV being measured in the degraded device.

V_{CE} Reading in lab	1200mV	
Original reading	240mV	This is in same range as collector
ΔV_{CE} Increase	960mV	resistance increase.

Prepared by: Alfred Poe
Failure Analysis Engineer

Date: 9/16/65

FAILURE ANALYSIS REPORT

Sheet 2 of 3

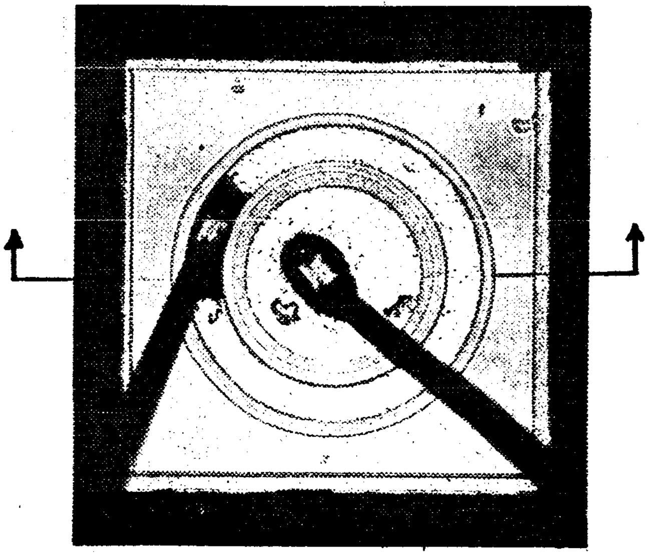

Photo 1

Unit developed a high $V_{CE(SAT)}$ after 3000 hours, 400mW, 150°C operation. Measurements indicated a 14 ohm resistance developed in the collector. Section was made through pellet as shown in photo 1 and photo 2.

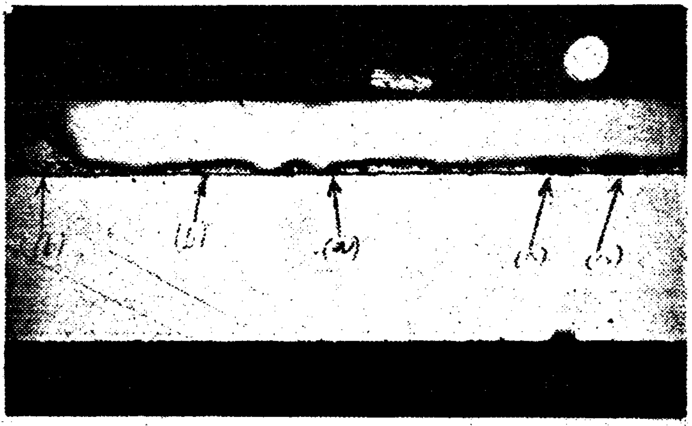

Photo 2 - Section

Voids are seen, although, not enough to explain a 14 ohm increase. The original wetting appears to be satisfactory, sufficient Au-Si eutectic. However, a thin hair line separation must be developing between eutectic and silicon. 300°C bake has 'healed' separation.

FAILURE ANALYSIS REPORT

Sheet 3 of Final

Section through collector contacts shows:

a. A few gas pockets - voids.
b. Adequate amount of silicon-gold eutectic soldering was performed initially.
c. High resistance is in a hairline separation between Si and eutectic due to:

    1. Slow chemical erosion of header salts and Si.
    2. High temperature acceleration at this area (power + high ambient).
    3. Possible Si-Ni eutectic embrittlement brought about by high temperature.

Conclusion:

Collector contact resistance increased due to thermal fatigue and cycling of Si, Si-Au eutectic interface. Interface weakened by long time high temperature deterioration in presence of entrapped plating salts.

FAILURE ANALYSIS REPORT

Sheet 1 of 6

Unit No.	Test Cell No.	Process	Failure Mode Category
A 419	419-204	A	A-2-b

Summary of Analysis: The cause of this failure has been determined to be degradation due to H_2O vapor pressure in the device, approximately 92 mm at 50°C. The failure indicator was an I_{CBO} degradation at the 1500 hour life test readout.

h_{FE} behavior:

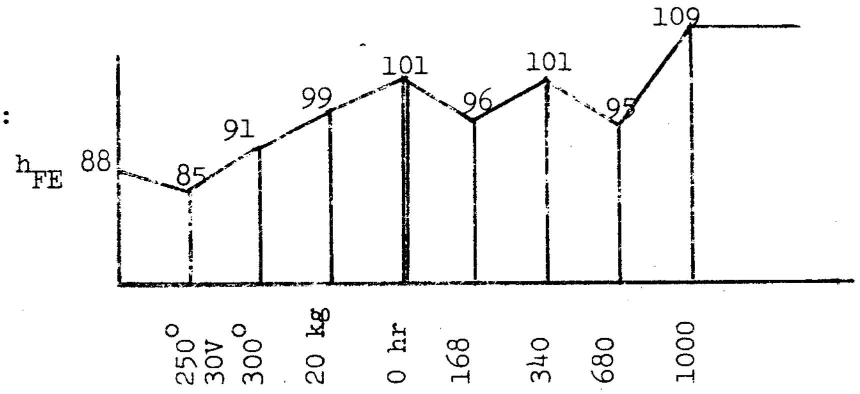

Note initial shifts after 300°C to 20kg and into power stress. No electrical stress was involved. Shift was possibly due to calibration error at 300°C measurement point. I_{CBO} was unstable at the 680 hour point.

Laboratory Measurements:

Indications of a conductive (ionic leakage) condition in device.

Prepared by: Alfred Poe
Failure Analysis Engineer

Date: 10/21/65

FAILURE ANALYSIS REPORT

Sheet 2 of 6

The following tests were performed to trace the presence of H_2O inside the transistor.

Initial Tests:

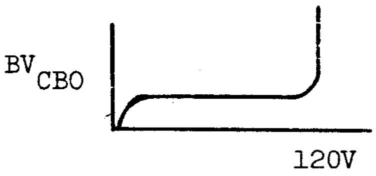

Curve tracer reverse leakage was very unstable. Mobile surface charges were characteristic of wet surfaces, cracks or extremely contaminated surfaces.

Leakage and Floating Emitter Potentials:

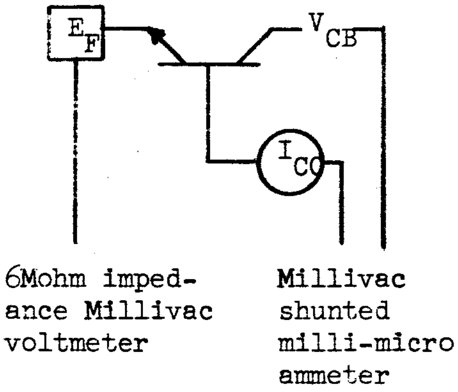

V_{CB}	I_{CO}	E_F
0	-0.9na	4.0mV
1	2.5na	2.0mV
10	14.0na	100 mV
20	16.0na	1.7 V

Current and voltage indication with 0 V_{CB} indicated galvanic action inside transistor, which was an indication of liquid on metal parts. High floating emitter response again indicated H_2O or cracks.

Hermeticity Tests:

Hermeticity Tests were performed to determine if H_2O leaked in from outside. The results were as follows:

(1)	Radiflo 10^{-9}cc/sec	No leak
(2)	4 hour laboratory boil test	Showed no change in parameters.

FAILURE ANALYSIS REPORT

Sheet 3 of 6

Dewpoint Test: This test was performed to check the level of H_2O contamination. The graphs of I_{CBO} versus temperature (0 to 70°C) were prepared during the analysis. The graphs show that the low point of the leakage current occurred at 50°C which represented the elimination of the H_2O component of the leakage current.

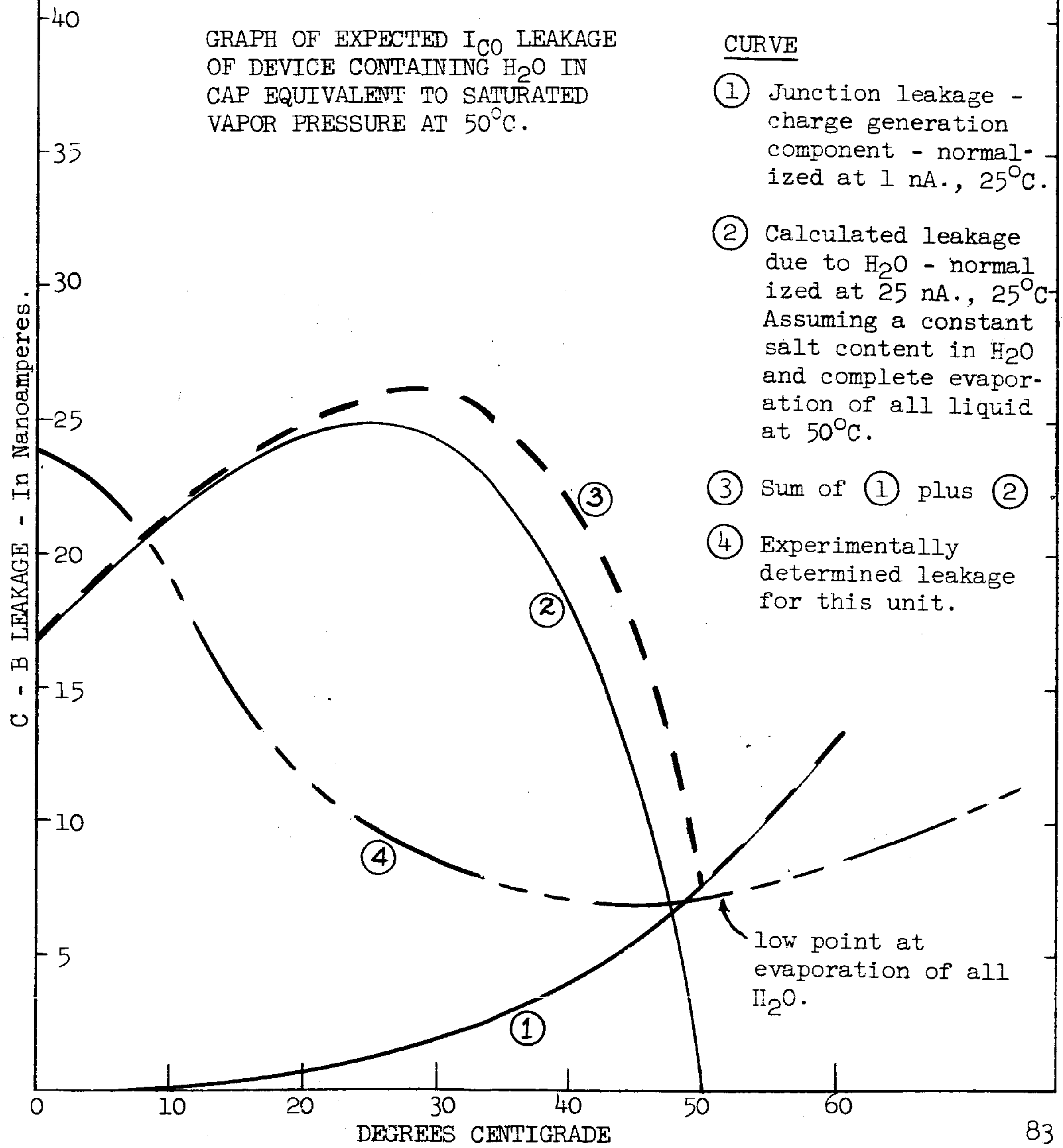

FAILURE ANALYSIS REPORT

Sheet 4 of 6

I_{CBO} behavior with H_2O:

I_{CBO} is made up of at least two components. It was assumed that no channel current component was present since channels were dispersed by the wet condition without a voltage stress.

a) The first component is from charge generation of carriers in the depletion layer, the normal junction reverse current which increases exponentially according to the equation.

$$I_{cg} = KT^{3/2} \; e^{-EG/2kT} \quad \text{(Ref. 1)}$$

K is a constant
T is °Kelvin
E_G = 1.21 ev
S_i = band gap energy
k = Boltzman's constant 8.63 x10 $^{-5}$ ev/^oK

Curve 1 shows a normalized plot of I_{cg} vsT - a typical charge generation starting with a value of 1na @ 25°C.

b) The second component is from conduction through layers of condensed H_2O. This will contribute a large leakage component if the H_2O has condensed on a critical surface such as the glass beads of the header and if any salts are present (most likely even on cleanest parts). If it is assumed from the low point in the Dew point test that all the H_2O has evaporated at 50°C, it is possible to estimate how much condensation takes place at lower temperatures. If conductivity of the solution, or condensed H_2O, would remain constant with temperature the conductance or leakage through the H_2O would be directly proportional to the amount of H_2O condensed. The amount of H_2O condensed is estimated as the saturated vapor pressure @ 50°C minus the vapor pressure at any lower temperature. Thus, H_2O cond. = 92.5 mm - vp_T.

However, H_2O conductivity falls very rapidly with decreasing temperature so that the decreasing temperature, while causing more H_2O to be deposited, is being compensated by the decreasing equivalent conduction of the H_2O.

Thus, a figure of merit for the level of H_2O leakage component = Quantity H_2O condensed x conductivity = $(92.5 - vp_T) \times L$

FAILURE ANALYSIS REPORT

Sheet 5 of 6

In the following calculation, conductivity (L) is estimated as follows:

A 1 ppm solution of NaCl is assumed to be formed by the condensed liquid. 1 ppm of NaCl is a concentration of 1.71 x 10^{-2} milli equivalent/liter - the constant factor to be multiplied by Λ, the equivalent NaCl conductance at any temperature, to give umho/cm (L_{NaCl}) the conductance of the NaCl ions directly. Total conductance L is the sum of the NaCl and H_2O ion conductances. Total $L_T = 1.71 (10^{-2}) (\Lambda) + L_{H_2O}$ (at any temperature).

Temp °C	mm sat vp H_2O Ref.2	H_2O condensed = (92.5-vp)	L_{H_2O} μmho/cm Ref.3	Λ cm² mho/g equiv Ref.4	L_{NaCl} umho/cm .0172	L solution = L_{NaCl} L_{H_2O} μmho/cm	Leakage I_{H_2O} = L x(H_2O condensed)
0	4.57	87.9mm	.012	67	1.15	1.16	102
10	9.2	83.3	.0227	90	1.54	1.56	130
15	12.8	79.7	.031	102	1.75	1.78	142
20	17.5	75	.0435	113.8	1.94	1.98	148
25	23.7	68.8	.055	126.4	2.17	2.22	153
30	31.8	60.7	.077	140	2.4	2.47	150
35	42.1	50.4	.091	153	2.62	2.71	136
40	55.3	37.2	.111	168	2.88	2.99	111.0
45	71.9	20.6	.142	183	3.14	3.28	67.6
50	92.5	0	.18	198	3.38	3.56	0

The last column is then normalized at a leakage value of 25na @ 25°C for plotting as Curve 2.

Ref. 1: A. B. Phillips Transistor Engineering pg. 132 McGraw Hill.

Ref. 2: Handbook Phys. & Chem.

Ref. 3: Conductivity of Pure H_2O - Mixed Bed Deionization of H_2O - Monet Chem. Eng. Progress Vol. 52 #7, Pg. 301.

Ref. 4: Equivalent conductance of Na Cl from Handbook of Phys. & Chem., Pg. 2357 - Calculated from ion conductances.

The plot of this expected leakage, last column and Curve (2), vs. temperature gives a peak value at about 25°C. A difference between the experimental curve (4) and the theoretical curve expected from the sum of H_2O leakage + I_{cg} Curve (3), can be compensated for if a constant salt concentration (1ppm) is not assumed, but the interaction of different concentrations in different areas is assumed. In practice, low temperature condensation must be more complete than that above 25°C, thus raising conduction (L) at lower temperatures.

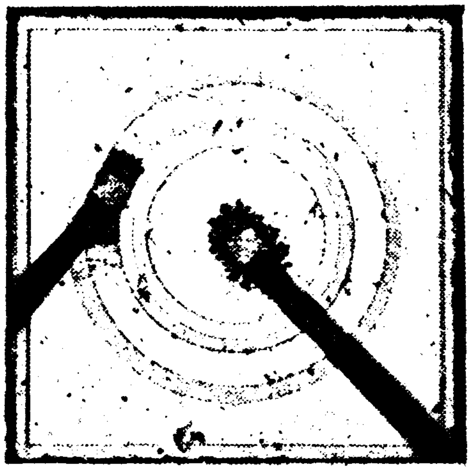

Further Confirming Observations:

Following dew point tests the device was decapped. The cap was found to be oxidized, again confirming the presence of oxidizing gases, such as H_2O. H_2O ordinarily will oxidize nickel very slowly. This unit, however, had undergone many hours of high temperature stressing.

FAILURE ANALYSIS REPORT

Sheet 1 of 2

Unit No.	Test Cell No.	Process	Failure Mode Category
A 528	419-201	A	Faulty Processing

Summary of Analysis: The cause of failure was a bulk degradation. The failure indicator was I_{EBO} degradation after the initial step of stress screen.

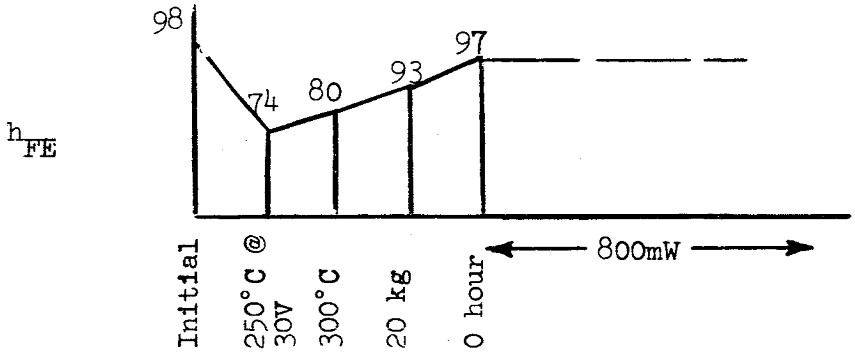

Data Indication:

I_{EBO} degraded after the first step stress. Although h_{FE} shows a severe drop after the 250°C - 30V stress, BV_{CEO} does not show any corresponding increase. Thus, the failure does not tie in with a real surface degradation of the emitter junction. In subsequent tests, h_{FE} recovered while the I_{EBO} failure still persists, indicating the probability of a bulk leakage characteristic.

Lab measurements show this condition also. A persistent bulk degradation condition appears to be indicated. Surface recombination (h_{FE}) is not degraded, but 5V I_{EBO} condition is increased.

Prepared by: Alfred Poe
Failure Analysis Engineer

Date: 9/17/65

FAILURE ANALYSIS REPORT

Sheet 2 of Final

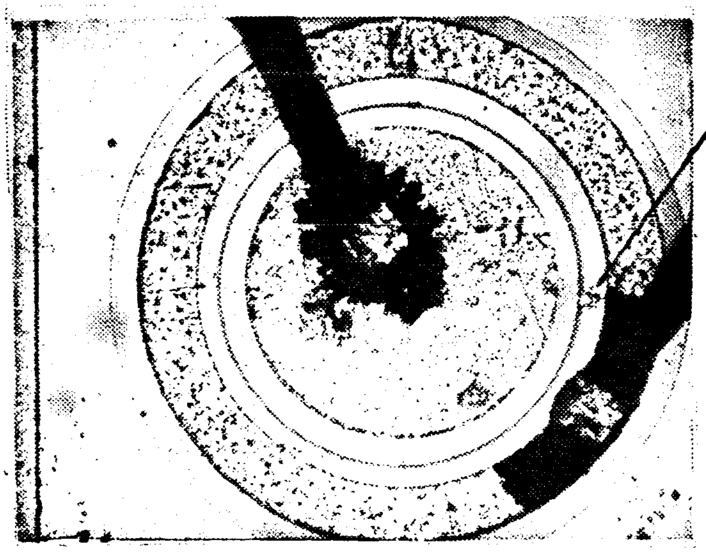

Bridge from manufacturing process. Leakage developed through thin emitter oxide.

Decapping:

See photo. Bulk degradation is an aluminum bridge extending from base ring to EB junction. High I_{EBO} leakage is through the emitter oxide. The bridge is not a gold alloy and is not under the oxide. A 10% KOH rinse was able to completely dissolve the bridge. Leakage developed by a metallic diffusion mechanism at high temperature through the thin emitter oxide.

Conclusion:

Definite failure would be screened out by second step stress. Noise at 100 kc is very low (in the 5th percentile) on initial test but became average during the test.

FAILURE ANALYSIS REPORT

Sheet 1 of 3

Unit No.	Test Cell No.	Process	Failure Mode Category
A 557	419-203	A	B-2-a

Summary of Analysis: The cause of this failure has been determined to be an emitter-base short. The failure indicator was an h_{FE} degradation at the 1000 hour life test readout.

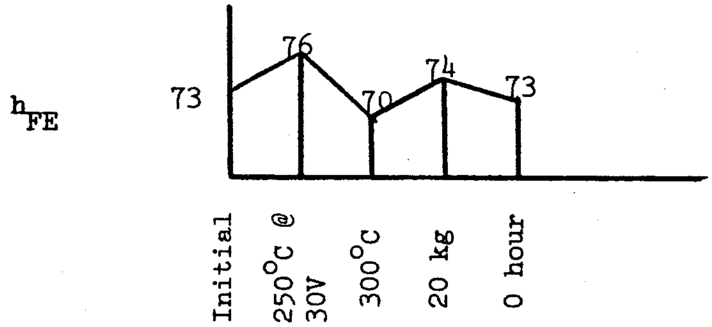

Data indicates h_{FE} failure at 1000 hours, 500mW life test.

Test Data (I_{EBO}): Indicates a dead short, 2 ohms.

Decap:

A gold bridge has been blased from the base bond into the emitter-base junction (see photos). This is usually due to a runaway condition. In this case, oxide chips are seen in this area (see photo 1).

Photo 1.

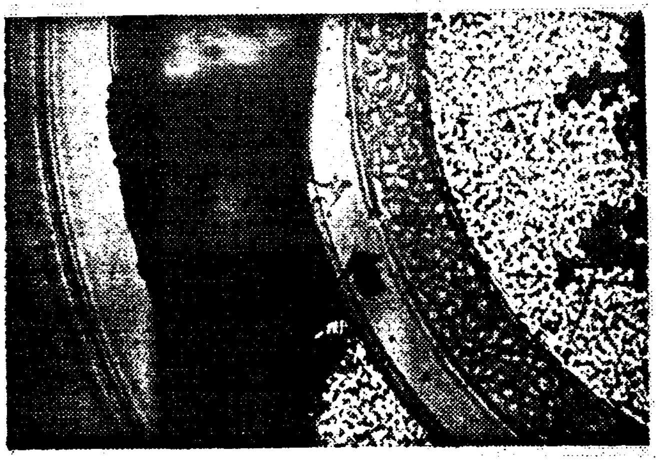

Prepared by: Alfred Poe
Failure Analysis Engineer

Date: 9/3/65

FAILURE ANALYSIS REPORT

Sheet 2 of 3

Photo 1:

Base bond area after test. Note gold bridge (see arrow) causing emitter-base short and an apparent oxide defect above it. The gold bridge did not initiate in the chipped section.

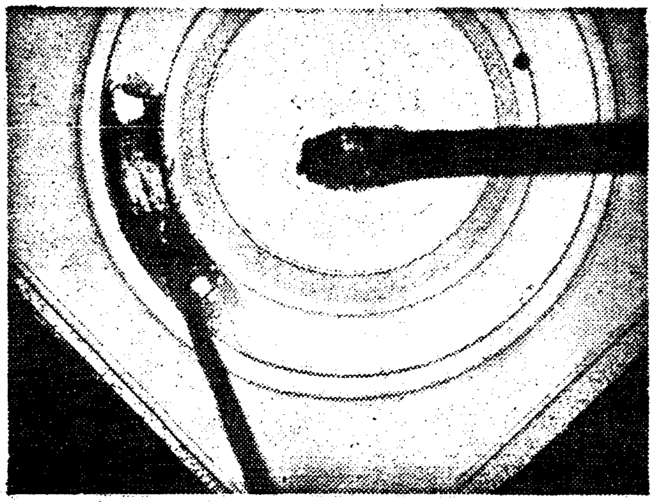

Photo 2

Etching:

Photos 2 and 3 show extensive chipping from TCB operation. Removal of metal shows cracks have propagated into the Silicon. Source of h_{FE} degradation and eventual short is this area of cracked and strained Silicon. Photo 2 shows intermediate etch operation. Selective etching of base wire in KCN - KOH solution 3 volts (+) on base.

Smaller darker area is area of original bond.

Boundary of Au-Al intermetallic growth

Gold bridge under oxide (a runaway)

Photo 3 - Etch completed

FAILURE ANALYSIS REPORT

Sheet 3 of Final

Photo 3:

Complete removal of metal in base bond area is shown. Short has appeared in this area in which a number of oxide chips have been identified growing out of the bond operation.

Conclusions:

Emitter-base shorts on life tests are caused by transients or by increases in I_E which will set up a reverse bias on the emitter-base junction. It is assumed in this case, that emitter-base runaway was accelerated or occurred at an earlier voltage than would have been the case for a device with no strains caused by the bond operation.

FAILURE ANALYSIS REPORT

Sheet 1 of 2

Unit No.	**Test Cell No.**	**Process**	**Failure Mode Category**
B 305	419-232	B	B-3-a

Summary of Analysis: Failure was caused by a bulk alloy degradation which resulted in an I_{EBO} failure at the 1500 hour point of the life test.

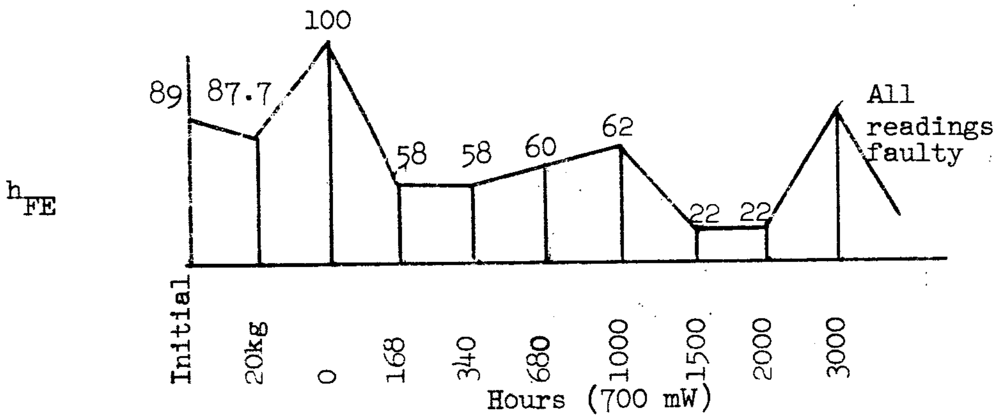

Test Data Indications

All readings at 3000 hour appear to be faulty. Unexplainable h_{FE} increase at 0 hour - no correlation with BV_{CEO}. Degradation at 168 hour. Data correlates BV_{CEO} increase and h_{FE} down severely. I_{EBO} not degraded until 1500 hour. V_{SAT} degraded at 2000 and 3000 hour readout.

Failure Analysis Laboratory Investigation:

I_{EBO} measures as severely degraded. A bakeout at 300°C, decapping and repeat baking did not change I_{EBO}. A bulk alloy type degradation was indicated. This must have started at 168 hours and progressed throughout the 700mW test.

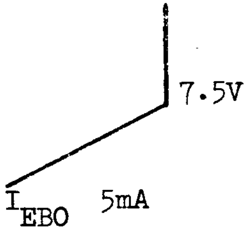

Prepared by: Alfred Poe
Failure Analysis Engineer

Date: 10/6/65

FAILURE ANALYSIS REPORT

Sheet 2 of Final

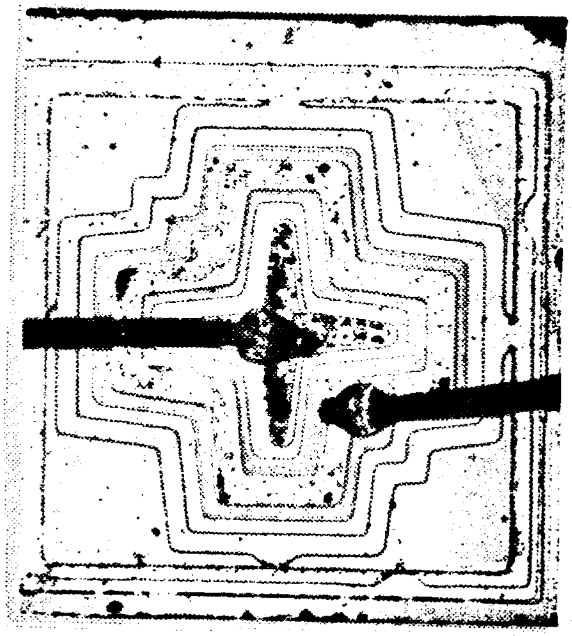

Photo shows emitter region has been operating at a very much higher temperature than the base. The aluminum is completely eroded off by chemical oxidation or by thermal operation at temperatures greater than 550°C. Destruction of aluminum is partially responsible for V_{SAT} increase.

FAILURE ANALYSIS REPORT

Sheet 1 of 2

Unit No.	Test Cell No.	Process	Failure Mode Category
B 354	419-233	B	E-8-b

Summary of Analysis: Failure was caused by an embedded conductive filament from collector to base. The failure was indicated as an I_{CBO} failure at the 168 hour readout on life test.

Test Data:

Data indicated the existence of a collector-base short of about 3 megohms. BV_{CEO} equals approximately 7V at 100 μa due to the intense emitter forward bias effect of the collector-base resistance. h_{FE} is slightly increased at 20 ma I_C and 5V. An increase of 100 μa at the 20 ma level is barely detectible.

Failure Analysis Laboratory Investigation:

Lab measurement indicated no failure, not short in any respect. The unit was decapped. Investigation and measurements could not locate any intermittence or faulty placement of wires which could intermittently short to case or pellet. Wires were spaced away from the pellet and case. H_2O tests on pellet showed it to be extremely stable in I_{CBO}, h_{FE} and other parameters. Pellet instability due to surface sensitivity is therefore unlikely.

Pellet inspection and etching (see photos on sheet 2) finally showed the problem to be a filament of conductive material firmly imbedded in the aluminum base and shorting into the pellet edge.

Prepared by: Alfred Poe
Failure Analysis Engineer

Date: 8/25/65

FAILURE ANALYSIS REPORT

Sheet 2 of Final

Pellet data indicated short. Lab electrical tests showed all parameters stable, low leakage and pellet very stable to H_2O vapor and electrical stressing. Wires were all well placed and could not have intermittently shorted. Note the filament resting to the left of the emitter wire approximately 0.15 mil wide and running from collector edge to base.

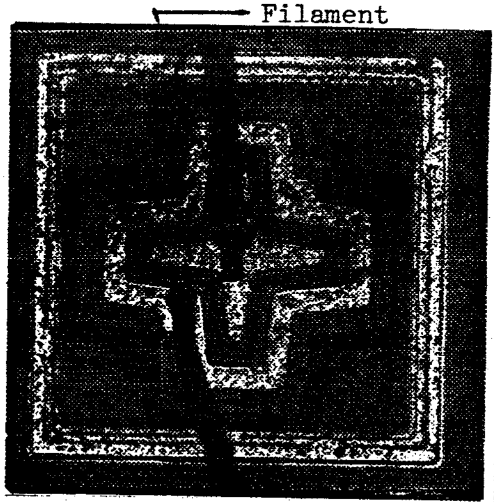

Pellet was washed in solvents, H_2O, filament still intact. Following a 10% NaOH - 30 sec. etch, filament is seen to have moved toward the right. The lower edge is still intact contacting the base ring area. It is evident how a 3 megohm short developed from C to B. The filament appears to have been an organic fiber which carbonized in power testing and became conductive.

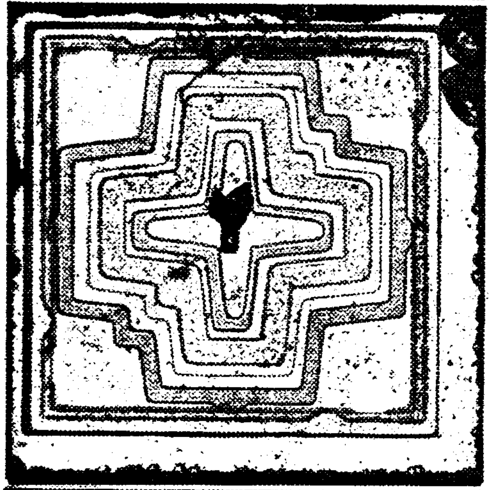

To further identify material of filament, HCL, H_2SO_4, HNO_3 solutions were used to clean surface. All failed to remove the filament. Finally a dilute HF wash lifted it off and left a clean undamaged oxide structure under it. Filament is probably organic, cellulose lint, from chemical reactions and appearance.

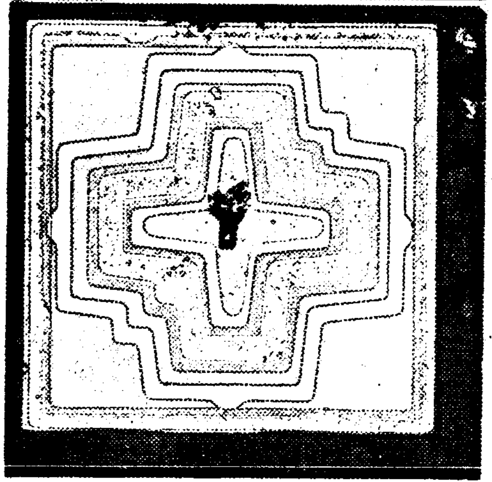

FAILURE ANALYSIS REPORT

Sheet 1 of 2

Unit No.	Test Cell No.	Process	Failure Mode Category
B 359	419-222	B	A-1-a

Summary of Analysis: The failure indicator was an h_{FE} and BV_{CEO} degradation at the 680 hour life test readout.

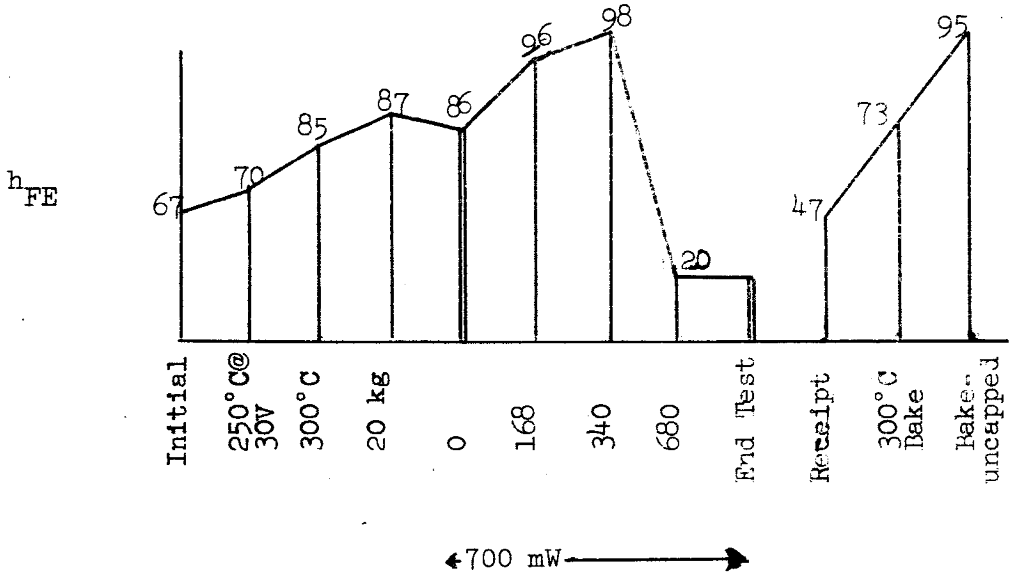

Data shows h_{FE} degradation at 680 hours after previous history of improving.

Laboratory Investigation:

Confirmed degraded h_{FE}

	h_{FE}		
	100 ua	20 na I_C	BV_{CEO}
h_{FE} on receipt	2	47	120V
After 300°C, 20 hour bake	8.2	73	95V
After decap and bake	14.5	95	90V

Unit is showing steady improvement in h_{FE} in laboratory measurements.

Prepared by: Alfred Poe
Failure Analysis Engineer

Date: 9/30/65

FAILURE ANALYSIS REPORT

Sheet 2 of Final

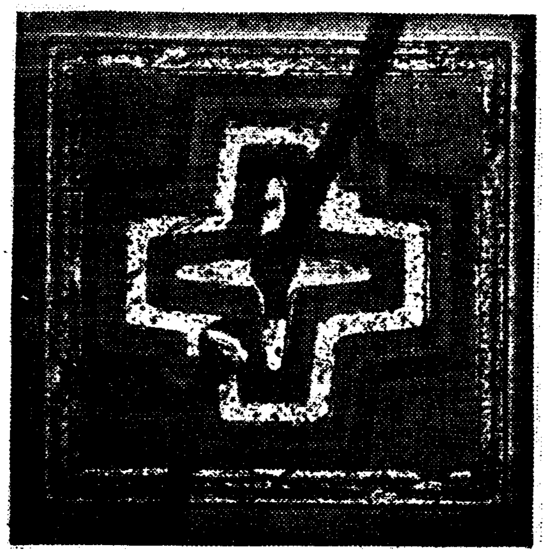

Visual inspection of pellet shows normal appearance.

FAILURE ANALYSIS REPORT

Sheet 1 of 2

Unit No.	Test Cell No.	Process	Failure Mode Category
B 446	419-231	B	D-1-a

Summary of Analysis: The cause of this failure has been determined to be base lead opening at the 2000 hour readout of the life test. The failure indicator was an h_{FE} degradation.

Test Data:

At Step 5 - high h_{FE} reading is inconsistent and probably incorrect. Data after Step 11 is consistent and indicates an open base at 2000 hour readout. I_{CO} readings are equipment leakage, h_{FE} reading 20 is an automatic indication of unit with no h_{FE}. $V_{(SATS)}$ are not readable. BV_{CEO} not involving base still reads.

Failure Analysis Laboratory Investigation:

Decapping shows a poor bond had been made on the base post. Very little intermetallic formation is in evidence at all three bond marks. No real contact had been made to gold. Probably due to contamination on post or oxide on aluminum. (See photos)

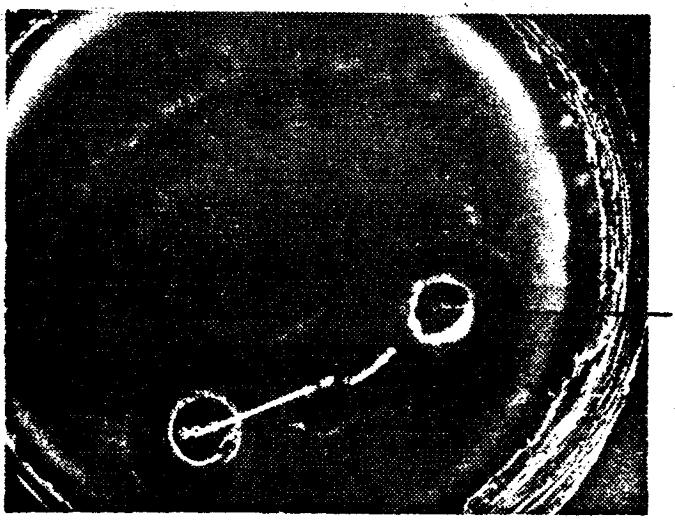

Photo 1

Prepared by: Alfred Poe
Failure Analysis Engineer

Date: 8/27/65

FAILURE ANALYSIS REPORT

Sheet 2 of Final

Base post with pressure points from wire bonding showing. Lack of intermetallic formations indicates poor initial contact had been made.

Photo 2

Enlarged photo of emitter post. Aluminum emitter wire still bonded to gold plated post. Note no Au-Al intermetallic is in evidence.

Photo 3

FAILURE ANALYSIS REPORT

Sheet 1 of Final

Unit No.	**Test Cell No.**	**Process**	**Failure Mode Category**
B 450	419-222	B	Not a failure

Summary of Analysis: This device failed because the external emitter lead broke off. The device was not otherwise damaged.

Collector-Base parameters were satisfactory. (BV_{CBO} = 122V, I_{CO} @ 60V = 1na).

The failure was determined to be metal fatigue.

Prepared by: Alfred Poe
Failure Analysis Engineer

Date: 8/27/65

FAILURE ANALYSIS REPORT

Sheet 1 of 2

Unit No.	Test Cell No.	Process	Failure Mode Category
B 515	419-227	B	D-1-a

Summary of Analysis: The cause of this failure has been determined to be a high resistance (Gold post - Aluminum wire) contact at emitter. The failure indicator was an intermittent h_{FE} and V_{SAT} condition.

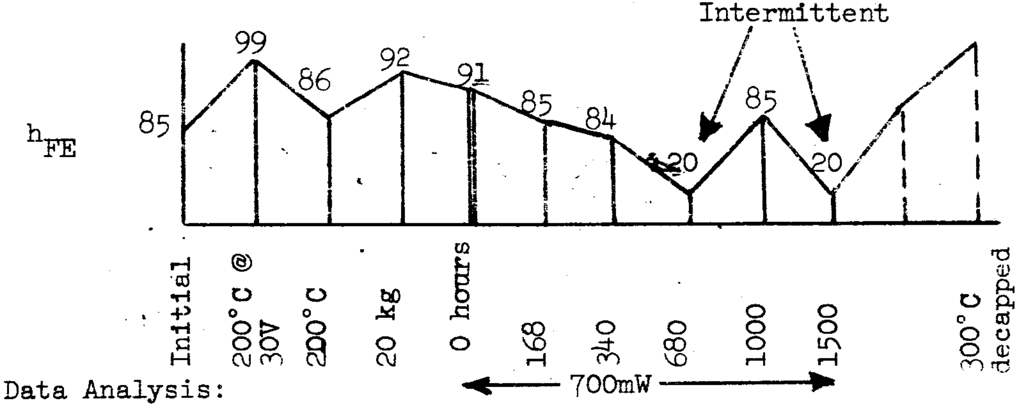

Test Data Analysis:

Indication of an intermittent condition leading to catastrophic performance was seen after the 700mW stress at the 680 hour readout. At this time, indication of a shorted collector to emitter is observed but no I_{CBO}. At the 1000 hour readout, the unit appears to recover. After 20 kg centrifuge, the collector to emitter appears to be open. V_{SAT} data indicates an increase in contact resistance.

Laboratory measurements:

Unit was baked for 16 hours at 300°C to determine h_{FE} behavior. Emitter post contact opened completely under this stress. h_{FE} increased from its slightly degraded value by re-establishing emitter contact with a probe. The cause of intermittence was determined to be a poor emitter post contact.

Prepared by: Alfred Poe
Failure Analysis Engineer

Date: 9/3/65

FAILURE ANALYSIS REPORT

Sheet 2 of Final

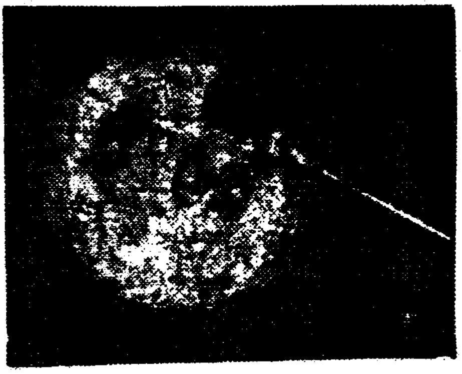

Photo of Emitter Post & Bond.

FAILURE ANALYSIS REPORT

Sheet 1 of 2

Unit No.	Test Cell No.	Process	Failure Mode Category
B 541	419-231	B	A-1-a, E-2-a

Summary of Analysis: Failure was caused by a hermetic seal leak and was indicated by a steadily increasing h_{FE} on life test.

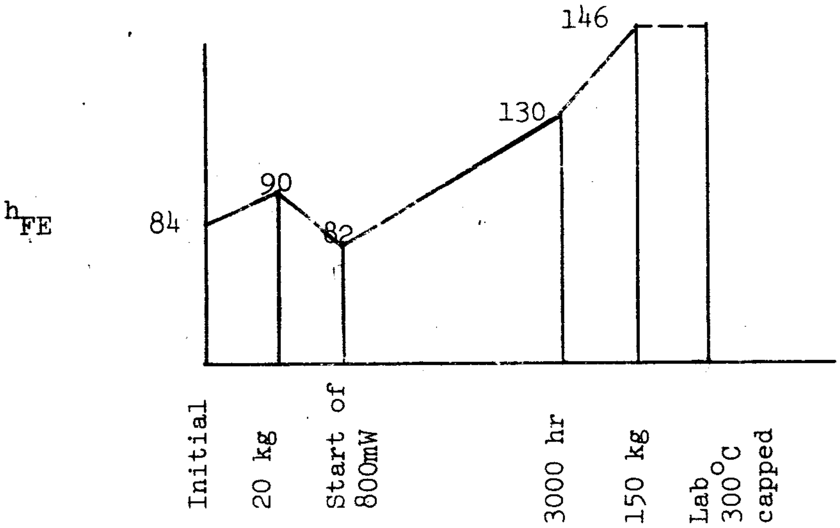

Data:

Data indicates a steady increase in h_{FE}. Increasing h_{FE} in a device frequently is indicative of operation under an oxygen or air ambient, ie, a hermetic leaker will frequently indicate this behavior.

Hermetic Tests:

Step 1. 4 hour boil in H_2O. Floating E potential and I_{CBO} response gave a positive indication of leak.

Step 2. HCL rinse to remove surface salts. Unit further degraded. Indication of HCl trapped in deep pore.

Step 3. Visual inspection shows glass cracked at emitter.

Prepared by: Alfred Poe
Failure Analysis Engineer

Date: 9/14/65

FAILURE ANALYSIS REPORT

Sheet 2 of Final

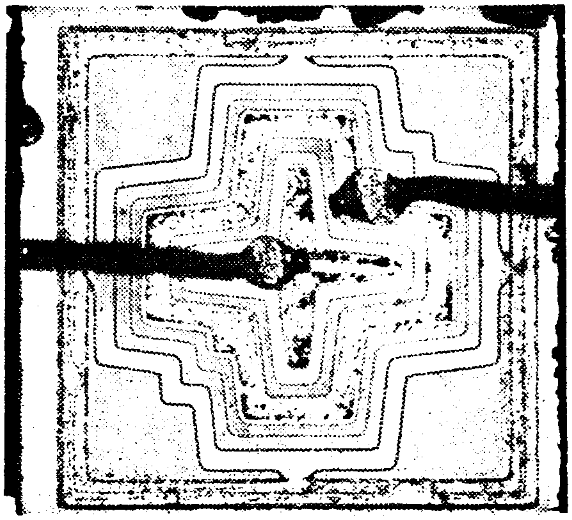

Photo 1

Step 4. Decap (see photo 1). Shows cap oxidized confirming leak. Pellet has not been damaged visually by exposure to ambient.

E_F readings and visual inspection indicate h_{FE} increase caused by leak in glass bead.

FAILURE ANALYSIS REPORT

Sheet 1 of 2

Unit No.	Test Cell No.	Process	Failure Mode Category
B 543	419-222	B	A-1-a

Summary of Analysis: Failure was caused by a surface change in the base, indicated as h_{FE} failure at the 2000 hour readout on life test.

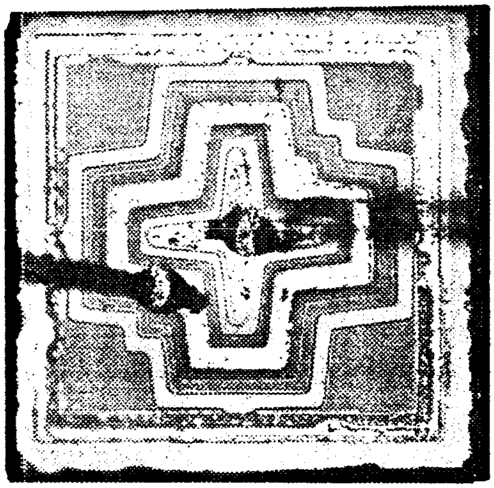

Data indicated severe h_{FE} degradation at 3000 hour. h_{FE} below readable level of 20.

Failure Analysis Laboratory investigation:

Test data indicated severe h_{FE} degradation. Laboratory tests confirmed h_{FE} degradation.

		$@I_C=100\mu A$	
	$h_{FE}@I_C=100\mu A$	BV_{CEO}	BV_{CBO}
As received	3.6	120	122
After 300°C bake	20.0	105	110
After 300°C repeat bake-uncapped	22.7	90	115

Prepared by: Alfred Poe
Failure Analysis Engineer

Date: 9/13/65

FAILURE ANALYSIS REPORT

Sheet 2 of 2

The h_{FE} degradation under high power represents a surface change in the base, toward N potential. The laboratory bakes represent surface potential changes back to the original condition. h_{FE} in air recovers more effectively than h_{FE} in cap. Breakdown voltages also follow the h_{FE} recovery and redistribution of charges on the collecto surface.

FAILURE ANALYSIS REPORT

Sheet 1 of 2

Unit No.	Test Cell No.	Process	Failure Mode Category
C 61	419-247	C	Not a failure

Summary of Analysis: Analysis of test and laboratory data indicates that this unit did not fail. The test readout (680 hour, 400mW @ 150°C) was obviously in error.

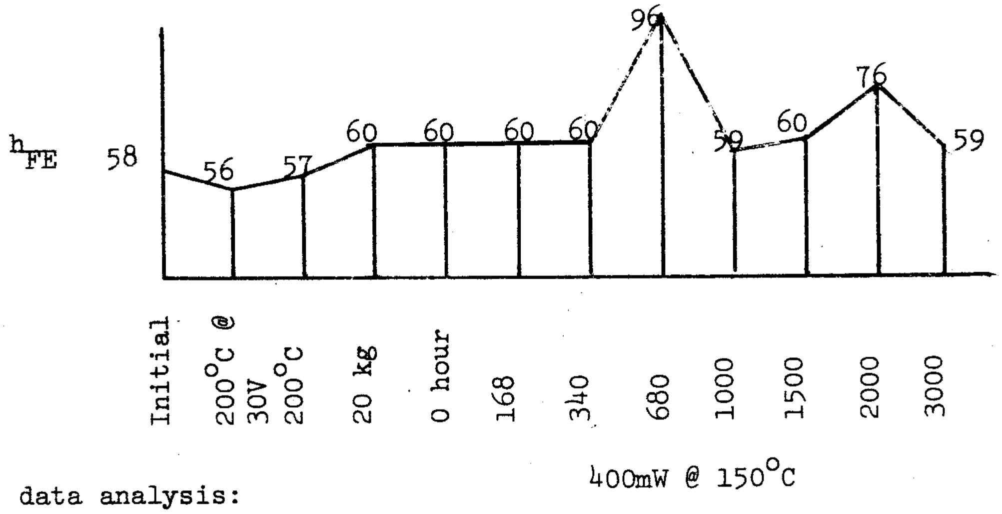

Test data analysis:

The only serious deviation from consistent data was the 680 hour readout. The following readouts of the same test stress were normal.

The 680 hour readout data was:

		Normal
I_{CBO}	297 na	less than 1 na
BV_{CEO}	63 V	110 V
h_{FE} @ 20 ma	96.6	59
$V_{CE(sat)}$	.097 V	.116 V

Prepared by: Alfred Poe
Failure Analysis Engineer

Date: 10/14/65

FAILURE ANALYSIS REPORT

Sheet 2 of Final

A drop in $V_{CE(sat)}$ of this magnitude is virtually impossible unless the unit is shorted from collector to emitter. An increase in h_{FE}, as indicated, goes along with a decrease in BV_{CEO} and again would go along with a collector - emitter increase in conductance, but by a much higher resistance.

For example:

For the ΔBV_{CEO} $R_{CE} = \frac{63V}{.1ma} = 630{,}000$ ohms

For Δh_{FE}

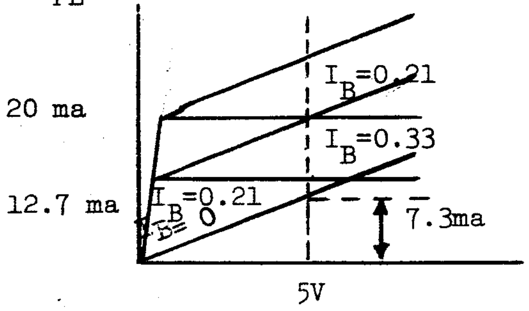

I_B = .21ma @ h_{FE} = 96
I_B = .33ma @ h_{FE} = 60
I_B = 0

Note: At 0 V_{CB}, base lines V_{CB} coincide for collector to emitter short.

The different I_B readings represent a shift in base line due to a collector to emitter short approximately equal to

$$R_{CE} = \frac{5.0V}{7.3ma} = 685 \text{ ohms}$$

The calculated R_{CE} shorts for the Δh_{FE} and ΔBV_{CEO} do not coincide. Therefore the 680 hour readings must be assumed to be erroneous.

FAILURE ANALYSIS REPORT

Sheet 1 of 2

Unit No.	**Test Cell No.**	**Process**	**Failure Mode Category**
C 98	419-247	C	B-2-a

Summary of Analysis: The cause of this failure has been determined to be a cracked junction under the intermetallic formations of the bonds. The failure indicator was an I_{CBO} degradation at the 680 hour readout on life test.

Laboratory Analysis:

All electrical data in laboratory indicates a cracked junction, through the emitter. This includes:

1. degraded h_{FE} at low currents
2. unstable emitter-base reverse characteristic
3. unstable I_{CBO} and I_{CES} reverse characteristic and I_{CES} not coinciding with I_{CBO}

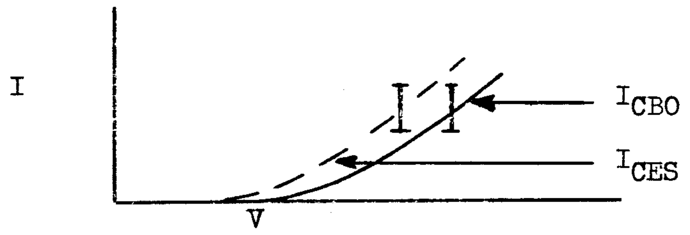

Readings confirmed on decapped, baked unit. High leakage was not caused by H_2O across glass beads of header. This was confirmed by disconnecting the emitter wire - E_F disappeared.

Prepared by: Alfred Poe
Failure Analysis Engineer

Date: 9/28/65

FAILURE ANALYSIS REPORT

Sheet 2 of Final

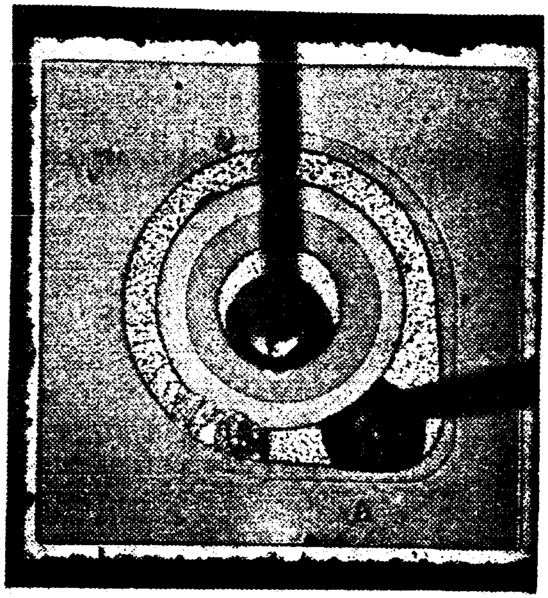

FAILURE ANALYSIS REPORT

Sheet 1 of 3

Unit No. C 147	**Test Cell No.** 410-246	**Process** C	**Failure Mode Category** Did not fail in Lift Test B-2-a in Lab Tests

Summary of Analysis: The cause of degradation in lab tests has been determined to be a crack which developed near the periphery of the gold-aluminum base bond intermetallic, apparently from differential expansions and contractions of the intermetallic and silicon beneath it.

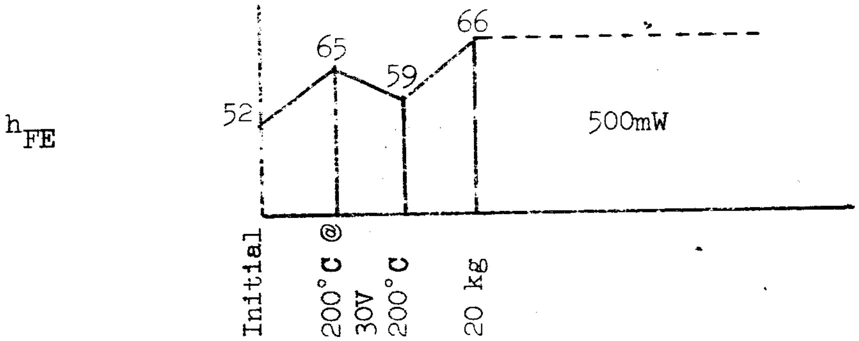

Test data analysis:

Data indicated small shifts in h_{FE} at 200°C @30V and 20 kg levels. Centrifuge should have no effect on h_{FE}. $V_{BE(sat)}$ readings are within the emitter specification of 15 - 25% shift.

Laboratory measurements:

h_{FE}: Emitter junction stable throughout laboratory tests. No indication of cracks.

I_{CBO} stable in bakeout at 300°C. Unit was decapped. In air bake, the unit was very unstable.

Etching off leads and contact showed a small crack in base, not in emitter. (see photos)

Prepared by: Alfred Poe
Failure Analysis Engineer

Date: 10/28/65

FAILURE ANALYSIS REPORT

Sheet 2 of 3

Conclusions:

Unit did not really degrade in life tests. Laboratory tests in uncapped condition rather than in capped ambient failed unit because of crack in junction area.

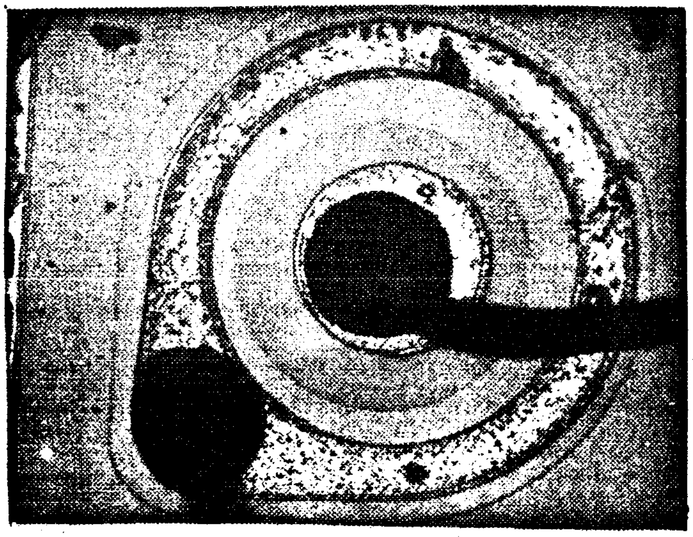

Unit did not show a degraded I_{CBO} in life tests. Some shift in h_{FE} was due to surface potential changes. At the 200°C @ 30V stress, h_{FE} increased 12.5%. This was within limits. In laboratory tests, severe degradation and I_{CBO} instability was seen after 300°C bake in air.

FAILURE ANALYSIS REPORT

Sheet 3 of Final

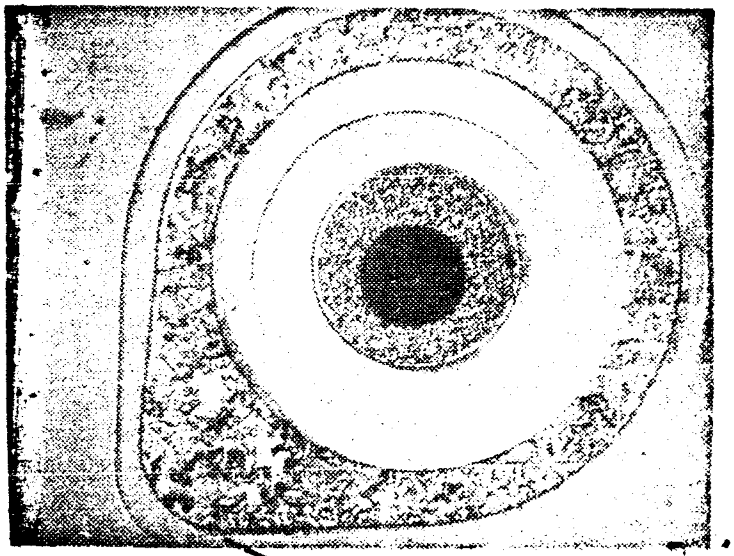

Etching in KOH and KCN to remove contact metals. A small knob of gold is still present in emitter contact area. Pitting indicates deep alloying of aluminum to silicon.

Note small crack just under base contact bond. This was responsible for I_{CBO} degradation. No cracks were seen in the emitter.

Discussion of results:

This device was stable under life tests performed at 200°C or less. In laboratory, the device was heated to 300°C and then showed the severe degradation indicated by devices from process C. The characteristics were very unstable indicating cracks in junctions.

Etching showed the crack developed near the periphery of the gold-aluminum intermetallic apparently from differential expansions and contractions of the intermetallic and silicon beneath it.

FAILURE ANALYSIS REPORT

Sheet 1 of 2

Unit No.	**Test Cell No.**	**Process**	**Failure Mode Category**
C 182	419-256	C	A-5-a

Summary of Analysis: The cause of this failure has been determined to be the effect of a 'microplasma site' in the collector-base junction. The failure was indicated as a BV_{CEO} shift at the 340 hour readout of the life test.

Test Data Analysis:

Increase in BV_{CEO} was seen in data during life test.

Laboratory Measurements:

Unit had a very low breakdown due to a microplasma type characteristic. BV_{CEO} 'snapped in' at this same artifically low breakdown voltage. It is normal for BV_{CBO} to vary by as much as 10V in life tests due to minor surface potential changes. In this case, BV_{CEO} followed these minor changes directly. BV_{CEO} was not increasing as a result of gain degradation which is the usual mechanism for BV_{CEO} shifting.

Bakeout at 300°C moved BV_{CBO} from 78V to 63V. As in the life test, BV_{CEO} followed this move in BV_{CBO}.

Visual inspection clearly showed a "microplasma site". A severe dislocation seen in the collector-base junction completely distorted the diffusion pattern. Small changes in surface potential at this site caused appreciable changes in the avalanche voltage.

Prepared by: Alfred Poe
Failure Analysis Engineer

Date: 10/6/65

FAILURE ANALYSIS REPORT

Sheet 2 of Final

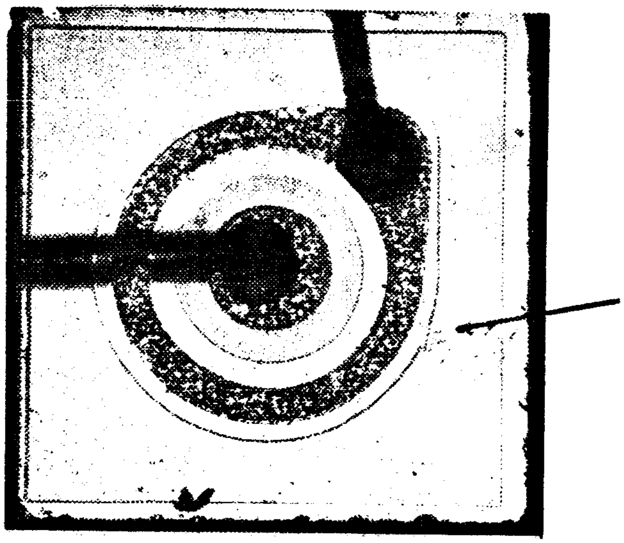

Junction defect causing microplasma like degradation in breakdown.

FAILURE ANALYSIS REPORT

Sheet 1 of 2

Unit No.	**Test Cell No.**	**Process**	**Failure Mode Category**
C 233	419-246	C	B-2-a

Summary of Analysis: The cause of this failure has been determined to be a crack in the collector-base junction. The failure indicator was an I_{CBO} degradation at the 168 hour life test readout.

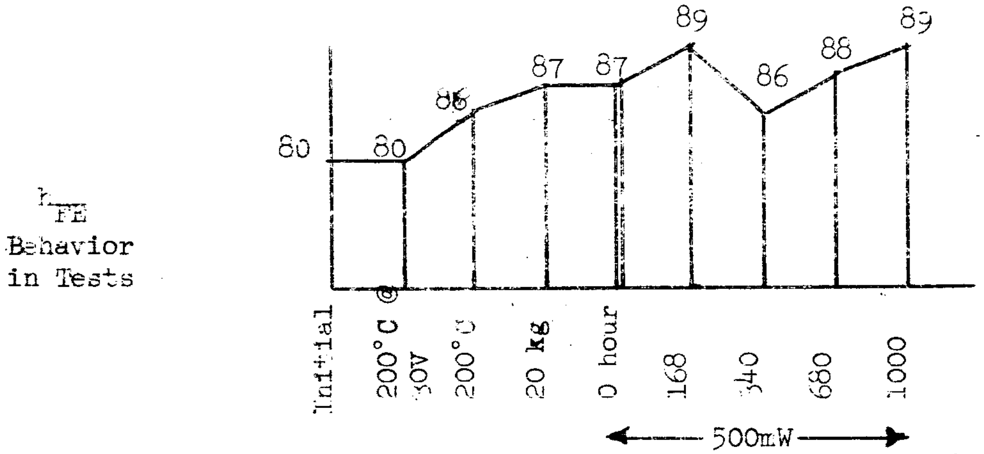

Test Data Analysis:

I_{CBO} indicated trouble in the power test, 168 hour readout.

Laboratory Measurements:

I_{CBO} measurements show severe inversion layer condition.

BV_{CEO} degraded - follows from high leakage I_{CBO}.

Bake: Collector junction completely recovered. After exposure to air, unit started to take on severe instability characteristic of "C" devices. I_{CBO} drift (no I_{CES} drift or h_{FE} change) indicated the collector-base junction was cracked.

Prepared by: Alfred Poe
Failure Analysis Engineer

Date: 9/7/65

FAILURE ANALYSIS REPORT

Sheet 2 of Final

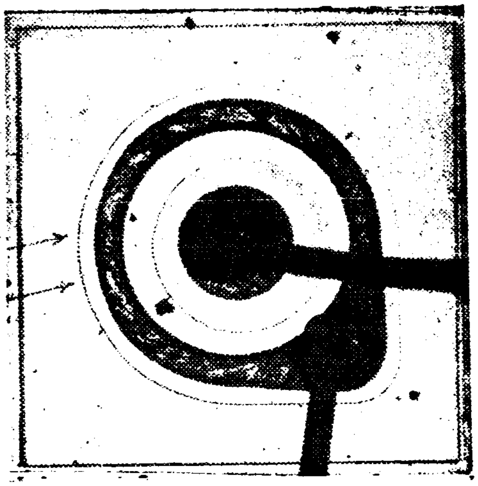

Decapped unit:

Cracks have appeared inside of pellet, not under bond as in other "C" units. These cracks believed to have been in device originally, contributing to "surface degradation" of unit.

FAILURE ANALYSIS REPORT

Sheet 1 of Final

Unit No.	Test Cell No.	Process	Failure Mode Category
C 275	419-247	C	D-3-a

Summary of Analysis: The cause of this failure has been determined to be a short between the base wire and pellet edge. The failure indicator was an I_{CBO} degradation at the 340 hour life test readout.

Test Data Analysis:

Data indicates an apparent short at the 340 hour readout during the 400mW test.

Laboratory Measurements:

Confirmed a collector-base short of approximately 14 ohms.

Decapped Unit:

Examination showed the base wire in contact with pellet edge. Confirms level of short measured. After probing wire of pellet, the unit completely recovered. Short occurred by wire sagging down during heat-power tests.

Short
Wire to edge

Prepared by: Alfred Poe
Failure Analysis Engineer

Date: 8/26/65

FAILURE ANALYSIS REPORT

Sheet 1 of 3

Unit No.	Test Cell No.	Process	Failure Mode Category
C 288	419-255	C	A-5-a

Summary of Analysis: The cause of this failure has been determined to be a defect in the base aluminum ring - probably a microcrack or faulty diffusion site which caused localized current hogging and I_{CBO} increase by surface inversion at this "hot spot".

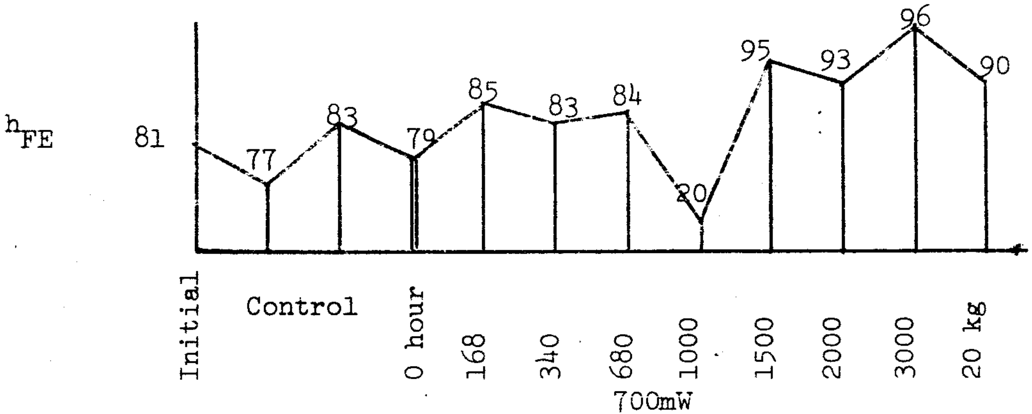

Test data analysis:

At the start of the test, a high value of BV_{CEO} (140V) and a low value of h_{FE} (=80), indicated a degraded condition of gain. During life test at 700mW, emitter-base surface potential changes improved gain, concurently lowering BV_{CEO}. Evidentially the 1000 hour readout is faulty.

I_{CBO} was failing at 168 hours of 700mW stress.

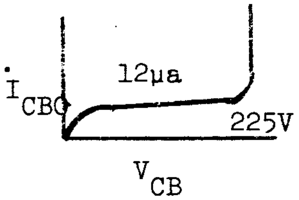

Laboratory measurements:

On receipt, I_{CBO} characteristics showed an inversion layer, high BV_{CBO} showed collector is inverted to intrinsic resistivity.

After 300°C for 16 hours bake

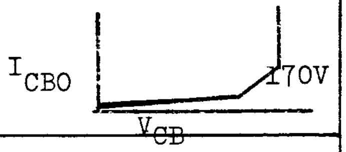

Prepared by: Alfred Poe
Failure Analysis Engineer

Date: 9/27/65

FAILURE ANALYSIS REPORT

Sheet 2 of 3

I_{CBO} level has recovered - inversion layer is gone. The collector is back to N surface potential sending avalanche breakdown to 170V. Bakeout reveals a microplasma type defect may be the source of the high leakage seen after power life.

Visual inspection and voltage drive under reverse bias revealed a "hot spot" location in the aluminum ring. This area was responsible for current hogging during life test and is the probable location of inversion layer due to high local temperature operation.

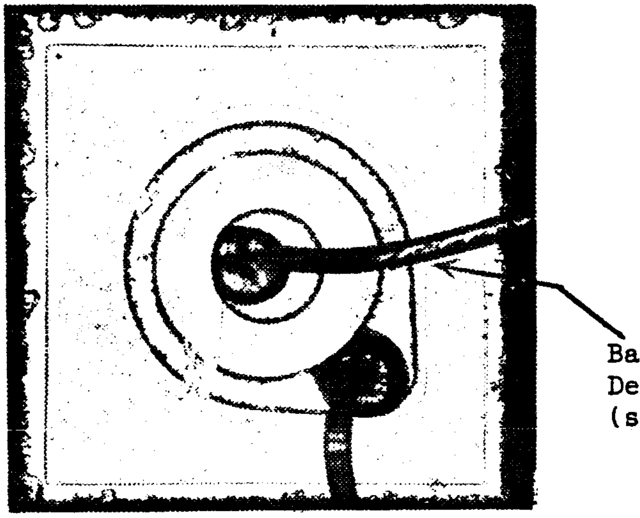

Base Ring
Defect Site
(shorted in lab)

Photo 1

Photo 1 shows device after life test and stressing in the laboratory at 2 watt level (see collector-base area). A short occurred in the aluminum ring just under the emitter wire and a bridge blasted across, base to emitter, at the base bond. This permanent damage occurred at power levels far below the capability of good devices. Base was in series with a 5K ohm resistance.

The base burn-out was the site of the microplasma like breakdown noted in the electrical characteristics. This area acted as a current hog during both life testing and during burn-out in the laboratory. Current density in this spot was high enough to raise local temperature greater than 575°C (the eutectic temperature of aluminum-silicon). Inversion occurred at this area during life test also due to the higher operating temperature. Inversion was "P" surface on collector since this would act to remove effective

FAILURE ANALYSIS REPORT

Sheet 3 of Final

junction from this localized defect area. After "recovery bake" in laboratory, junction moved back to original metallurgical location, intersecting the defect area again and giving the "microplasma" type breakdown noted.

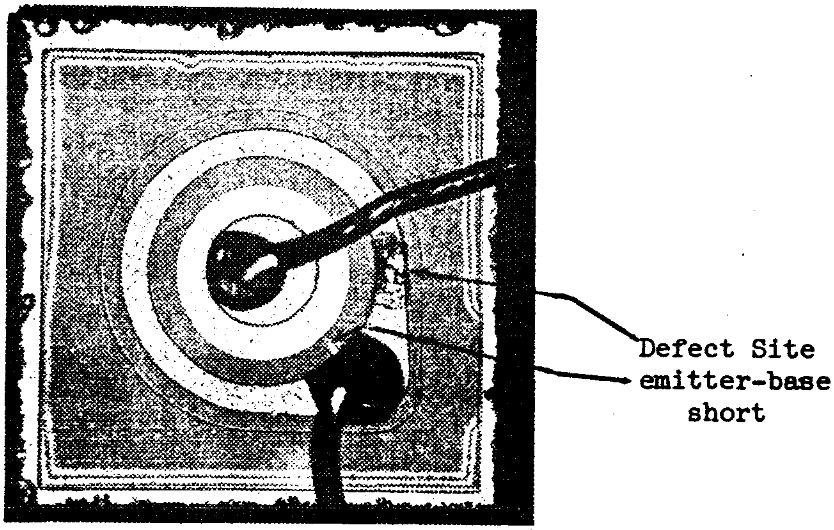

Photo 2

Photo 2 shows device after etch in 10% NaOH to clear away aluminum. Emitter wire has been moved to fully expose the "hot spot" in the aluminum ring.

Aluminum smear in the original photo 1 did not contribute appreciably to failure.

Emitter-base short bridge occurred after the collector-base short and is not related to any reliability degradation in this case.

FAILURE ANALYSIS REPORT

Sheet 1 of 4

Unit No.	Test Cell No.	Process	Failure Mode Category
C 293	419-242	C	Not a Failure

Summary of Analysis: This unit did not fail during the High Stress Screen or the 700 mW life test. A Laboratory analysis was undertaken to determine if any differences could be detected between this unit and other Process C devices, a majority of which failed under high stress level tests.

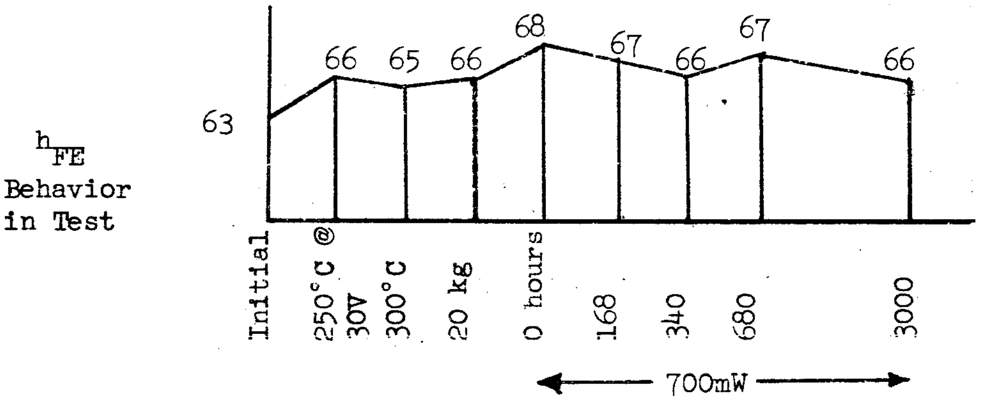

Conclusion: The mechanism which caused the other highly stressed units to fail (microcrack formation under the bonds) was also found in this device. In this case, the microcrack condition did not cause degradation of the parameters, although laboratory measurements at current levels lower than those used in parameter tests indicated the presence of these cracks.

Laboratory Measurements:

Initial Measurements

1) The h_{FE}, at the 100 µA level of I_C, was noted to appear degraded. This is a possible symptom of microcracks in the emitter.

Prepared by: Alfred Poe **Date:** 10/28/65
Failure Analysis Engineer

FAILURE ANALYSIS REPORT

Sheet 2 of 4

2) After a 300°C bake (similar to the stress screen), there was a large improvement noted in the 100 μA h_{FE}.

3) After decap and exposure to air: BV_{CBO} was considerably degraded.

4) After 300°C bake in air: Extreme instability of I_{CBO} was noted. Devices acted cracked in the collector-base junction.

5) Photos: Etch photos were taken. Cracks appeared under bond - sections were taken.

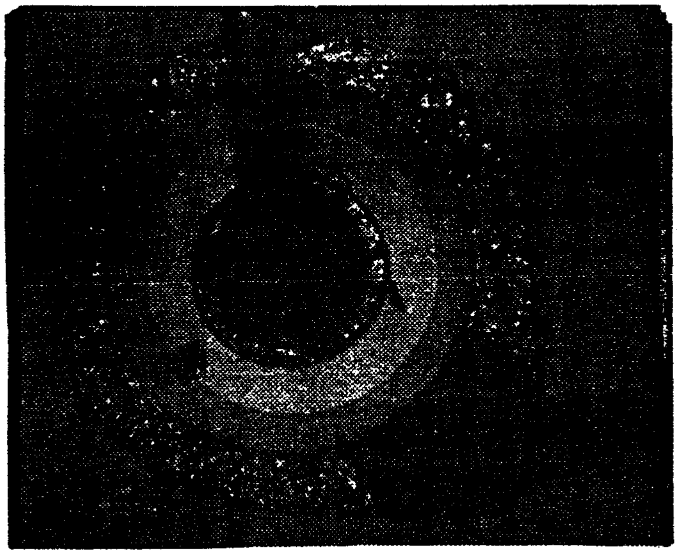

Photo 1. Mag 103X

Unit showed characteristics of a cracked collector-base junction. No cracks are visible in this photo. The following photos show cracks surrounding bonds, shown up after chemical removal of deeply alloyed aluminum contacts.

FAILURE ANALYSIS REPORT

Sheet 3 of 4

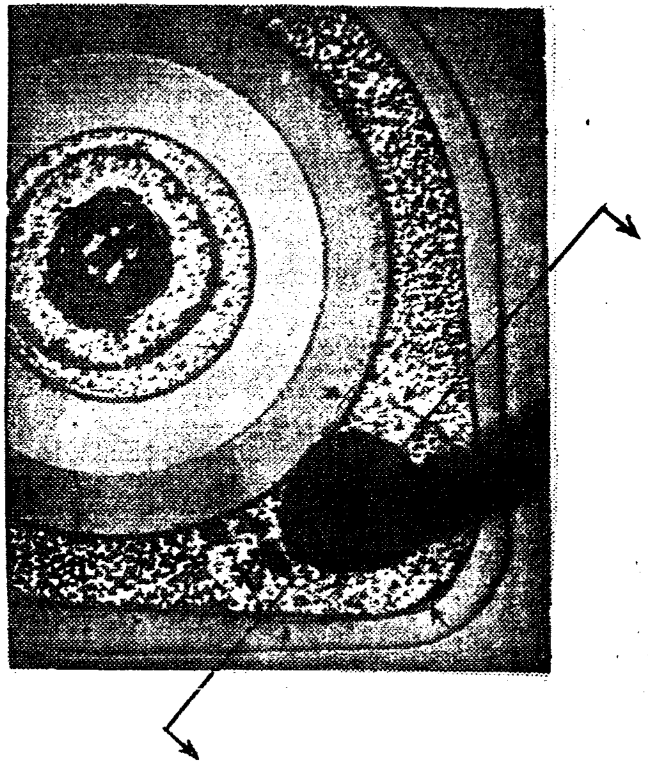

Photo 2. Mag 148X

Note cracks surrounding the base bond under the intermetallic formation of photo 1. Aluminum and intermetallics were chemically removed by a cyanide etch.

Section to show up cracks was made as shown in following photos.

FAILURE ANALYSIS REPORT

Sheet 4 of Final

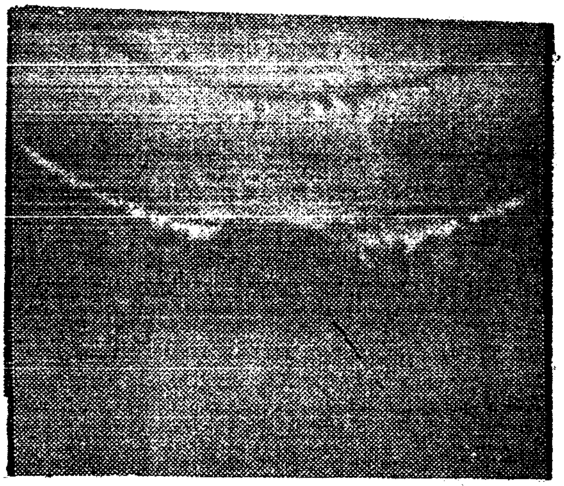

Photo 3

This is a top view of the photo 4 specimen potted **in translucent** compound to show exactly where the section **intersected the specimen** surface. Note cracks.

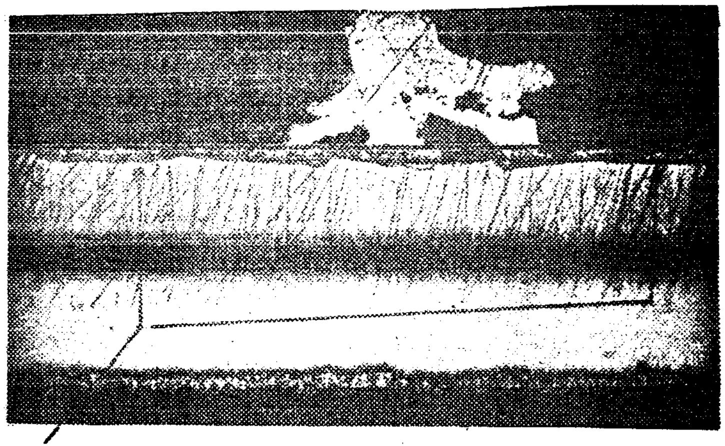

Crack
Locations   Photo 4 Mag 304X

Cross section through base bond of C 293. Section shows **intersection** of cracks at surface with dimensions **corresponding to those in photo** 2. Intermetallic growth greater than 1 mil **high.**

FAILURE ANALYSIS REPORT

Sheet 1 of 4

Unit No.	**Test Cell No.**	**Process**	**Failure Mode Category**
C 301	419-242	C	Not a failure

Summary of Analysis: This device did not fail.

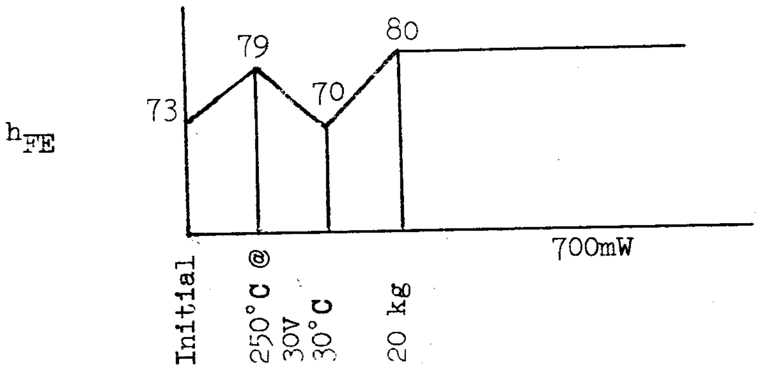

Test data analysis:

Δ h_{FE} change between 300°C bake and 20 kg stress indicates calibration error rather than a real change.

This device, a survivor of high stress testing, was used to study the oxide structures of the Process C units.

Prepared by: Alfred Poe
Failure Analysis Engineer

Date: 10/28/65

FAILURE ANALYSIS REPORT

Sheet 2 of 4

Photo 1

Photo 1 is of a "C" type unit used for oxide thickness studies. This particular device survived 300°C bake without developing "crack" electrical characteristics.

FAILURE ANALYSIS REPORT

Sheet 3 of 4

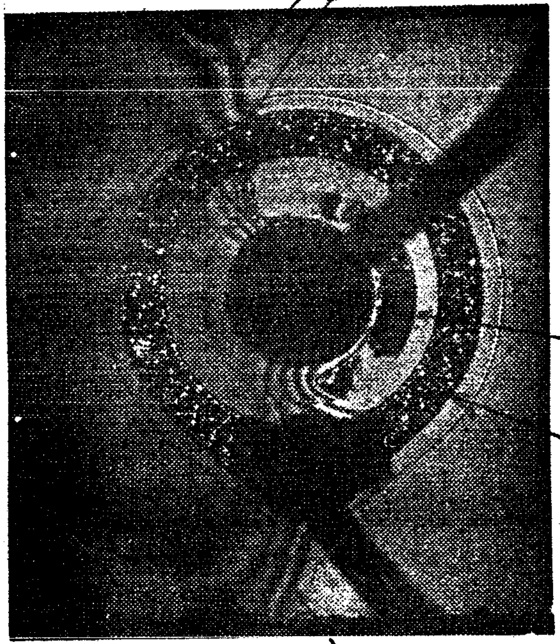

Acid has undercut mask considerably showing up interference fringes easily. No difference between base and collector oxides.

To determine oxide thicknesses, the left side of the pellet was coated with paraffin wax and the unit then etched in concentrated HF for 25 seconds. SiO_2 is completely removed in the unmasked area and the heavy undercutting action of the acid makes counting of interference fringes and calculation of SiO_2 thickness relatively easy.

Note 1: The dark area inside the emitter is not residual SiO_2 but an electrochemical deposition of Si film into N+ areas from the HF reaction.

Note 2: The aluminum ring is very deeply alloyed into the silicon and so has not been appreciably removed by the HF treatment.

FAILURE ANALYSIS REPORT

Sheet 4 of Final

Note 3: The collector and base oxides appear to be identical both being 4 interference fringes deep and purple in color - 6300 angstroms.

The emitter oxide is a shade of green thicker than the base - collector - 4¼ fringes or about 7100 angstroms thick.

FAILURE ANALYSIS REPORT

Sheet 1 of 2

Unit No.	**Test Cell No.**	**Process**	**Failure Mode Category**
C 363	419-255	C	B-2-a

Summary of Analysis: The cause of this failure has been determined to be cracks in base and emitter bond area. Device was indicated to be an I_{CBO} failure at the 2000 hour life test readout.

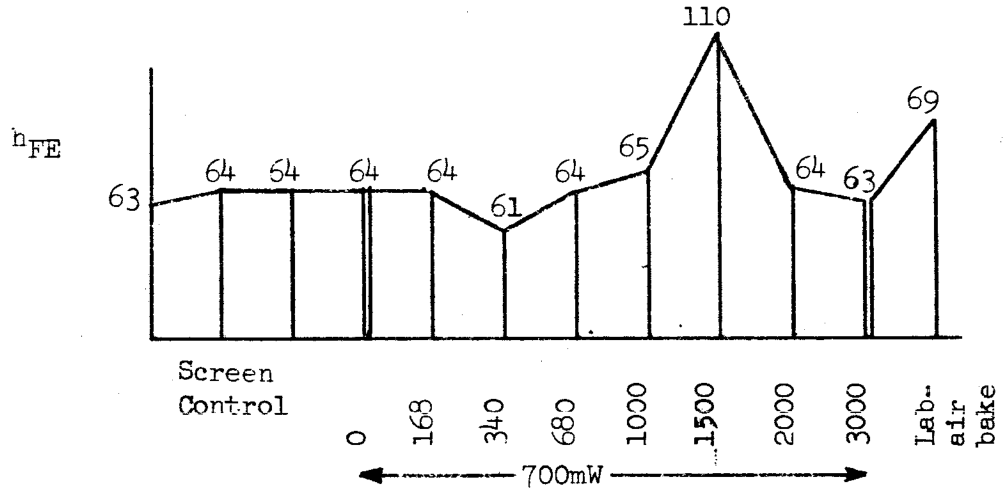

Test Data Analysis:

The very high h_{FE} reading and the high BV_{CEO} reading were contradictory and could very safely be assumed to be incorrect. The contradiction was probably due to faulty equipment. The high I_{CBO} indicated a real degradation, which probably was due to cracks.

Laboratory Analysis:

Baked at 300°C. I_{CBO} now unstable, h_{FE} improved. No E_F or other indications of cracks.

Etch (KOH and KCN); Cracks in base of emitter area were visible (see photos). Emitter bond cracks probably did not penetrate.

Prepared by: Alfred Poe **Date:** 10/1/65

Failure Analysis Engineer

FAILURE ANALYSIS REPORT

Sheet 2 of Final

After decapping - no defects visible to explain increase in I_{CBO} after 700mW stress and instability in air after bake.

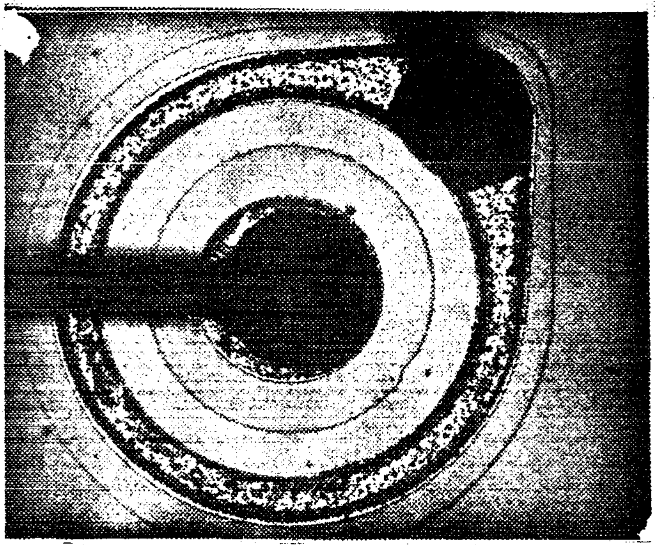

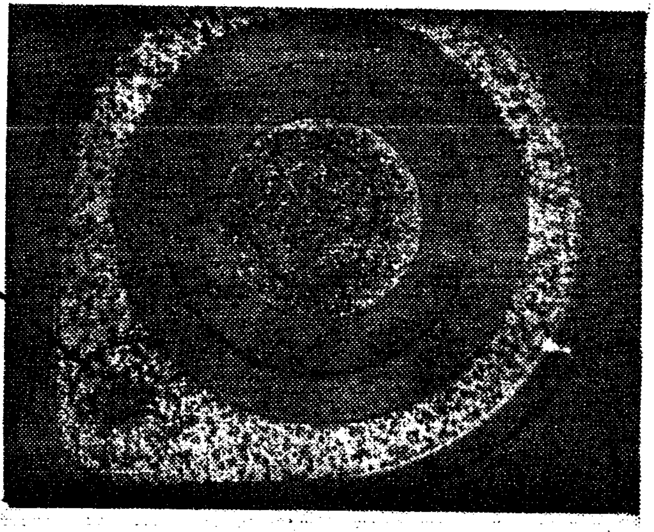

Bond area cracks

After etching both wires and contacts of pellet using KCN and KOH.

Cracks in contact surface were visible in base surrounding pellet ball bond. These are probably deep enough to penetrate the collector-base junction. Similar crack areas in emitter were probably more shallow. No emitter cracks were indicated electrically.

FAILURE ANALYSIS REPORT

Sheet 1 of 3

Unit No.	**Test Cell No.**	**Process**	**Failure Mode Category**
C 400	419-246	C	B-2-a

Summary of Analysis: The cause of this failure has been determined to be a crack extending across both junctions of the unit. The failure indicator was a small I_{CBO} degradation at the 1000 hour life test readout.

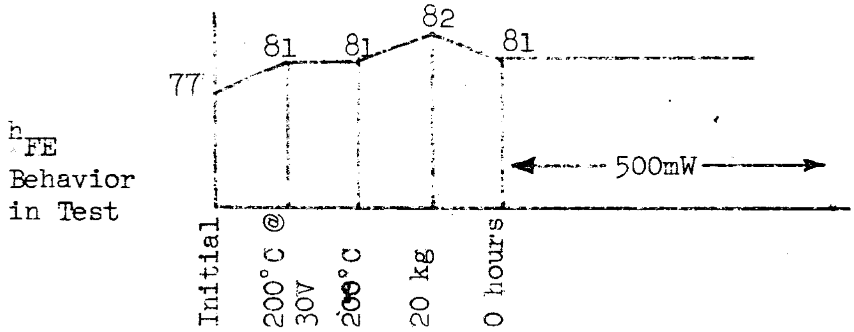

Test Data Analysis:

Test data indicated that this unit operated normally until the final 150 kg centrifuge stress. This condition was similar to other failures observed for this process type and was indicative of cracks in the bond area.

Laboratory Analysis:

Failure analysis procedure for this failure was similar to others for this process type, which were concluded to be a crack in a junction. The unit was decapped and sections were made. Visual inspection (see photos) concluded a crack was the cause of this failure.

Prepared by: Alfred Poe
Failure Analysis Engineer

Date: 10/14/65

FAILURE ANALYSIS REPORT

Sheet 2 of 3

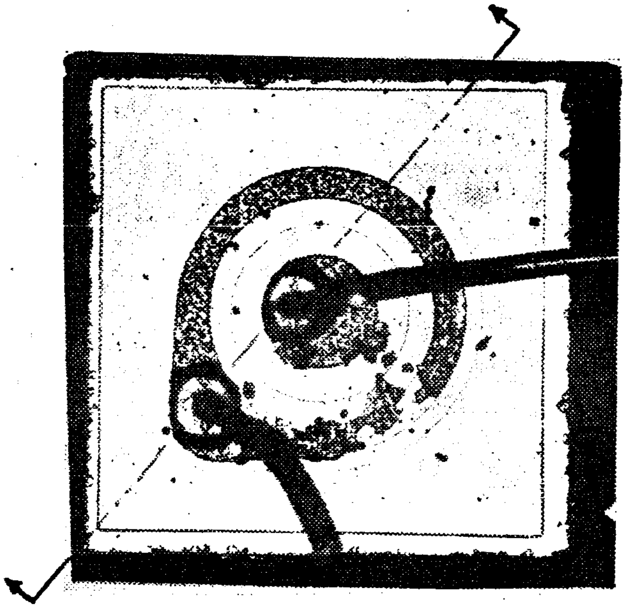

Photo 1 Mag 60X

Electrical evidence of cracks in emitter not confirmed by visual inspection.

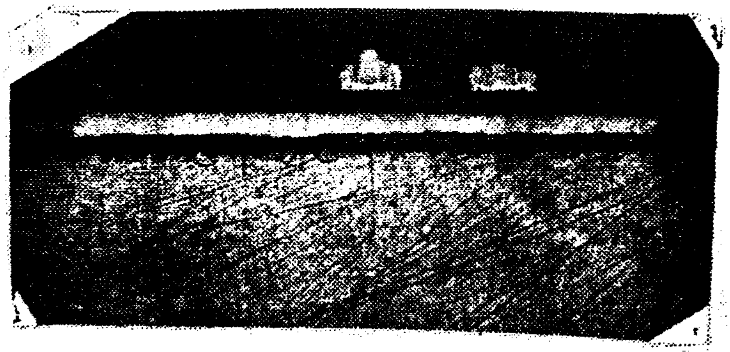

Photo 2 Mag 60.7X

Photo 2 is a section through both bonds which shows:

1. Separation between Si-Au eutectic solder and header metal. V_{SAT} data does not show this characteristic.

FAILURE ANALYSIS REPORT

Sheet 3 of Final

2. Shows very shallow diffusion being used.

3. Photo 3 shows a crack under emitter bond, indicated by electrical parameters.

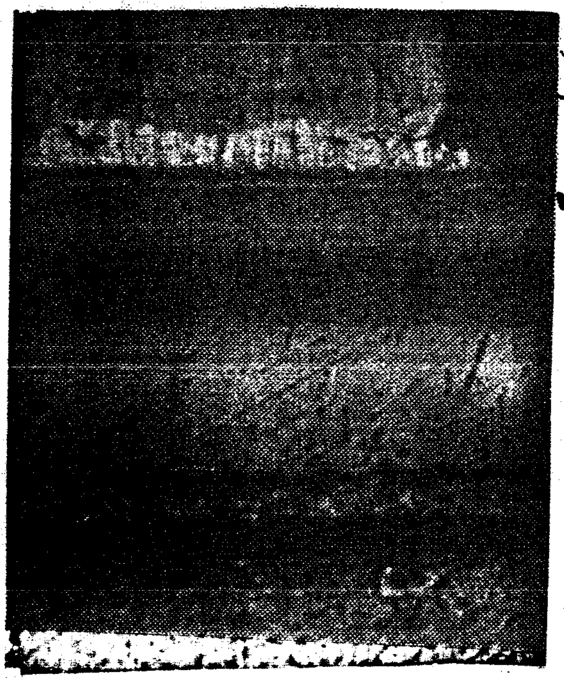

Defect in periphery of bond appearing to be a crack penetrating both junctions.

CB junction depth = 0.21 mil
EB junction depth = 0.07 mil

Photo 3 Mag 401X

Concludions:

Slight crack found in analysis contributes to degradation of I_{CBO} limits. Crack condition characteristic of Process C devices.

FAILURE ANALYSIS REPORT

Sheet 1 of 2

Unit No.	Test Cell No.	Process	Failure Mode Category
C 406	419-255	C	A-2-b

Summary of Analysis: Device began to show I_{CBO} degradation of the surface inversion layer type at the 168 hour readout of the life test.

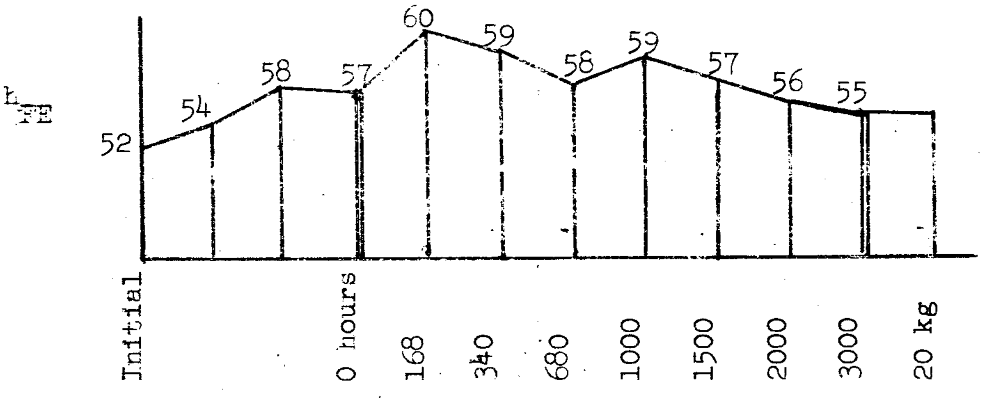

h_{FE} behavior indicates favorable surface potential improvement up to 1000 and 1500 hours. The unit started to degrade slightly after this time. BV_{CEO} is increased corresponding to h_{FE} decrease.

I_{CO} degradation noted early in 700mW stress.

Laboratory Measurements:

Shows a typical inversion layer.

Prepared by: Alfred Poe
Failure Analysis Engineer

Date: 9/21/65

FAILURE ANALYSIS REPORT

Sheet 2 of Final

Severely contaminated header - gases and migrating ions will contribute to inversion layer formation

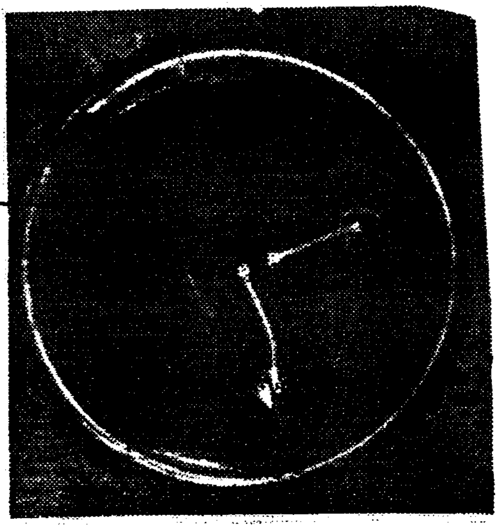

Photo 1

Decapped:

Note that the header is severely contaminated (photo 1). **Device is** cracked. **However,** crack is so severe it is hard to believe characteristics could have been so good. An emitter crack with no floating emitter response at high voltage is very rare. It will be assumed that the crack occurred in the decap operation. Extreme contamination will contribute to inversion.

Severe crack - assumed caused in decap operation.

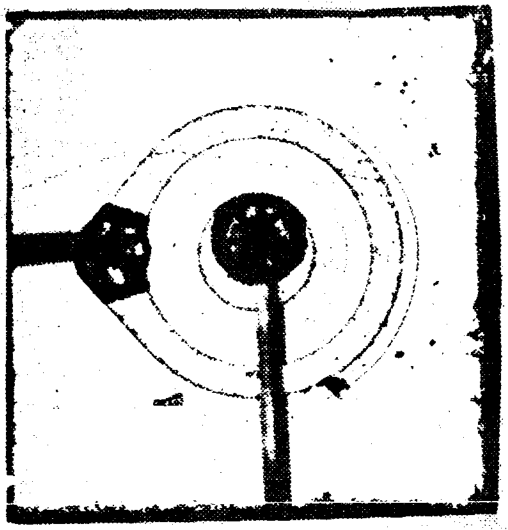

FAILURE ANALYSIS REPORT

Sheet 1 of 2

Unit No.	**Test Cell No.**	**Process**	**Failure Mode Category**
C 505	419-246	C	B-2-a

Summary of Analysis: The cause of this failure has been determined to be due to junction microcracks developing the bond areas under the gold-aluminum intermetallics. These have resulted in the degrading h_{FE} shown in the chart and increasing I_{CBO} during 500mW testing.

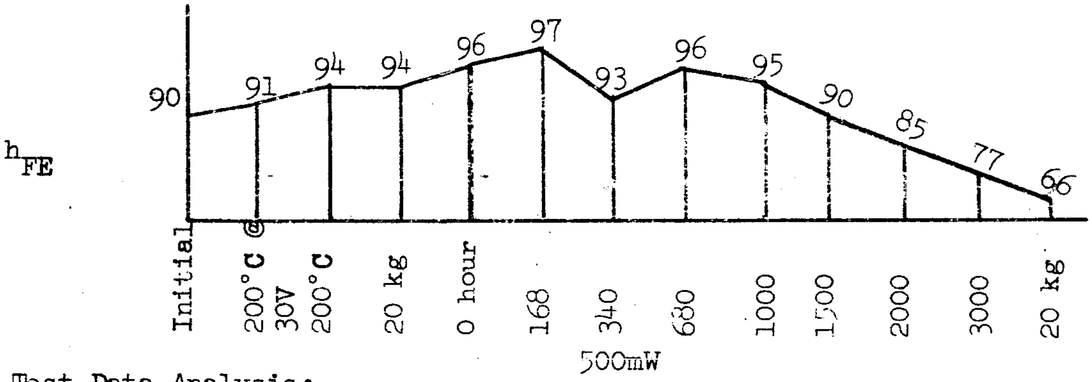

Test Data Analysis:

Gain h_{FE} started to shift in life test at 1000 hour readout, with BV_{CEO} increasing and h_{FE} dropping.
At end of test, I_{CBO} and h_{FE} both degraded.

Laboratory Measurements:

Although h_{FE} severely degraded, no emitter crack was evident in data.

300°C bake: h_{FE} worse. No emitter crack evident.

Decap and 300°C bake: Emitter cracks now in evidence. Strong E_F response.

Prepared by: Alfred Poe
Failure Analysis Engineer

Date: 10/22/65

FAILURE ANALYSIS REPORT

Sheet 2 of 2

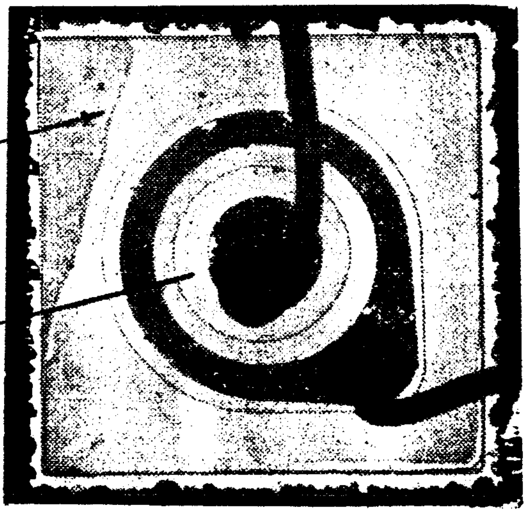

Collector oxide stained by uneven defective etch techniques

Emitter junction extremely unstable after decap and bake - acts cracked from electrical indications

FAILURE ANALYSIS REPORT

Sheet 1 of 3

Unit No.	**Test Cell No.**	**Process**	**Failure Mode Category**
C 576	419-242	C	Not a failure

Summary of Analysis: This unit did not fail during the High Stress Screen or the 700 mW life test. A Laboratory analysis was undertaken to determine if any differences could be detected between this unit and other Process C devices, a majority of which failed under high stress level tests. The mechanism which caused the other highly stressed units to fail (microcracks under the bonds) was also found in this unit. In this case, the microcrack condition did not cause parameter degradation.

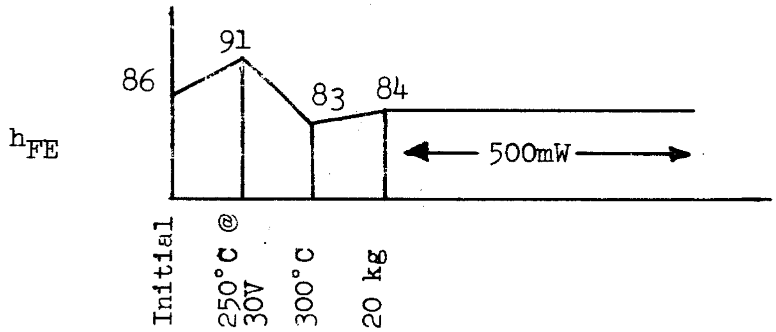

Test Data Analysis:

h_{FE} deviations were within specification. Many units measured showed the same pattern of deviation. 150kg centrifuge reading probably was faulty. Tests did not degrade this device, since all the variations were within the specification.

Laboratory Measurements:

1) Slight E_F indication (symptom of cracks)
2) Unit was decapped. Degrading E_F was noted. Bake at 300°C caused breakdown, h_{FE}, floating emitter potential degradation. Emitter cracks became larger or more severe, as a result of this treatment.

Prepared by: Alfred Poe
Failure Analysis Engineer

Date: 10/28/65

FAILURE ANALYSIS REPORT

Sheet 2 of 3

Photo shows stained header. This contamination did not degrade device.

Section made through emitter

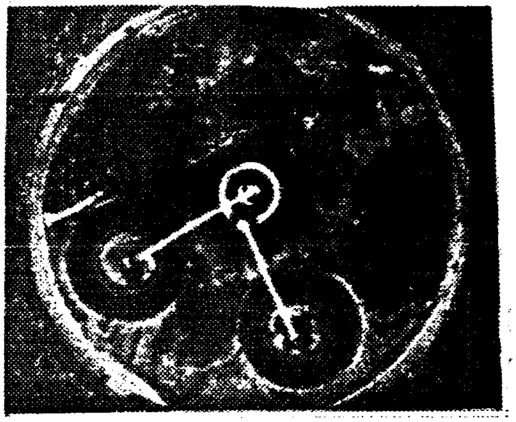

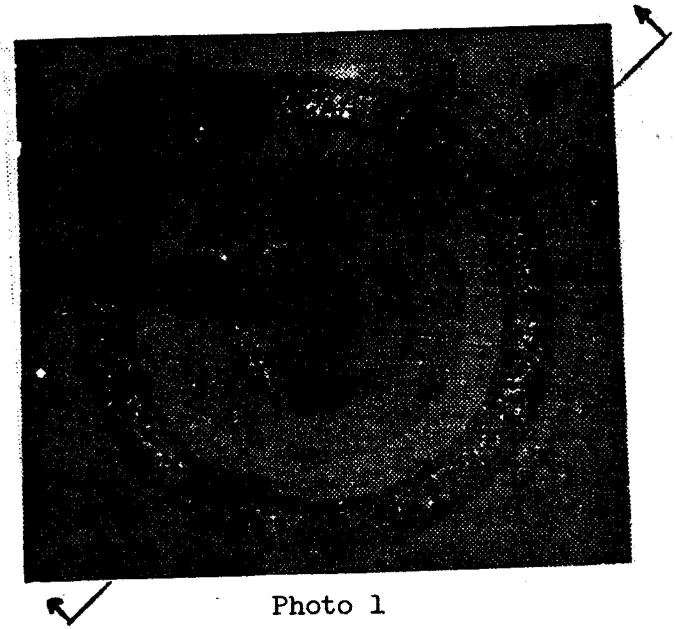

Photo 1

Photo of pellet (photo 1) giving electrical indications of cracked emitter and collector junction. Crack is not visible in photo. Section was made as shown.

FAILURE ANALYSIS REPORT

Sheet 3 of Final

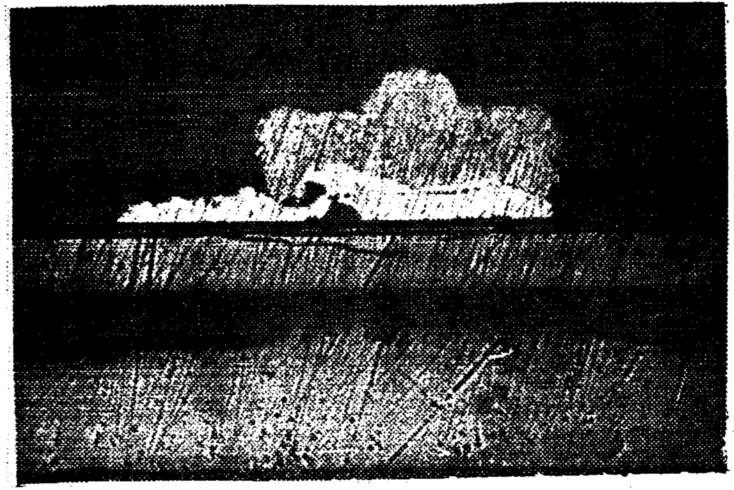

Photo 2

Photo 2 shows a section through the bond which reveals a crack under the intermetallic formations of the bond. Intermetallic (Au_5Al_2) under bond was over 1 mil thick. The fracture had the appearance of being caused by contraction of metal over it, placing the silicon in tension during the cool from 300°C.

Type A unit after 300°C @ 1000 hour bake

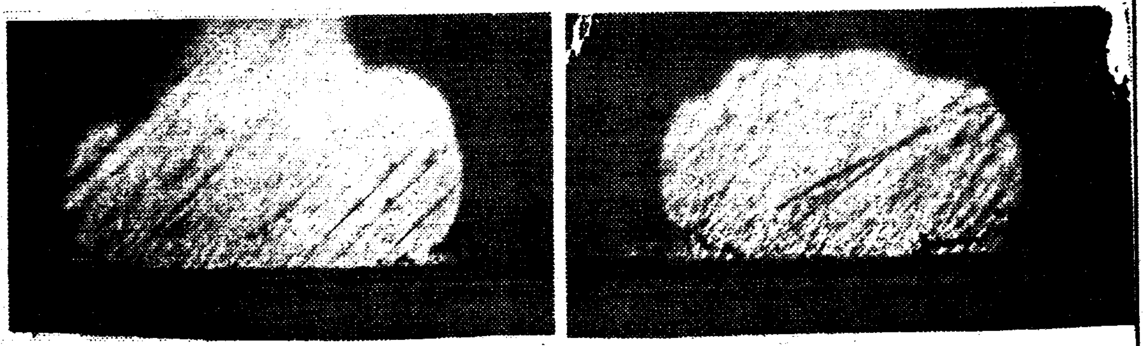

Gold ball bonds were made to A type units and aged. Sections show that the thickness of the intermetallics under bond was 0.25 mil at left and 0.4 at right - less than that formed with C devices. Collector-base junction = 0.32 mil.

F. PROGRAM FAILURE RESPONSE CODE

A Failure Response Code, which would be different from the Failure Mode Code, was developed as a convenient means of noting the device response to stress. The meaning of each digit in the code is defined in the following table:

	First Group		Second Group	Third Group (Response Category Limit Passed)
1	I_{CBO}	1	Initial Value	1
2	I_{EBO}	2	After 1st step	2
9	BV_{CEO}	2S	1st Step Shift	3
13	h_{FE}	3	After 3rd Step	4
15	V_{CE} (SAT)	3S	3rd Step Shift	
16	V_{BE} (SAT)	4	After 4th Step	
660	Noise 100 cps, 1mA	4S	4th Step Shift	
661	Noise 1000 cps, 1mA			
662	Noise 1000 cps, 30mA			
663	Noise 100 Kc, 30mA			

In Addition, the second group is extended to include Steps 5 through 16 using 5S, 6S, etc. as the shift items for each step. The second group is extended as follows:

5 = 00 hours Life Test Readout
6 = 170 hours Life Test Readout
7 = 340 hours Life Test Readout
8 = 680 hours Life Test Readout
9 = 1,000 hours Life Test Readout
10 = 1,500 hours Life Test Readout
11 = 2,000 hours Life Test Readout
12 = 3,000 hours Life Test Readout
13 = 30 Kg Centrifuge Test Following Life Test
14 = 50 Kg Centrifuge Test Following Life Test
15 = 90 Kg Centrifuge Test Following Life Test
16 = 150 Kg Centrifuge Test Following Life Test

The failure response categories identified as 1, 2, 3 and 4 correspond to units that meet the original specifications, units that would meet a normal high reliability end-of-life requirements, units that meet catastrophic limits, and units that shifted beyond catastrophic limits. Thus, each response category identifies a further degree of shift of these critical parameters. The specification limits, or percent shift, which define the response categories are listed in the following table:

	1	2	3	4
I_{CBO}	10nA	10-100nA	100-1000nA	> 1 uA
I_{EBO}	10nA	10-100nA	100-1000nA	> 1 uA
BV_{CEO}	40V	30-40V	20-30V	< 20V
BV_{CEO} % Shift	15%	25%	50%	> 50%
h_{FE}	40-120	35-40 & 120-150	28-35 & 150-180	< 28 or > 180
h_{FE} % Shift	15%	15-25%	25-50%	> 50%
V_{CE} (SAT)% Shift	15%	15-25%	25-50%	> 50%
V_{BE} (SAT)% Shift	15%	15-25%	25-50%	> 50%

The Failure Response Code is only useful when the raw data is being analyzed, and is included here for completeness. An example of the use of the code is given for the Process A devices which were screened out and not placed on life test.

UNIT NO.	FAILURE RESPONSE CODE
A240	(1-2-4)
A285	(1-2-3)
A110	(1-2-4) (9-2S-3) (9-2S-2)
A186	(1-2-4) (9-2S-3)
A294	(2-1-3) (2-2-3) (2-3-4)
A192	(1-2-4) (9-2-4)

SECTION V. NOISE STUDY

A. RESULTS OF THE NOISE STUDY

1. Screening to Noise Limits. Figure 3 shows the cumulative distribution of noise current for units later found to be good and for those later found to be bad. From this Figure it is possible to see that a limit of 5 picoamperes would have removed 10% of the bad units and 5% of the good units. Progressive lowering of the screening limit could have removed 40% of the bad and 18% of the good. Thus, screening to noise could have removed approximately twice as large a percentage of units which would have later failed as the percentage of units that would have been removed that would not have failed.

When the noise was measured after a period of operation, the screen was improved. Figure 4 shows the distribution of the noise readings after the transistor was operated. In this case, a limit of 5 picoamperes would have removed 2% of the good units and 18% of the bad units. At 4 picoamperes, the ratio became 7% of good units versus 42% of bad units. This method is roughly twice as effective as the initial screen.

A test at these low collector currents can result in transistor noise which is comparable to the test equipment noise. A review of the specifications and performance of the QuanTech Noise Analyzer showed that the flattening of the distribution below 3 picoamperes is probably caused by equipment input noise. The use of a higher noise measurement frequency improves the equipment noise ratio but decreases the effectiveness in detecting unreliability. Figure 5 shows the noise distribution comparison of good and failed units when the same transistors are measured initially at 1000 cycles.

2. Correlation of Noise and Transistor Parameters. Noise is not equally effective as a screen for all failure modes. Figure 6

shows the distribution of noise values found for units which later failed h_{FE} and for those which later failed $V_{CE(SAT)}$. The units which later failed $V_{CE(SAT)}$ showed a much lower noise than was expected from the total distribution. The units which later failed h_{FE} did not have the high noise values expected, but did have a significant difference in the mean noise values.

A period of operation is required to produce the higher noise levels found in the units which degrade. Figure 7 shows the effect of a period of operation. When compared with Figure 6, it can be seen that noise increased on all failures, but $V_{CE(SAT)}$ failures had less than the expected noise and h_{FE} failures had more than the expected noise. The $V_{CE(SAT)}$ relation suggests the need for exploring initial noise for very low noise units.

3. Comparative Screening. If the collector current is increased from 5 microamperes to 1 milliampere, and the 100 cycle noise current is used, the ability of an initial test to eliminate units which would later fail can be improved. The following table of values for a lot stressed to a 45 percent failure, shows I_{CBO} to be the most effective screen. $V_{BE(SAT)}$; the upper limit of h_{FE}; 1000∿, 30 mA noise; 100 cycle; and 1000 cycle, 5 microampere noise could also be effective.

Parameter Measured	% of lot Rejected	% Bad of Screen Rejected
No screen	0	0
I_{CBO} @ V_{CB} = 20V	15	100
I_{EBO} @ V_{EB} = 5V	15	45
BV_{CEO} @ I_C = 0.1mA	15	45
h_{FE} @ V_{CE} = 5V, I_C = 20mA	7	71
$V_{CE(SAT)}$ @ I_C = 50mA, I_B = 5mA	8	38
$V_{BE(SAT)}$ @ I_C = 50mA, I_B = 5mA	8	75
I_n @ 5ua, 100 cps, BW = 20 cps	9	55
1000 cps, BW = 200 cps	12	50
I_n @ 30mA, 1000 cps, BW = 200 cps	7	71
100 kc, BW = 20 kc	7	43

% Bad in Lot = 45.

The noise current at 1,000 cycles and 30mA showed the greatest screening effectiveness as an individual test, but every unit which was eliminated by the screen could have been eliminated by either the I_{CBO} or the 100 cycle noise screen. Therefore the 1,000 cycle, 30mA noise test would not be economic. Screening to other parameters such as I_{EBO}, BV_{CEO}, $V_{CE(SAT)}$ and noise at 5uA, 1000 cycle would not improve the efficiency.

B. NOISE STUDY LITERATURE SEARCH

Refer to the Bibliography for the complete literature references shown below.

Noise readings made at the time of the initial test on transistors which later fail tend to have a higher noise current than units which will not fail. Noise can be due to two or more factors within the device. One such factor could be the flicker noise generated by contacts.

Van der Ziel, (1) reporting on the work of Williams and Thatcher (2) and on the work of Christenson and Pearson (3) reports that when flicker noise is measured in semiconductors, it often masks the noise found in the material. The work was based on research samples available in 1959 and present technology would keep the contact noise lower in most cases, but any poor contact could develop flicker noise. Other details in (1) show that flicker noise has been associated with contacts between grains of a material. Pearson, (13) has established that a wet atmosphere can also cause flicker noise. It could be expected that flicker noise due to damp atmospheres would contribute to the total noise measured in a semiconductor.

Brophy & Bess, (14) (15) (16), have shown that stress and high temperature can cause noise due to the plastic deformation of the crystal. Process C was shown to have stress cracks under the lead bonds. It could be expected that the stresses set up by the lead bonding operation would cause flicker noise. The cracks themselves, if partially developed, could be expected to contribute to the noise by the same mechanism as contacts between grains.

Brophy also found, (17), that noise is caused by the "Seebeck" or thermoelectric effect. Hot spots, which are often observable visually or photographically due to light emission, would also cause fluctuations in temperature generating thermoelectric noise voltages. Slow states of charges upon the surface, (18), are also a cause of flicker noise. Noise could thus be expected to be associated with any form of ion contamination in the can or in the surface layers of the oxides.

It was not the purpose of this contract to re-investigate the noise phenomenon, but the literature showed many mechanisms that produce noise which could be associated with failure mechanisms. From a practical standpoint, no semiconductor could be completely free from such mechanisms and would also generate noise due to those mechanisms which have no relation to reliability.

C. NOISE SCREENING RELATED TO MANUFACTURING PROCESSES

One value of noise would not be suitable for application to all vendors and processes supplied to a single specification. Figure 8 shows the comparative, cumulative distribution of noise readings for the three different processes. Process C was expected to have the greatest failure rate. Quarterly Report 3, Section 7, showed that Processes A and B had small failure rates but relatively high noise when compared with Process C. Paragraph 7.11 of the 3rd Quarterly Report, shows the effectiveness of screening to the upper 85th percentile of noise.

If all three lots were screened to the 85th percentile (52 picoamperes) of Process C, 30% of Process A and 32% of Process B would be rejected. In any direct comparison, the most reliable transistor lots could have the highest rejection to a noise specification.

The relations shown are characteristic of noise relationships for different processes. In normal production experience, the distribution of any parameter may shift from time to time, due to small manufacturing variations. The semiconductor yield is dependent upon many variables, and frequently the step taken to "correct" one parameter will shift the distribution of other parameters. If all the parameters were screened to remove the top 15% for the purpose of improving reliability, it would probably be impossible for any manufacturer to meet the total specification.

If all of the sources of failure, or noise sources were removed, the manufacturer would be unnecessarily penalized for the extra effort by the loss of 15% of the good units. Also, if a distribution is cut in the center for any reason, the top 15% could be the center of the original distribution, and this screen would be inefficient since it would remove more good units than bad units.

D. NOISE CURRENT EFFECTIVENESS

Figure 6 shows the 100 cps noise current distribution values, before the first stress, for all units, for units which failed $V_{CE(SAT)}$, and for units which failed h_{FE}. Figure 7 shows the 100 cycle noise current distribution for all units, for the units which later failed h_{FE}, and for the units which later failed $V_{CE(SAT)}$ after the first stress.

The noise found in the $V_{CE(SAT)}$ failures for the initial measurement was relatively low in comparison with all units. There may be a reason for less noise at the higher $V_{CE(SAT)}$ values, but this could not be determined. Figure 7 shows that 20% of the units which failed $V_{CE(SAT)}$ had higher noise after the initial period of operation, and that this noise was less than the noise observed in the entire distribution. In the case of the h_{FE} failures, noise for a substantial portion of the units was higher than the noise for the entire distribution. Thus, it may be concluded that noise current associated with failure tended to increase following a period of operation.

This analysis tended to confirm the suggested relation between noise and hot spots. If a hot spot were present due to a microplasma, degradation would be expected after a small amount of operation, and could be associated with an h_{FE} degradation. A larger sample experiment would be necessary to confirm this effect.

E. LOW FREQUENCY NOISE SCREENING EFFECTIVENESS

Low frequency noise as a means of detecting failures was expected to show the best results. This was due to the assumption that low frequency noise is associated with slow surface states.

Van der Zeil (1, page 52) reasons that slow states are stored charges and that the charge leaks away with a time constant related to resistivity and charge. This theory is confirmed by observing the behavior pattern of the low frequency meter (100 cycle) on the Noise Analyzer which is very unsteady on some transistors. Fluctuation in the 100 cycle meter can approximately double during the observation time.

Assuming that the slow surface states have a time period of seconds or minutes, it is possible to understand the erratic action of the meter. This also agrees with the observation of the distribution of noise readings at different frequencies for units which later failed. For example, at the 100 cycle noise reading, Process B showed the clearest distinction between noise in units which failed and in those which did not fail. Operation of the unit increased the noise generated by the mechanism associated with degradation. A review of previous Quarterly Reports showed that discrete shifts occur in some transistors and that these shifts are also very similar to the behavior of the 100 cycle noise meter.

The analysis thus tended to confirm that noise at lower frequencies should be expected to be present in transistors having failure mechanisms such as contact noise and hot spots, where current would shift abruptly from one path to another.

SECTION VI. PROCESS DETAILS

A. ELECTRICAL SPECIFICATION

The transistors investigated were purchased to the JEDEC registered specification for the 2N718A. The three devices investigated represent three variations to meet the same specification. These are:

Process A - Double Diffused, with Au to Al contacts.

Process B - Double Diffused epitaxial, with Al to Al contacts.

Process C - Triple Diffused, with Au to Al contacts.

Joint Electron Device Engineering Council

REGISTRATION DATA

2N718A

General Description

This transistor is an NPN double diffused silicon general purpose transistor designed for a wide variety of high performance amplifiers and high speed switching applications.

Absolute Maximum Ratings

A. Maximum Temperature

1. Storage Temperature	-65°C to +300°C
2. Junction Temperature, T_J operating	+200°C Max.
3. Total Dissipation at case temperature 25°C	1.8 Watts
at case temperature 100°C	1.0 Watts
at ambient temperature 25°C	0.5 Watts

B. Maximum Voltage

1. Emitter to Base Voltage, V_{EB}	- 7 volts
2. Collector to Base Voltage, V_{CB}	- 75 volts
3. Collector to Emitter Voltage, V_{CER} (R_{BE} - 10 ohms)	- 50 volts
4. Collector to Emitter Voltage, V_{CEO}	- 32 volts

Electrical Characteristics at 25°C

A. Static Characteristics	Min.	Max.
1. Collector Current, I_{CBO}	-	10 nA
Collector Voltage, $V_{CB} = 60$ V.		
2. Collector Current, I_{CBO}	-	10 uA
Collector Voltage, $V_{CB} = 60$ V.		
$T_A = +150^{\circ}C$		
3. Collector Breakdown Voltage, BV_{CBO}	75 V	-
$I_C = 100$ uA		
4. Emitter Current, I_{EBO}	-	10 nA
Emitter Voltage, $V_{EB} = +5$ V.		
5. Emitter Breakdown Voltage, BV_{EBO}	+ 7 V	-
$I_E = 100$ uA, $I_C = 0$		
6. Collector to Emitter Sustaining Voltage, $V_{CER(sust.)}$	+50 V	-
($R_{BE} \leq 10$ Ohms, $I_C = 100$ mA, pulsed)		
7. Collector Saturation Voltage, $V_{CE(SAT)}$	-	+1.5 V
$I_B = 15$ mA, $I_C = 150$ mA		
8. Base Saturation Voltage, $V_{BE(SAT)}$	-	+1.3 V
$I_B = 15$ mA, $I_C = 150$ mA		

Electrical Characteristics at 25°C (Cont'd)	**Min.**	**Max.**
B. Small Signal Characteristics		
1. Small Signal Current Gain, h_{fe}		
$I_C = 1$ mA, $V_C = 5$ V	30	100
$I_C = 5$ mA, $V_C = 10$ V	35	150
2. Input Resistance, h_{ib}		
$I_C = 1$ mA, $V_C = 5$ V	24	34
$I_C = 5$ mA, $V_C = 10$ V	4	8
3. Voltage Feedback Ratio, h_{rb}		
$I_C = 1$ mA, $V_C = 5$ V	-	3×10^{-4}
$I_C = 1$ mA, $V_C = 10$ V	-	3×10^{-4}
4. Output Conductance, h_{ob}		
$I_C = 1$ mA, $V_C = 5$ V	0.1 μmho	0.5 μmho
$I_C = 5$ mA, $V_C = 10$ V	0.1 μmho	1.0 μmho
5. High Frequency Current Gain, h_{fe}	3.0	-
$I_C = 50$ mA, $V_C = 10$ V, f = 20 MC		
6. Output Capacitance, C_{ob}	-	25 pf
$I_E = 0$ mA, $V_{CB} = 10$ V		
7. Input Capacitance, C_{ib}	-	80 pf
$I_C = 0$ mA, $V_{EB} = -0.5$ V		
8. Noise Figure, NF	-	12 db
$I_C = .3$ mA, $V_C = 10$ V, f = 1000 cps $R_G = 510\ \Omega$, 1 cycle bandwidth		

Electrical Characteristics at 25°C (Cont'd)	Min.	Max.
C. Large Signal Characteristics		
1. D.C. Pulse Current Gain, h_{FE}	40	120
$I_C = 150$ mA, $V_{CE} = 10$ V		
2. D.C. Pulse Current Gain, h_{FE}	20	-
$I_C = 500$ mA, $V_{CE} = 10$ V		
3. D.C. Current Gain, h_{FE}		
$I_C = 10$ mA, $V_{CE} = 10$ V, $T = 25°C$	35	-
$I_C = 10$ mA, $V_{CE} = 10$ V, $T = -55°C$	20	-
4. D.C. Current Gain, h_{FE}	20	-
$I_C = 0.1$ mA, $V_{CE} = 10$ V		
5. Switching Time $t_d + t_r + t_f$	-	30 nsec
Thermal Characteristics		
A. Thermal Resistance, Junction to Case, 0_{J-C}	-	97.0°C/W

Packaging

A. JEDEC TO - 18

B. Lead Connections:

1. Lead 1 - Emitter
2. Lead 2 - Base
3. Lead 3 - Collector (Connected to Case)

B. PROCESS DIFFERENCES

Units made by the three separate processes as supplied by NASA were electrically measured, then opened and analyzed to determine any differences which could change the effectiveness of the screening methods being studied.

The following table shows a summary of the physical measurements:

	PROCESS A	PROCESS B	PROCESS C
Pellet Size - Mil	32 X 32	25 X 25	40 X 40
C.B. Dia. - Mil	24	17 Tip to Tip	27 Teardrop
E.B. Dia. - Mil	15	10.7 " " "	15
E Contact Dia. - Mil	13		10
Base Area Mil^2	542	169	616
Emit Area Mil^2	176	46	176
Emit Perimeter - Mil	47	37.2	47
Contacts	Alum	Alum	Alum
Wire	2 Mil Au	0.85 Mil Al	2 Mil Au
Caps	Nickel	Nickel	Nickel
Gas Analysis N_2	98 %	99%	98%
O_2	0	0	1%
CO_2	2%	0.1%	1%
Ar	-	0.25%	0.25%
Volume (micron liters)	27	23	44

C. PHYSICAL AND FABRICATION DETAILS

		PROCESS A	PROCESS B	PROCESS C
1.	Header and Cap	TO-18 Header TO-18 Cap	TO-18 Header TO-18 Cap	TO-46 Header TO-18 Cap (Gas Volume is Larger)
2.	Oxide Thickness	Base 8-9000 Å Emitter - 5000 Å	- 7000 Å - 7500 Å	
3.	Bonding	Wedge	Wedge	Ball

D. PHOTOGRAPHS OF THE PHYSICAL APPEARANCE OF THE PELLETS.

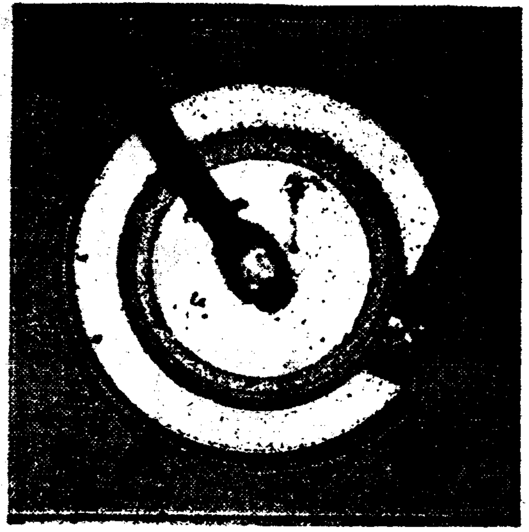

PROCESS A

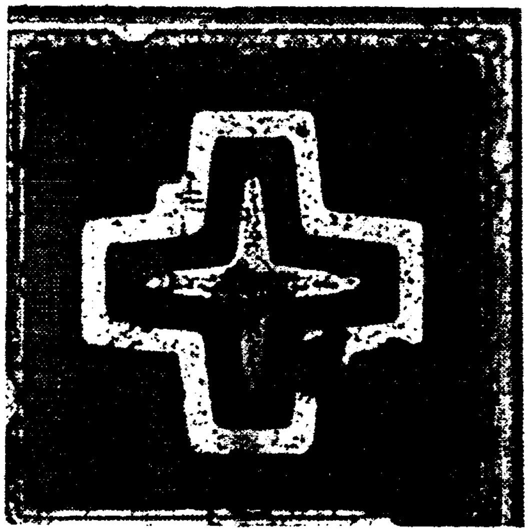

PROCESS B

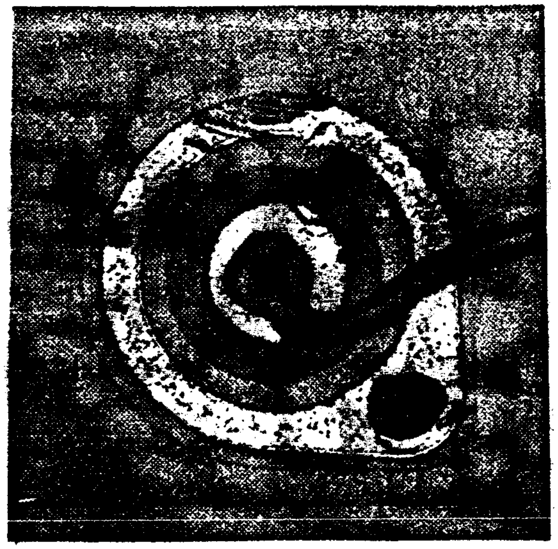

PROCESS C

TABLE 1.

3000 HOUR LIFE TEST FAILURE RATES

STRESS SCREEN		P = 800 mW V_{CB}=20V, T_A=25°C			P = 700 mW V_{CB}=20V, T_A=25°C			P = 500 mW V_{CB}=20V, T_A=25°C			P = 400 mW V_{CB}=20V, T_A=150°			P = 200 mW V_{CB}=20V, T_A=150°		
		Unit Khr	FR 1	FR 2	Unit Khr	FR 1	FR 2	Unit Khr	FR 1	FR 2	Unit Khr	FR 1	FR 2	Unit Khr	FR 1	FR 2
PROCESS A	HIGH	39	7.9	7.9	66	1.4	1.4	168	2.5	2.5	36	14	14	66	4.7	3.4
	MODERATE	39	2.4	2.4	87	1.1	1.1	231	2.3	2.3	42	7.4	5.4	87	2.3	2.3
	CENTRIFUGE	21	9.6	9.6	48	4.2	4.2	117	5.4	5.4	21	4.4	4.4	48	4.2	4.2
	NONE	21	9.6	9.6	42	4.7	4.7	108	6.8	6.2	21	4.4	4.4	42	2.2	2.2
PROCESS B	HIGH	18	23	18	54	19	14	171	10	8.6	39	16	11	78	13	5.8
	MODERATE	39	21	18	81	5.2	4.2	201	4.1	1.8	39	5.2	5.2	78	2.6	2.6
	CENTRIFUGE	21	30	29	39	16	11	117	7.2	3.3	21	9.6	9.6	42	7.4	5.5
	NONE	18	17	17	39	7.9	7.9	99	8.4	3.9	18	17	12	39	5.2	2.7
PROCESS C	HIGH	3	67	67	15	21	24	6	51	51	--	--	--	--	--	--
	MODERATE	30	14	14	63	21	20	162	6.4	3.2	12	43	43	54	12	9.1
	CENTRIFUGE	27	31	31	48	11	7.8	123	6.8	5.0	27	27	24	48	13	2.9
	NONE	24	31	29	54	25	23	150	4.9	0.7	27	23	14	51	8.1	4.7

Unit Khr = Accumulated test hours in thousands of hours.
FR 1 = Failure Rate in % per 1000 hours, 60% Confidence Level - Total Failures.
FR 2 = Failure Rate in % per 1000 hours, 60% Confidence Level - Burn-in Failures removed.

TABLE 2.

3000 HOUR LIFE TEST RESULTS AFTER HIGH STRESS SCREEN

		P = 800 mW V_{CB}=20V, T_A=25°C					P = 700 mW V_{CB}=20V, T_A=25°C					P = 500 mW V_{CB}=20V, T_A=25°C					P = 400 mW V_{CB}=20V, T_A=150°					P = 200 mW V_{CB}=20V, T_A=150°				
		Good	Response Category				Good	Response Category				Good	Response Category				Good	Response Category				Good	Response Category			
			1	2	3	4		1	2	3	4		1	2	3	4		1	2	3	4		1	2	3	4
PROCESS A	Start High Stress Screen	14					26					73					14					28				
	End High Stress Screen	13			1		22	2	1		1	56	13	4			12	1			1	22	4			2
	End Burn-in	13					22					56					12					21		1		
	End Life Test	11				2	22					53		1		2	8		2	1	1	20		1		
PROCESS B	Start High Stress Screen	10					22					70					13					28				
	End High Stress Screen	6			1	3	18		1	1	2	57		7	2	4	13					26		2		
	End Burn-in	4		1		1	13		2	3		52		3		2	10		3			19		6		1
	End Life Test	3		1			9		2		2	41		2	1	8	8		1		1	17		2		
PROCESS C	Start High Stress Screen	6					16					6														
	End High Stress Screen	1			1	4	5		2	4	5	2		1	1	2										
	End Burn-in	1					3	1		1		2														
	End Life Test	0				1	2		1			0		1	1											

TABLE 3.

3000 HOUR LIFE TEST RESULTS AFTER MODERATE STRESS SCREEN

		P = 800 mW V_{CB}=20V, T_A=25°C					P = 700 mW V_{CB}=20V, T_A=25°C					P = 500 mW V_{CB}=20V, T_A=25°C					P = 400 mW V_{CB}=20V, T_A=150°					P = 200 mW V_{CB}=20V, T_A=150°				
		Good	Response Category				Good	Response Category				Good	Response Category				Good	Response Category				Good	Response Category			
			1	2	3	4		1	2	3	4		1	2	3	4		1	2	3	4		1	2	3	4
PROCESS A	Start Moderate Stress Screen	13					29					78					14					29				
	End Moderate Stress Screen	13					29					77	1				14					29				
	End Burn-in	13					29					77					13		1			29				
	End Life Test	13					29					73		1		3	12				1	28		1		
PROCESS B	Start Moderate Stress Screen	14					29					70					14					29				
	End Moderate Stress Screen	13				1	27	1		1		67		2		1	13				1	26		2		1
	End Burn-in	10		2		1	26				1	62		4	1		13					26				
	End Life Test	6		2		2	24				2	60				2	12				1	25		1		
PROCESS C	Start Moderate Stress Screen	14					28					79					14					28				
	End Moderate Stress Screen	10	1		2	1	21		5	1	1	54	3	15	4	3	4			2	8	18		3	3	4
	End Burn-in	10					18		3			47	1	1	4	1	4					16		1		1
	End Life Test	7		1	1	1	9		1	3	5	44		3			0			1	3	13		1		2

TABLE 4.

3000 HOUR LIFE TEST RESULTS AFTER CENTRIFUGE ONLY SCREEN

		P = 800 mW V_{CB}=20V, T_A=25°C					P = 700 mW V_{CB}=20V, T_A=25°C					P = 500 mW V_{CB}=20V, T_A=25°C					P = 400 mW V_{CB}=20V, T_A=150°					P = 200 mW V_{CB}=20V, T_A=150°				
		Good	Response Category				Good	Response Category				Good	Response Category				Good	Response Category				Good	Response Category			
			1	2	3	4		1	2	3	4		1	2	3	4		1	2	3	4		1	2	3	4
PROCESS A	Start Centrifuge Only Screen	7					16					39					7					16				
	End Centrifuge Only Screen	7					16					39					7					16				
	End Burn-in	7					16					38	1				7					16				
	End Life Test	6				1	15		1			33				5	7					15		1		
PROCESS B	Start Centrifuge Only Screen	7					15					40					7					15				
	End Centrifuge Only Screen	7					13			1	1	39		1			7					14	1			
	End Burn-in	5				2	10				3	33	1	2		3	7					13			1	
	End Life Test	2		1		2	8				2	31		1		1	6		1			12			1	
PROCESS C	Start Centrifuge Only Screen	10					19					52					10					20				
	End Centrifuge Only Screen	9		1			16	1	1	1		41	3	6	2		9	1				16	4			
	End Burn-in	6		1		2	14		1		1	37	1	1		2	6		1	1	1	11		2		3
	End Life Test	2		2		2	12				2	33		2	2		3		1	1	1	11				

TABLE 5.

3000 HOUR LIFE TEST RESULTS AFTER NO SCREEN

		P = 800 mW V_{CB}=20V, T_A=25°C					P = 700 mW V_{CB}=20V, T_A=25°C					P = 500 mW V_{CB}=20V, T_A=25°C					P = 400 mW V_{CB}=20V, T_A=150°					P = 200 mW V_{CB}=20V, T_A=150°				
		Good	Response Category				Good	Response Category				Good	Response Category				Good	Response Category				Good	Response Category			
			1	2	3	4		1	2	3	4		1	2	3	4		1	2	3	4		1	2	3	4
PROCESS A	Start	7					14					38					7					14				
	Electrical Screen Rejects																									
	End Burn-in	7					14					36	1			1	7					14				
	End Life Test	6				1	13		1			31				5	7					14				
PROCESS B	Start	6					13					37					7					14				
	Electrical Screen Rejects																					13		1		
	End Burn-in	6					13					33		1	1	2	6				1	12		1		
	End Life Test	4		1		1	11		2			30		2		1	5				1	12				
PROCESS C	Start	10					20					55					10					20				
	Electrical Screen Rejects	8			1	1	18	1			1	50	1	2		2	9		1			17	1	2		
	End Burn-in	5		2	1		12			2	4	44		2	2	2	5		2		2	15		1	1	
	End Life Test	2		1	2		6		3	2	1	44					4			1		14				1

TABLE 6.

CENTRIFUGE FAILURES AFTER HIGH STRESS SCREEN AND LIFE TEST

Process	Centrifuge Stress (Y_1 Axis)	$P = 800$ mW	$P = 700$ mW	$P = 500$ mW	$P = 400$ mW	$P = 200$ mW
		V_{CB}=20 V	V_{CB}=20 V	V_{CB}=20 V	V_{CB}=20 V	V_{CB}=20 V
		$T_A = 25^oC$	$T_A = 25^oC$	$T_A = 25^oC$	$T_A = 150^oC$	$T_A = 150^oC$
A	Initial	14	26	73	14	25
	End 20 Kg	4	4	8	1	1
	End 150 Kg	2	17	47	1	17
B	Initial	10	22	70	13	28
	End 20 Kg	7	9	8	0	0
	End 150 Kg	0	8	1	0	0
C	Initial	--	6	16	--	6
	End 20 Kg		2	1		1
	End 150 Kg		3	11		4

Devices were considered to have failed if they exhibited an electrical open following the test.

The number of devices listed under Initial were the number of devices subjected to the centrifuge test.

TABLE 7.

CENTRIFUGE FAILURES AFTER MODERATE STRESS SCREEN AND LIFE TEST

Process	Centrifuge Stress (Y_1 Axis)	$P = 800$ mW $V_{CB}=20$ V $T_A = 25^{\circ}$C	$P = 700$ mW $V_{CB}=20$ V $T_A = 25^{\circ}$C	$P = 500$ mW $V_{CB}=20$ V $T_A = 25^{\circ}$C	$P = 400$ mW $V_{CB}=20$ V $T_A = 150^{\circ}$C	$P = 200$ mW $V_{CB}=20$ V $T_A = 150^{\circ}$C
A	Initial	13	29	78	14	29
	End 20 Kg	2	0	5	1	0
	End 150 Kg	4	21	55	2	21
B	Initial	14	29	70	14	29
	End 20 Kg	4	4	3	0	1
	End 150 Kg	0	19	49	4	22
C	Initial	14	28	79	10	28
	End 20 Kg	4	1	4	6	1
	End 150 Kg	1	21	55	1	20

Devices were considered to have failed if they exhibited an electrical open following the test.

The number of devices listed under Initial were the number of devices subjected to the centrifuge test.

TABLE 8.

CENTRIFUGE FAILURES AFTER CENTRIFUGE STRESS SCREEN AND LIFE TEST

Process	Centrifuge Stress (Y_1 Axis)	P = 800 mW V_{CB}=20 V T_A = 25°C	P = 700 mW V_{CB}=20 V T_A = 25°C	P = 500 mW V_{CB}=20 V T_A = 25°C	P = 400 mW V_{CB}=20 V T_A = 150°C	P = 200 mW V_{CB}=20 V T_A = 150°C
A	Initial	7	16	39	7	16
	End 20 Kg	1	1	5	0	1
	End 150 Kg	0	11	25	0	11
B	Initial	7	15	40	7	15
	End 20 Kg	4	4	4	0	0
	End 150 Kg	0	7	26	0	11
C	Initial	10	19	52	10	20
	End 20 Kg	6	1	2	3	1
	End 150 Kg	1	2	38	1	14

Devices were considered to have failed if they exhibited an electrical open following the test.

The number of devices listed under Initial were the number of devices subjected to the centrifuge test.

TABLE 9.

CENTRIFUGE FAILURES AFTER NO STRESS SCREEN AND LIFE TEST

Process	Centrifuge Stress (Y_1 Axis)	P = 800 mW	P = 700 mW	P = 500 mW	P = 400 mW	P = 200 mW
		V_{CB}=20 V	V_{CB}=20 V	V_{CB}=20 V	V_{CB}=20 V	V_{CB}=20 V
		T_A = 25°C	T_A = 25°C	T_A = 25°C	T_A = 150°C	T_A = 150°C
A	Initial	7	14	38	7	14
	End 20 Kg	1	0	4	0	0
	End 150 Kg	0	10	26	1	10
B	Initial	6	13	37	7	14
	End 20 Kg	3	1	3	2	0
	End 150 Kg	0	9	24	0	10
C	Initial	10	20	55	10	20
	End 20 Kg	5	1	4	5	2
	End 150 Kg	1	14	38	0	13

Devices were considered to have failed if they exhibited an electrical open following the test.

The number of devices listed under Initial were the number of devices subjected to the centrifuge test.

TABLE 10.

ALL STRESSES COMBINED CENTRIFUGE FAILURES AFTER STRESS SCREEN AND LIFE TEST

Process	Centrifuge Stress (Y_1 Axis)	P = 800 mW V_{CB}=20 V T_A = 25°C	P = 700 mW V_{CB}=20 V T_A = 25°C	P = 500 mW V_{CB}=20 V T_A = 25°C	P = 400 mW V_{CB}=20 V T_A = 150°C	P = 200 mW V_{CB}=20 V T_A = 150°C	All Life Tests Combined
A	Initial	41	85	228	42	84	480
	End 20 Kg	8	5	22	2	2	39
	End 150 Kg	6	59	153	4	59	281
B	Initial	37	79	217	41	86	460
	End 20 Kg	18	18	18	2	1	57
	End 150 Kg	0	43	100	4	43	190
C	Initial	34	73	202	30	74	413
	End 20 Kg	15	5	11	14	5	50
	End 150 Kg	3	40	142	2	51	238

Devices were considered to have failed if they exhibited an electrical open following the test.

The number of devices listed under Initial were the number of devices subjected to the centrifuge test.

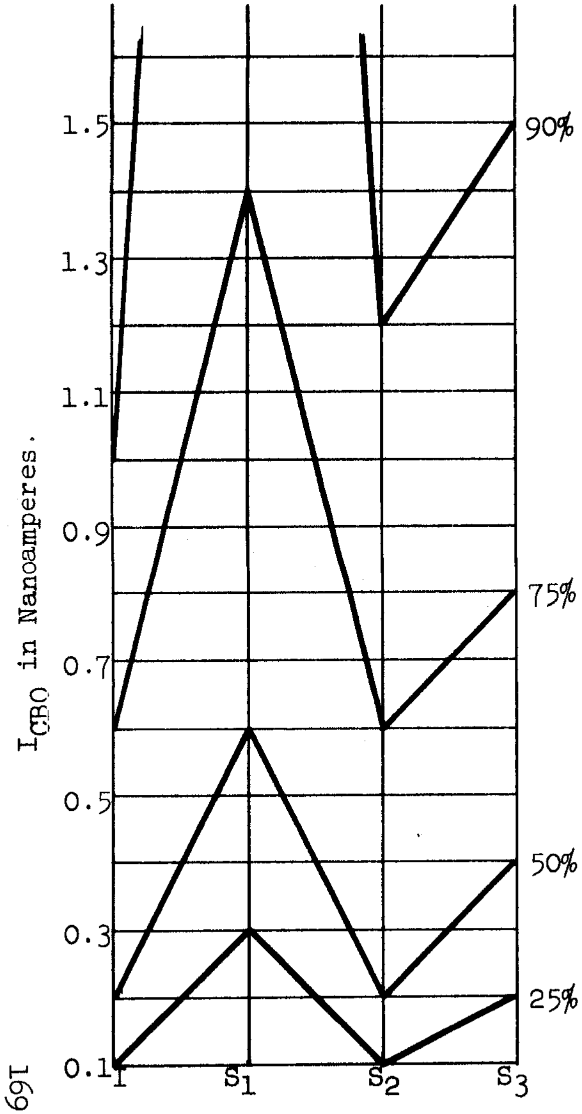

PROCESS: A. TABLE 11.

HIGH STRESS SCREEN.

I_{CBO} DISTRIBUTION (AT V_{CB} = 60 V.).

	INITIAL	S_1	S_2	S_3
MINIMUM	< 0.1	< 0.1	< 0.1	< 0.1
5 PERCENTILE	< 0.1	0.1	< 0.1	< 0.1
10 PERCENTILE	< 0.1	0.2	< 0.1	< 0.1
25 PERCENTILE	0.1	0.3	0.1	0.2
50 PERCENTILE	0.2	0.6	0.2	0.4
75 PERCENTILE	0.6	1.4	0.6	0.8
90 PERCENTILE	1.0	27.5	1.2	1.5
95 PERCENTILE	1.4	657.3	1.4	2.0
MAXIMUM	3.1	6.9 uA	2.3	3.4

Stress S_1 = 168 hours at 250°C., with V_{CB} = 30 V.

Stress S_2 = 168 hours at 300°C.

Stress S_3 = 25 Kg. centrifuge - Y_1 plane only.

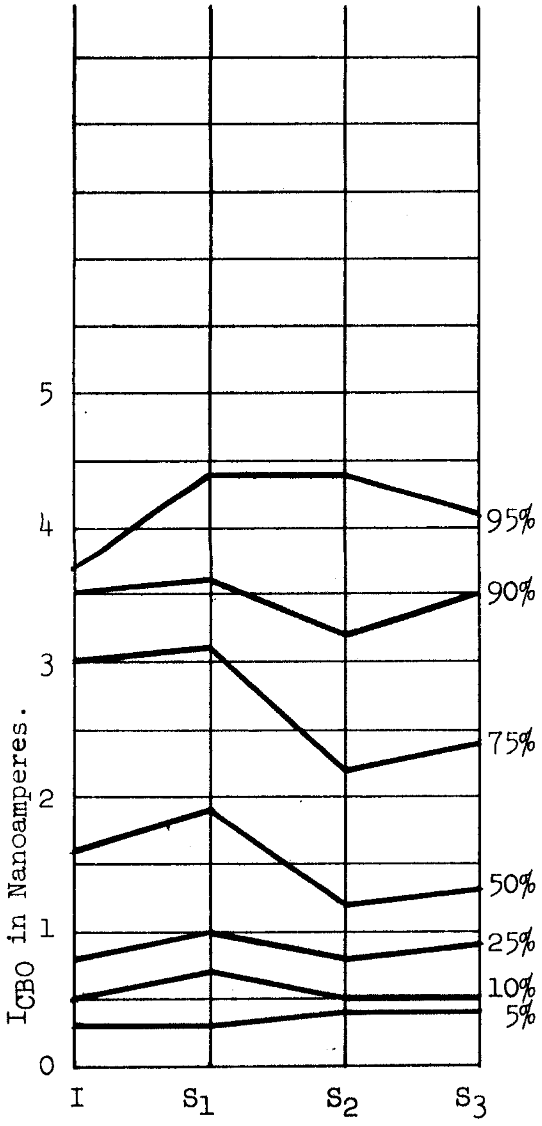

TABLE 12.

PROCESS: B.

HIGH STRESS SCREEN.

I_{CBO} DISTRIBUTION (AT V_{CB} = 60 V.).

	INITIAL	S_1	S_2	S_3
MINIMUM	< 0.1	< 0.1	0.2	< 0.1
5 PERCENTILE	0.3	0.3	0.4	0.4
10 PERCENTILE	0.5	0.7	0.5	0.5
25 PERCENTILE	0.8	1.0	0.8	0.9
50 PERCENTILE	1.6	1.9	1.2	1.3
75 PERCENTILE	3.0	3.1	2.2	2.4
90 PERCENTILE	3.5	3.6	3.2	3.5
95 PERCENTILE	3.7	4.4	4.4	4.1
MAXIMUM	4.2	2.4uA	48uA	42uA

Stress S_1 = 168 hours at 250°C., with V_{CB} = 30 V.

Stress S_2 = 168 hours at 300°C.

Stress S_3 = 25 Kg. centrifuge - Y_1 plane only.

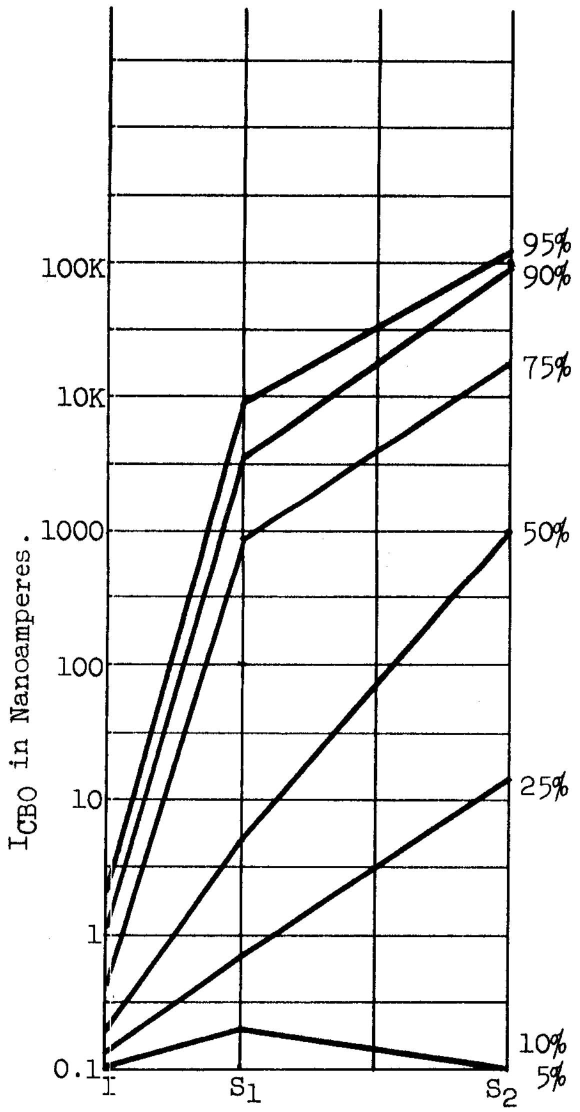

TABLE 13.

PROCESS: C.

HIGH STRESS SCREEN.

I_{CBO} DISTRIBUTION (AT V_{CB} = 60 V.).

	INITIAL	S_1	S_2	S_3 *
MINIMUM	0.1	0.1	0.1	
5 PERCENTILE	0.1	0.2	0.1	
10 PERCENTILE	0.1	0.2	0.1	
25 PERCENTILE	0.1	0.7	13.8	
50 PERCENTILE	0.2	5.0	1 uA	
75 PERCENTILE	0.4	830.0	17.1 uA	
90 PERCENTILE	1.2	3.4 uA	100 uA	
95 PERCENTILE	2.1	8.9 uA	100 uA	
MAXIMUM	2.7	21.0 uA	100 uA	

Stress S_1 = 168 hours at 250°C. with V_{CB} = 30 V.

Stress S_2 = 168 hours at 200°C.

Stress S_3 = 25 Kg. centrifuge - Y_1 plane only.

* Summary Data for S_3 stress not shown due to the severity of S_2 stress and removal of 50% of devices.

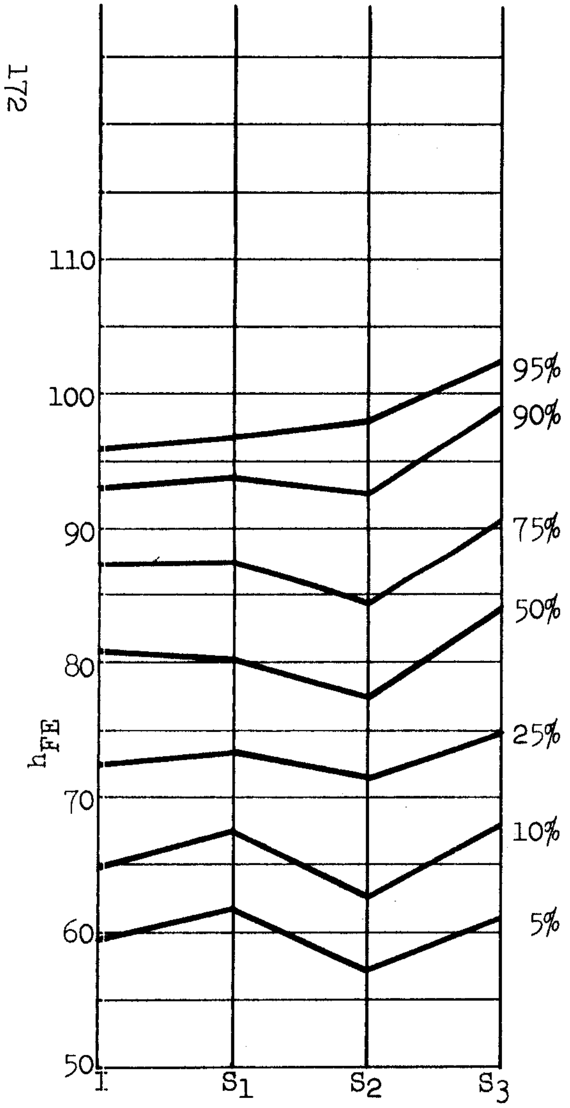

TABLE 14.

PROCESS: A.

HIGH STRESS SCREEN.

h_{FE} DISTRIBUTION (AT I_C = 20 mA., V_{CE} = 5 V.)

	INITIAL	S_1	S_2	S_3
MINIMUM	49.5	47.8	3.5	3.5
5 PERCENTILE	59.5	61.9	57.2	61.0
10 PERCENTILE	64.9	67.5	62.7	67.9
25 PERCENTILE	72.4	73.3	71.5	74.9
50 PERCENTILE	80.9	80.2	77.3	83.9
75 PERCENTILE	87.3	87.6	84.3	90.6
90 PERCENTILE	93.1	93.9	92.7	98.9
95 PERCENTILE	95.9	96.9	98.0	102.3
MAXIMUM	103.7	105.9	109.5	120.8

Stress S_1 = 168 hours at 250°C., with V_{CB} = 30 V.

Stress S_2 = 168 hours at 300°C.

Stress S_3 = 25 Kg. centrifuge - Y_1 plane only.

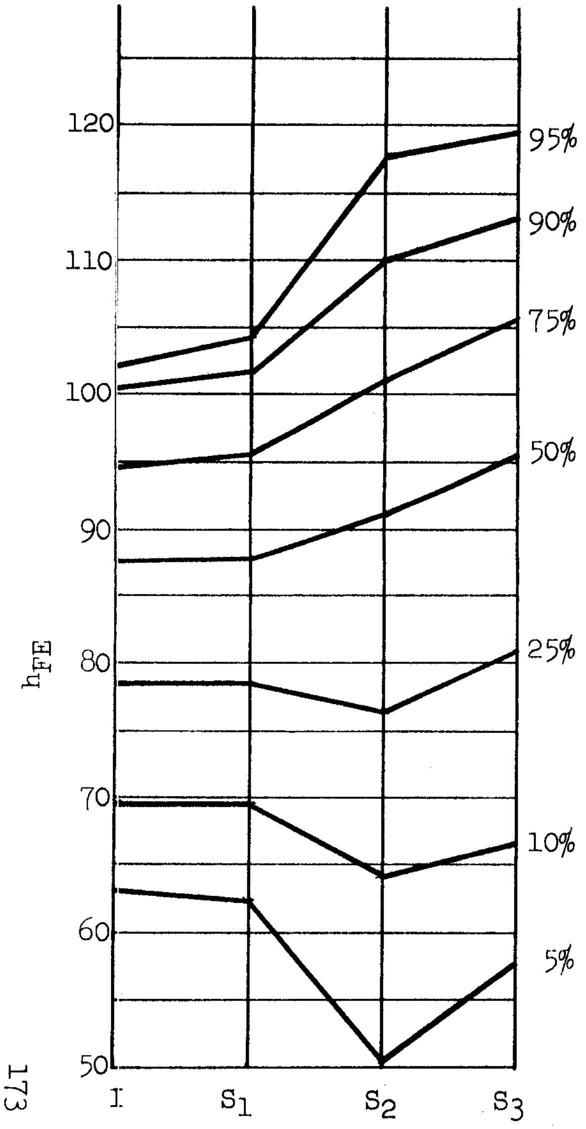

TABLE 15.

PROCESS: B.

HIGH STRESS SCREEN.

h_{FE} DISTRIBUTION (AT I_C = 20 mA., V_{CE} = 5 V.).

	INITIAL	S_1	S_2	S_3
MINIMUM	47.7	52.4	< 20	<20
5 **PERCENTILE**	63.2	62.3	50.6	57.7
10 **PERCENTILE**	69.6	69.6	64.2	66.6
25 **PERCENTILE**	78.5	78.6	76.3	80.9
50 **PERCENTILE**	87.7	88.0	91.2	95.4
75 **PERCENTILE**	94.8	95.7	101.1	105.5
90 **PERCENTILE**	100.5	101.8	110.0	113.1
95 **PERCENTILE**	102.1	104.2	117.8	119.5
MAXIMUM	121.9	107.6	186.8	163.5

Stress S_1 = 168 hours at 250°C., with V_{CB} = 30 V.

Stress S_2 = 168 hours at 300°C.

Stress S_3 = 25 Kg. centrifuge - Y_1 plane only.

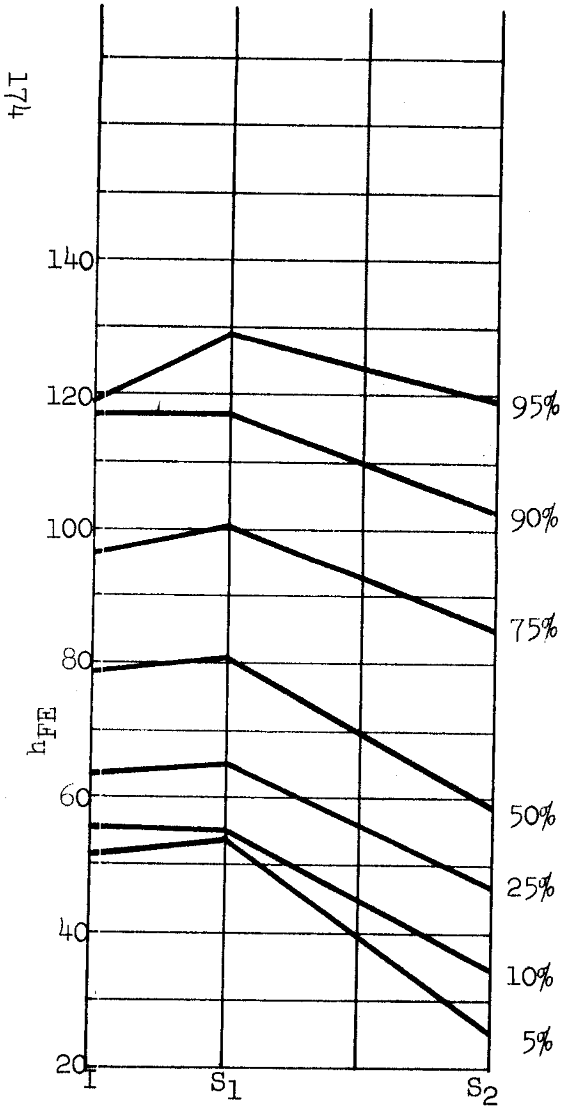

TABLE 16.

PROCESS: C.

HIGH STRESS SCREEN.

h_{FE} DISTRIBUTION (AT I_C = 20 mA., V_{CE} = 5 V.).

	INITIAL	S_1	S_2	S_3 *
MINIMUM	47.3	53.5	20	
5 PERCENTILE	51.4	54.0	25.4	
10 PERCENTILE	55.3	54.7	34.4	
25 PERCENTILE	63.6	65.1	46.9	
50 PERCENTILE	78.5	80.8	58.6	
75 PERCENTILE	96.3	100.4	85.3	
90 PERCENTILE	116.9	117.2	103.1	
95 PERCENTILE	119.2	129.0	119.5	
MAXIMUM	125.9	>200	200	

Stress S_1 = 168 hours at 250°C. with V_{C3} = 30 V.

Stress S_2 = 168 hours at 300°C.

Stress S_3 = 25 Kg. centrifuge - Y_1 plane only.

* Summary Data for S_3 stress not shown due to the severity of S_2 stress and removal of 50% of devices.

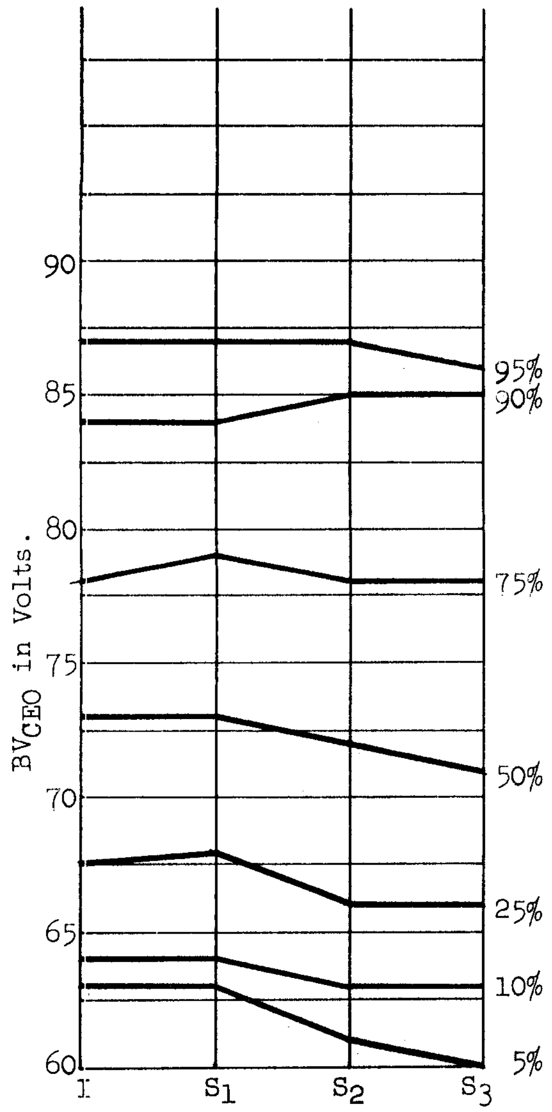

TABLE 17.

PROCESS: B.

HIGH STRESS SCREEN.

BV_{CEO} DISTRIBUTION (AT I_C = 100 uA.).

	INITIAL	S_1	S_2	S_3
MINIMUM	62	55	8	8
5 PERCENTILE	63	63	61	60
10 PERCENTILE	64	64	63	63
25 PERCENTILE	67.5	68	66	66
50 PERCENTILE	73	73	72	71
75 PERCENTILE	78	79	78	78
90 PERCENTILE	84	84	85	85
95 PERCENTILE	87	87	87	86
MAXIMUM	93	93	105	101

Stress S_1 = 168 hours at 250°C., with V_{CB} = 30 V.

Stress S_2 = 168 hours at 300°C.

Stress S_3 = 25 Kg. centrifuge - Y_1 plane only.

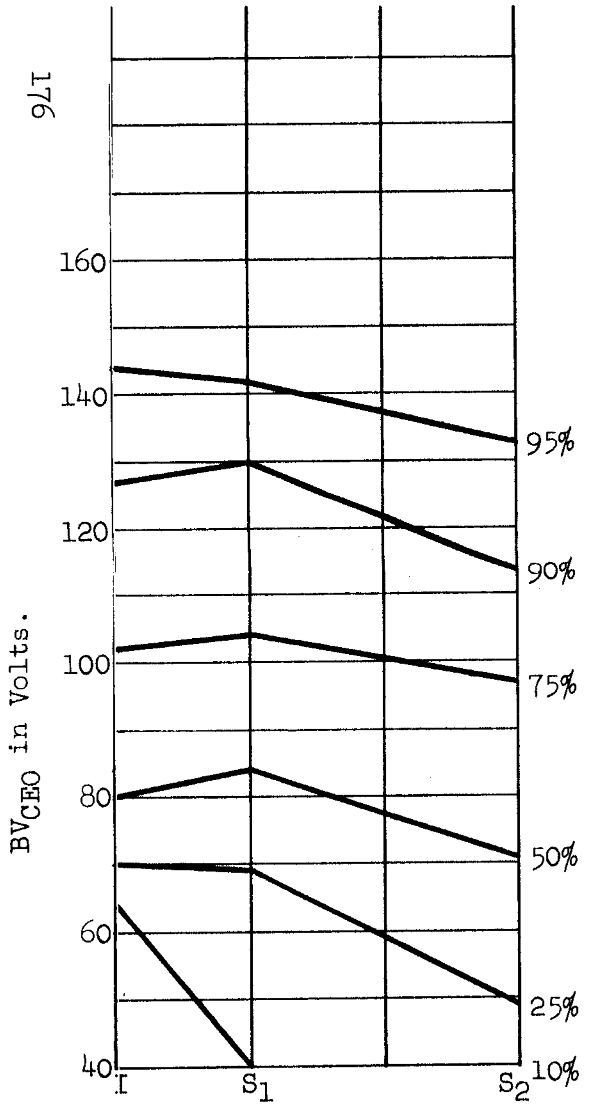

TABLE 18.

PROCESS: C.

HIGH STRESS SCREEN.

BV$_{CEO}$ DISTRIBUTION (AT I_C = 100 uA.).

	INITIAL	S_1	S_2	S_3 *
MINIMUM	56	4	0	
5 PERCENTILE	62	5	1	
10 PERCENTILE	64	40	8	
25 PERCENTILE	70	69	49	
50 PERCENTILE	80	84	71	
75 PERCENTILE	102	104	97	
90 PERCENTILE	127	130	114	
95 PERCENTILE	144	142	133	
MAXIMUM	152	174	220 **	

Stress S_1 = 168 hours at 250°C., with V_{CB} = 30 V.

Stress S_2 = 168 hours at 300°C.

Stress S_3 = 25 Kg. centrifuge - Y_1 plane only.

* Summary Data for S_3 stress not shown due to the severity of S_2 stress and removal of 50% of devices.

** Appears as open emitter.

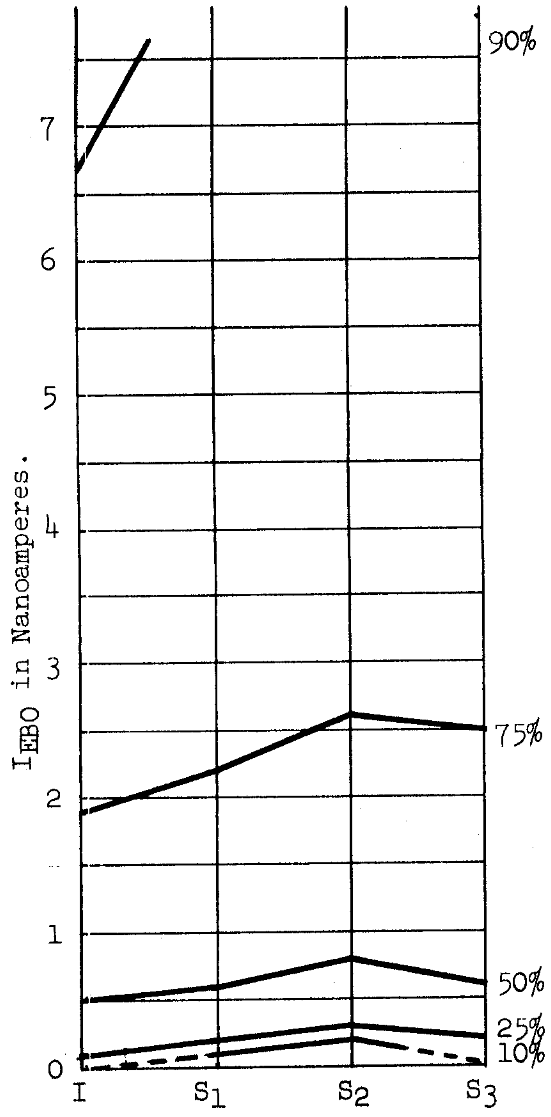

TABLE 19.

PROCESS; B.

HIGH STRESS SCREEN.

I_{EBO} DISTRIBUTION (AT V_{EB} = 5 V.).

	INITIAL	S_1	S_2	S_3
MINIMUM	< 0.1	< 0.1	< 0.1	< 0.1
5 PERCENTILE	< 0.1	< 0.1	0.1	< 0.1
10 PERCENTILE	< 0.1	0.1	0.2	< 0.1
25 PERCENTILE	0.1	0.2	0.3	0.2
50 PERCENTILE	0.5	0.6	0.8	0.6
75 PERCENTILE	1.9	2.2	2.6	2.5
90 PERCENTILE	6.7	8.5	10.6	7.8
95 PERCENTILE	16.2	22.3	34.3	19.5
MAXIMUM	104.1	61.3	240.2	237.6

Stress S_1 = 168 hours at 250°C., with V_{CB} = 30 V.

Stress S_2 = 168 hours at 300°C.

Stress S_3 = 25 Kg. centrifuge - Y_1 plane only.

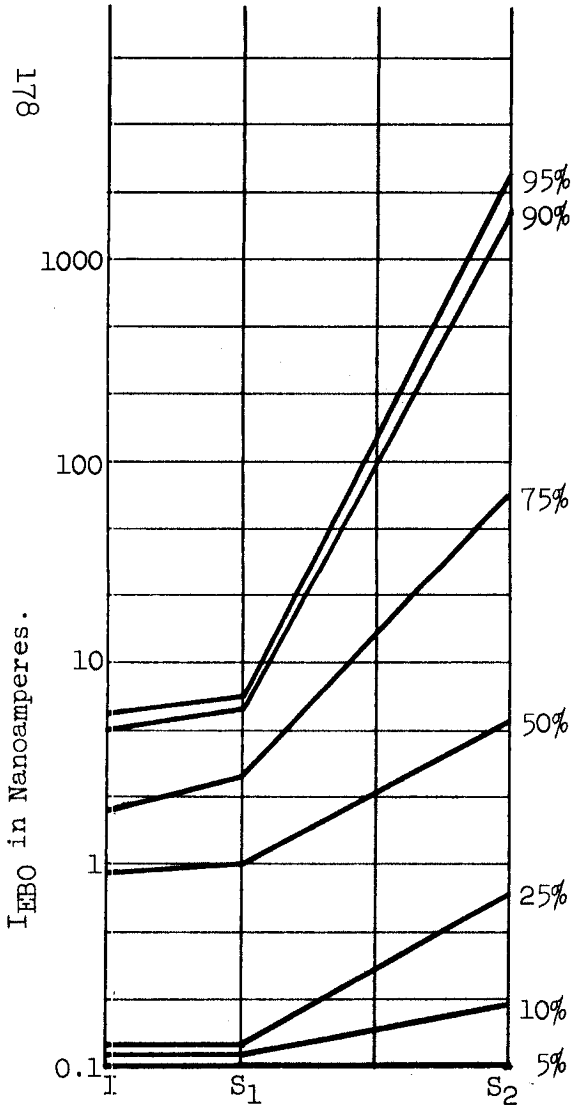

TABLE 20.

PROCESS: C.

HIGH STRESS SCREEN.

I_{EBO} DISTRIBUTION (AT V_{EB} = 5 V.).

	INITIAL	S_1	S_2	S_3 *
MINIMUM	0.1	0.1	0.1	
5 PERCENTILE	0.1	0.1	0.1	
10 PERCENTILE	0.1	0.1	0.2	
25 PERCENTILE	0.1	0.1	0.7	
50 PERCENTILE	0.9	1.0	5.0	
75 PERCENTILE	1.8	2.7	69.7	
90 PERCENTILE	4.4	5.5	1.7 uA	
95 PERCENTILE	5.3	6.7	2.5 uA	
MAXIMUM	9.6	21.8	23.9 uA	

Stress S_1 = 168 hours at 250°C., with V_{CB} = 30 V.

Stress S_2 = 168 hours at 300°C.

Stress S_3 = 25 Kg. centrifuge - Y_1 plane only.

* Summary Data for S_3 stress not shown due to the severity of S_2 stress and removal of 50% of devices.

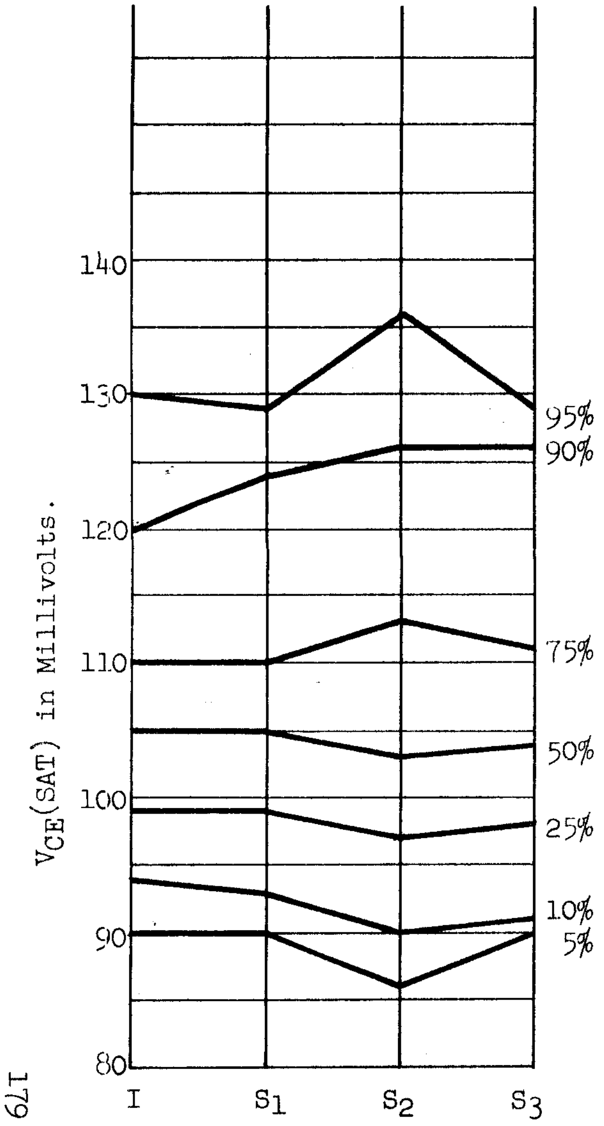

TABLE 21.

PROCESS: B.

HIGH STRESS SCREEN.

V_{CE}(SAT) DISTRIBUTION (AT I_C = 50 mA., I_B = 5 mA.).

	INITIAL	S_1	S_2	S_3
MINIMUM	75	73	75	84
5 PERCENTILE	90	90	86	90
10 PERCENTILE	94	93	90	91
25 PERCENTILE	99	99	97	98
50 PERCENTILE	105	105	103	104
75 PERCENTILE	110	110	113	111
90 PERCENTILE	120	124	126	126
95 PERCENTILE	130	129	136	129
MAXIMUM	135	155	>10 V	>10 V

Stress S_1 = 168 hours at 250°C., with V_{CB} = 30 V.

Stress S_2 = 168 hours at 300°C.

Stress S_3 = 25 Kg. centrifuge - Y_1 plane only.

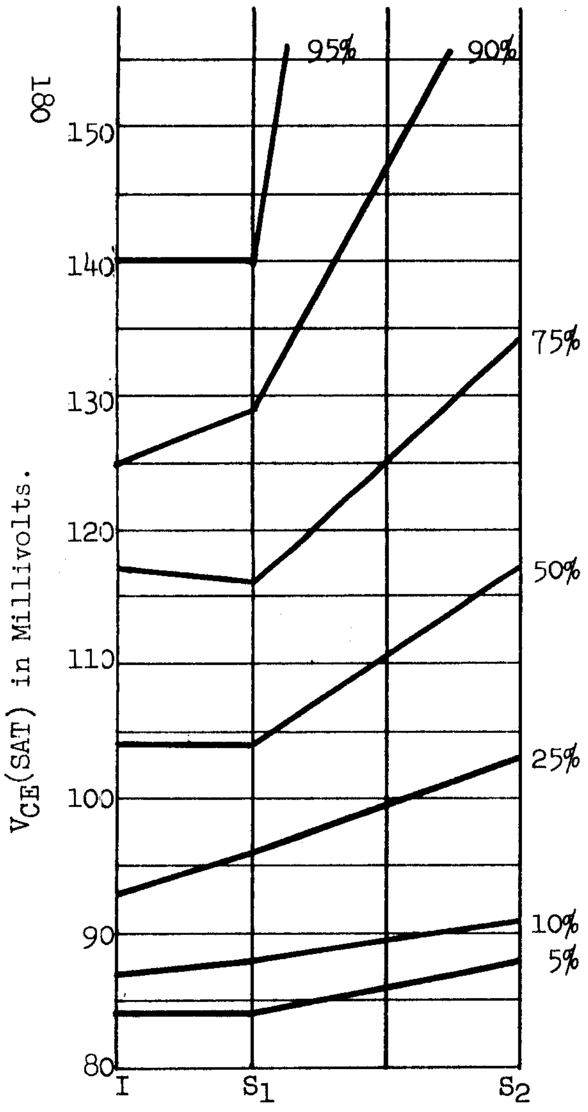

TABLE 22.

PROCESS: C.

HIGH STRESS SCREEN.

V_{CE}(SAT) DISTRIBUTION (AT I_C = 50 mA., I_B = 5 mA.).

	INITIAL	S_1	S_2	S_3 *
MINIMUM	80	83	80	
5 PERCENTILE	84	84	88	
10 PERCENTILE	87	88	91	
25 PERCENTILE	93	96	103	
50 PERCENTILE	104	104	117	
75 PERCENTILE	117	116	134	
90 PERCENTILE	125	129	165	
95 PERCENTILE	140	140	434	
MAXIMUM	146	148	10 V	

Stress S_1 = 168 hours at 250°C., with V_{CB} = 30 V.

Stress S_2 = 168 hours at 300°C.

Stress S_3 = 25 Kg. centrifuge - Y_1 plane only.

* Summary Data for S_3 stress not shown due to the severity of S_2 stress and removal of 50% of devices.

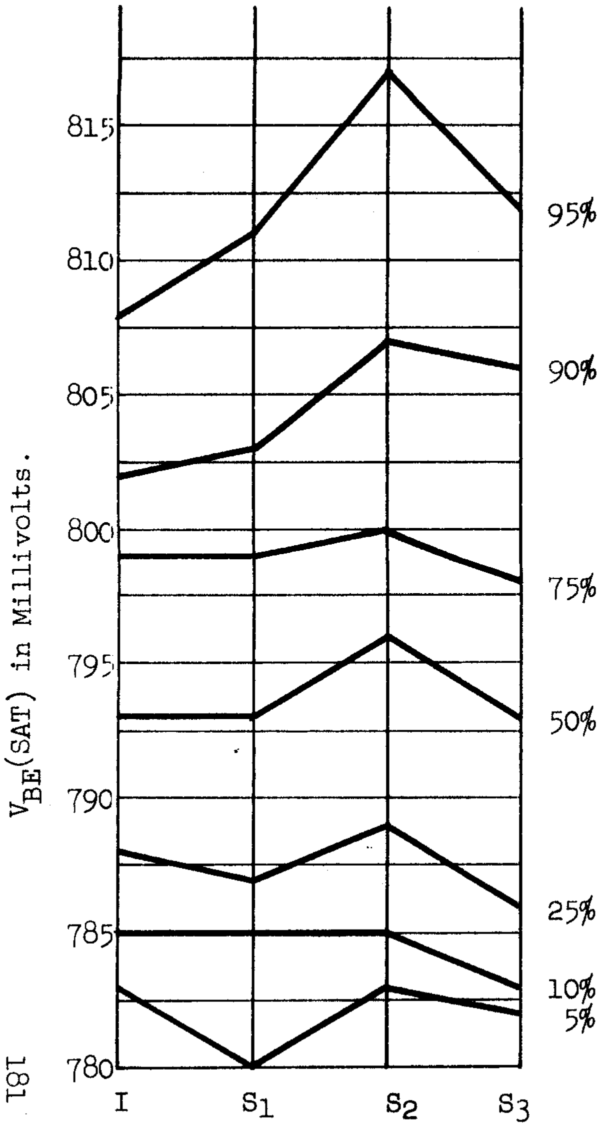

TABLE 23.

PROCESS: B.

HIGH STRESS SCREEN.

V_{BE}(SAT) DISTRIBUTION (AT I_C = 50 mA., I_B = 5 mA.).

	INITIAL	S_1	S_2	S_3
MINIMUM	780	779	718	779
5 PERCENTILE	783	780	783	782
10 PERCENTILE	785	785	785	783
25 PERCENTILE	788	787	789	786
50 PERCENTILE	793	793	796	793
75 PERCENTILE	799	799	800	798
90 PERCENTILE	802	803	807	806
95 PERCENTILE	808	811	817	812
MAXIMUM	819	837	>10 V	>10 V

Stress S_1 = 168 hours at 250°C., with V_{CB} = 30 V.

Stress S_2 = 168 hours at 300°C.

Stress S_3 = 25 Kg. centrifuge - Y_1 plane only.

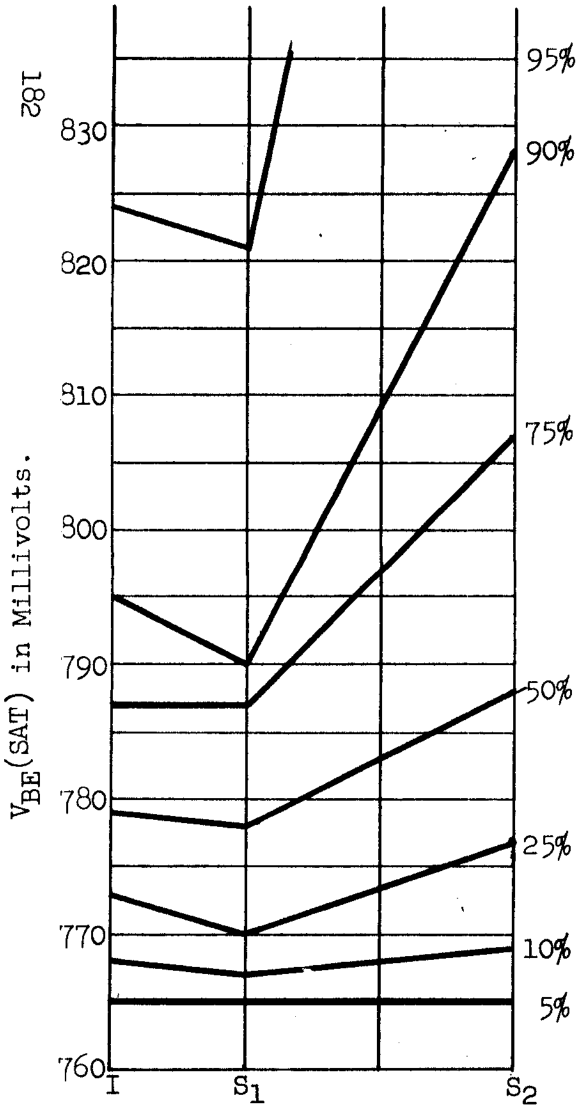

TABLE 24.

PROCESS: C.

HIGH STRESS SCREEN.

V_{BE}(SAT) DISTRIBUTION (AT I_C = 50 mA., I_B = 5 mA.).

	INITIAL	S_1	S_2	S_3 *
MINIMUM	762	758	758	
5 PERCENTILE	765	765	765	
10 PERCENTILE	768	767	769	
25 PERCENTILE	773	770	777	
50 PERCENTILE	779	778	788	
75 PERCENTILE	787	787	807	
90 PERCENTILE	795	790	828	
95 PERCENTILE	824	821	916	
MAXIMUM	842	829	> 10 V	

Stress S_1 = 168 hours at 250°C., with V_{CB} = 30 V.

Stress S_2 = 168 hours at 300°C.

Stress S_3 = 25 Kg. centrifuge - Y_1 plane only.

* Summary Data for S_3 stress not shown due to the severity of S_2 stress and removal of 50% of devices.

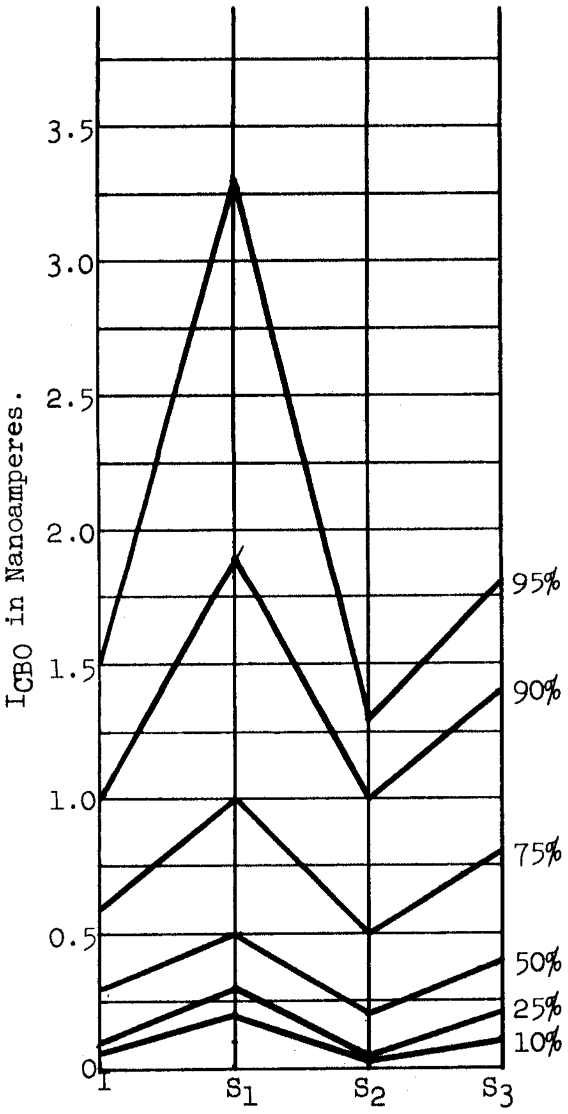

TABLE 25.

PROCESS: A.

MODERATE STRESS SCREEN.

I_{CBO} DISTRIBUTION (AT V_{CB} = 60 V.).

	INITIAL	S_1	S_2	S_3
MINIMUM	< 0.1	< 0.1	< 0.1	< 0.1
5 PERCENTILE	< 0.1	0.1	< 0.1	0.1
10 PERCENTILE	< 0.1	0.2	< 0.1	0.1
25 PERCENTILE	0.1	0.3	< 0.1	0.2
50 PERCENTILE	0.3	0.5	0.2	0.4
75 PERCENTILE	0.6	1.0	0.5	0.8
90 PERCENTILE	1.0	1.9	1.0	1.4
95 PERCENTILE	1.5	3.3	1.3	1.8
MAXIMUM	2.5	320.2	25.4	26.1

Stress S_1 = 168 hours at 200°C., with V_{CB} = 30 V.

Stress S_2 = 168 hours at 200°C.

Stress S_3 = 25 Kg. centrifuge - Y_1 plane only.

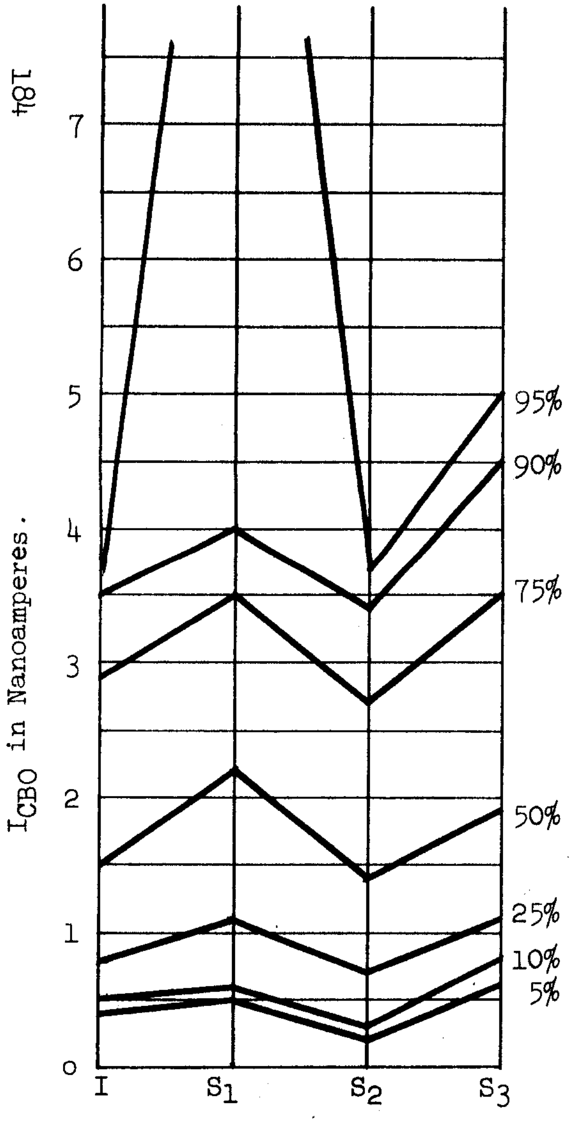

TABLE 26.

PROCESS: B.

MODERATE STRESS SCREEN.

I_{CBO} DISTRIBUTION (AT V_{CB} = 60 V.).

	INITIAL	S_1	S_2	S_3
MINIMUM	0.1	< 0.1	< 0.1	0.1
5 PERCENTILE	0.4	0.5	0.2	0.6
10 PERCENTILE	0.5	0.6	0.3	0.8
25 PERCENTILE	0.8	1.1	0.7	1.1
50 PERCENTILE	1.5	2.2	1.4	1.9
75 PERCENTILE	2.9	3.5	2.7	3.5
90 PERCENTILE	3.5	4.0	3.4	4.5
95 PERCENTILE	3.7	11.7	3.7	5.0
MAXIMUM	4.9	197 uA	4.5	6.1

Stress S_1 = 168 hours at 200°C., with V_{CB} = 30 V.

Stress S_2 = 168 hours at 200°C.

Stress S_3 = 25 Kg. centrifuge - Y_1 plane only.

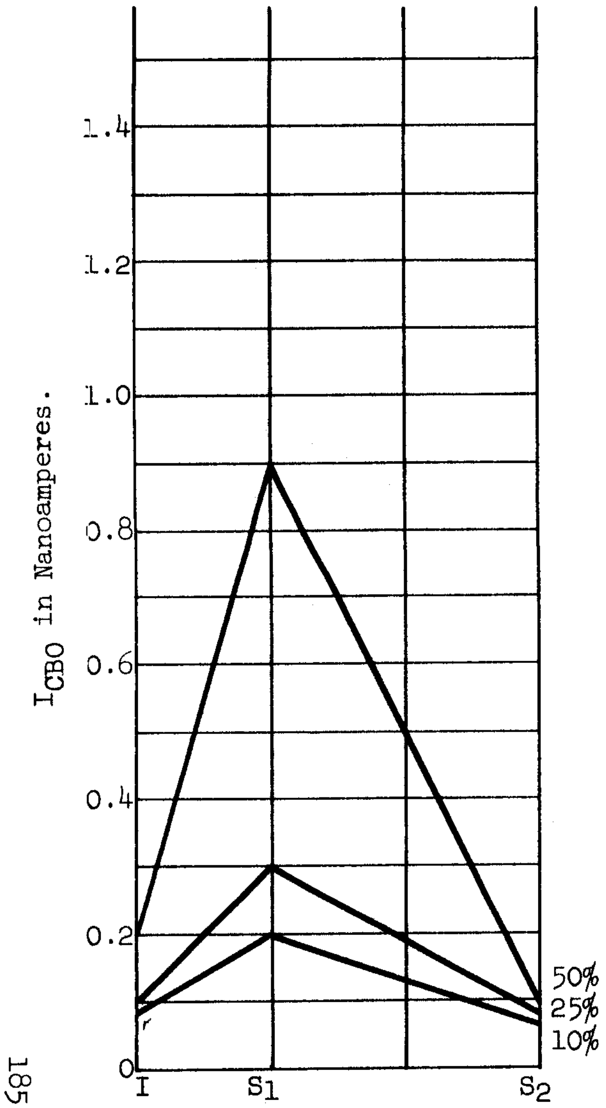

TABLE 27.

PROCESS: C.

MODERATE STRESS SCREEN.

I_{CBO} DISTRIBUTION (AT V_{CB} = 60 V.).

	INITIAL	S_1	S_2	S_3 *
MINIMUM	< 0.1	< 0.1	< 0.1	
5 PERCENTILE	< 0.1	< 0.1	< 0.1	
10 PERCENTILE	< 0.1	0.2	< 0.1	
25 PERCENTILE	0.1	0.3	< 0.1	
50 PERCENTILE	0.2	0.9	0.1	
75 PERCENTILE	0.4	11.2	0.3	
90 PERCENTILE	1.1	3.1 uA	1.5	
95 PERCENTILE	1.5	10.5 uA	22.4	
MAXIMUM	12.0	17.5 uA	17.4 uA	

Stress S_1 = 168 hours at 200°C., with V_{CB} = 30 V.

Stress S_2 = 168 hours at 200°C.

Stress S_3 = 25 Kg. centrifuge - Y_1 plane only.

* Summary Data of S_3 stress not shown due to removal of 16% of units after S_2 stress.

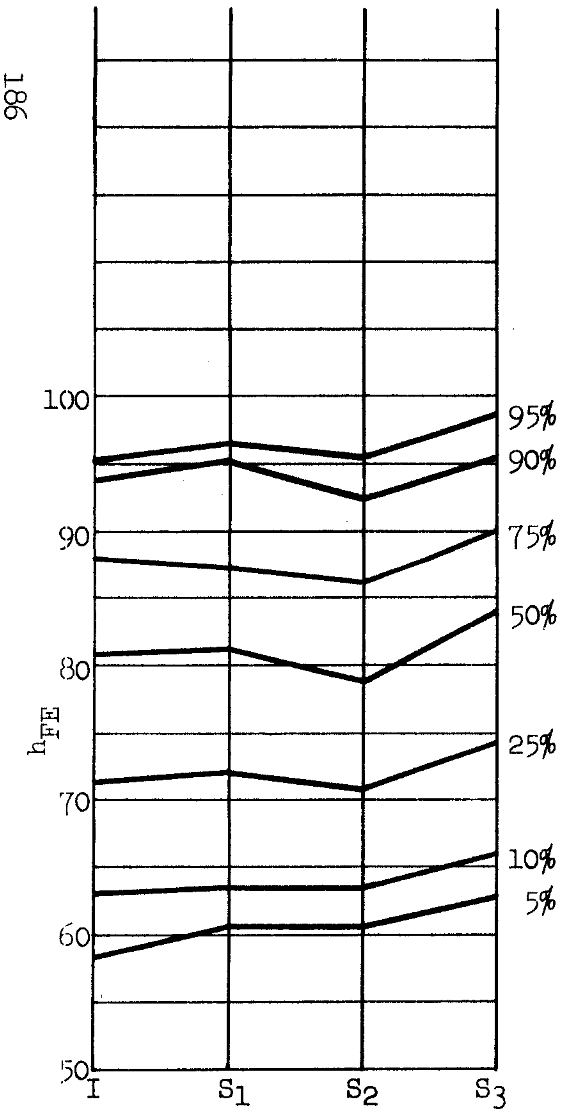

TABLE 28.

PROCESS: A.

MODERATE STRESS SCREEN.

h_{FE} DISTRIBUTION (AT I_C = 20 mA., V_{CE} = 5 V.).

	INITIAL	S_1	S_2	S_3
MINIMUM	36.9	43.0	49.5	50.6
5 PERCENTILE	58.4	60.7	60.7	62.9
10 PERCENTILE	63.0	63.4	63.3	66.1
25 PERCENTILE	71.3	72.1	70.8	74.3
50 PERCENTILE	80.9	81.2	78.9	84.1
75 PERCENTILE	88.1	87.2	86.1	90.0
90 PERCENTILE	93.9	95.2	92.5	95.5
95 PERCENTILE	95.2	96.6	95.4	98.7
MAXIMUM	99.5	101.0	103.7	105.5

Stress S_1 = 168 hours at 200°C., with V_{CB} = 30 V.

Stress S_2 = 168 hours at 200°C.

Stress S_3 = 25 Kg. centrifuge - Y_1 plane only.

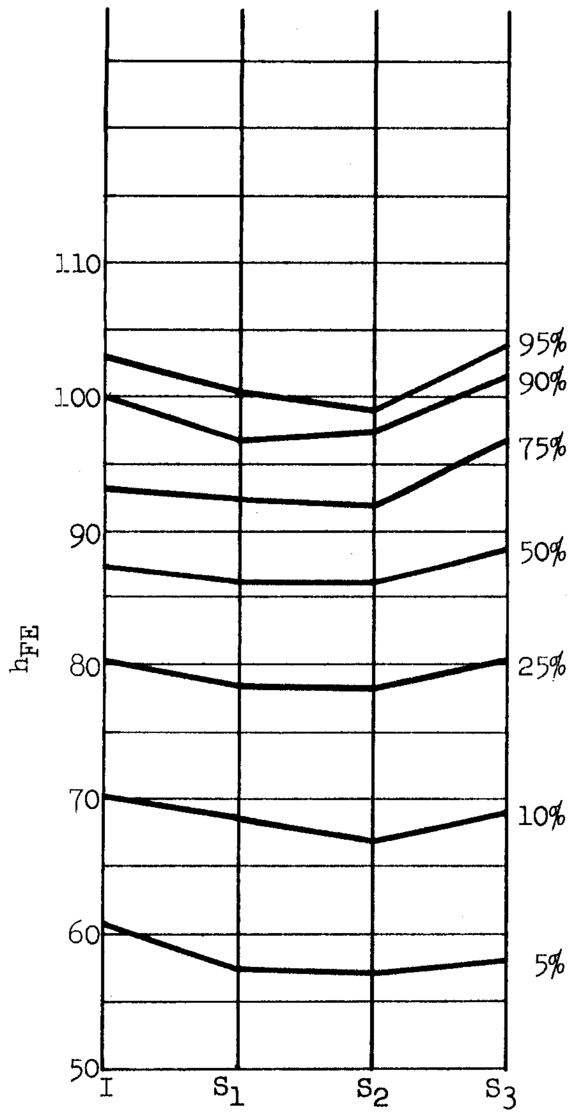

TABLE 29.

PROCESS: B.

MODERATE STRESS SCREEN.

h_{FE} DISTRIBUTION (AT I_C = 20 mA., V_{CE} = 5 V.).

	INITIAL	S_1	S_2	S_3
MINIMUM	56.5	< 20.0	< 27.0	< 2.0
5 PERCENTILE	60.8	57.6	57.2	58.0
10 PERCENTILE	70.1	68.7	66.9	69.0
25 PERCENTILE	80.2	78.6	78.3	80.2
50 PERCENTILE	87.3	86.1	86.1	88.7
75 PERCENTILE	93.2	92.5	92.1	96.7
90 PERCENTILE	99.9	96.9	97.5	101.4
95 PERCENTILE	103.0	100.3	99.0	103.7
MAXIMUM	159.2	105.3	107.6	107.9

Stress S_1 = 168 hours at 200°C., with V_{CB} = 30 V.

Stress S_2 = 168 hours at 200°C.

Stress S_3 = 25 Kg. centrifuge - Y_1 plane only.

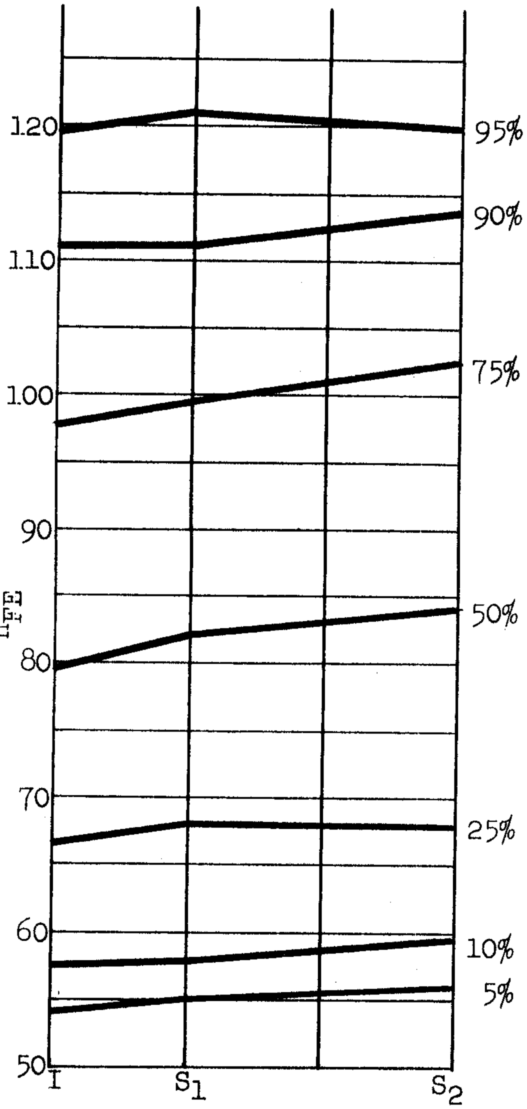

TABLE 30.

PROCESS: C.

MODERATE STRESS SCREEN.

h_{FE} DISTRIBUTION (AT I_C = 20 mA., V_{CE} = 5 V.).

	INITIAL	S_1	S_2	S_3 *
MINIMUM	49.5	49.4	51.0	
5 PERCENTILE	54.1	55.1	56.0	
10 PERCENTILE	57.6	58.0	59.5	
25 PERCENTILE	66.7	68.1	67.9	
50 PERCENTILE	79.7	82.1	84.0	
75 PERCENTILE	97.8	99.5	102.6	
90 PERCENTILE	111.1	111.2	113.7	
95 PERCENTILE	119.7	121.0	119.9	
MAXIMUM	138.9	167.8	133.6	

Stress S_1 = 168 hours at 200°C., with V_{CB} = 30 V.

Stress S_2 = 168 hours at 200°C.

Stress S_3 = 25 Kg. centrifuge - Y_1 plane only.

* Summary Data for S_3 stress not shown due to removal of 16% of units after S_2 stress.

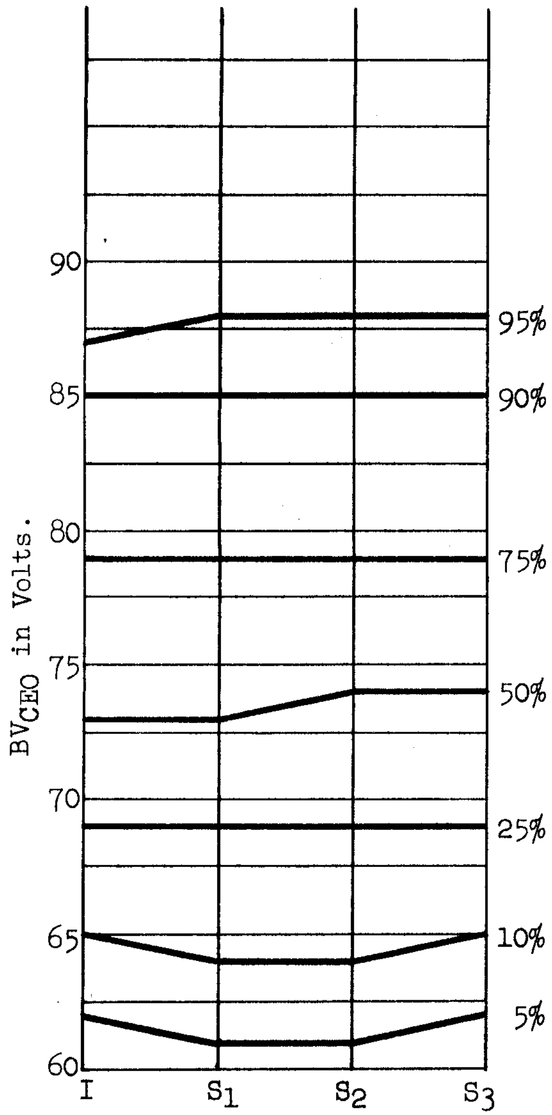

TABLE 31.

PROCESS: B.

MODERATE STRESS SCREEN.

BV$_{CEO}$ DISTRIBUTION (AT I_C = 100 uA.).

	INITIAL	S_1	S_2	S_3
MINIMUM	59	52	59	60
5 PERCENTILE	62	61	61	62
10 PERCENTILE	65	64	64	65
25 PERCENTILE	69	69	69	69
50 PERCENTILE	73	73	74	74
75 PERCENTILE	79	79	79	79
90 PERCENTILE	85	85	85	85
95 PERCENTILE	87	88	88	88
MAXIMUM	94	95	106	106

Stress S_1 = 168 hours at 200°C., with V_{CB} = 30 V.

Stress S_2 = 168 hours at 200°C.

Stress S_3 = 25 Kg. centrifuge - Y_1 plane only.

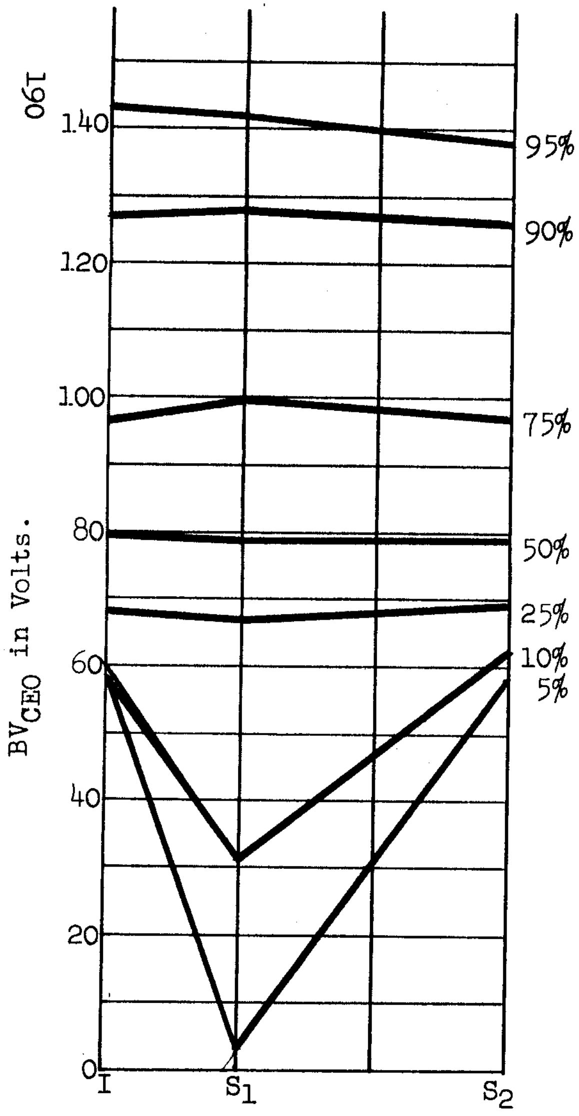

TABLE 32.

PROCESS: C.

MODERATE STRESS SCREEN.

BV$_{CEO}$ IDSTRIBUTION (AT I_C = 100 uA.).

	INITIAL	S_1	S_2	S_3 *
MINIMUM	45.2	0.6	56	
5 PERCENTILE	58.0	3.3	58	
10 PERCENTILE	60.0	31.3	62	
25 PERCENTILE	68.0	67.0	69	
50 PERCENTILE	79.4	79.0	79	
75 PERCENTILE	96.4	99.6	97	
90 PERCENTILE	127.0	128.0	126	
95 PERCENTILE	143.0	142.0	138	
MAXIMUM	159.0	170.0	160	

Stress S_1 = 168 hours at 200°C., with V_{CB} = 30 V.

Stress S_2 = 168 hours at 200°C.

Stress S_3 = 25 Kg. centrifuge - Y_1 plane only.

* Summary Data for S_3 stress not shown due to removal of 16% of units after S_2 stress.

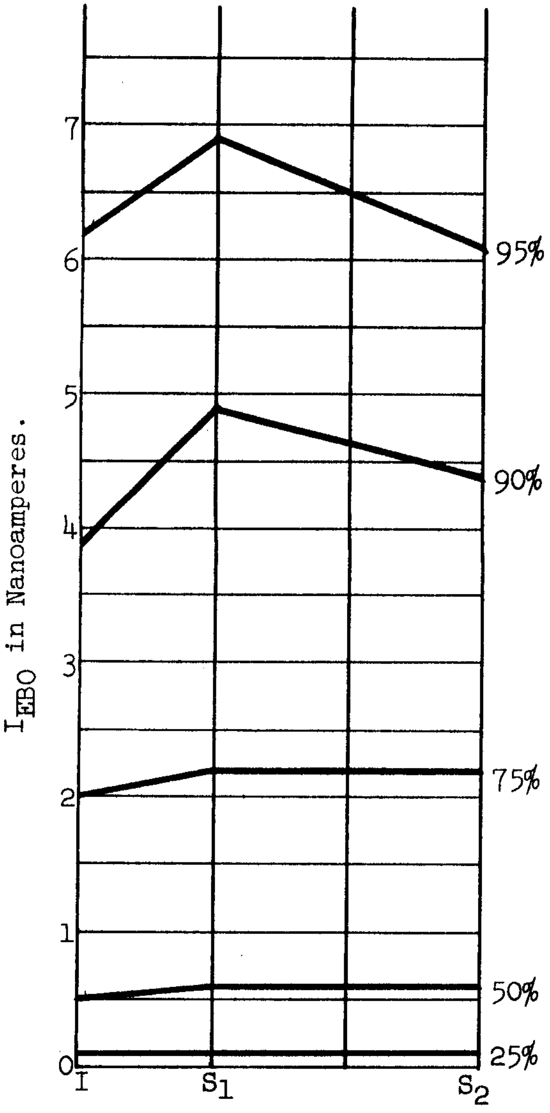

TABLE 33.

PROCESS: C.

MODERATE STRESS SCREEN.

I_{EBO} DISTRIBUTION (AT V_{EB} = 5 V.).

	INITIAL	S_1	S_2	S_3 *
MINIMUM	< 0.1	< 0.1	< 0.1	
5 PERCENTILE	< 0.1	< 0.1	< 0.1	
10 PERCENTILE	< 0.1	< 0.1	< 0.1	
25 PERCENTILE	0.1	0.1	0.1	
50 PERCENTILE	0.5	0.6	0.6	
75 PERCENTILE	2.0	2.2	2.2	
90 PERCENTILE	3.9	4.9	4.4	
95 PERCENTILE	6.2	6.9	6.1	
MAXIMUM	9.2	11.2	9.4	

Stress S_1 = 168 hours at 200°C., with V_{CB} = 30 V.

Stress S_2 = 168 hours at 200°C.

Stress S_3 = 25 Kg. centrifuge - Y_1 plane only.

* Summary Data for S_3 stress not shown due to removal of 16% of units after S_2 stress.

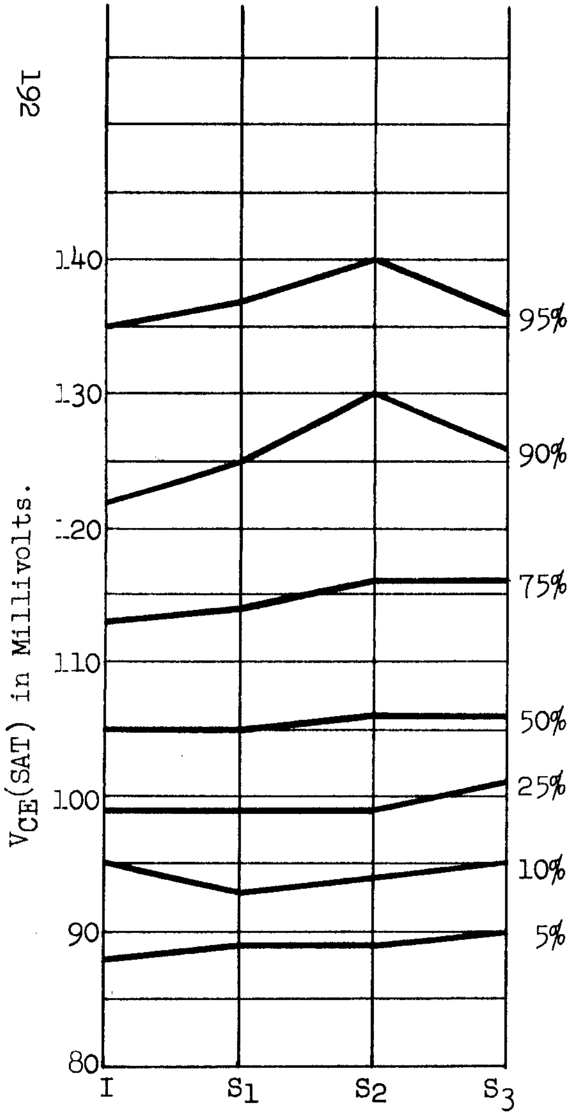

TABLE 34.

PROCESS: B.

MODERATE STRESS SCREEN.

V_{CE}(SAT) **DISTRIBUTION** (AT I_C = 50 mA., I_B = 5 mA.).

	INITIAL	S_1	S_2	S_3
MINIMUM	85	83	84	84
5 PERCENTILE	88	89	89	90
10 PERCENTILE	95	93	94	95
25 PERCENTILE	99	99	99	101
50 PERCENTILE	105	105	106	106
75 PERCENTILE	113	114	116	116
90 PERCENTILE	122	125	130	126
95 PERCENTILE	135	137	140	136
MAXIMUM	140	>10 V	>10 V	>10 V

Stress S_1 = 168 hours at 200°C., with V_{CB} = 30 V.

Stress S_2 = 168 hours at 200°C.

Stress S_3 = 25 Kg. centrifuge - Y_1 plane only.

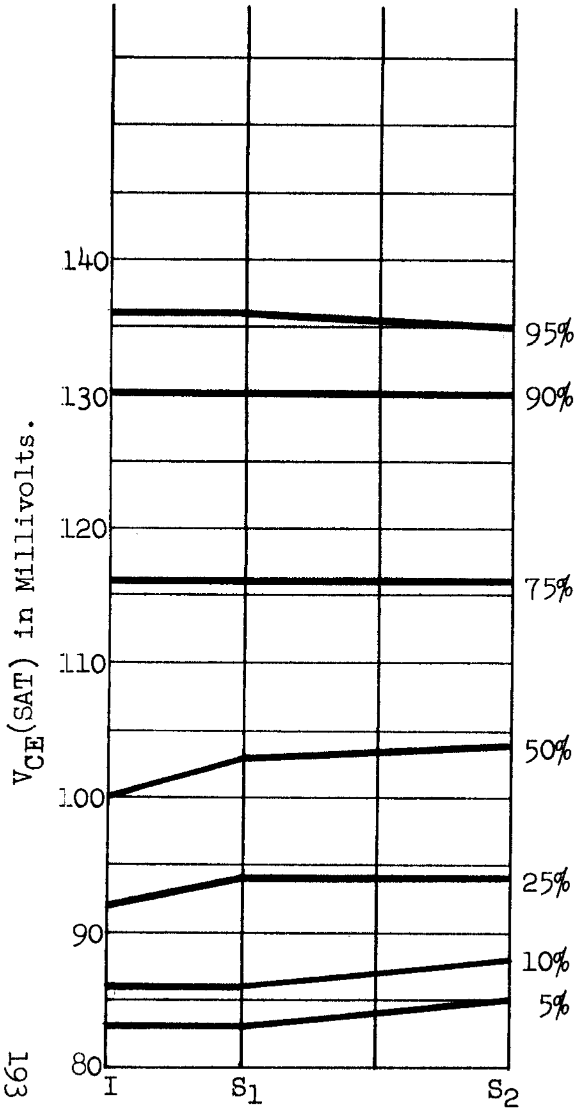

TABLE 35.

PROCESS: C.

MODERATE STRESS SCREEN.

V_{CE}(SAT) **DISTRIBUTION** (AT I_C = 50 mA., I_B = 5 mA.).

	INITIAL	S_1	S_2	S_3 *
MINIMUM	78	77	78	
5 PERCENTILE	83	83	85	
10 PERCENTILE	86	86	88	
25 PERCENTILE	92	94	94	
50 PERCENTILE	100	103	104	
75 PERCENTILE	116	116	116	
90 PERCENTILE	130	130	130	
95 PERCENTILE	136	136	135	
MAXIMUM	147	150	150	

Stress S_1 = 168 hours at 200°C., with V_{CB} = 30 V.

Stress S_2 = 168 hours at 200°C.

Stress S_3 = 25 Kg. centrifuge - Y_1 plane only.

* Summary Data for S_3 stress not shown due to removal of 16% of units after S_2 stress.

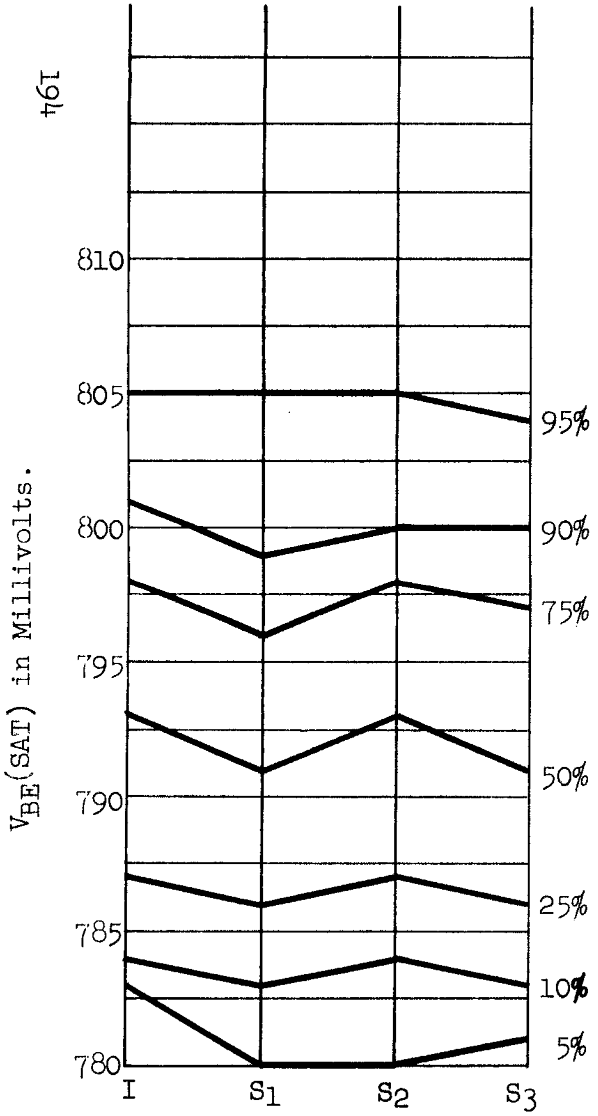

TABLE 36.

PROCESS: B.

MODERATE STRESS SCREEN.

V_{BE}(SAT) DISTRIBUTION (AT I_C = 50 mA, I_B = 5 mA.).

	INITIAL	S_1	S_2	S_3
MINIMUM	780	778	720	779
5 PERCENTILE	783	780	780	781
10 PERCENTILE	784	783	784	783
25 PERCENTILE	787	786	787	786
50 PERCENTILE	793	791	793	791
75 PERCENTILE	798	796	798	797
90 PERCENTILE	801	799	800	800
95 PERCENTILE	805	805	805	804
MAXIMUM	826	>10 V	>10 V	>10 V

Stress S_1 = 168 hours at 200°C., with V_{CB} = 30 V.

Stress S_2 = 168 hours at 200°C.

Stress S_3 = 25 Kg. centrifuge - Y_1 plane only.

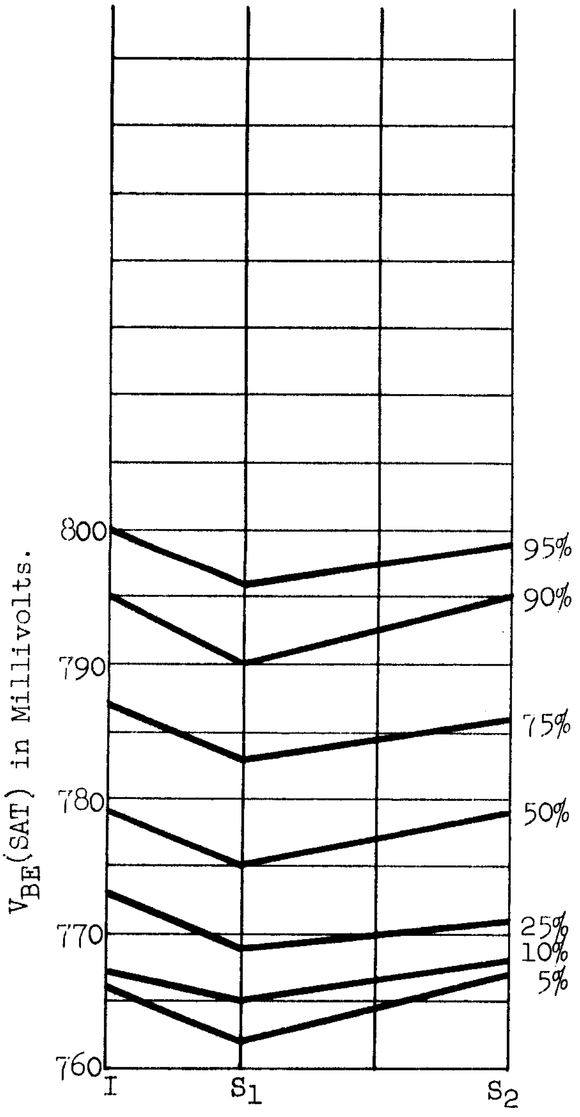

TABLE 37.

PROCESS: C.

MODERATE STRESS SCREEN.

V_{BE}(SAT) DISTRIBUTION (AT I_C = 50 mA., I_B = 5 mA.).

	INITIAL	S_1	S_2	S_3 *
MINIMUM	757	757	760	
5 PERCENTILE	766	762	767	
10 PERCENTILE	767	765	768	
25 PERCENTILE	773	769	771	
50 PERCENTILE	779	775	779	
75 PERCENTILE	787	783	786	
90 PERCENTILE	795	790	795	
95 PERCENTILE	800	796	799	
MAXIMUM	850	838	840	

Stress S_1 = 168 hours at 200°C., with V_{CB} = 30 V.

Stress S_2 = 168 hours at 200°C.

Stress S_3 = 25 Kg. centrifuge - Y_1 plane only.

* Summary Data for S_3 stress not shown due to removal of 16% of units after S_2 stress.

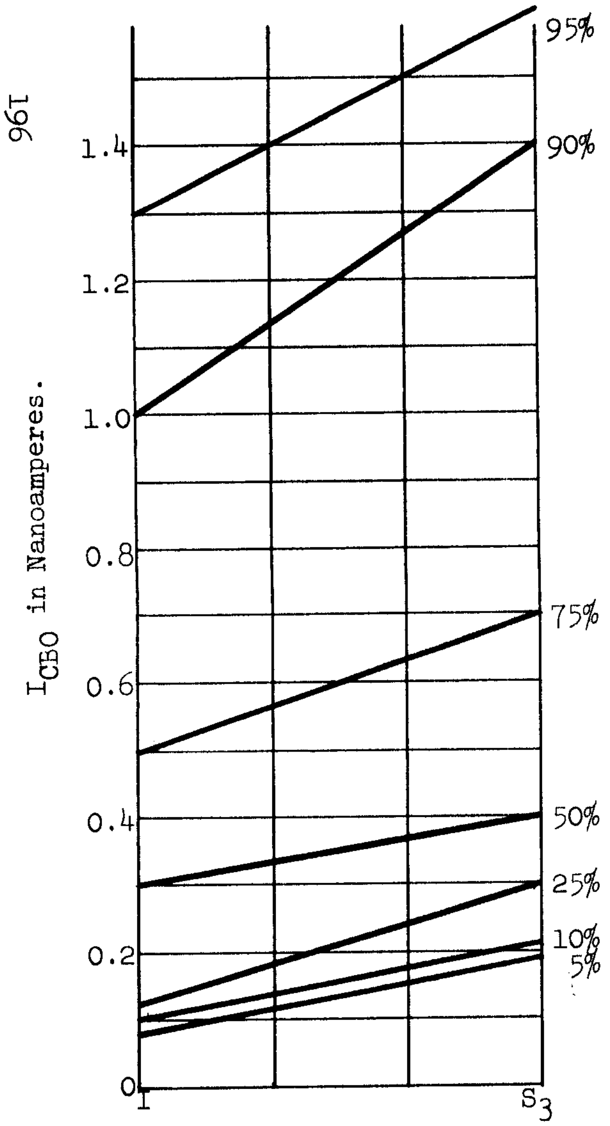

TABLE 38.

PROCESS: A.

CENTRIFUGE ONLY STRESS.

I_{CBO} DISTRIBUTION (AT V_{CB} = 60 V.).

	INITIAL	S_3		
MINIMUM	< 0.1	< 0.1		
5 PERCENTILE	< 0.1	0.2		
10 PERCENTILE	0.1	0.2		
25 PERCENTILE	0.1	0.3		
50 PERCENTILE	0.3	0.4		
75 PERCENTILE	0.5	0.7		
90 PERCENTILE	1.0	1.4		
95 PERCENTILE	1.3	1.6		
MAXIMUM	2.1	1.9		

Stress S_3 = 25 Kg. centrifuge - Y_1 plane only.

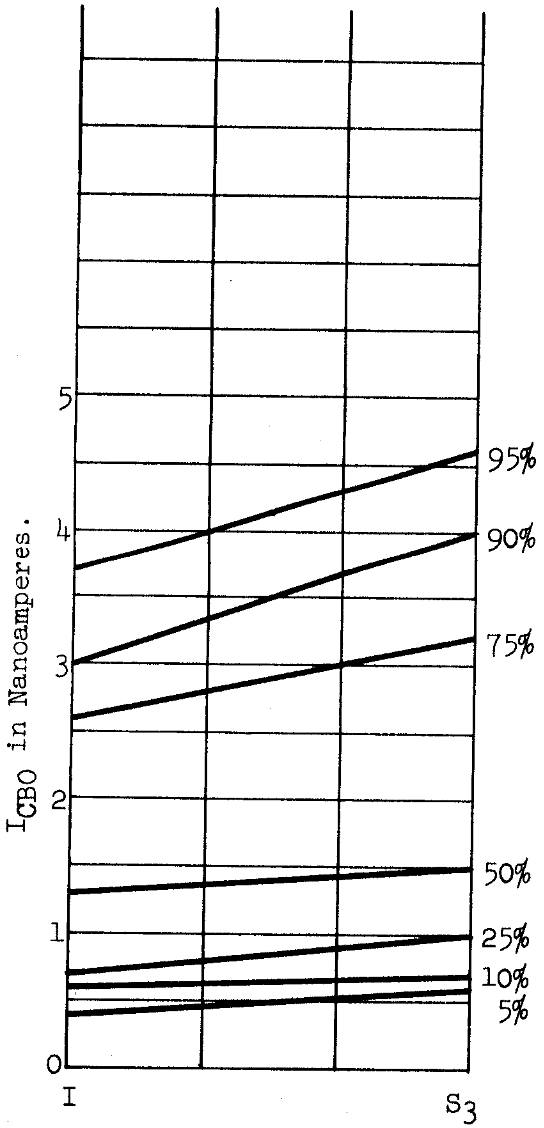

TABLE 39.

PROCESS: B.

CENTRIFUGE ONLY SCREEN.

I_{CBO} DISTRIBUTION (AT V_{CB} = 60 V.).

	INITIAL	S_3		
MINIMUM	0.2	0.4		
5 PERCENTILE	0.4	0.6		
10 PERCENTILE	0.6	0.7		
25 PERCENTILE	0.7	1.0		
50 PERCENTILE	1.3	1.5		
75 PERCENTILE	2.6	3.2		
90 PERCENTILE	3.0	4.0		
95 PERCENTILE	3.7	4.6		
MAXIMUM	4.2	5.8		

Stress S_3 = 25 Kg. centrifuge - Y_1 plane only.

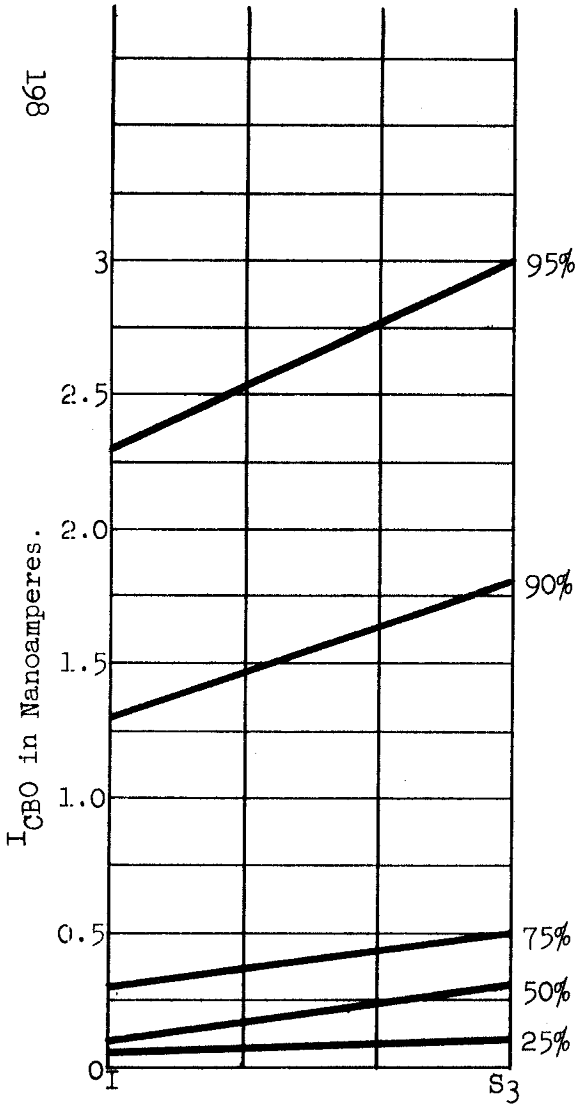

TABLE 40.

PROCESS: C.

CENTRIFUGE ONLY SCREEN.

I_{CBO} DISTRIBUTION (AT V_{CB} = 60 V.).

	INITIAL	S_3		
MINIMUM	< 0.1	< 0.1		
5 **PERCENTILE**	< 0.1	< 0.1		
10 **PERCENTILE**	< 0.1	< 0.1		
25 **PERCENTILE**	< 0.1	0.1		
50 **PERCENTILE**	0.1	0.3		
75 **PERCENTILE**	0.3	0.5		
90 **PERCENTILE**	1.3	1.8		
95 **PERCENTILE**	2.3	3.0		
MAXIMUM	7.2	6.0		

Stress S_3 = 25 Kg. centrifuge - Y_1 plane only.

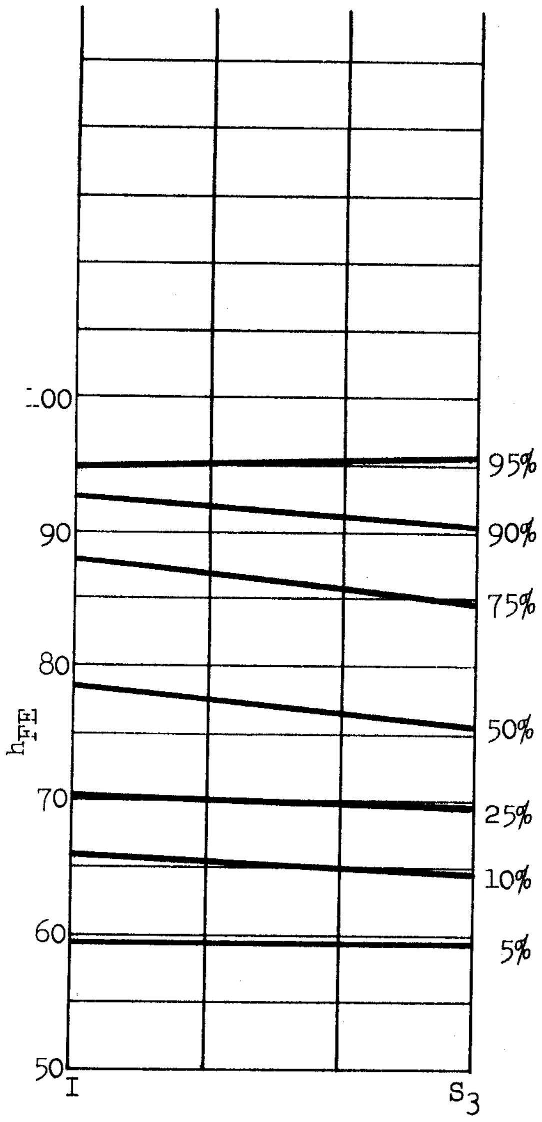

TABLE 41.

PROCESS: A.

CENTRIFUGE ONLY STRESS.

h_{FE} DISTRIBUTION (AT I_C = 20 mA., V_{CE} = 5 V.).

	INITIAL	S_3		
MINIMUM	49.1	48.1		
5 PERCENTILE	59.5	59.4		
10 PERCENTILE	66.0	64.6		
25 PERCENTILE	70.3	69.5		
50 PERCENTILE	78.3	75.7		
75 PERCENTILE	87.9	84.7		
90 PERCENTILE	92.6	90.5		
95 PERCENTILE	94.9	95.7		
MAXIMUM	98.5	99.5		

Stress S_3 = 25 Kg. centrifuge - Y_1 plane only.

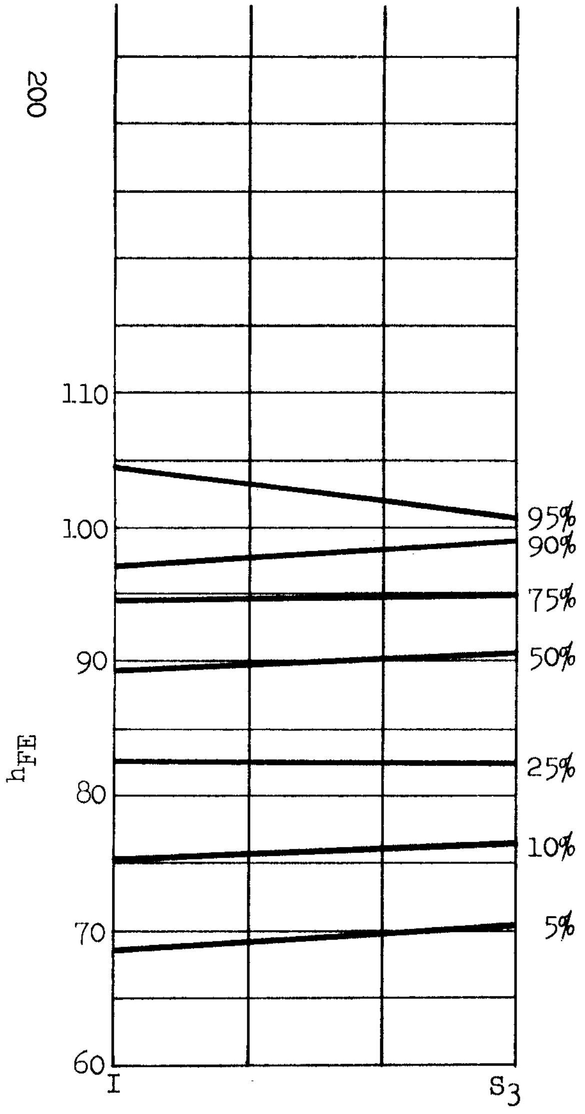

TABLE 42.

PROCESS: B.

CENTRIFUGE ONLY SCREEN.

h_{FE} **DISTRIBUTION** (AT I_C = 20 mA., V_{CE} = 5 V.).

	INITIAL	S_3		
MINIMUM	66.1	68.4		
5 PERCENTILE	68.7	70.5		
10 PERCENTILE	75.2	76.4		
25 PERCENTILE	82.5	82.4		
50 PERCENTILE	89.2	90.6		
75 PERCENTILE	94.6	94.9		
90 PERCENTILE	97.0	99.0		
95 PERCENTILE	104.6	100.8		
MAXIMUM	107.0	108.7		

Stress S_3 = 25 Kg. centrifuge - Y_1 plane only.

TABLE 43.

PROCESS: C.

CENTRIFUGE ONLY SCREEN.

h_{FE} DISTRIBUTION (AT I_C = 20 ma., V_{CE} = 5 V.).

	INITIAL	S_3		
MINIMUM	45.2	47.2		
5 PERCENTILE	50.6	51.2		
10 PERCENTILE	53.5	54.9		
25 PERCENTILE	63.0	66.2		
50 PERCENTILE	82.6	82.2		
75 PERCENTILE	100.5	100.5		
90 PERCENTILE	114.6	112.5		
95 PERCENTILE	120.1	116.6		
MAXIMUM	125.3	126.8		

Stress S_3 = 25 Kg. centrifuge - Y_1 plane only.

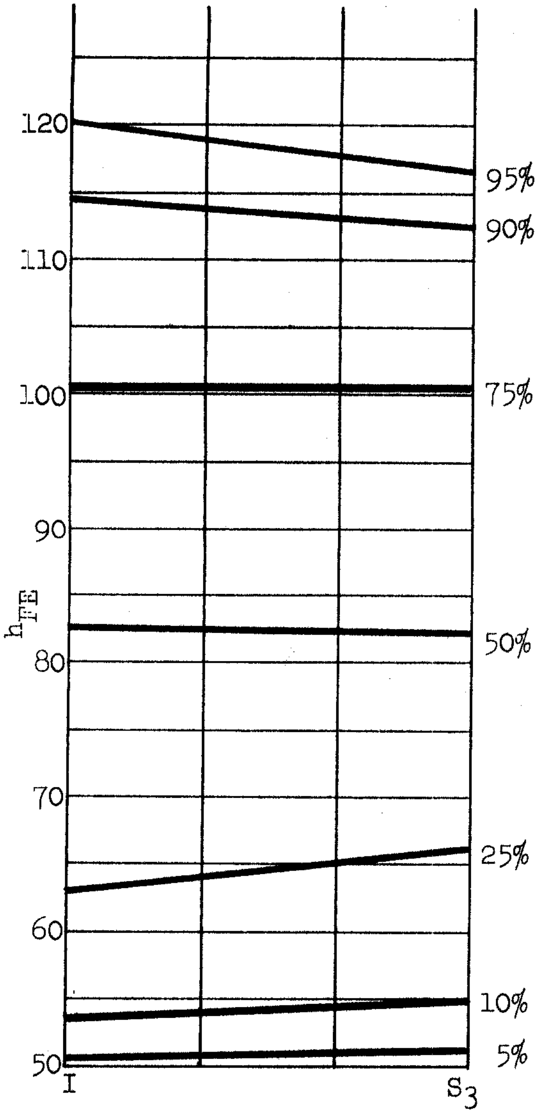

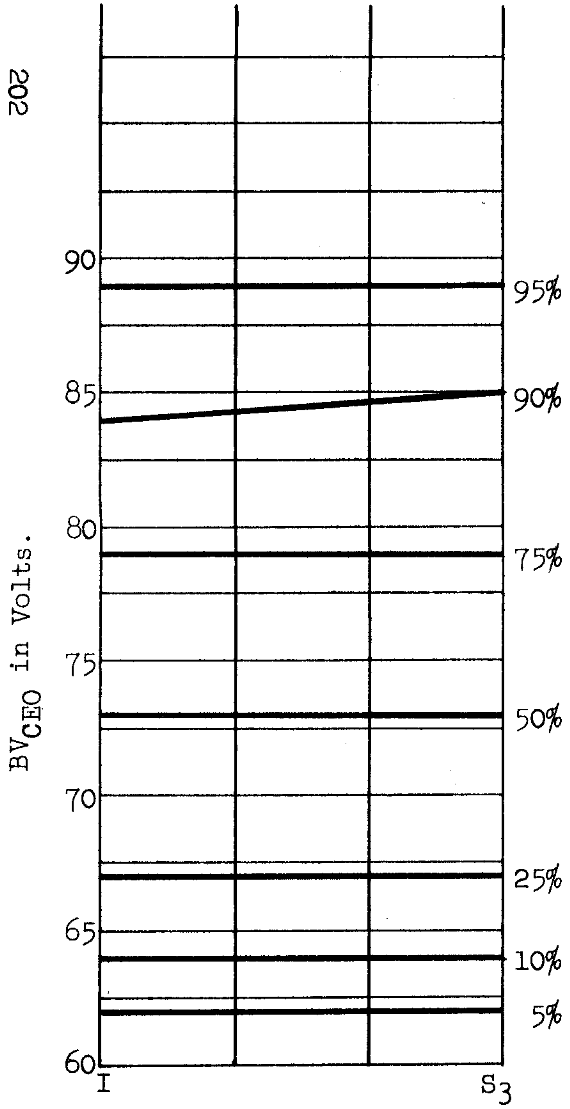

TABLE 44.

PROCESS: B.

CENTRIFUGE ONLY SCREEN.

BV$_{CEO}$ DISTRIBUTION (AT I_C = 100 uA.).

	INITIAL	S_3		
MINIMUM	60.3	60.5		
5 PERCENTILE	62.0	62.0		
10 PERCENTILE	64.0	64.0		
25 PERCENTILE	67.0	67.0		
50 PERCENTILE	73.0	73.0		
75 PERCENTILE	79.0	79.0		
90 PERCENTILE	84.0	85.0		
95 PERCENTILE	89.0	89.0		
MAXIMUM	90.0	90.0		

Stress S_3 = 25 Kg. centrifuge - Y_1 plane only.

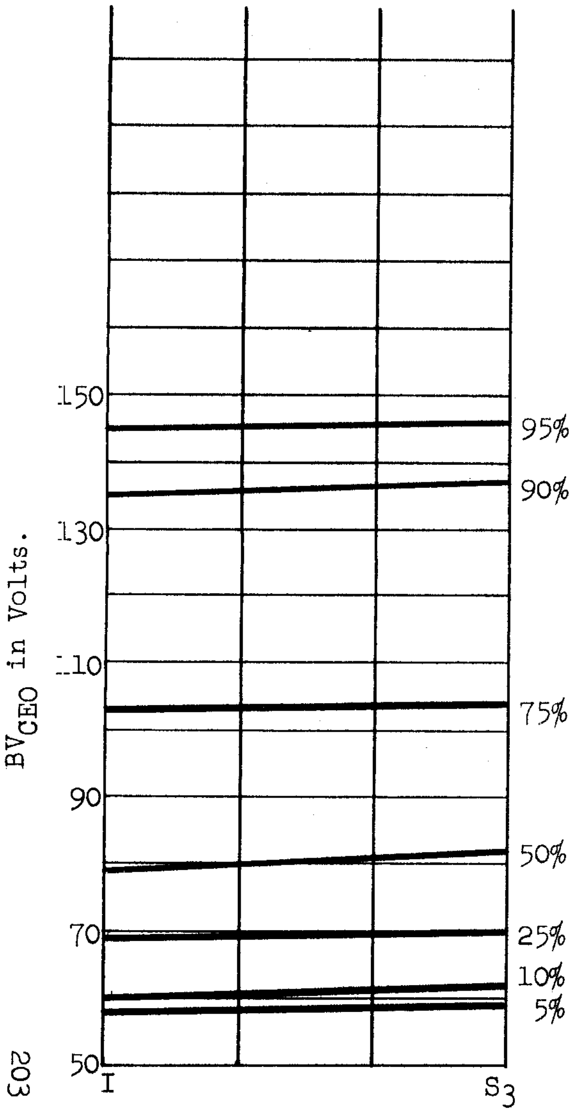

TABLE 45.

PROCESS: C.

CENTRIFUGE ONLY SCREEN.

BV_{CEO} DISTRIBUTION (AT I_C = 100 uA.).

	INITIAL	S_3		
MINIMUM	42	52		
5 PERCENTILE	58	59		
10 PERCENTILE	60	62		
25 PERCENTILE	69	70		
50 PERCENTILE	79	82		
75 PERCENTILE	103	104		
90 PERCENTILE	135	137		
95 PERCENTILE	145	146		
MAXIMUM	164	166		

Stress S_3 = 25 Kg. centrifuge - Y_1 plane only.

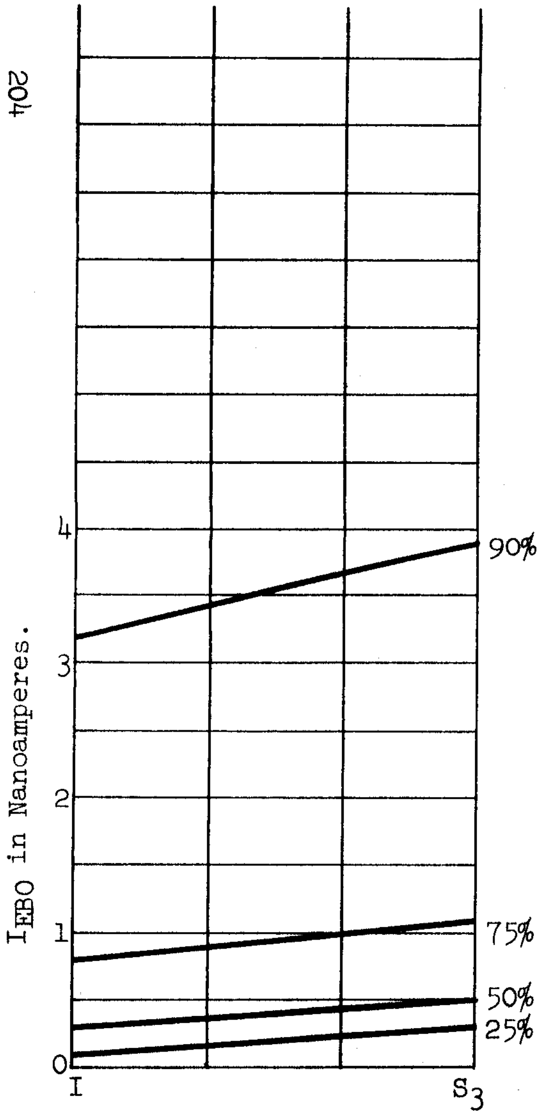

TABLE 46.

PROCESS: B.

CENTRIFUGE ONLY SCREEN.

I_{EBO} DISTRIBUTION (AT V_{EB} = 5 V.).

	INITIAL	S_3		
MINIMUM	< 0.1	< 0.1		
5 PERCENTILE	< 0.1	0.1		
10 PERCENTILE	< 0.1	0.2		
25 PERCENTILE	0.1	0.3		
50 PERCENTILE	0.3	0.5		
75 PERCENTILE	0.8	1.1		
90 PERCENTILE	3.2	3.9		
95 PERCENTILE	9.7	11.3		
MAXIMUM	27.9	31.5		

Stress S_3 = 25 Kg. centrifuge - Y_1 plane only.

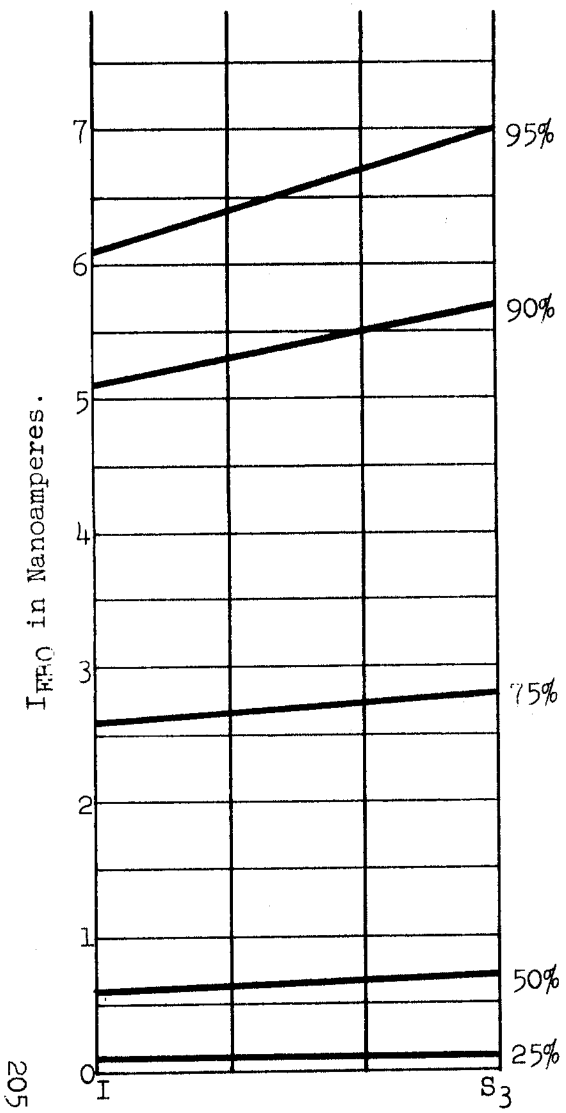

TABLE 47.

PROCESS: C.

CENTRIFUGE ONLY SCREEN.

I_{EBO} DISTRIBUTION (AT V_{EB} = 5 V.).

	INITIAL	S_3		
MINIMUM	< 0.1	< 0.1		
5 **PERCENTILE**	< 0.1	< 0.1		
10 **PERCENTILE**	< 0.1	< 0.1		
25 **PERCENTILE**	0.1	0.1		
50 **PERCENTILE**	0.6	0.7		
75 **PERCENTILE**	2.6	2.8		
90 **PERCENTILE**	5.1	5.7		
95 **PERCENTILE**	6.1	7.0		
MAXIMUM	14.0	12.2		

Stress S_3 = 25 Kg. centrifuge -- Y_1 plane only.

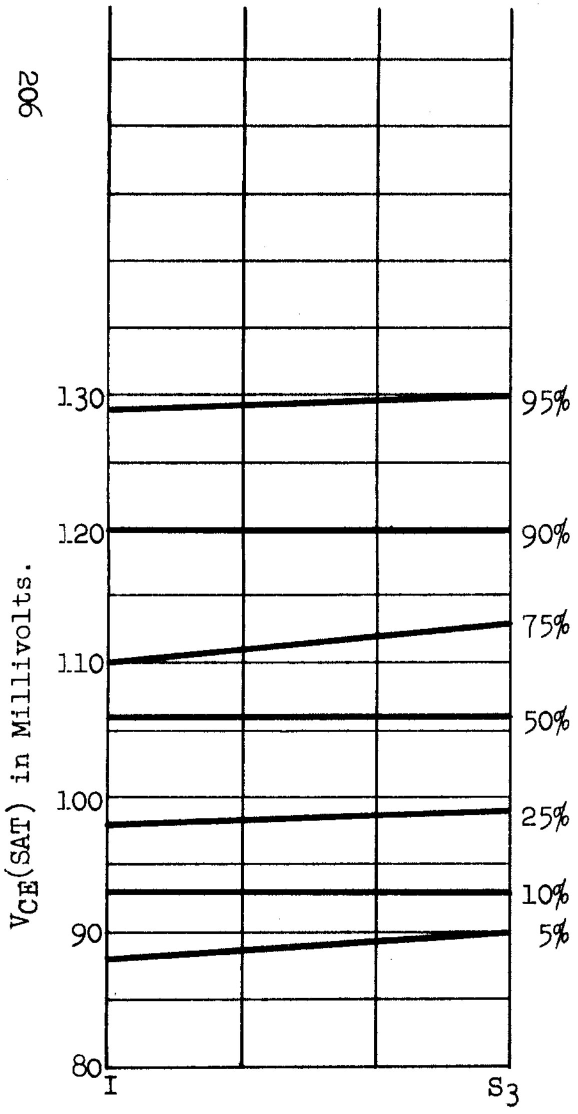

TABLE 48.

PROCESS: B.

CENTRIFUGE ONLY SCREEN.

V_{CE}(SAT) DISTRIBUTION (AT I_C = 50 mA., I_B = 5 mA.).

	INITIAL	S_3		
MINIMUM	85	87		
5 PERCENTILE	88	90		
10 PERCENTILE	93	93		
25 PERCENTILE	98	99		
50 PERCENTILE	106	106		
75 PERCENTILE	110	113		
90 PERCENTILE	120	120		
95 PERCENTILE	129	130		
MAXIMUM	136	138		

Stress S_3 = 25 Kg. centrifuge - Y_1 plane only.

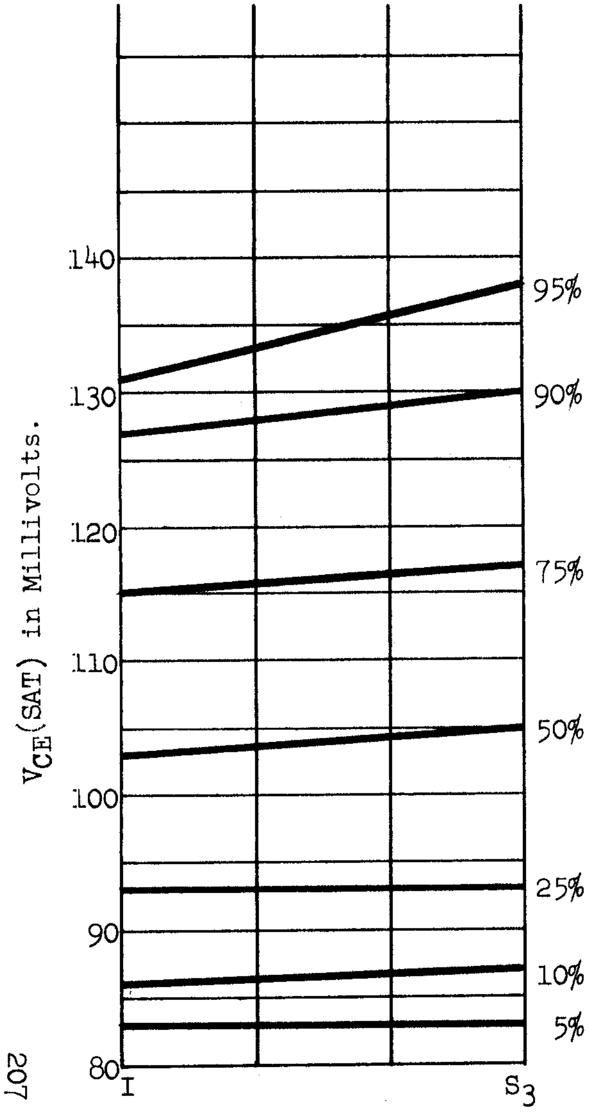

TABLE 49.

PROCESS: C.

CENTRIFUGE ONLY SCREEN.

V_{CE}(SAT) DISTRIBUTION (AT I_C = 50 mA., I_B = 5 mA.).

	INITIAL	S_3		
MINIMUM	69	73		
5 PERCENTILE	83	83		
10 PERCENTILE	86	87		
25 PERCENTILE	93	93		
50 PERCENTILE	103	105		
75 PERCENTILE	115	117		
90 PERCENTILE	127	130		
95 PERCENTILE	131	138		
MAXIMUM	165	168		

Stress S_3 = 25 Kg. centrifuge - Y_1 plane only.

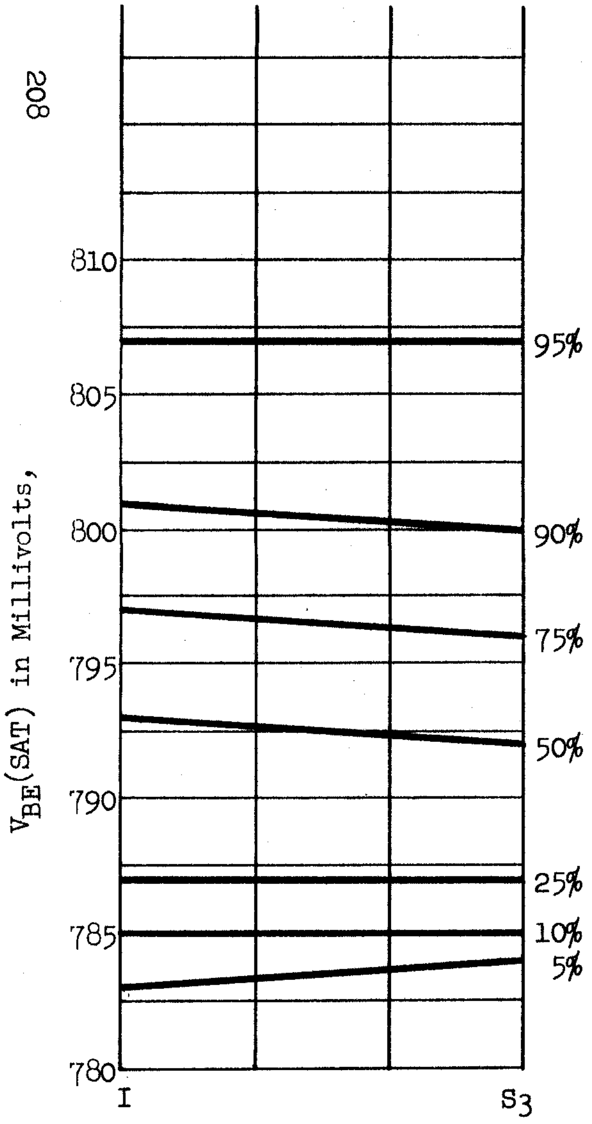

TABLE 50.

PROCESS: B.

CENTRIFUGE ONLY SCREEN.

V_{BE}(SAT) DISTRIBUTION (AT I_C = 50 mA., I_B = 5 mA.).

	INITIAL	S_3		
MINIMUM	780	780		
5 PERCENTILE	783	784		
10 PERCENTILE	785	785		
25 PERCENTILE	787	787		
50 PERCENTILE	793	792		
75 PERCENTILE	797	796		
90 PERCENTILE	801	800		
95 PERCENTILE	807	807		
MAXIMUM	820	820		

Stress S_3 = 25 Kg. centrifuge - Y_1 plane only.

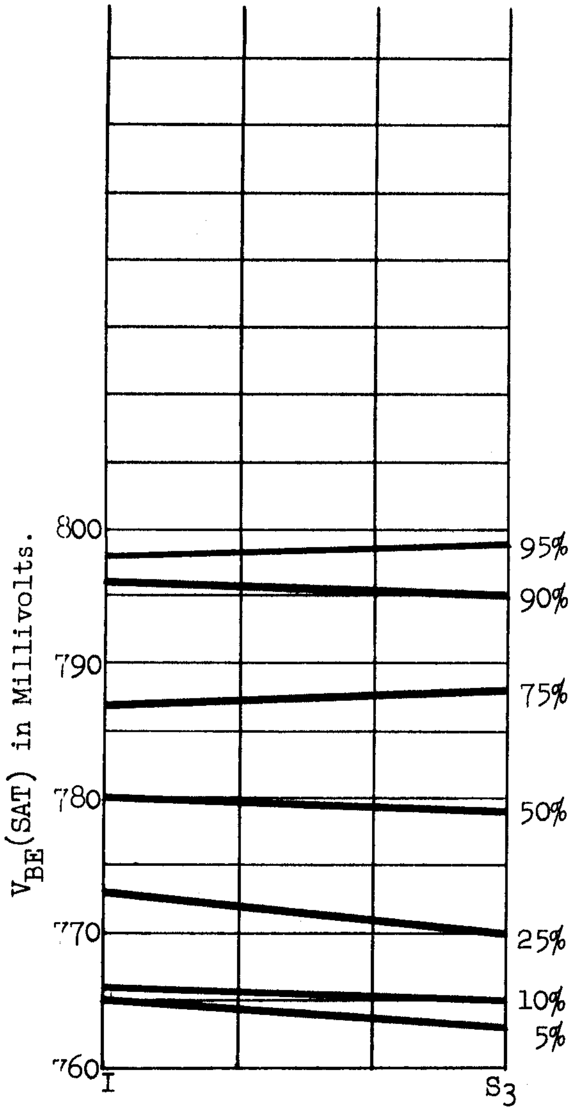

TABLE 51.

PROCESS: C.

CENTRIFUGE ONLY SCREEN.

V_{BE}(SAT) DISTRIBUTION (AT I_C = 50 mA., I_B = 5 mA.).

	INITIAL	S_3		
MINIMUM	697	760		
5 PERCENTILE	765	763		
10 PERCENTILE	766	765		
25 PERCENTILE	773	770		
50 PERCENTILE	780	779		
75 PERCENTILE	787	788		
90 PERCENTILE	796	795		
95 PERCENTILE	798	799		
MAXIMUM	848	848		

Stress S_3 = 25 Kg. centrifuge - Y_1 plane only.

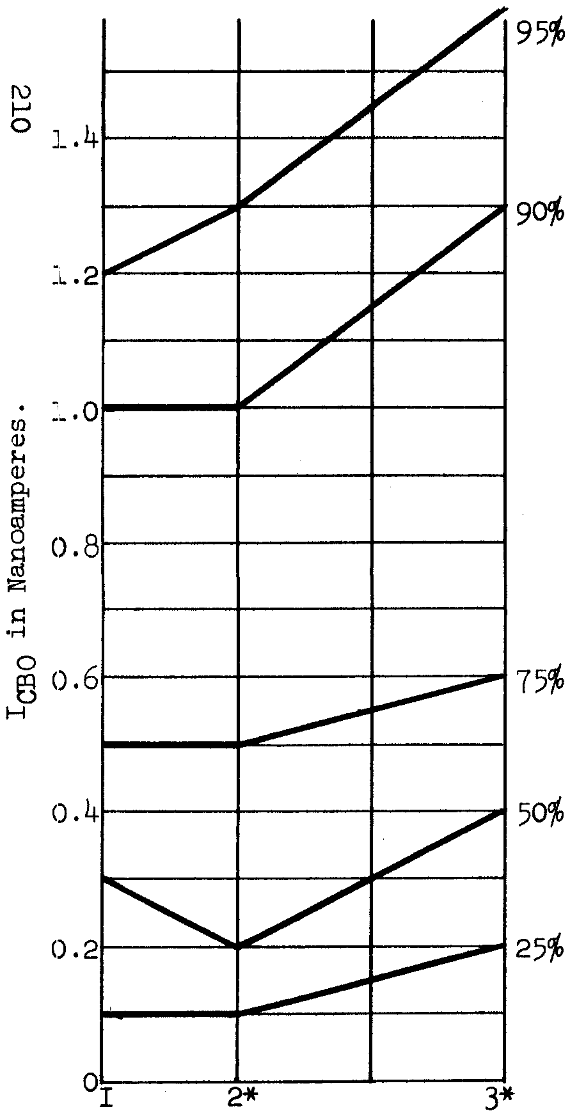

TABLE 52.

PROCESS: A.

CONTROL LOT.

I_{CBO} DISTRIBUTION (AT V_{CB} = 60 V.).

	INITIAL	2nd Read*	3rd Read*	
MINIMUM	< 0.1	< 0.1	< 0.1	
5 PERCENTILE	< 0.1	< 0.1	< 0.1	
10 PERCENTILE	0.1	< 0.1	0.1	
25 PERCENTILE	0.1	0.1	0.2	
50 PERCENTILE	0.3	0.2	0.4	
75 PERCENTILE	0.5	0.5	0.6	
90 PERCENTILE	1.0	1.0	1.3	
95 PERCENTILE	1.2	1.3	1.6	
MAXIMUM	2.1	2.1	2.4	

* Second Reading = Control lot read after 7 weeks from Initial.

* Third Reading = Control lot read after 10 weeks from Initial.

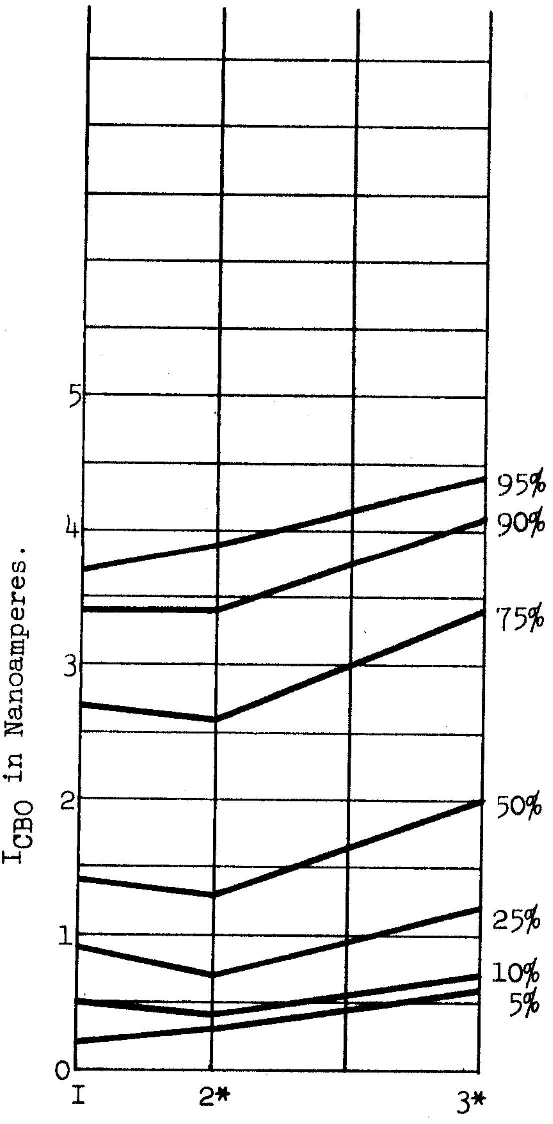

TABLE 53.

PROCESS: B.

CONTROL LOT.

I_{CBO} DISTRIBUTION (AT V_{CB} = 60 V.).

	INITIAL	2nd Read*	3rd Read*	
MINIMUM	< 0.1	< 0.1	0.2	
5 PERCENTILE	0.2	0.3	0.6	
10 PERCENTILE	0.5	0.4	0.7	
25 PERCENTILE	0.9	0.7	1.2	
50 PERCENTILE	1.4	1.3	2.0	
75 PERCENTILE	2.7	2.6	3.4	
90 PERCENTILE	3.4	3.4	4.1	
95 PERCENTILE	3.7	3.9	4.4	
MAXIMUM	4.5	5.1	6.0	

* Second Reading = Control lot read after 7 weeks from Initial.

* Third Reading = Control lot read after 10 weeks from Initial.

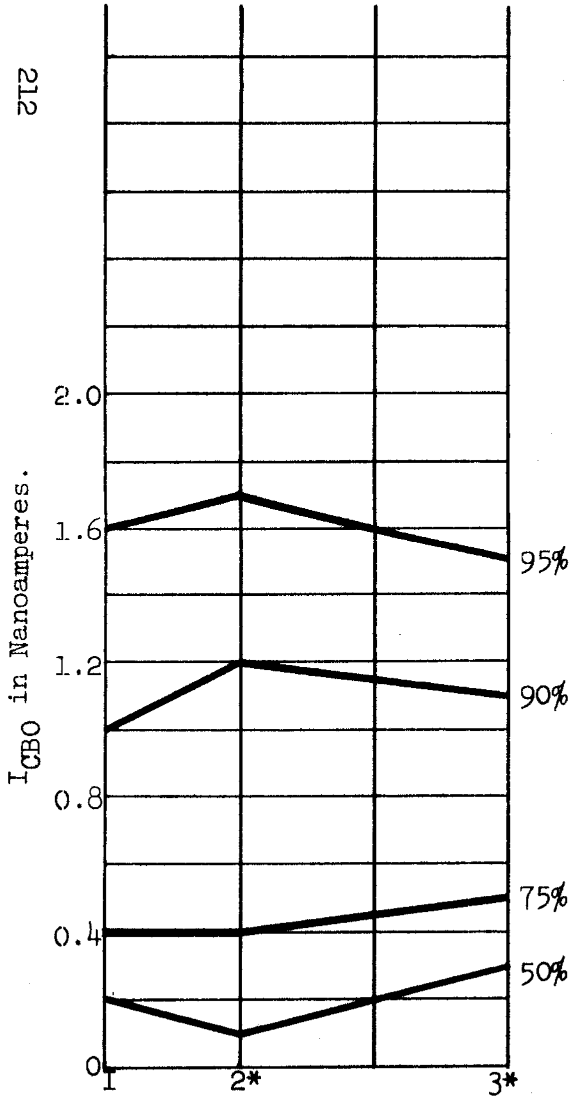

TABLE 54.

PROCESS: C.

CONTROL LOT.

I_{CBO} DISTRIBUTION (AT V_{CB} = 60 V.).

	INITIAL	2nd Read*	3rd Read*	
MINIMUM	< 0.1	< 0.1	< 0.1	
5 PERCENTILE	< 0.1	< 0.1	< 0.1	
10 PERCENTILE	< 0.1	< 0.1	0.1	
25 PERCENTILE	0.1	< 0.1	0.1	
50 PERCENTILE	0.2	0.1	0.3	
75 PERCENTILE	0.4	0.4	0.5	
90 PERCENTILE	1.0	1.2	1.1	
95 PERCENTILE	1.6	1.7	1.5	
MAXIMUM	15.5	5.3	6.4	

* Second Reading = Control lot read after 7 weeks from Initial.

* Third Reading = Control lot read after 10 weeks from Initial.

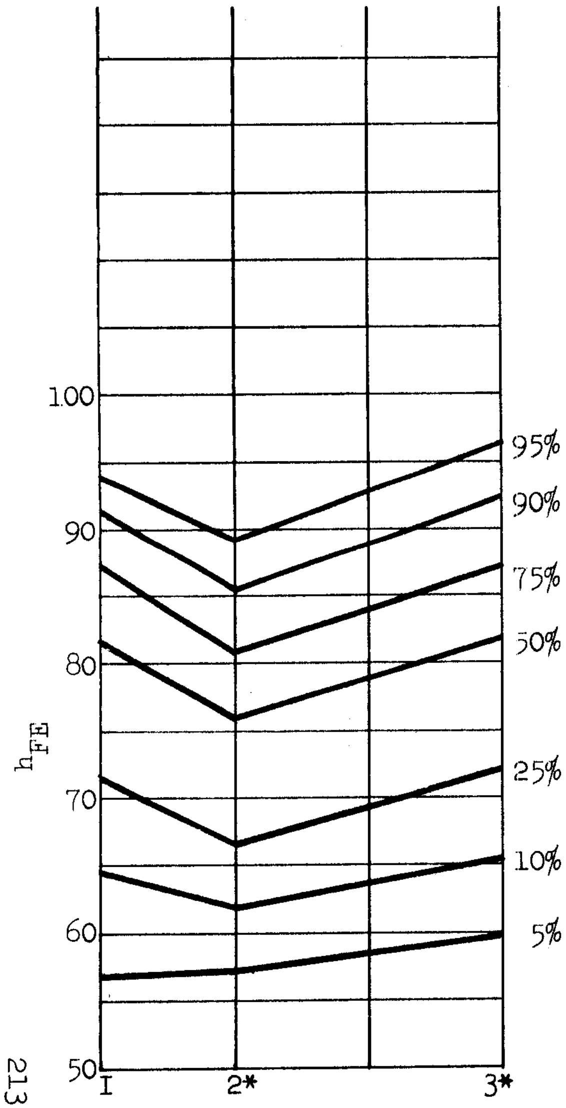

TABLE 55.

PROCESS: A.

CONTROL LOT.

h_{FE} DISTRIBUTION (AT I_C = 20 mA., V_{CE} = 5 V.).

	INITIAL	2nd Read*	3rd Read*	
MINIMUM	36.5	48.2	49.6	
5 PERCENTILE	56.9	57.2	59.8	
10 PERCENTILE	64.4	62.0	65.5	
25 PERCENTILE	71.3	66.5	72.1	
50 PERCENTILE	81.4	76.0	81.8	
75 PERCENTILE	87.0	80.9	87.1	
90 PERCENTILE	91.3	85.4	92.3	
95 PERCENTILE	93.9	89.2	96.3	
MAXIMUM	97.6	96.6	99.7	

* Second **Reading** = Control lot read after 7 weeks from Initial.

* Third **Reading** = Control lot read after 10 weeks from Initial.

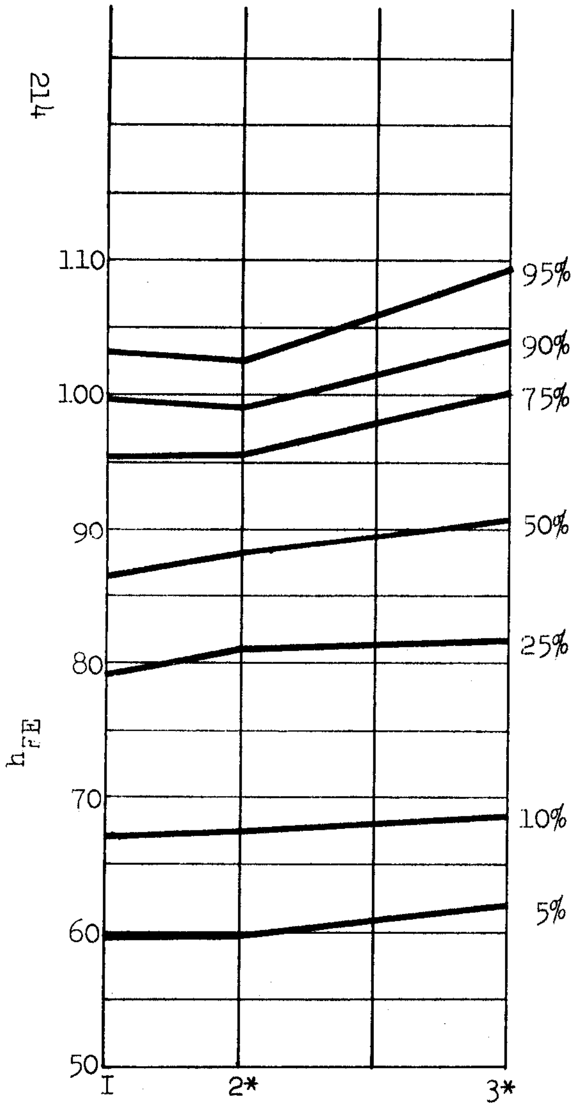

TABLE 56

PROCESS: B.

CONTROL LOT.

h_{FE} DISTRIBUTION (AT I_C = 20 mA., V_{CE} = 5 V.).

	INITIAL	2nd Read*	3rd Read*	
MINIMUM	41.1	55.8	56.0	
5 PERCENTILE	59.6	59.8	62.0	
10 PERCENTILE	67.0	67.3	68.3	
25 PERCENTILE	79.2	81.1	81.6	
50 PERCENTILE	86.4	88.0	90.7	
75 PERCENTILE	95.3	95.7	100.1	
90 PERCENTILE	99.7	99.0	104.0	
95 PERCENTILE	103.1	102.6	109.3	
MAXIMUM	107.6	104.2	222.8	

* Second **Reading** = **C**ontrol lot read after 7 weeks from Initial.

* Third **Reading** = **C**ontrol lot read after 10 weeks from Initial.

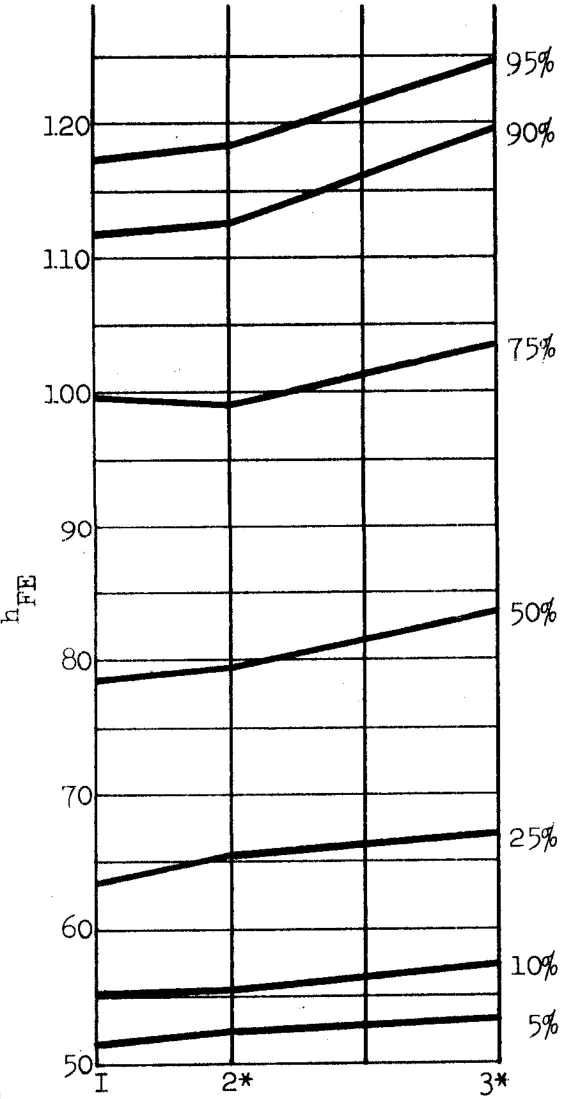

TABLE 57.

PROCESS: C.

CONTROL LOT.

h_{FE} DISTRIBUTION (AT I_C = 20 mA., V_{CE} = 5 V.).

	INITIAL	2nd Read *	3rd Read *	
MINIMUM	46.7	46.9	48.0	
5 PERCENTILE	51.6	52.5	53.3	
10 PERCENTILE	55.1	55.5	57.2	
25 PERCENTILE	63.6	65.6	67.0	
50 PERCENTILE	78.6	79.4	83.6	
75 PERCENTILE	99.7	99.0	103.4	
90 PERCENTILE	111.8	112.7	119.4	
95 PERCENTILE	117.3	118.2	124.5	
MAXIMUM	136.3	138.5	137.9	

* Second Reading = Control lot read after 7 weeks from Initial.

* Third Reading = Control lot read after 10 weeks from Initial.

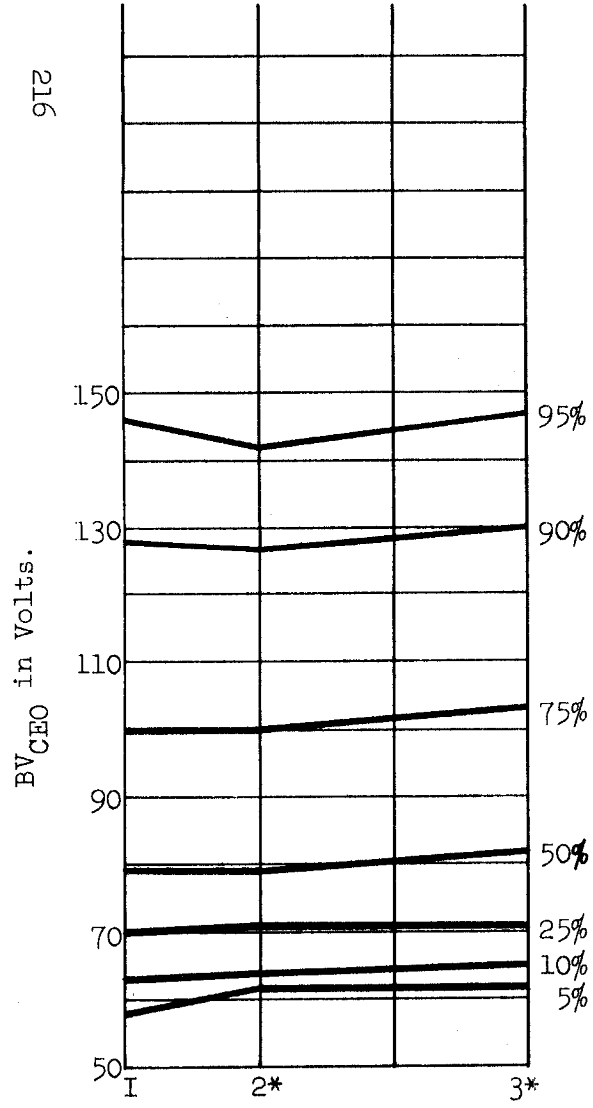

TABLE 58.

PROCESS: C.

CONTROL LOT.

BV_{CEO} DISTRIBUTION (AT I_C = 100 uA.).

	INITIAL	2nd Read *	3rd Read *	
MINIMUM	53	53	52	
5 PERCENTILE	58	62	62	
10 PERCENTILE	63	64	65	
25 PERCENTILE	70	71	71	
50 PERCENTILE	79	79	82	
75 PERCENTILE	100	100	103	
90 PERCENTILE	128	127	130	
95 PERCENTILE	146	142	147	
MAXIMUM	161	162	162	

* Second **Reading** = **C**ontrol lot read after 7 weeks from Initial.

* Third **Reading** = **C**ontrol lot read after 10 weeks from Initial.

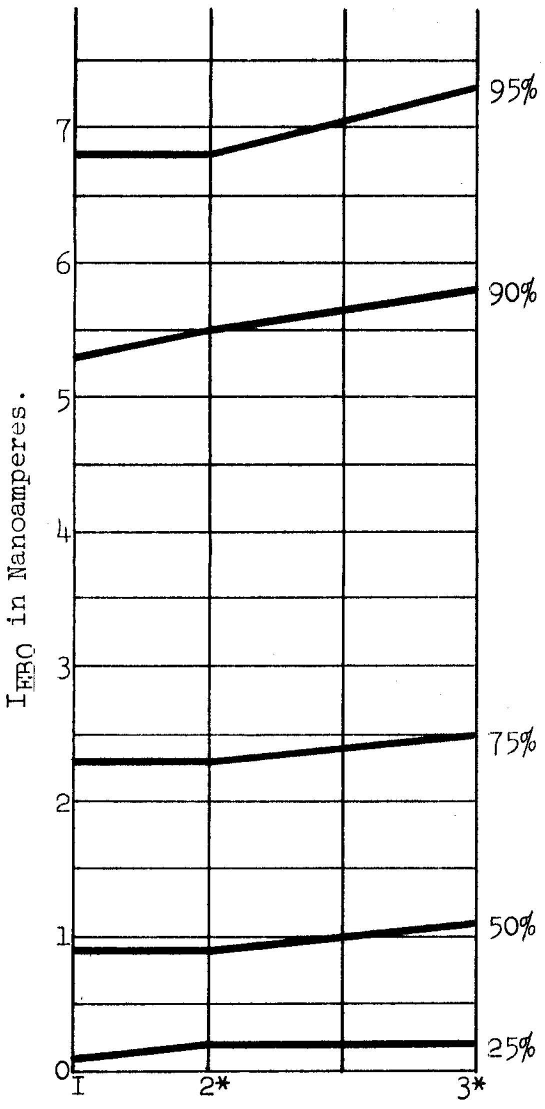

TABLE 59.

PROCESS: C.

CONTROL LOT.

I_{EBO} DISTRIBUTION (AT V_{EB} = 5 V.).

	INITIAL	2nd Read *	3rd Read *	
MINIMUM	< 0.1	< 0.1	< 0.1	
5 PERCENTILE	< 0.1	< 0.1	< 0.1	
10 PERCENTILE	< 0.1	< 0.1	< 0.1	
25 PERCENTILE	0.1	0.2	0.2	
50 PERCENTILE	0.9	0.9	1.1	
75 PERCENTILE	2.3	2.3	2.5	
90 PERCENTILE	5.3	5.5	5.8	
95 PERCENTILE	6.8	6.8	7.3	
MAXIMUM	7.7	7.9	8.6	

* Second Reading = Control lot read after 7 weeks from Initial.

* Third Reading = Control lot read after 10 weeks from Initial.

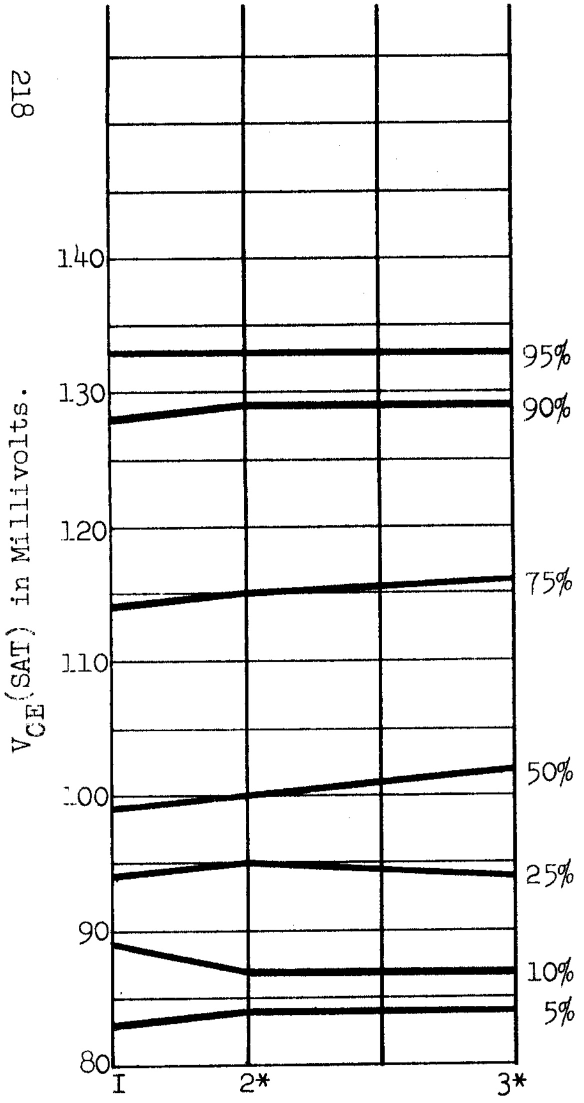

TABLE 60.

PROCESS: C.

CONTROL LOT.

V_{CE}(SAT) DISTRIBUTION (AT I_C = 50 mA., I_B = 5 mA.).

	INITIAL	2nd Read *	3rd Read *	
MINIMUM	79	16	15	
5 PERCENTILE	83	84	84	
10 PERCENTILE	89	87	87	
25 PERCENTILE	94	95	94	
50 PERCENTILE	99	100	102	
75 PERCENTILE	114	115	116	
90 PERCENTILE	128	129	129	
95 PERCENTILE	133	133	133	
MAXIMUM	149	145	146	

* Second Reading = Control lot read after 7 weeks from Initial.

* Third Reading = Control lot read after 10 weeks from Initial.

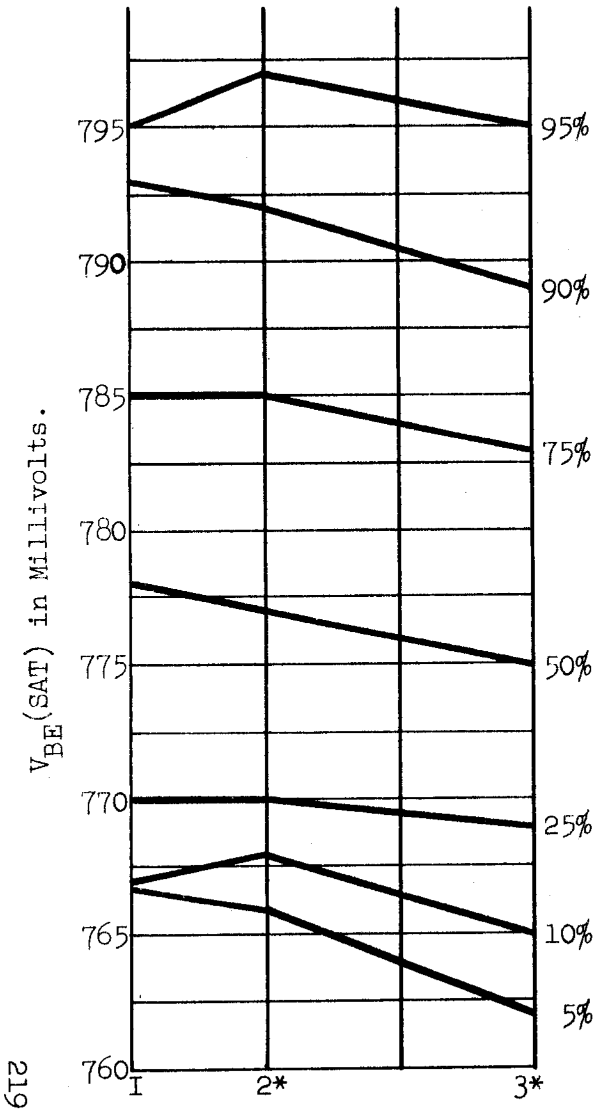

TABLE 61.

PROCESS: A.

CONTROL LOT.

V_{BE}(SAT) DISTRIBUTION (AT I_C = 50 mA., I_B = 5 mA.).

	INITIAL	2nd Read *	3rd Read *	
MINIMUM	765	693	688	
5 PERCENTILE	767	766	762	
10 PERCENTILE	767	768	765	
25 PERCENTILE	770	770	769	
50 PERCENTILE	778	777	775	
75 PERCENTILE	785	785	783	
90 PERCENTILE	793	792	789	
95 PERCENTILE	795	797	795	
MAXIMUM	817	1059	813	

* Second Reading = Control lot read after 7 weeks from Initial.

* Third Reading = Control lot read after 10 weeks from Initial.

PROCESS A. HIGH STRESS SCREEN. TABLE 62.

I_{CBO} DISTRIBUTION CHANGES WITH LIFE TEST.

	I_{CBO} (V_{CB} = 60 V.) (Nanoamperes).								
HRS.	INIT.	168	340	680	1000	1500	2000	3000	
Min	0.2	0.5	<0.1	<0.1	0.1	<0.1	<0.1		P=800mW. V_{CB}=20V. T_A=25°C.
5%	0.2	0.6	<0.1	<0.1	0.1	<0.1	<0.1		
10%	0.2	0.6	<0.1	<0.1	0.1	<0.1	<0.1		
25%	0.3	0.7	0.2	0.1	0.2	0.1	<0.1		
50%	0.4	1.1	0.5	0.5	0.5	0.2	0.3		
75%	0.7	1.5	0.8	0.9	0.9	0.6	0.5		
90%	1.3	2.0	1.4	1.3	1.3	1.0	0.9		
95%	1.5	2.3	1.7	1.5	1.5	1.2	1.0		
Max	1.5	2.3	1.7	1.5	1.5	1.2	1.0		
Min	<0.1	0.4	<0.1	<0.1	<0.1	<0.1	<0.1	0.3	P=700mW. V_{CB}=20V. T_A=25°C.
5%	<0.1	0.4	<0.1	<0.1	<0.1	<0.1	<0.1	0.3	
10%	<0.1	0.4	<0.1	<0.1	<0.1	<0.1	<0.1	0.5	
25%	0.1	0.7	0.1	0.1	0.2	<0.1	0.2	0.5	
50%	0.3	1.0	0.4	0.3	0.4	0.3	0.6	0.7	
75%	1.0	1.9	1.3	1.2	1.3	0.9	2.4	1.4	
90%	1.4	2.7	2.6	2.1	2.6	1.8	7.9	2.6	
95%	2.1	3.0	4.0	4.5	6.7	25.3	20.8	22.0	
Max	2.3	3.2	4.6	6.4	8.9	44.4	31.0	36.9	
Min	<0.1	<0.1	0.2	0.6	<0.1	<0.1	<0.1	<0.1	P=500mW. V_{CB}=20V. T_A=25°C.
5%	<0.1	<0.1	0.5	0.8	<0.1	<0.1	<0.1	<0.1	
10%	<0.1	<0.1	0.5	1.0	<0.1	0.2	<0.1	<0.1	
25%	0.1	<0.1	0.6	1.0	0.1	0.3	0.1	<0.1	
50%	0.2	0.4	0.8	1.2	0.3	0.5	0.2	0.2	
75%	0.4	0.6	1.0	1.7	0.7	0.7	0.7	0.6	
90%	1.1	0.7	2.0	2.4	1.6	1.7	1.6	1.9	
95%	1.4	1.1	2.5	3.3	2.8	2.1	2.7	5.7	
Max	2.5	101.2	32.9	10.2	>1 mA	7.8	9.3	35.0	
Min	<0.1	0.4	0.1	<0.1	<0.1	<0.1	<0.1	<0.1	P=400mW. V_{CB}=20V. T_A=150°C.
5%	<0.1	0.4	0.1	<0.1	<0.1	<0.1	<0.1	<0.1	
10%	<0.1	0.5	0.1	0.1	0.1	<0.1	<0.1	<0.1	
25%	<0.1	0.7	0.3	0.2	0.2	<0.1	<0.1	0.1	
50%	0.2	0.8	0.4	0.6	0.6	0.3	0.4	0.5	
75%	0.4	1.3	0.7	1.0	3.4	1.0	1.4	22.4	
90%	0.8	3.0	3.2	5.1	14.6	47.3	157.9	627.7	
95%	0.9	4.2	5.3	6.3	22.9	83.5	279.4	---	
Max	0.9	4.2	5.3	6.3	22.9	83.5	279.4	---	

TABLE 62. (CONTINUED).

HRS.	INIT.	168	340	680	1000	1500	2000	3000	
Min	<0.1	0.6	<0.1	<0.1	<0.1	<0.1	<0.1	<0.1	
5%	<0.1	0.6	<0.1	<0.1	<0.1	<0.1	<0.1	<0.1	
10%	<0.1	0.6	0.1	<0.1	0.1	0.1	<0.1	0.1	
25%	<0.1	0.8	0.2	0.2	0.3	0.1	0.1	0.1	P=200mW.
50%	0.2	0.9	0.5	0.4	0.4	0.3	0.3	0.4	V_{CB}=20V.
75%	0.4	1.4	1.0	1.0	1.2	0.8	1.1	1.2	T_A=150°C.
90%	0.9	13.5	2.0	1.9	1.8	1.5	1.9	1.9	
95%	1.5	127.7	109.1	11.1	6.4	4.8	2.4	196.2	
Max	2.0	142.4	196.6	18.6	10.1	7.3	2.6	354.1	

TABLE 62 GRAPH.

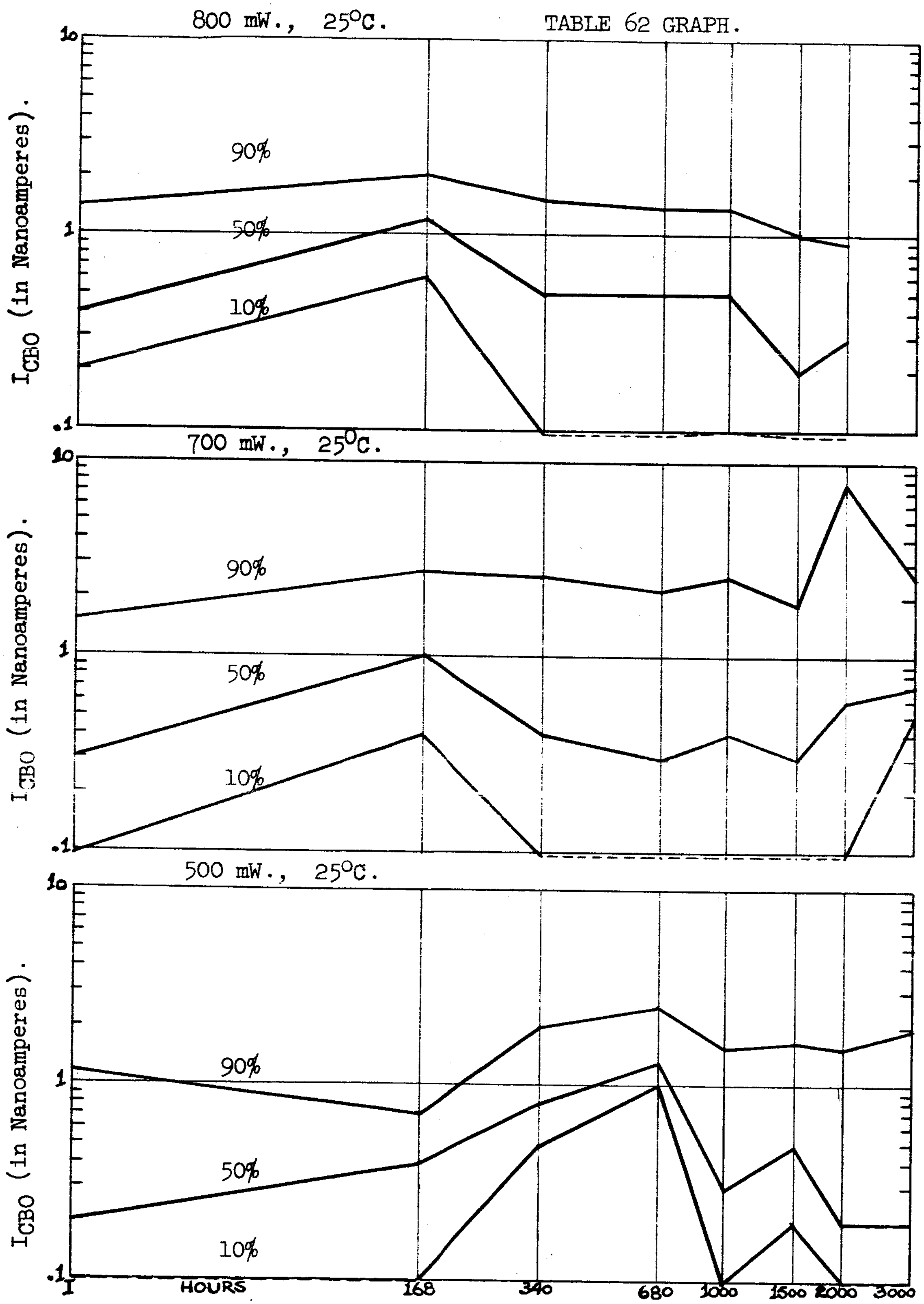
800 mW., 25°C.

700 mW., 25°C.

500 mW., 25°C.

TABLE 62 GRAPH.

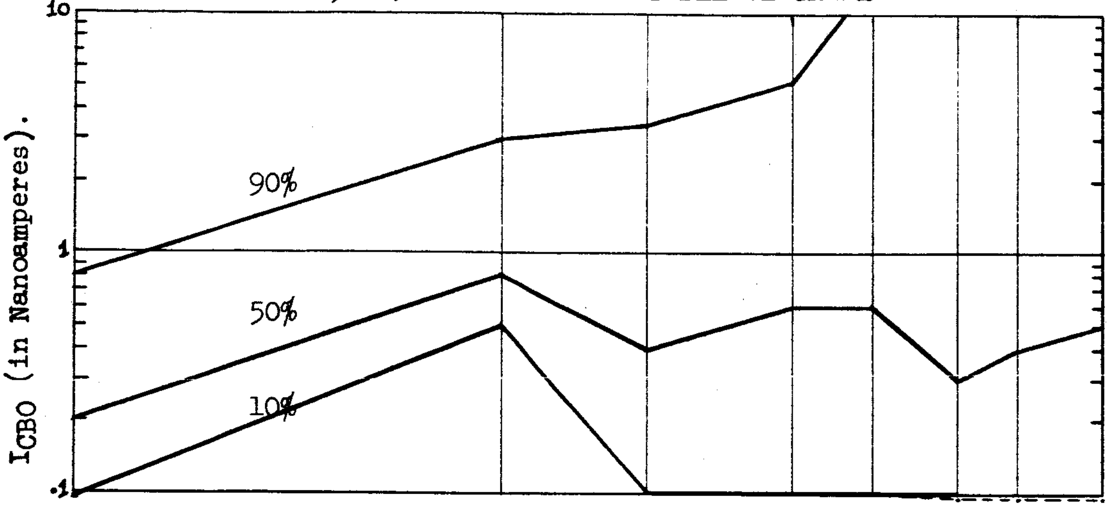
400 mW., 150°C.

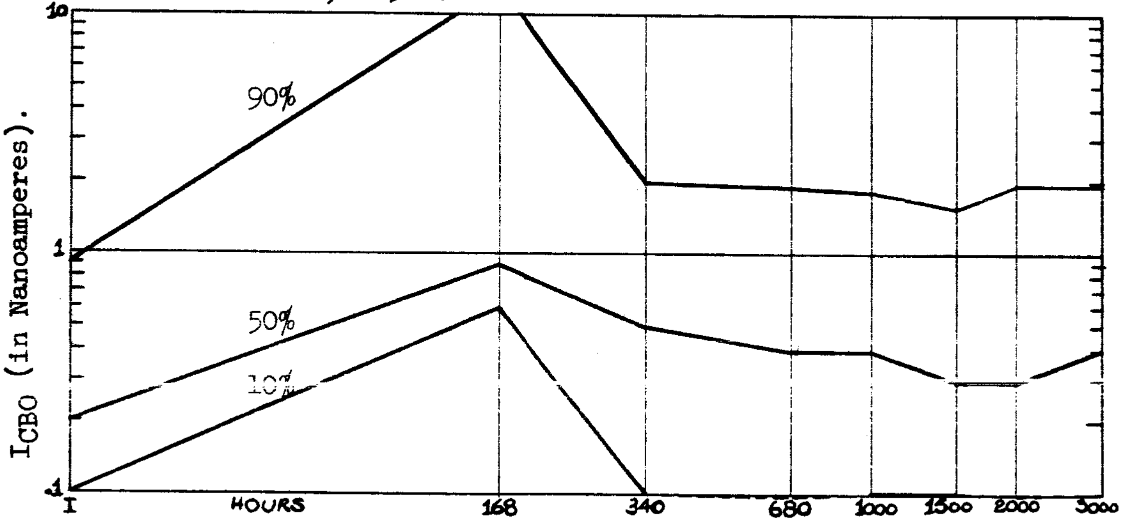
200 mW., 150°C.

PROCESS B. HIGH STRESS SCREEN. TABLE 63.

I_{CBO} DISTRIBUTION CHANGES WITH LIFE TEST.

	I_{CBO} (V_{CB} = 60 V.) (Nanoamperes).								
HRS.	INIT.	168	340	680	1000	1500	2000	3000	
Min	<0.1	0.6	0.3	0.1	1.0	0.2	1.1	0.5	
5%	<0.1	0.6	0.3	0.1	1.0	0.2	1.1	0.5	
10%	0.1	0.6	0.3	0.1	1.0	0.2	1.1	0.5	
25%	0.4	1.0	0.6	0.3	1.2	0.4	1.1	0.7	P=800mW.
50%	0.8	2.9	1.8	1.0	3.0	0.5	1.9	1.2	V_{CB}=20V.
75%	1.7	14.2	7.8	3.2	7.7	2.2	2.9	2.2	T_A=25°C.
90%	3.3	98.2	47.5	39.1	54.4	2.8	3.5	926.1	
95%	3.4	132.0	62.8	58.3	54.4	2.8	3.5	926.1	
Max	3.4	132.0	62.8	58.3	54.4	2.8	3.5	926.1	
Min	<0.1	0.5	0.1	<0.1	<0.1	0.6	<0.1	<0.1	
5%	<0.1	0.5	0.1	<0.1	<0.1	0.6	<0.1	<0.1	
10%	<0.1	0.5	0.2	0.2	0.1	0.7	0.2	<0.1	
25%	0.1	0.9	0.5	0.3	0.2	1.0	0.2	0.2	P=700mW.
50%	0.4	1.4	0.9	0.7	0.5	1.4	0.4	1.0	V_{CB}=20V.
75%	1.3	2.4	2.2	1.9	1.6	2.4	0.8	1.7	T_A=25°C.
90%	6.9	17.0	17.0	31.0	2.8	4.0	2.4	276.3	
95%	557.8	94.2	322.1	678.2	124.1	141.6	46.0	---	
Max	>1 uA	123.1	531.6	---	223.1	165.7	80.0	---	
Min	0.1	0.6	0.7	<0.1	0.1	<0.1	<0.1	0.2	
5%	0.2	0.8	1.1	0.4	0.2	0.1	<0.1	0.3	
10%	0.3	1.1	1.3	0.5	0.4	0.2	0.1	0.4	
25%	0.7	1.3	1.6	0.8	0.7	0.5	0.5	0.7	P=500mW.
50%	1.0	1.9	2.2	1.6	1.3	1.1	1.1	1.4	V_{CB}=20V.
75%	2.5	3.6	3.4	3.0	2.7	2.5	2.4	3.0	T_A=25°C.
90%	3.2	4.6	6.5	7.8	7.8	3.3	3.6	5.8	
95%	4.4	91.7	70.3	32.3	152.6	7.9	24.4	26.3	
Max	13.3	---	---	---	---	686.7	---	---	
Min	0.1	1.2	0.7	0.5	0.5	<0.1	0.3	0.5	
5%	0.1	1.2	0.7	0.5	0.5	<0.1	0.3	0.5	
10%	0.2	1.2	0.8	0.5	0.5	0.2	0.3	0.5	
25%	0.5	1.5	1.1	0.9	0.8	0.8	0.5	0.8	P=400mW.
50%	0.8	1.8	1.5	1.2	1.0	1.0	0.6	1.2	V_{CB}=20V.
75%	1.5	2.5	2.1	1.7	1.6	1.4	1.5	1.7	T_A=150°C.
90%	2.3	3.1	3.8	2.2	10.1	2.0	2.0	3.6	
95%	2.5	3.2	4.6	2.5	15.5	2.2	2.2	4.2	
Max	2.5	3.2	4.6	2.5	15.5	2.2	2.2	4.2	

TABLE 63. (CONTINUED).

HRS.	INIT.	168	340	680	1000	1500	2000	3000	
Min	0.3	0.6	0.5	0.3	0.2	0.2	1.0	0.4	
5%	0.3	0.7	0.5	0.4	0.2	0.2	1.0	0.4	
10%	0.4	0.9	0.7	0.5	0.3	0.3	1.0	0.5	
25%	1.1	1.5	1.2	1.1	0.7	0.5	1.6	1.3	P=200mW.
50%	2.0	2.7	2.4	2.0	1.8	1.3	2.3	2.0	V_{CB}=20V.
75%	3.1	3.6	3.4	2.7	2.5	2.7	3.2	3.0	T_A=150°C.
90%	3.7	25.7	22.3	6.1	14.5	4.5	5.2	4.6	
95%	18.6	134.9	211.2	190.3	135.3	91.5	68.4	14.6	
Max	30.0	199.9	359.4	329.7	236.4	151.7	109.3	18.9	

TABLE 63 GRAPH.

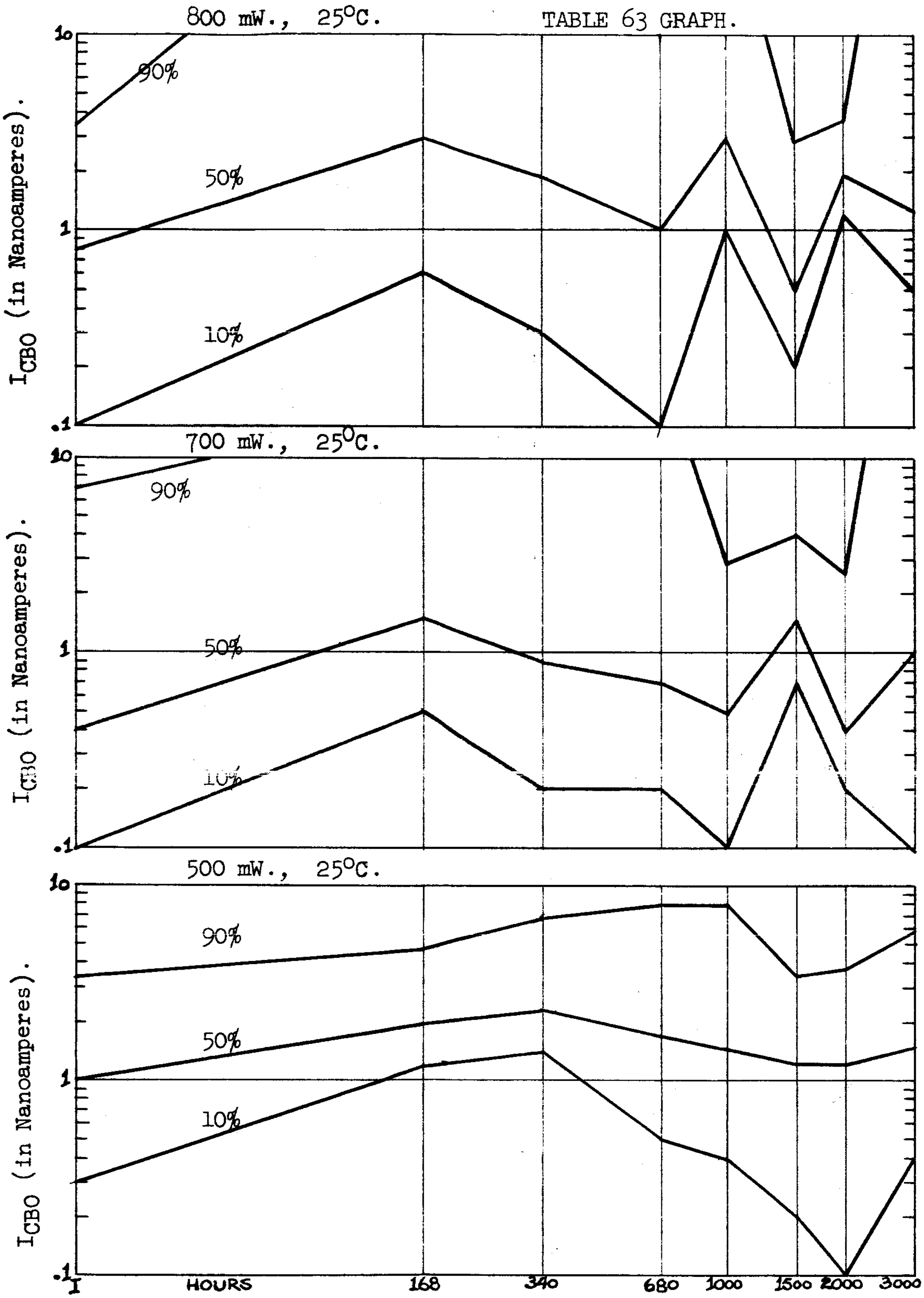

TABLE 63 GRAPH.

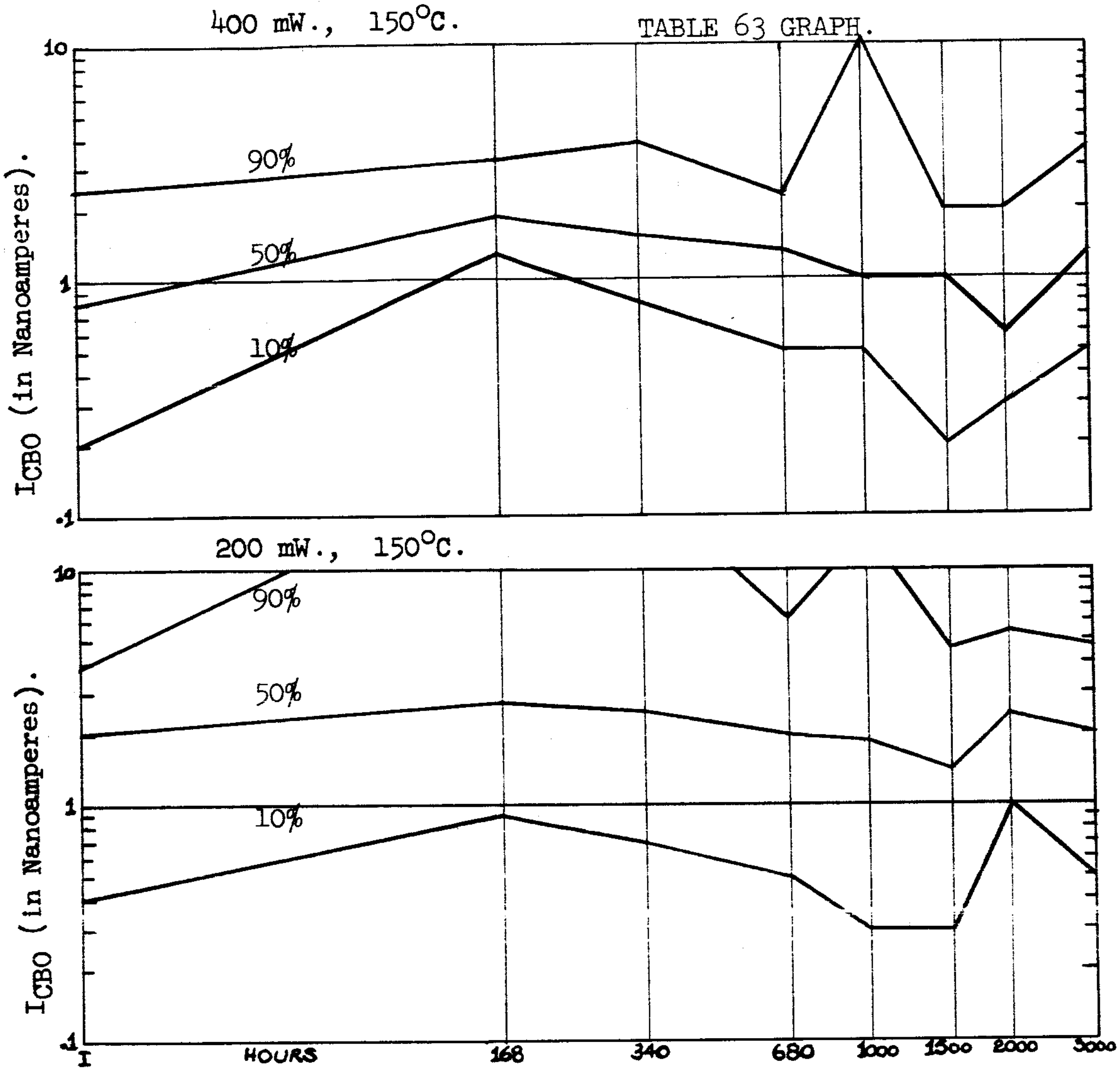

PROCESS C. HIGH STRESS SCREEN. TABLE 64.

I_{CBO} DISTRIBUTION CHANGES WITH LIFE TEST.

	I_{CBO} (V_{CB} = 60 V.) (Nanoamperes).								
HRS.	INIT.	168	340	680	1000	1500	2000	3000	
Min	0.2	1.1	0.6	0.6	0.4	0.4	0.8	<0.1	P=800mW. V_{CB}=20V. T_A=25°C.
5%	0.2	1.1	0.6	0.6	0.4	0.4	0.8	<0.1	
10%	0.2	1.1	0.6	0.6	0.4	0.4	0.8	<0.1	
25%	0.2	9.7	41.3	39.7	9.0	0.5	1.3	1.1	
50%	504.4	50.0	91.6	71.5	68.8	131.2	33.1	13.7	
75%	>1 uA	607.0	421.6	331.9	295.8	293.7	504.6	394.2	
90%	>1 uA	908.9	808.1	662.8	640.9	494.0	918.4	---	
95%	>1 uA	908.9	808.1	662.8	640.9	494.0	918.4	---	
Max	>1 uA	908.9	808.1	662.8	640.9	494.0	918.4	---	
Min	<0.1	0.7	1.0	0.5	0.5	0.1	0.1	<0.1	P=700mW. V_{CB}=20V. T_A=25°C.
5%	<0.1	0.7	1.0	0.5	0.5	0.1	0.1	<0.1	
10%	<0.1	0.8	1.0	0.5	0.5	0.2	0.2	0.2	
25%	0.2	1.0	1.3	0.6	0.7	0.7	0.5	1.0	
50%	1.5	5.1	11.7	6.3	7.5	5.2	12.6	9.8	
75%	533.1	94.9	57.5	77.9	106.3	83.4	125.9	129.0	
90%	>1 uA	---	---	---	765.9	504.7	---	---	
95%	>1 uA	---	---	---	---	---	---	---	
Max	>1 uA	---	---	---	---	---	---	---	
Min	0.3	0.3	0.1	0.5	10.6	0.3	0.2	0.4	P=500mW. V_{CB}=20V. T_A=25°C.
5%	0.3	0.3	0.1	0.5	10.6	0.3	0.2	0.4	
10%	0.3	0.3	0.1	0.5	10.6	0.3	0.2	0.4	
25%	0.3	0.5	2.1	6.7	24.2	7.2	5.3	7.8	
50%	169.0	9.5	76.1	67.0	730.2	53.6	43.9	32.6	
75%	>1 uA	354.3	761.3	---	---	---	---	---	
90%	>1 uA	---	---	---	---	---	---	---	
95%	>1 uA	---	---	---	---	---	---	---	
Max	>1 uA	---	---	---	---	---	---	---	

TABLE 64 GRAPH.

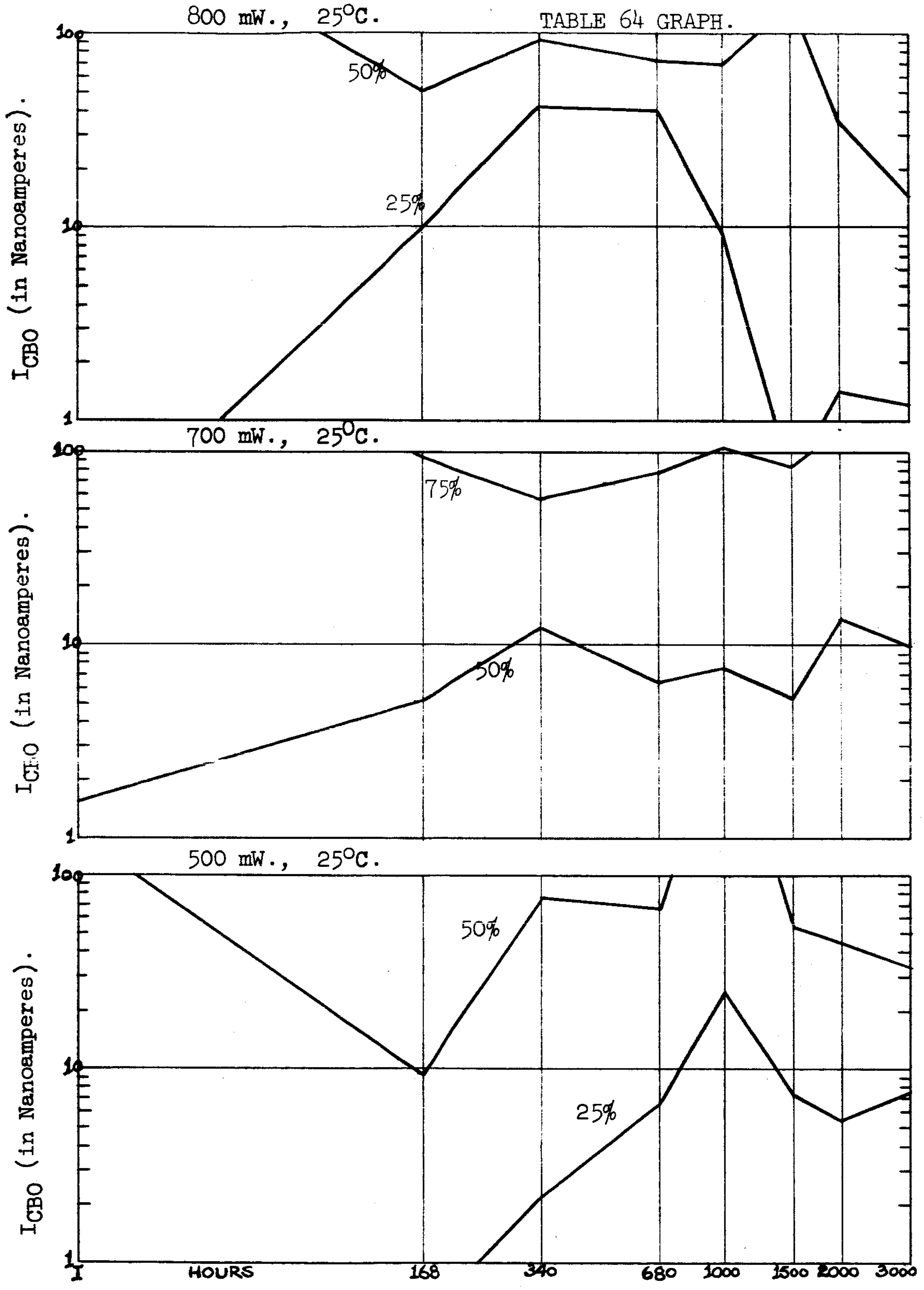

PROCESS A. HIGH STRESS SCREEN. TABLE 65.

h_{FE} DISTRIBUTION CHANGES WITH LIFE TEST.

	h_{FE} (I_C = 20 mA., V_{CE} = 5 V.)								
HRS.	INIT.	168	340	680	1000	1500	2000	3000	
Min	59	57	20	57	58	58	20		P=800mW. V_{CB}=20V. T_A=25°C.
5%	59	57	20	57	58	58	20		
10%	64	63	38	63	64	64	38		
25%	78	80	74	80	81	81	81		
50%	82	86	82	84	85	86	85		
75%	91	93	93	92	93	95	98		
90%	102	103	98	101	102	103	104		
95%	105	106	99	104	105	108	105		
Max	105	106	99	104	105	108	105		
Min	67	69	65	20	69	20	20	20	P=700mW. V_{CB}=20V. T_A=25°C.
5%	68	69	65	41	70	20	20	20	
10%	69	70	70	68	73	64	20	20	
25%	74	74	73	72	76	73	71	70	
50%	82	83	79	82	86	83	80	78	
75%	89	89	87	88	102	91	90	90	
90%	99	98	98	101	904	106	105	104	
95%	105	104	106	104	978	113	116	121	
Max	106	106	107	106	---	118	125	134	
Min	51	48	20	20	20	20	20	20	P=500mW. V_{CB}=20V. T_A=25°C.
5%	62	61	41	61	20	20	20	20	
10%	69	65	64	65	51	53	53	53	
25%	77	75	74	73	65	69	70	69	
50%	86	83	84	82	76	78	79	80	
75%	92	86	90	89	84	90	91	90	
90%	99	97	97	99	99	99	101	100	
95%	104	101	101	103	102	106	108	108	
Max	119	116	116	---	118	119	121	120	
Min	64	58	64	53	63	64	64	20	P=400mW. V_{CB}=20V. T_A=150°C.
5%	64	58	64	53	63	64	64	20	
10%	73	60	65	60	67	67	68	42	
25%	84	81	86	81	87	88	89	83	
50%	89	89	88	84	93	96	98	102	
75%	100	94	98	90	104	108	107	110	
90%	106	97	103	100	109	112	115	119	
95%	107	97	104	104	109	115	118	119	
Max	107	97	104	104	109	115	118	119	

TABLE 65. (CONTINUED).

HRS.	INIT.	168	340	680	1000	1500	2000	3000	
Min	54	54	54	53	52	53	58	53	
5%	56	56	56	56	55	55	59	56	
10%	60	60	59	60	58	59	60	59	
25%	74	75	72	74	74	71	81	74	P=200mW.
50%	83	83	82	82	82	83	84	84	V_{CB}=20V.
75%	90	90	88	89	87	88	96	89	T_A=150°C.
90%	104	99	98	104	102	104	1687	1055	
95%	118	115	114	120	119	117	6221	1278	
Max	122	123	124	125	123	117	7071	1349	

TABLE 65 GRAPH.

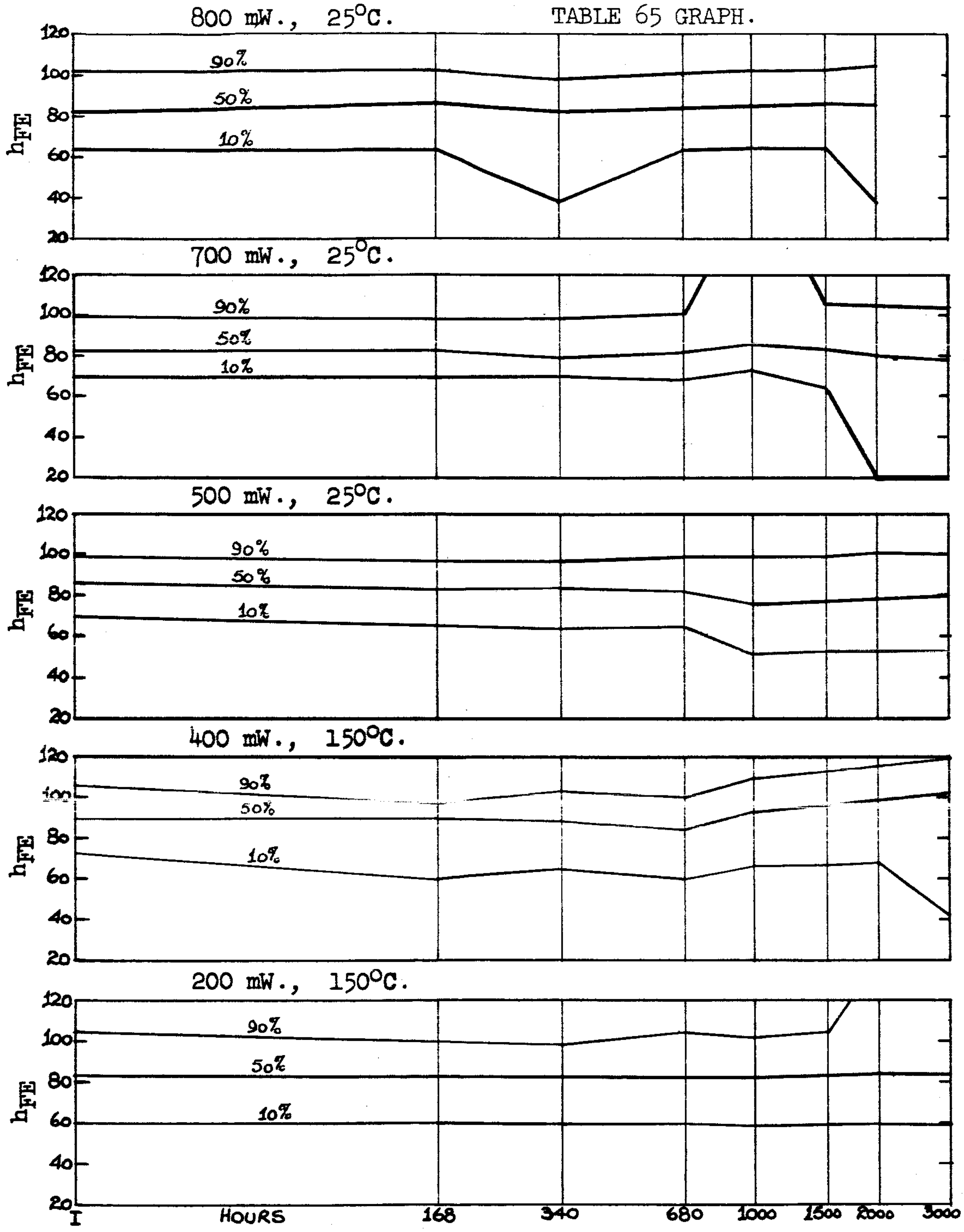

PROCESS B. HIGH STRESS SCREEN. TABLE 66.

h_{FE} DISTRIBUTION CHANGES WITH LIFE TEST.

	h_{FE} (I_C = 20 mA., V_{CE} = 5 V.)								
HRS.	INIT.	168	340	680	1000	1500	2000	3000	
Min	67	20	67	20	68	20	34	20	P=800mW. V_{CB}=20V. T_A=25°C.
5%	67	20	67	20	68	20	34	20	
10%	68	40	68	20	68	20	34	20	
25%	77	75	74	70	82	20	60	29	
50%	92	96	92	96	99	86	98	75	
75%	110	108	109	115	113	109	121	106	
90%	151	119	158	159	122	124	129	131	
95%	174	121	179	185	122	125	129	131	
Max	174	121	179	185	122	125	129	131	
Min	49	54	58	20	20	34	20	20	P=700mW. V_{CB}=20V. T_A=25°C.
5%	50	56	59	20	20	38	20	20	
10%	56	60	62	20	20	66	20	20	
25%	86	83	84	86	86	89	23	86	
50%	99	98	99	99	99	102	91	101	
75%	109	106	112	118	117	134	116	145	
90%	118	158	162	167	162	163	153	160	
95%	128	175	180	634	178	183	168	179	
Max	131	185	189	---	187	186	177	179	
Min	55	72	20	69	20	20	20	20	P=500mW. V_{CB}=20V. T_A=25°C.
5%	70	74	73	75	71	20	20	20	
10%	75	76	77	78	74	72	20	20	
25%	86	86	83	85	85	84	83	82	
50%	99	99	95	99	97	97	98	97	
75%	109	111	106	111	111	113	112	113	
90%	115	117	115	121	117	124	123	122	
95%	121	130	126	140	142	143	141	143	
Max	153	147	153	153	148	155	153	157	
Min	61	61	62	58	60	61	60	57	P=400mW. V_{CB}=20V. T_A=150°C.
5%	61	61	62	58	60	61	60	57	
10%	67	66	68	63	66	67	60	59	
25%	82	85	87	82	86	87	87	88	
50%	99	94	100	89	97	98	98	100	
75%	112	108	107	103	109	110	111	112	
90%	130	129	145	145	153	178	183	188	
95%	137	138	159	168	171	212	220	228	
Max	137	138	159	168	171	212	220	228	

TABLE 66. (CONTINUED).

HRS.	INIT.	168	340	680	1000	1500	2000	3000	
Min	64	65	64	61	63	64	64	64	
5%	65	65	64	61	64	65	65	65	
10%	66	67	68	65	66	67	68	69	
25%	85	84	83	79	82	83	83	83	P=200mW.
50%	98	98	98	92	96	98	98	98	V_{CB}=20V.
75%	112	108	107	100	110	110	111	111	T_A=150°C.
90%	118	115	114	107	117	119	119	120	
95%	125	116	120	112	120	124	123	126	
Max	129	117	122	115	121	127	125	128	

TABLE 66 GRAPH.

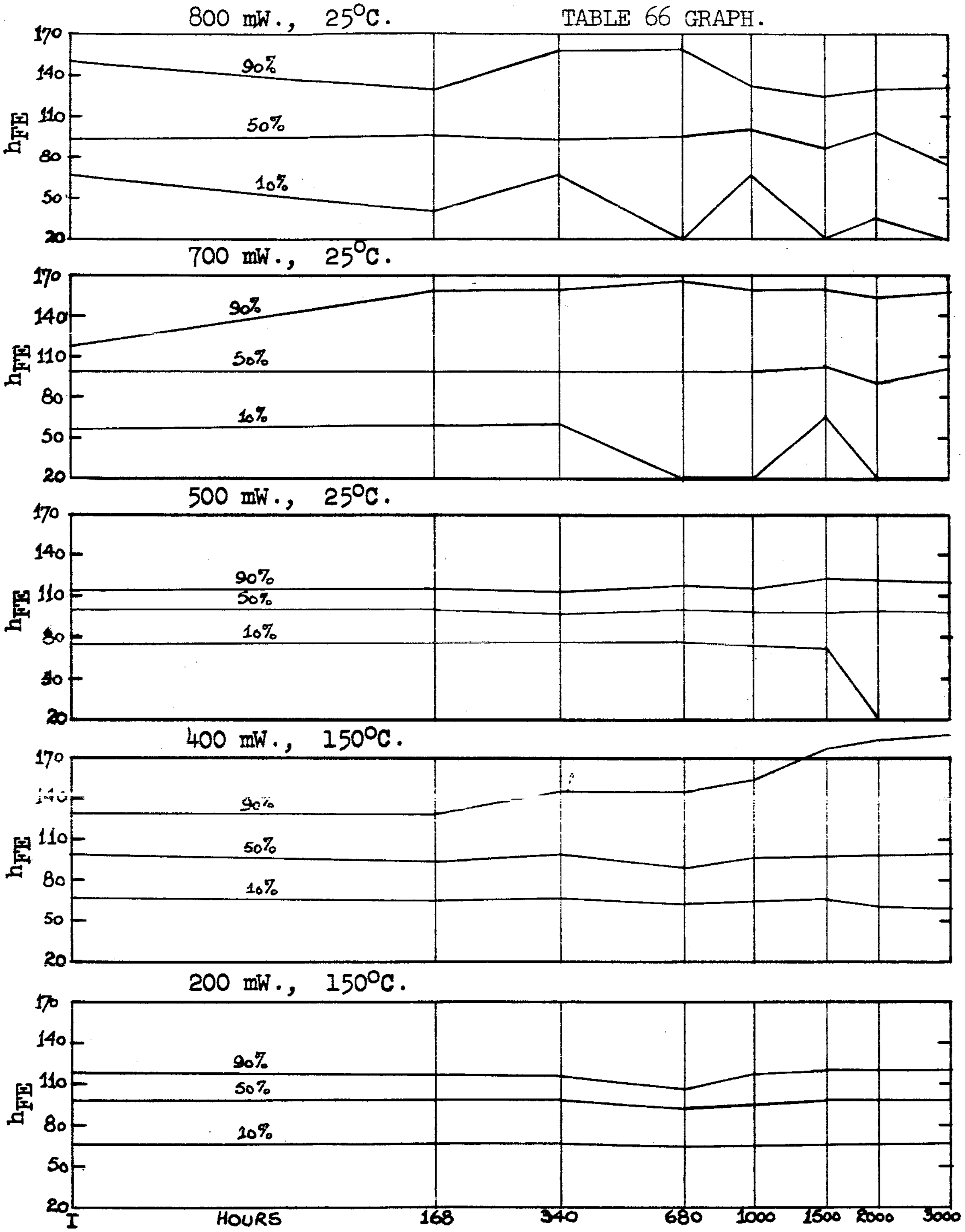

PROCESS C. HIGH STRESS SCREEN. TABLE 67.

h_{FE} DISTRIBUTION CHANGES WITH LIFE TEST.

	h_{FE} (I_C = 20 mA., V_{CE} = 5 V.)								
HRS.	INIT.	168	340	680	1000	1500	2000	3000	
Min	51	46	46	45	46	20	20		P=800mW. V_{CB}=20V. T_A=25°C.
5%	51	46	46	45	46	20	20		
10%	51	46	46	45	46	20	20		
25%	55	51	50	49	49	43	20		
50%	69	68	63	67	68	68	58		
75%	89	82	79	82	84	84	93		
90%	129	115	107	114	117	119	117		
95%	129	115	107	114	117	119	117		
Max	129	115	107	114	117	119	117		
Min	49	48	47	49	48	49	48	50	P=700mW. V_{CB}=20V. T_A=25°C.
5%	49	48	47	49	48	49	48	50	
10%	50	51	49	51	50	51	50	50	
25%	55	54	53	54	54	54	54	53	
50%	69	69	68	69	69	69	67	68	
75%	102	101	100	101	101	101	101	101	
90%	124	123	121	123	122	124	124	123	
95%	131	130	128	131	129	131	130	129	
Max	131	130	128	131	129	131	130	129	
Min	43	43	37	32	31	31	29	28	P=500mW. V_{CB}=20V. T_A=25°C.
5%	43	43	37	32	31	31	29	28	
10%	43	43	37	32	31	31	29	28	
25%	53	52	51	47	48	49	49	48	
50%	64	66	67	64	67	68	70	71	
75%	86	81	81	78	81	83	85	84	
90%	111	108	108	103	105	108	114	109	
95%	111	108	108	103	105	108	114	109	
Max	111	108	108	103	105	108	114	109	

TABLE 67 GRAPH.

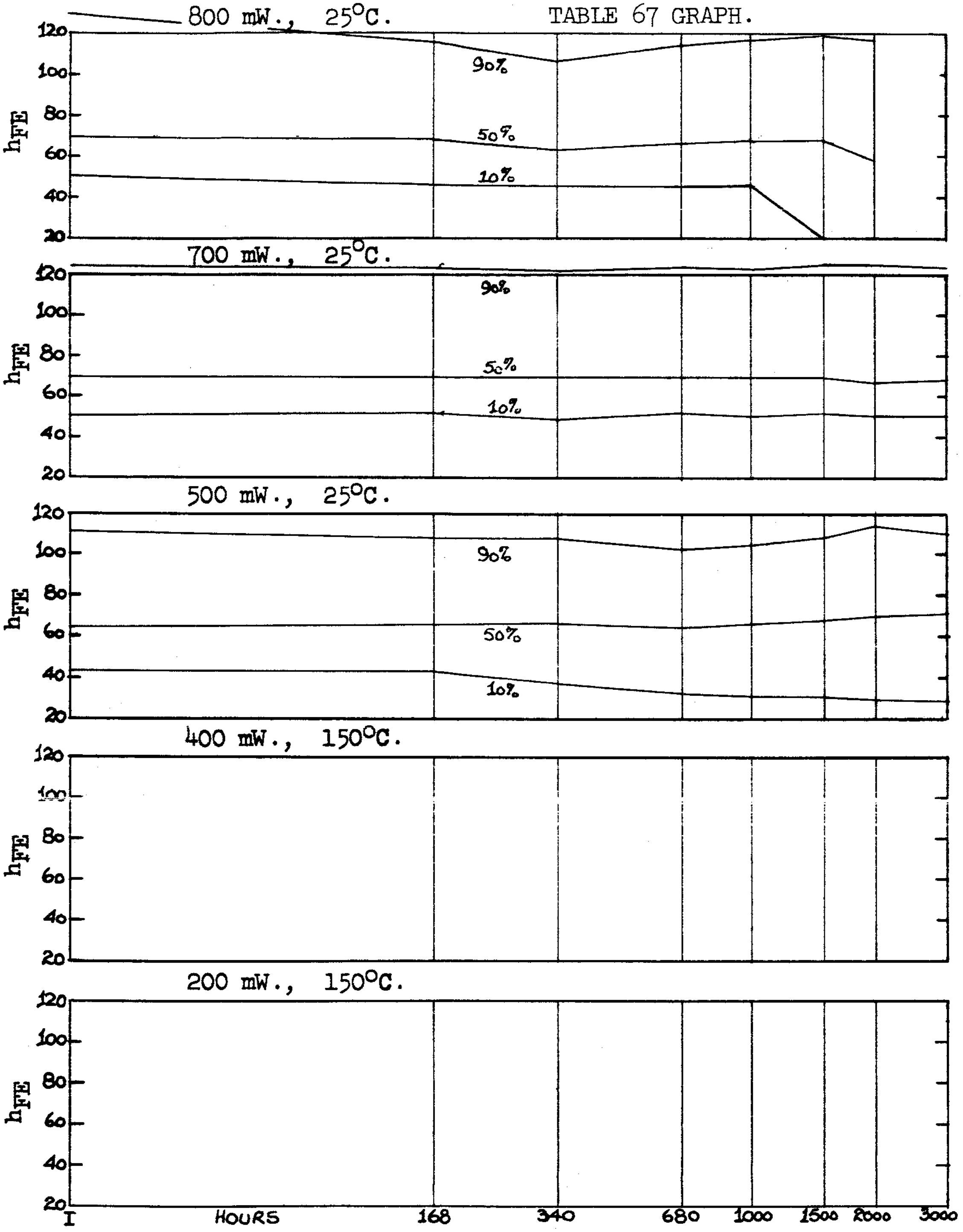

I_{CBO} DISTRIBUTION CHANGES WITH LIFE TEST.

HRS.	I_{CBO} (V_{CB} = 60 V.) (Nanoamperes).								
	INIT.	168	340	680	1000	1500	2000	3000	
Min	<0.1	<0.1	0.1	<0.1	0.2	<0.1	<0.1	<0.1	P=800mW. V_{CB}=20V. T_A=25°C.
5%	<0.1	<0.1	0.1	<0.1	0.2	<0.1	<0.1	<0.1	
10%	0.1	0.3	0.2	0.1	0.2	<0.1	<0.1	<0.1	
25%	0.1	0.5	0.2	0.2	0.2	0.1	0.2	0.1	
50%	0.3	0.9	0.4	0.4	0.4	0.5	0.3	0.4	
75%	0.5	1.9	1.7	1.5	1.6	1.2	2.7	3.2	
90%	1.5	4.9	4.9	3.0	2.5	1.9	7.5	6.5	
95%	2.0	6.9	6.9	3.7	2.5	2.0	9.3	6.8	
Max	2.0	6.9	6.9	3.7	2.5	2.0	9.3	6.8	
Min	<0.1	0.5	<0.1	<0.1	<0.1	<0.1	<0.1	0.3	P=700mW. V_{CB}=20V. T_A=25°C.
5%	<0.1	0.5	<0.1	<0.1	<0.1	<0.1	<0.1	0.4	
10%	<0.1	0.6	<0.1	<0.1	<0.1	<0.1	<0.1	0.5	
25%	0.1	0.7	0.1	0.1	0.1	0.1	<0.1	0.5	
50%	0.2	0.9	0.4	0.3	0.1	0.2	0.3	0.7	
75%	0.9	1.7	1.1	1.1	0.3	0.7	1.0	1.5	
90%	1.0	2.0	1.3	1.3	1.3	1.1	1.3	1.9	
95%	1.9	2.9	2.3	2.2	2.2	1.9	2.1	3.2	
Max	2.7	3.7	3.1	3.0	3.0	2.4	2.7	3.4	
Min	<0.1	<0.1	0.4	0.8	<0.1	<0.1	<0.1	<0.1	P=500mW. V_{CB}=20V. T_A=25°C.
5%	0.1	<0.1	0.4	0.9	<0.1	0.1	<0.1	<0.1	
10%	0.1	<0.1	0.5	1.0	0.1	0.2	<0.1	<0.1	
25%	0.2	0.1	0.7	1.1	0.3	0.3	0.1	0.1	
50%	0.3	0.4	0.9	1.3	0.6	0.5	0.3	0.4	
75%	0.9	0.6	1.5	1.8	1.2	1.3	1.0	1.0	
90%	1.3	1.2	2.1	2.5	2.0	1.7	1.4	1.7	
95%	2.4	2.3	3.4	3.4	3.8	2.7	2.1	2.6	
Max	26.5	7.4	3.5	4.5	71 uA	3.9	3.5	6.8	
Min	<0.1	0.6	<0.1	<0.1	0.1	<0.1	<0.1	<0.1	P=400mW. V_{CB}=20V. T_A=150°C.
5%	<0.1	0.6	<0.1	<0.1	0.1	<0.1	<0.1	<0.1	
10%	<0.1	0.6	<0.1	0.1	0.2	0.1	<0.1	0.1	
25%	0.1	0.7	0.3	0.3	0.4	0.2	0.2	0.3	
50%	0.3	0.9	0.5	0.4	0.6	0.3	0.4	0.6	
75%	0.5	1.1	0.7	0.6	3.0	0.5	0.6	1.2	
90%	1.3	17.1	16.7	14.8	14.3	5.7	4.7	1.9	
95%	1.3	32.1	31.7	27.8	16.3	10.0	7.7	2.3	
Max	1.3	32.1	31.7	27.8	16.3	10.0	7.7	2.3	

TABLE 68. (CONTINUED).

HRS.	INIT.	168	340	680	1000	1500	2000	3000	
Min	<0.1	0.4	0.1	<0.1	<0.1	<0.1	<0.1	<0.1	
5%	<0.1	0.5	0.2	<0.1	<0.1	<0.1	<0.1	<0.1	
10%	0.1	0.5	0.2	<0.1	0.1	<0.1	<0.1	<0.1	
25%	0.2	0.7	0.2	0.2	0.2	0.1	0.1	0.1	P=200mW.
50%	0.3	0.8	0.4	0.4	0.3	0.3	0.2	0.3	V_{CB}=20V.
75%	0.6	1.2	0.7	0.6	0.8	0.4	0.5	0.5	T_A=150°C.
90%	1.3	2.0	1.6	1.6	1.5	1.4	1.2	1.3	
95%	2.0	4.6	2.1	2.1	5.9	1.6	1.8	1.8	
Max	2.3	6.3	2.4	2.5	9.5	1.8	2.0	2.2	

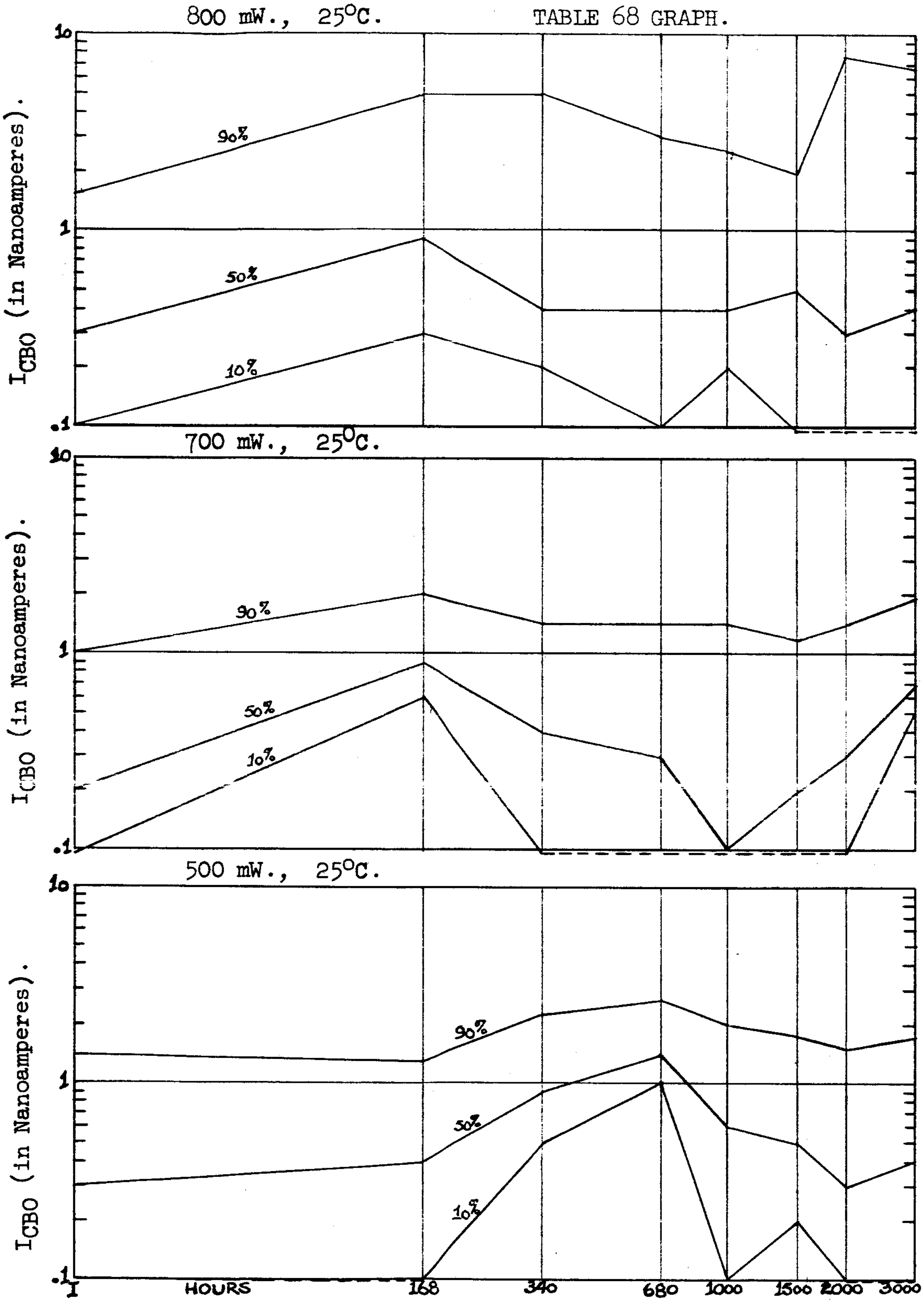
TABLE 68 GRAPH.

400 mW., 150°C. TABLE 68 GRAPH.

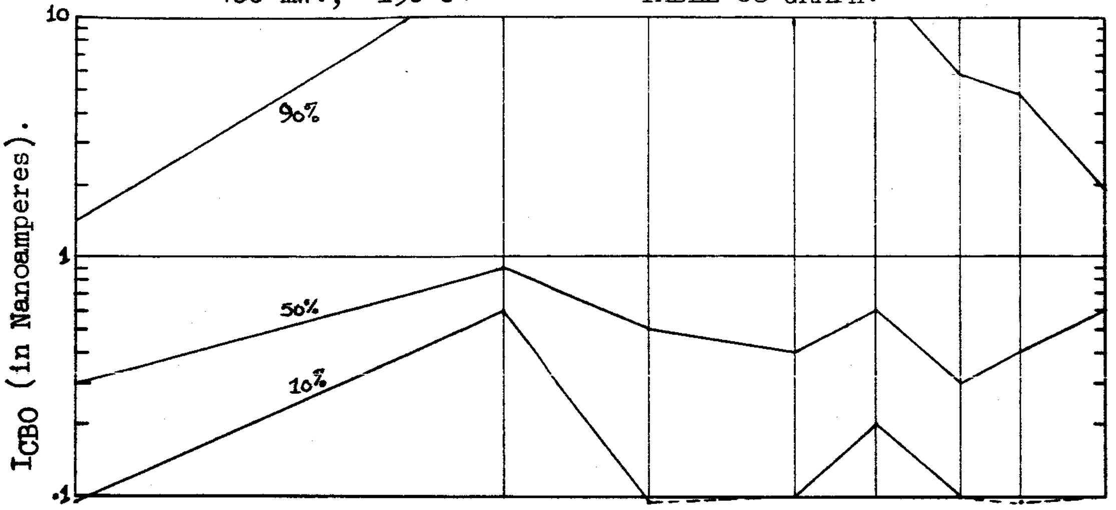

200 mW., 150°C.

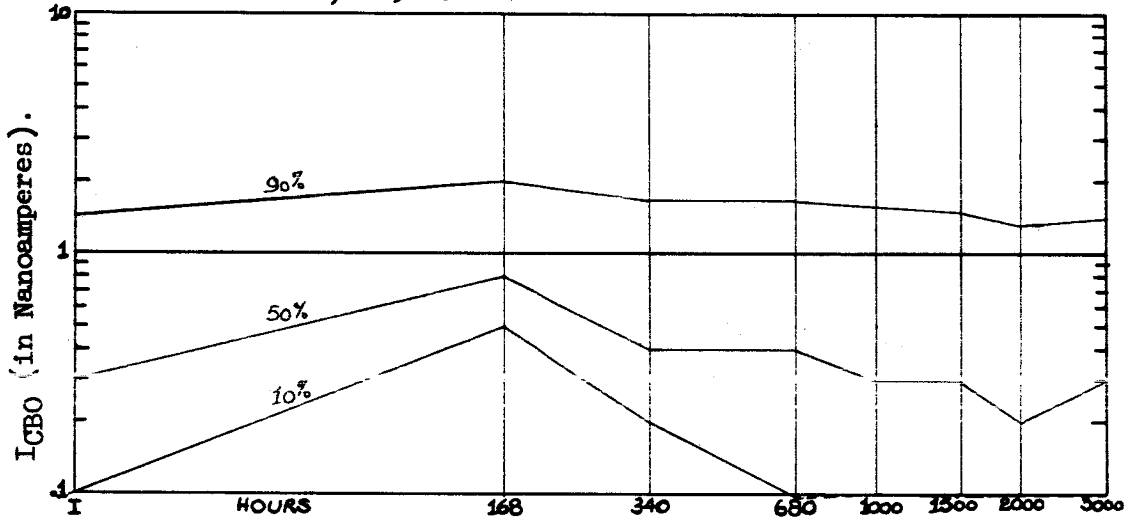

I_{CBO} DISTRIBUTION CHANGES WITH LIFE TEST.

	I_{CBO} (V_{CB} = 60 V.) (Nanoamperes).								
HRS.	INIT.	168	340	680	1000	1500	2000	3000	
Min	0.2	0.9	0.3	0.2	0.3	<0.1	<0.1	0.6	
5%	0.2	0.9	0.3	0.2	0.3	<0.1	<0.1	0.6	
10%	0.3	0.9	0.3	0.3	0.4	0.1	0.2	0.6	
25%	0.9	1.6	0.9	0.7	0.9	0.3	0.4	0.7	P=800mW.
50%	1.5	1.8	1.2	1.0	1.2	1.0	1.0	1.0	V_{CB}=20V.
75%	3.5	4.1	3.8	3.2	3.5	2.3	1.7	1.3	T_A=25°C.
90%	4.6	4.9	4.4	501.8	4.2	3.5	3.2	3.2	
95%	4.6	5.0	4.4	---	4.2	3.7	3.7	3.6	
Max	4.6	5.0	4.4	---	4.2	3.7	3.7	3.6	
Min	<0.1	0.8	0.2	0.2	0.4	<0.1	0.2	0.2	
5%	0.2	0.9	0.3	0.2	0.4	<0.1	0.3	0.2	
10%	0.4	0.9	0.4	0.3	0.5	0.1	0.3	0.2	
25%	1.0	1.8	1.1	0.9	1.3	1.0	0.7	0.9	P=700mW.
50%	2.2	3.4	2.8	1.8	2.0	1.6	1.0	1.3	V_{CB}=20V.
75%	3.6	4.5	3.5	2.7	3.5	3.3	2.9	3.3	T_A=25°C.
90%	4.7	5.1	4.4	3.8	4.5	4.2	3.7	4.0	
95%	4.9	9.8	6.9	3.9	4.8	502.7	3.9	4.4	
Max	5.0	14.4	9.2	3.9	4.8	---	3.9	4.5	
Min	0.2	0.9	1.3	0.4	0.3	0.2	0.3	0.5	
5%	0.4	1.0	1.3	0.5	0.6	0.3	0.4	0.7	
10%	0.5	1.2	1.5	0.7	0.7	0.5	0.6	1.0	
25%	0.9	1.6	1.9	1.0	1.1	0.9	1.0	1.3	P=500mW.
50%	2.1	3.4	3.3	2.3	2.5	2.4	2.3	2.6	V_{CB}=20V.
75%	3.7	4.5	4.2	3.5	3.5	3.4	3.4	4.0	T_A=25°C.
90%	4.1	5.0	4.6	3.9	4.0	4.3	4.2	4.6	
95%	4.5	13.2	13.9	17.9	18.7	5.1	5.6	9.7	
Max	4.8	196.4	121.8	57.6	29.4	34.2	38.3	31.1	
Min	0.2	0.7	0.5	0.3	0.1	0.2	<0.1	0.3	
5%	0.2	0.7	0.5	0.3	0.1	0.2	<0.1	0.3	
10%	0.2	0.8	0.5	0.4	0.1	0.3	0.1	0.4	
25%	0.4	1.1	0.6	0.5	0.4	0.4	0.3	0.6	P=400mW.
50%	1.9	2.5	2.2	1.8	1.3	1.6	1.6	0.8	V_{CB}=20V.
75%	4.4	4.6	4.2	3.9	3.1	3.6	4.1	3.6	T_A=150°C.
90%	5.1	5.1	4.6	4.3	3.5	4.1	4.4	4.3	
95%	5.4	5.3	4.6	4.5	3.5	4.2	4.4	4.6	
Max	5.4	5.3	4.6	4.5	3.5	4.2	4.4	4.6	

TABLE 69. (CONTINUED).

HRS.	INIT.	168	340	680	1000	1500	2000	3000	
Min	0.4	0.8	0.6	0.5	0.5	0.3	1.1	0.1	
5%	0.5	0.9	0.7	0.5	0.5	0.4	1.1	0.3	
10%	0.6	1.2	0.8	0.5	0.6	0.4	1.2	0.9	
25%	0.9	1.5	1.2	1.0	0.9	0.9	1.5	1.2	P=200mW.
50%	1.4	2.0	1.7	1.6	1.3	1.7	2.1	1.7	V_{CB}=20V.
75%	3.2	3.7	3.7	3.4	2.9	3.3	3.7	3.7	T_A=150°C.
90%	3.8	4.2	4.6	5.0	4.0	4.3	4.5	4.3	
95%	4.6	4.8	5.6	7.0	6.8	29.3	7.2	7.1	
Max	4.8	5.0	6.1	7.9	9.0	52.1	7.7	9.5	

TABLE 69 GRAPH.

800 mW., 25°C.

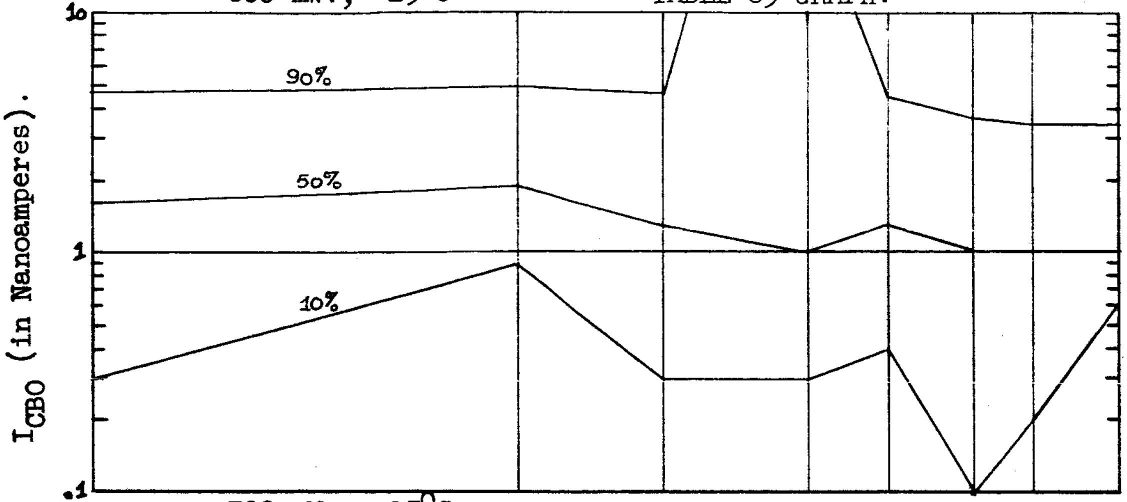

700 mW., 25°C.

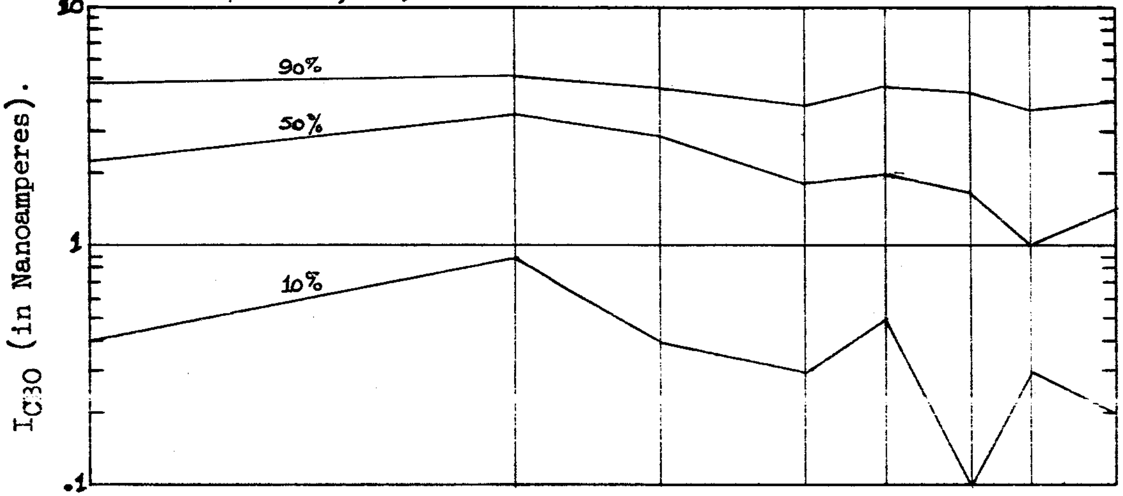

500 mW., 25°C.

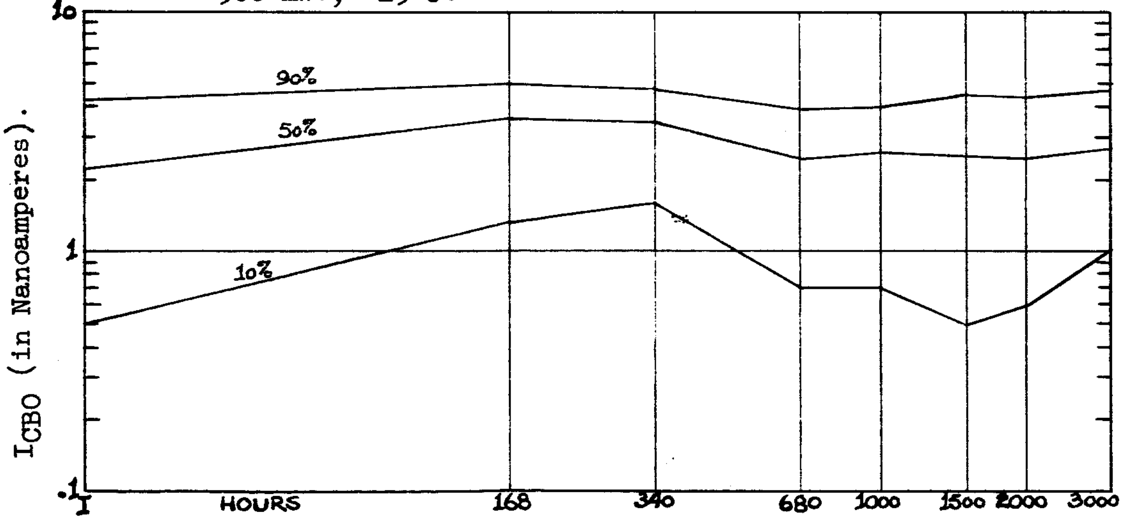

TABLE 69 GRAPH.

400 mW., 150°C.

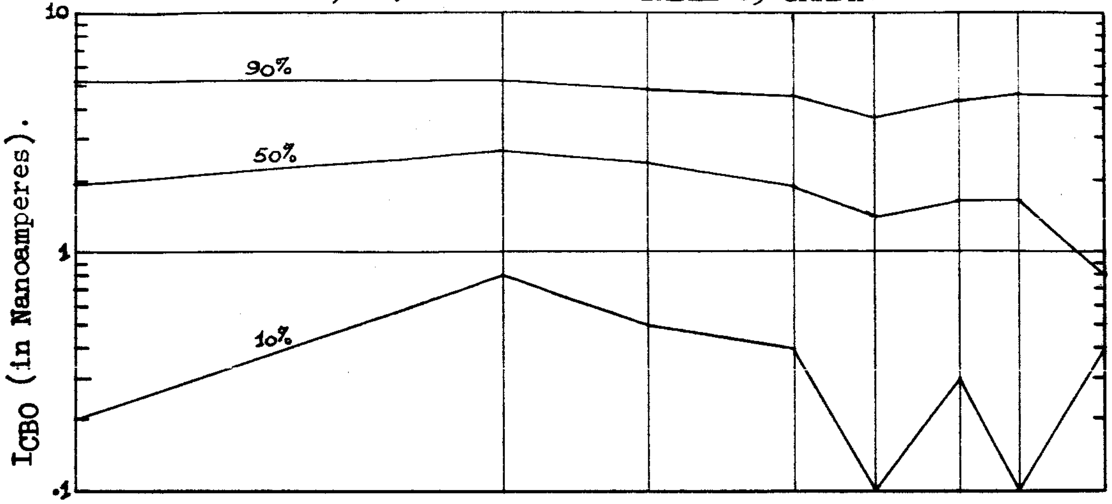

200 mW., 150°C.

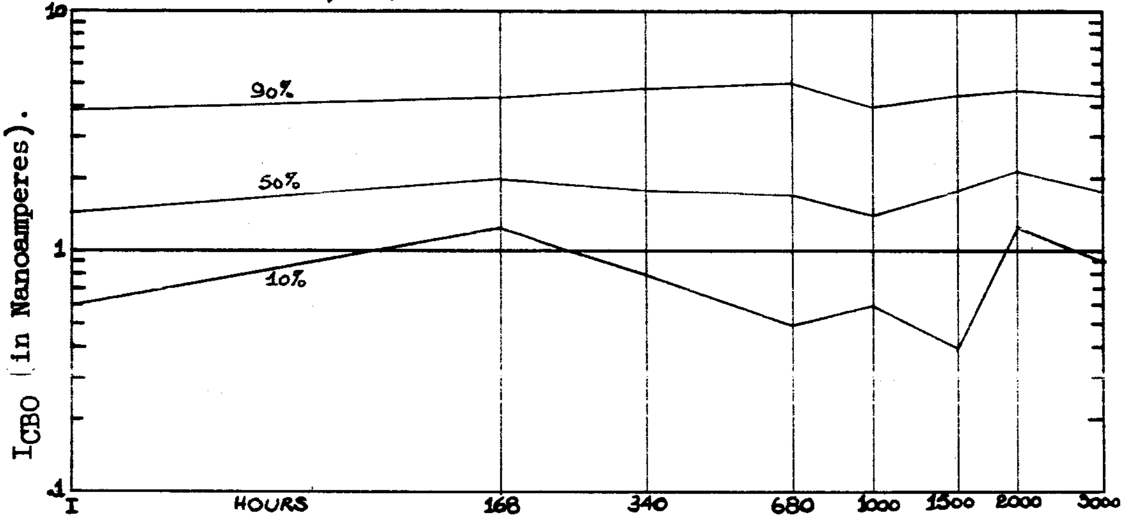

PROCESS C. MODERATE STRESS SCREEN. TABLE 70.

I_{CBO} DISTRIBUTION CHANGES WITH LIFE TEST.

	I_{CBO} (V_{CB} = 60 V.) (Nanoamperes).								
HRS.	INIT.	168	340	680	1000	1500	2000	3000	
Min	<0.1	0.4	<0.1	<0.1	<0.1	<0.1	<0.1	<0.1	P=800mW. V_{CB}=20V. T_A=25°C.
5%	<0.1	0.4	<0.1	<0.1	<0.1	<0.1	<0.1	<0.1	
10%	<0.1	0.4	<0.1	<0.1	0.1	<0.1	<0.1	<0.1	
25%	0.2	0.6	0.3	0.2	0.3	0.1	0.5	0.2	
50%	0.5	0.9	1.0	0.6	0.7	0.8	1.9	1.8	
75%	0.8	2.1	2.1	1.8	1.9	1.4	30.1	14.6	
90%	1.0	124.3	379.2	405.1	440.2	512.4	592.2	331.9	
95%	1.1	220.8	745.3	802.9	875.0	---	---	363.0	
Max	1.1	220.8	745.3	802.9	875.0	---	---	363.0	
Min	<0.1	0.4	<0.1	<0.1	<0.1	<0.1	<0.1	0.1	P=700mW. V_{CB}=20V. T_A=25°C.
5%	<0.1	0.5	<0.1	<0.1	<0.1	<0.1	0.1	0.2	
10%	<0.1	0.6	0.2	<0.1	0.2	<0.1	0.3	0.5	
25%	<0.1	0.7	0.2	0.1	0.3	0.1	0.4	0.7	
50%	0.1	0.9	0.5	0.3	0.4	0.4	1.0	1.6	
75%	0.2	1.4	1.2	1.2	1.5	3.3	204.9	562.4	
90%	0.6	3.6	31.2	44.3	58.5	581.0	---	---	
95%	8.0	6.5	62.2	134.8	148.4	---	---	---	
Max	14.0	7.0	73.8	174.5	187.0	---	---	---	
Min	<0.1	0.3	0.7	<0.1	<0.1	<0.1	<0.1	<0.1	P=500mW. V_{CB}=20V. T_A=25°C.
5%	<0.1	0.4	0.8	<0.1	0.1	<0.1	<0.1	<0.1	
10%	<0.1	0.4	1.0	<0.1	0.1	<0.1	<0.1	<0.1	
25%	<0.1	0.5	1.0	0.2	0.2	0.1	0.1	0.1	
50%	<0.1	0.7	1.3	0.4	0.4	0.3	0.3	0.3	
75%	0.2	1.2	1.9	1.1	1.4	0.7	1.6	1.7	
90%	0.6	4.0	5.4	5.9	13.0	6.7	11.6	19.1	
95%	2.3	23.7	22.2	31.3	45.3	17.9	24.5	102.9	
Max	7.6	58.1	179.1	938.0	---	---	---	---	
Min	<0.1	0.4	0.1	0.1	0.2	0.1	<0.1	<0.1	P=400mW. V_{CB}=20V. T_A=150°C.
5%	<0.1	0.4	0.1	0.1	0.2	0.1	<0.1	<0.1	
10%	<0.1	0.5	0.2	0.2	0.3	0.2	<0.1	<0.1	
25%	<0.1	0.7	0.6	0.5	2.6	0.3	0.2	0.1	
50%	0.4	1.3	2.4	4.6	72.9	3.9	0.3	0.4	
75%	0.4	4.1	229.0	325.2	---	---	409.2	155.4	
90%	0.8	236.2	---	---	---	---	---	366.7	
95%	0.9	417.0	---	---	---	---	---	451.8	
Max	0.9	417.0	---	---	---	---	---	451.8	

TABLE 70. (CONTINUED).

HRS.	INIT.	168	340	680	1000	1500	2000	3000	
Min	<0.1	0.2	<0.1	<0.1	<0.1	<0.1	<0.1	<0.1	
5%	<0.1	0.3	<0.1	<0.1	<0.1	<0.1	<0.1	<0.1	
10%	<0.1	0.5	<0.1	<0.1	0.1	<0.1	0.1	<0.1	
25%	<0.1	0.7	<0.1	0.1	0.2	<0.1	0.2	0.1	P=200mW.
50%	0.2	0.9	0.4	0.5	0.4	0.2	0.3	0.5	V_{CB}=20V.
75%	0.4	1.4	1.6	7.0	1.5	4.8	4.4	25.9	T_A=150°C.
90%	2.0	27.2	56.3	45.2	12.2	82.1	47.0	460.7	
95%	24.3	39.6	137.4	139.1	75.5	236.9	659.0	---	
Max	34.3	44.1	169.6	205.0	121.4	260.5	---	---	

TABLE 70 GRAPH.

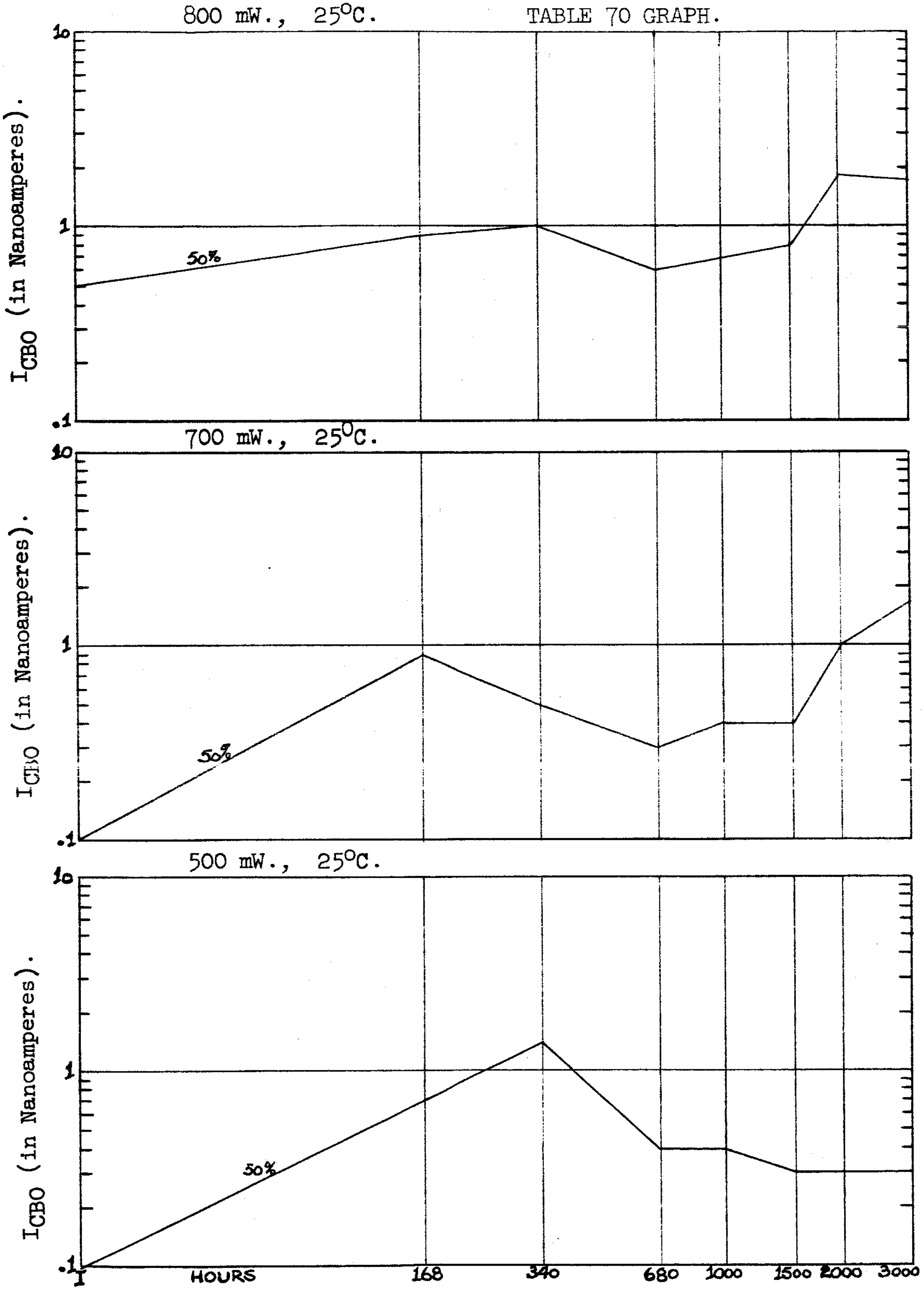

800 mW., 25°C.

700 mW., 25°C.

500 mW., 25°C.

TABLE 70 GRAPH.

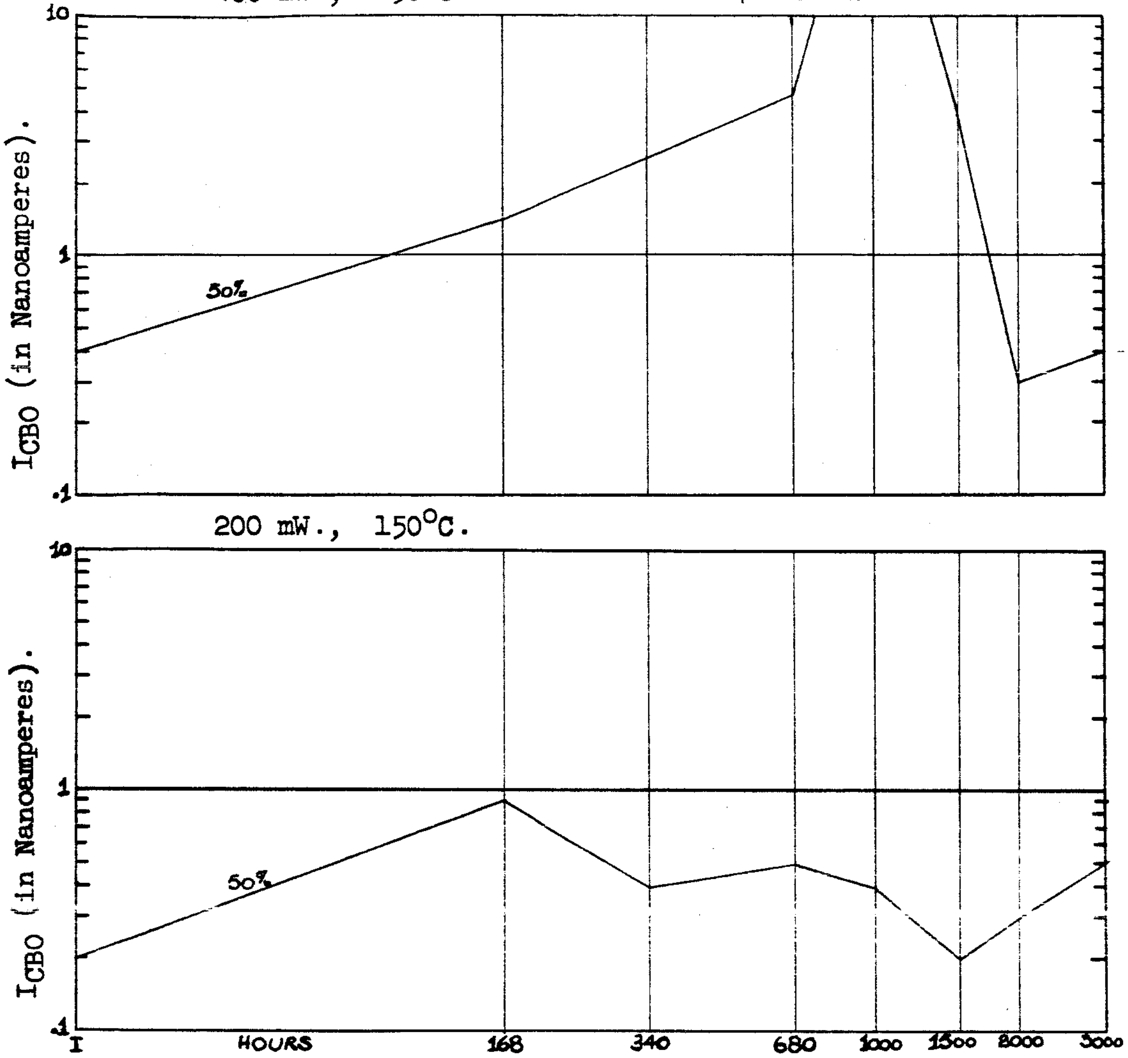

400 mW., 150°C.

200 mW., 150°C.

PROCESS A. MODERATE STRESS SCREEN. TABLE 71.

h_{FE} DISTRIBUTION CHANGES WITH LIFE TEST.

	h_{FE} (I_C = 20 mA., V_{CE} = 5 V.)								
HRS.	INIT.	168	340	680	1000	1500	2000	3000	
Min	67	68	64	20	20	20	20	20	P=800mW. V_{CB}=20V. T_A=25°C.
5%	67	68	64	20	20	20	20	20	
10%	68	68	64	44	44	20	20	20	
25%	73	74	75	70	71	66	55	66	
50%	88	89	91	87	90	87	79	85	
75%	92	92	94	90	92	91	90	90	
90%	98	97	100	97	99	98	99	101	
95%	100	98	102	99	101	99	102	105	
Max	100	98	102	99	101	99	102	105	
Min	62	60	63	63	63	62	60	20	P=700mW. V_{CB}=20V. T_A=25°C.
5%	63	63	64	64	64	64	61	40	
10%	67	66	67	66	66	67	66	63	
25%	77	77	77	77	77	77	74	73	
50%	84	83	84	84	85	85	83	83	
75%	90	90	89	90	92	91	90	88	
90%	98	94	92	99	99	100	98	99	
95%	102	100	97	103	103	103	103	102	
Max	105	105	99	106	106	105	104	103	
Min	53	54	52	52	20	20	20	20	P=500mW. V_{CB}=20V. T_A=25°C.
5%	64	64	62	62	20	52	20	20	
10%	68	65	64	64	54	57	54	54	
25%	77	75	74	72	64	66	64	64	
50%	87	82	83	80	77	80	79	79	
75%	92	90	91	87	89	91	89	89	
90%	97	96	96	91	95	97	95	95	
95%	99	98	97	94	97	98	97	96	
Max	103	103	102	96	186	101	99	98	
Min	57	57	59	19	55	56	56	20	P=400mW. V_{CB}=20V. T_A=150°C.
5%	57	57	59	19	55	56	56	20	
10%	62	60	62	37	60	60	60	38	
25%	67	66	66	59	65	66	66	66	
50%	87	86	86	77	82	84	83	82	
75%	91	91	92	85	88	90	91	90	
90%	97	98	99	92	96	97	98	95	
95%	98	98	100	93	97	98	100	97	
Max	98	98	100	93	97	98	100	97	

TABLE 71. (CONTINUED).

HRS.	INIT.	168	340	680	1000	1500	2000	3000	
Min	62	62	62			62	61	62	
5%	64	64	63			63	63	63	
10%	66	65	65			65	65	66	
25%	71	71	70			70	69	71	P=200mW.
50%	83	80	79			80	81	82	V_{CB}=20V.
75%	89	87	86			87	87	88	T_A=150°C.
90%	98	96	95			97	95	97	
95%	102	100	99			99	101	102	
Max	102	101	101			101	101	102	

TABLE 71 GRAPH.

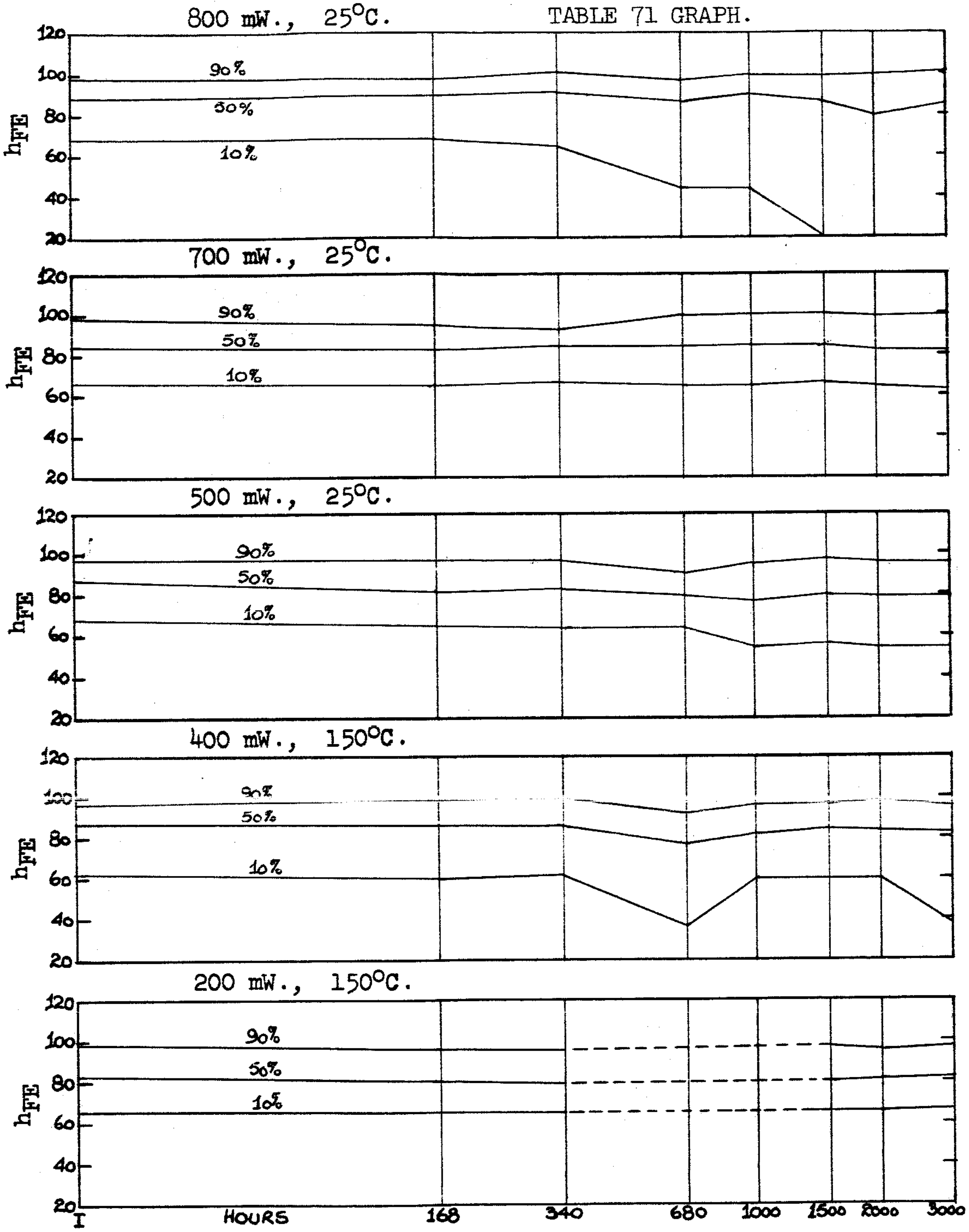

PROCESS B. MODERATE STRESS SCREEN. TABLE 72.

h_{FE} DISTRIBUTION CHANGES WITH LIFE TEST.

	h_{FE} (I_C = 20 mA., V_{CE} = 5 V.)								
HRS.	INIT.	168	340	680	1000	1500	2000	3000	
Min	61	63	63	62	63	20	20	20	
5%	61	63	63	62	63	20	20	20	
10%	65	67	68	66	67	45	20	20	
25%	77	78	79	77	78	79	74	60	P=800mW.
50%	94	96	91	96	96	100	97	89	V_{CB}=20V.
75%	98	101	103	100	103	108	112	114	T_A=25°C.
90%	104	111	113	112	113	116	124	679	
95%	105	112	115	114	115	119	132	917	
Max	105	112	115	114	115	119	132	917	
Min	67	20	65	20	20	20	20	72	
5%	69	44	69	20	44	20	20	75	
10%	73	73	74	68	73	70	70	82	
25%	85	84	85	82	85	86	85	89	P=700mW.
50%	93	92	91	92	94	94	95	100	V_{CB}=20V.
75%	102	99	101	103	103	107	104	110	T_A=25°C.
90%	105	105	109	108	110	112	109	114	
95%	108	106	112	112	115	116	113	116	
Max	109	107	115	115	116	117	116	117	
Min	36	47	20	57	57	58	20	20	
5%	58	58	57	59	59	60	58	57	
10%	67	70	66	69	69	70	68	65	
25%	84	85	82	83	84	86	84	83	P=500mW.
50%	93	93	91	93	93	96	97	96	V_{CB}=20V.
75%	101	101	96	100	94	102	103	104	T_A=25°C.
90%	103	106	103	106	106	107	106	108	
95%	105	108	105	108	107	109	109	109	
Max	108	110	108	109	109	113	119	115	
Min	77	75	75	72	77	78	83	84	
5%	77	75	75	72	77	78	83	84	
10%	77	76	75	73	77	78	83	84	
25%	87	82	81	77	80	81	83	89	P=400mW.
50%	94	91	90	89	94	95	97	98	V_{CB}=20V.
75%	97	96	97	95	101	102	103	103	T_A=150°C.
90%	105	104	550	100	105	106	137	136	
95%	106	108	---	103	108	108	164	162	
Max	106	108	---	103	108	108	164	162	

TABLE 72. (CONTINUED).

HRS.	INIT.	168	340	680	1000	1500	2000	3000	
Min	56	56	20	20	20	20	55	20	
5%	57	58	38	38	37	38	57	38	
10%	70	68	59	59	58	59	68	59	
25%	75	76	77	76	75	77	78	77	P=200mW.
50%	88	87	86	88	87	87	89	89	V_{CB}=20V.
75%	97	97	95	97	96	98	98	98	T_A=150°C.
90%	107	108	105	106	106	103	109	108	
95%	108	109	107	110	108	107	112	113	
Max	108	109	109	111	110	109	114	114	

TABLE 72 GRAPH.

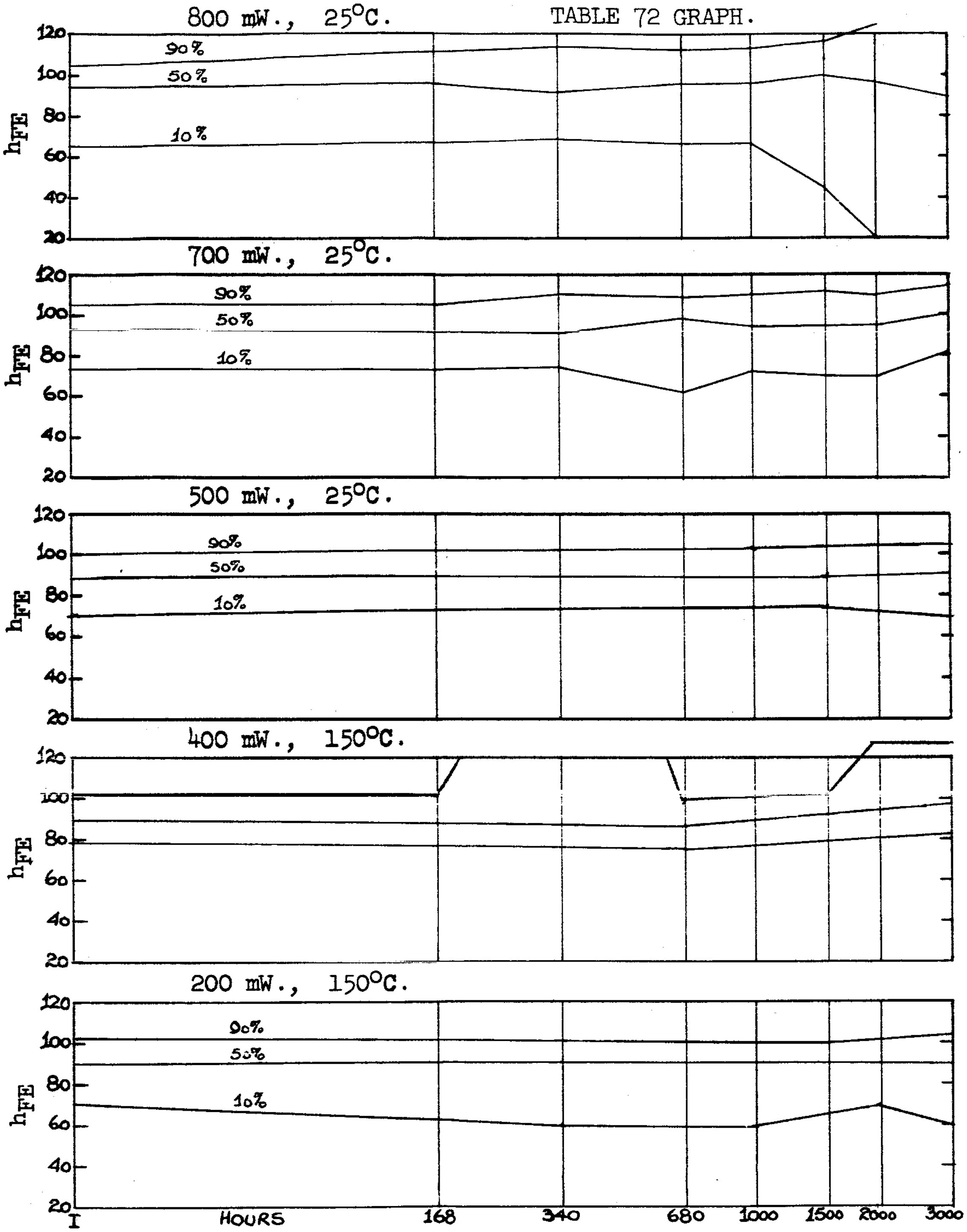

PROCESS C. MODERATE STRESS SCREEN. TABLE 73.

h_{FE} DISTRIBUTION CHANGES WITH LIFE TEST.

	h_{FE} (I_C = 20 mA., V_{CE} = 5 V.)								
HRS.	INIT.	168	340	680	1000	1500	2000	3000	
Min	54	55	55	55	55	55	54	53	P=800mW. V_{CB}=20V. T_A=25°C.
5%	54	55	55	55	55	55	54	53	
10%	60	61	61	60	61	61	60	54	
25%	66	67	68	67	68	68	67	59	
50%	81	80	80	80	81	82	77	77	
75%	107	107	105	105	107	108	107	107	
90%	112	112	114	112	113	114	113	112	
95%	114	115	116	115	115	116	115	113	
Max	114	115	116	115	115	116	115	113	
Min	55	56	20	56	57		44	46	P=700mW. V_{CB}=20V. T_A=25°C.
5%	56	57	36	57	58		50	50	
10%	59	60	57	60	61		57	57	
25%	68	68	63	67	68		63	64	
50%	90	89	81	87	88		87	87	
75%	110	110	105	109	111		109	112	
90%	132	134	120	133	136		134	134	
95%	136	137	134	134	138		136	136	
Max	139	139	138	135	140		137	136	
Min	53	53	53	53	54	55	25		P=500mW. V_{CB}=20V. T_A=25°C.
5%	57	57	56	56	57	57	53		
10%	60	61	61	60	62	63	56		
25%	74	72	71	73	75	76	70		
50%	84	84	82	84	85	87	80		
75%	102	103	101	102	103	105	99		
90%	121	122	120	121	124	125	118		
95%	133	132	130	128	134	138	129		
Max	139	141	139	134	141	143	134		
Min	59	20	20	19	20	20	20	20	P=400mW. V_{CB}=20V. T_A=150°C.
5%	59	20	20	19	20	20	20	20	
10%	60	39	39	33	27	30	20	20	
25%	63	60	60	56	54	60	20	20	
50%	104	92	84	76	78	93	58	45	
75%	118	115	112	101	105	114	126	84	
90%	121	120	121	109	117	249	149	111	
95%	122	121	122	111	119	374	156	116	
Max	122	121	122	111	119	374	156	116	

TABLE 73. (CONTINUED).

HRS.	INIT.	168	340	680	1000	1500	2000	3000	
Min	53	20	52	19	50	20	20	20	
5%	55	34	54	33	53	37	37	20	
10%	60	56	60	57	59	60	59	56	
25%	70	66	69	66	66	68	68	68	P=200mW.
50%	89	85	87	83	88	89	88	87	V_{CB}=20V.
75%	104	103	104	100	103	106	105	103	T_A=150°C.
90%	116	117	115	111	113	117	115	118	
95%	123	123	122	118	119	123	121	124	
Max	127	127	126	122	123	127	125	128	

TABLE 73 GRAPH.

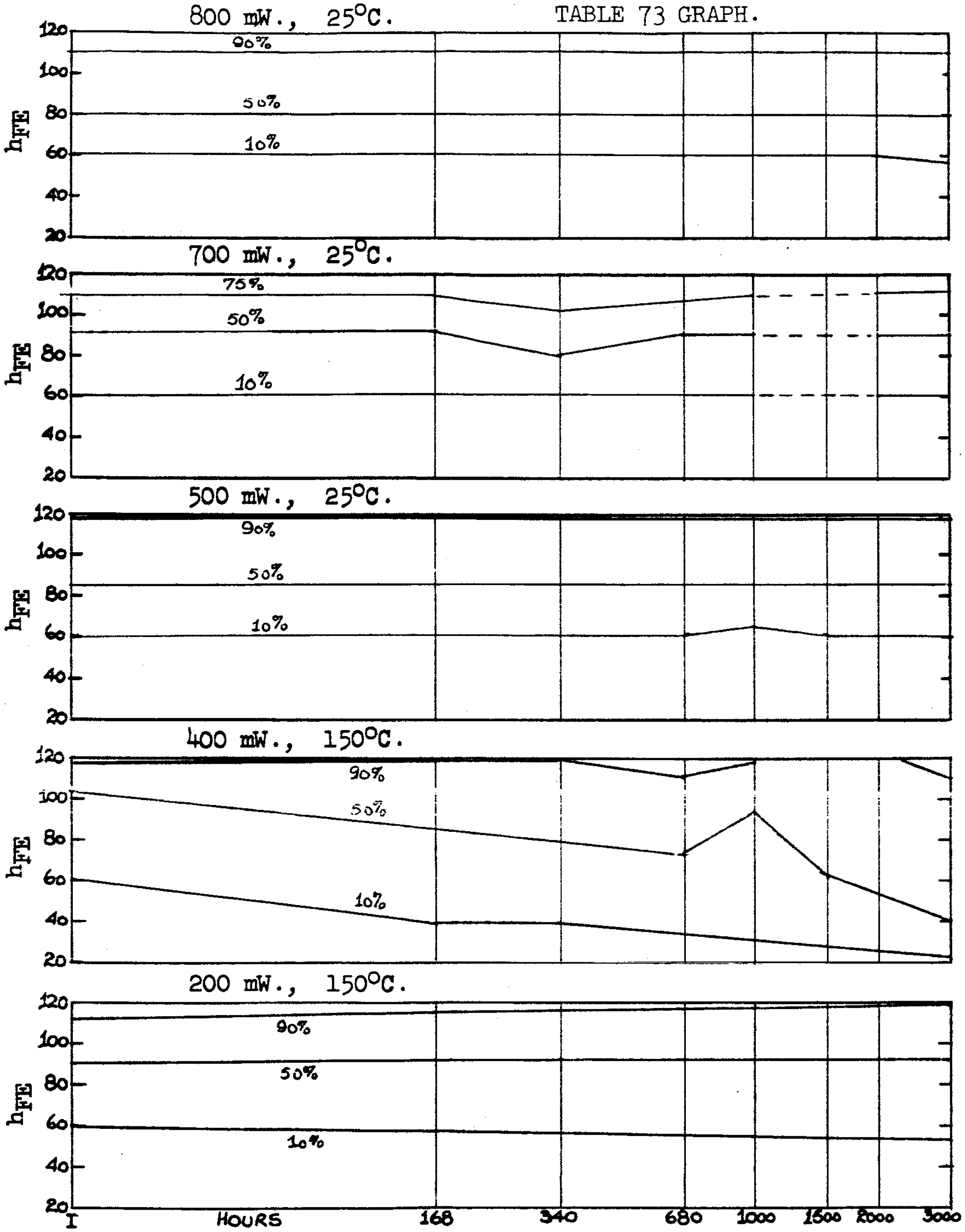

PROCESS A. CENTRIFUGE ONLY SCREEN. TABLE 74.

I_{CBO} DISTRIBUTION CHANGES WITH LIFE TEST.

	I_{CBO} (V_{CB} = 60 V.) (Nanoamperes).								
HRS.	INIT.	168	340	680	1000	1500	2000	3000	
Min	0.1	0.5	0.1	<0.1	<0.1	<0.1	<0.1	<0.1	P=800mW. V_{CB}=20V. T_A=25°C.
5%	0.1	0.5	0.1	<0.1	<0.1	<0.1	<0.1	<0.1	
10%	0.1	0.5	0.1	<0.1	<0.1	<0.1	<0.1	<0.1	
25%	0.1	0.7	0.2	<0.1	0.1	0.1	0.3	<0.1	
50%	0.4	0.8	0.4	0.2	0.3	0.2	0.3	0.1	
75%	0.7	1.0	0.8	0.5	1.2	0.5	1.5	1.6	
90%	1.9	2.2	1.8	1.5	1.7	1.0	2.6	3.2	
95%	1.9	2.2	1.8	1.5	1.7	1.0	2.6	3.2	
Max	1.9	2.2	1.8	1.5	1.7	1.0	2.6	3.2	
Min	0.1	0.6	0.2	<0.1	0.1	<0.1	0.3	<0.1	P=700mW. V_{CB}=20V. T_A=25°C.
5%	0.1	0.6	0.2	<0.1	0.1	<0.1	0.3	<0.1	
10%	0.2	0.7	0.2	<0.1	0.2	<0.1	0.3	0.1	
25%	0.3	0.8	0.2	0.1	0.3	0.2	0.4	0.4	
50%	0.5	1.0	0.5	0.4	0.6	0.4	0.7	0.9	
75%	1.1	1.4	0.9	0.9	1.1	0.7	1.1	1.5	
90%	1.1	1.8	1.3	1.0	1.3	3.6	31.1	30.6	
95%	1.4	1.9	1.4	1.0	1.3	9.5	40.3	92.5	
Max	1.4	1.9	1.4	1.0	1.3	9.5	40.3	92.5	
Min	0.1	<0.1	0.5	0.8	<0.1	<0.1	<0.1	<0.1	P=500mW. V_{CB}=20V. T_A=25°C.
5%	0.1	<0.1	0.5	0.8	<0.1	<0.1	<0.1	<0.1	
10%	0.1	<0.1	0.5	1.0	0.1	0.1	<0.1	<0.1	
25%	0.2	<0.1	0.7	1.0	0.2	0.1	0.1	<0.1	
50%	0.4	0.4	0.8	1.2	0.3	0.3	0.3	0.3	
75%	0.9	0.5	1.3	1.6	0.8	0.7	0.8	1.0	
90%	1.3	0.7	2.1	2.0	1.3	1.4	1.5	1.9	
95%	1.6	2.2	2.3	2.6	1.5	1.6	3.4	---	
Max	1.8	4.1	4.0	4.0	3.3	3.4	---	---	
Min	0.2	0.5	0.2	0.3	<0.1	<0.1	<0.1	<0.1	P=400mW. V_{CB}=20V. T_A=150°C.
5%	0.2	0.5	0.2	0.3	<0.1	<0.1	<0.1	<0.1	
10%	0.2	0.5	0.2	0.3	<0.1	<0.1	<0.1	<0.1	
25%	0.3	0.7	0.3	0.3	0.2	7.5	<0.1	<0.1	
50%	0.3	0.9	0.4	0.3	0.3	25.0	0.2	0.5	
75%	0.4	0.9	0.7	0.6	0.5	40.0	0.4	1.0	
90%	0.7	1.2	0.7	0.7	0.8	70.0	1.0	9.6	
95%	0.7	1.2	0.7	0.7	0.8	70.0	1.0	9.6	
Max	0.7	1.2	0.7	0.7	0.8	70.0	1.0	9.6	

TABLE 74. (CONTINUED).

HRS.	INIT.	168	340	680	1000	1500	2000	3000	
Min	0.1	0.6	0.3	<0.1	0.1	<0.1	<0.1	<0.1	P=200mW. V_{CB}=20V. T_A=150°C.
5%	0.1	0.6	0.3	<0.1	0.1	<0.1	<0.1	<0.1	
10%	0.1	0.8	0.3	<0.1	0.1	<0.1	0.1	<0.1	
25%	0.3	0.9	0.6	0.3	0.2	0.2	0.3	0.1	
50%	0.4	1.1	0.8	0.5	0.4	0.4	0.5	0.4	
75%	1.2	1.7	1.3	1.2	1.1	0.8	1.0	1.1	
90%	1.4	1.9	245.5	1.3	1.2	1.0	1.2	1.3	
95%	1.5	2.0	814.9	1.3	1.2	1.0	1.3	1.4	
Max	1.5	2.0	814.9	1.3	1.2	1.0	1.3	1.4	

TABLE 74 GRAPH.

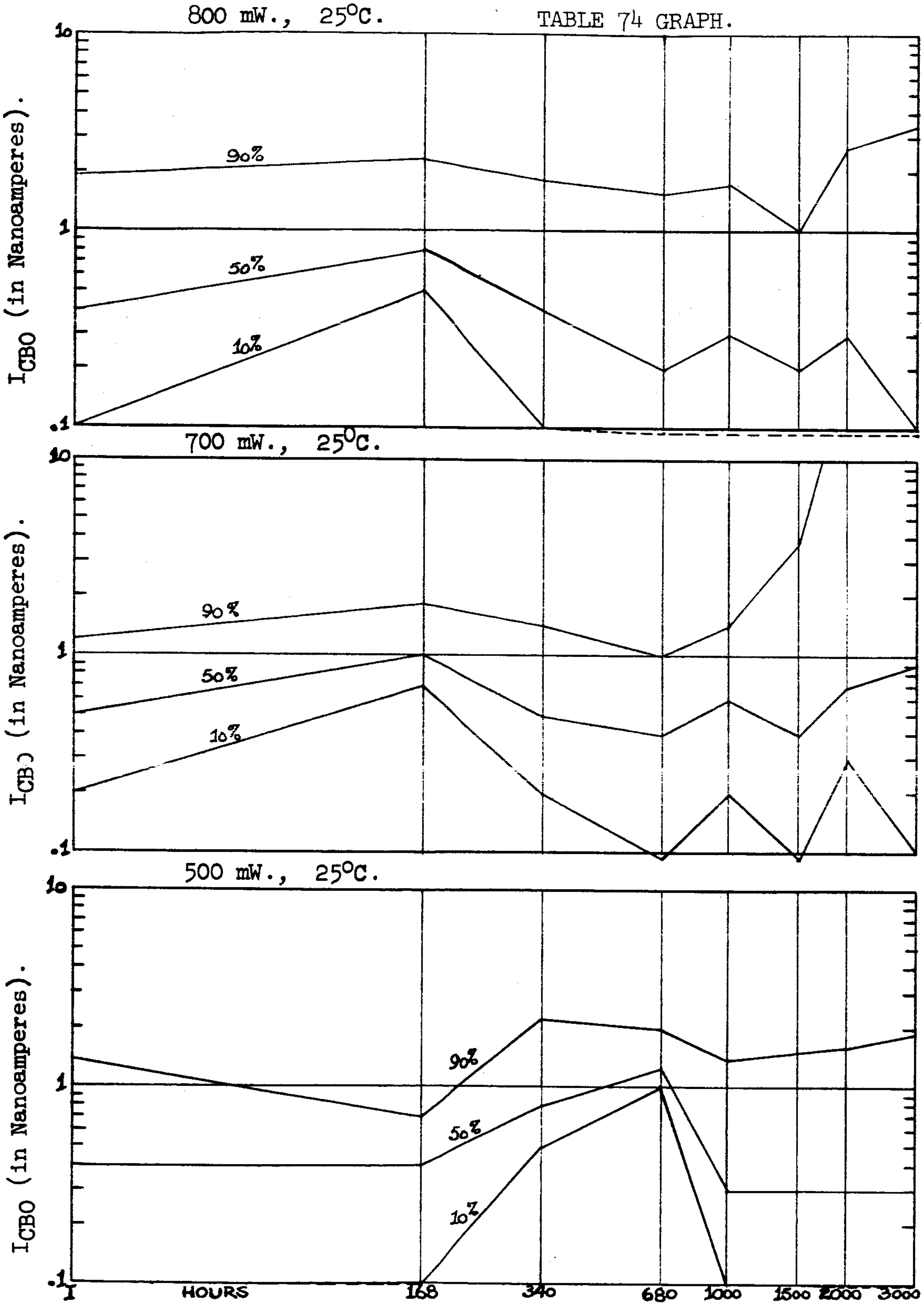
800 mW., 25°C.

700 mW., 25°C.

500 mW., 25°C.

400 mW., 150°C. TABLE 74 GRAPH.

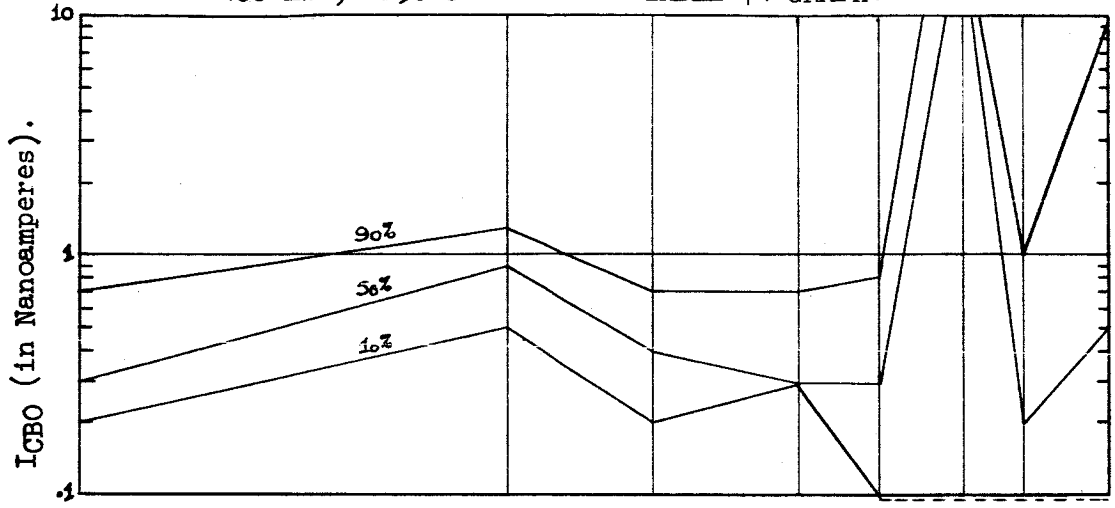

200 mW., 150°C.

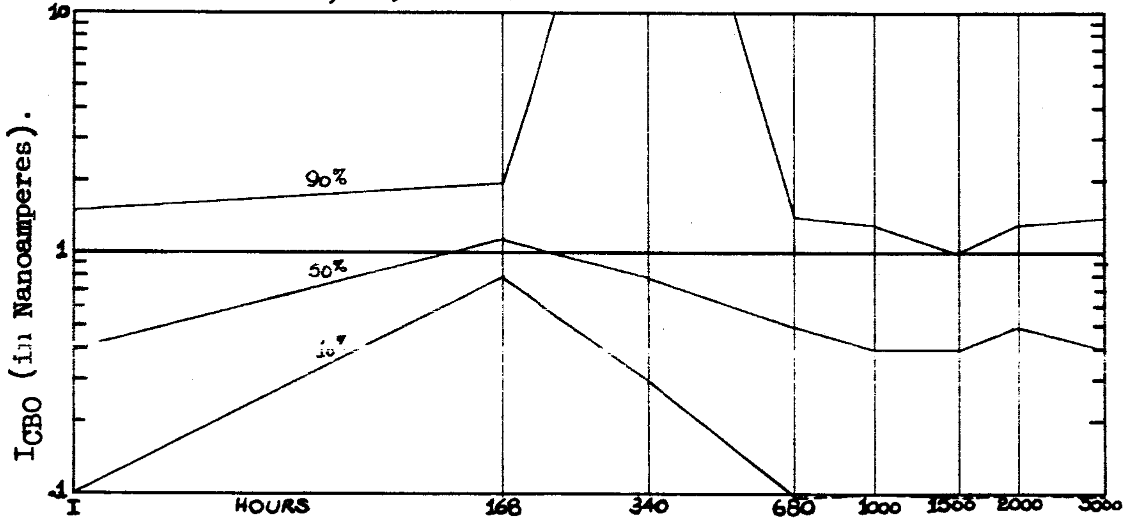

PROCESS B. CENTRIFUGE ONLY SCREEN. TABLE 75.

I_{CBO} DISTRIBUTION CHANGES WITH LIFE TEST.

	I_{CBO} (V_{CB} = 60 V.) (Nanoamperes).								
HRS.	INIT.	168	340	680	1000	1500	2000	3000	
Min	0.6	1.3	0.9	0.8	0.8	0.4	<0.1	0.1	
5%	0.6	1.3	0.9	0.8	0.8	0.4	<0.1	0.1	
10%	0.6	1.3	0.9	0.8	0.8	0.4	<0.1	0.1	
25%	1.6	1.9	1.7	0.9	1.3	1.0	<0.1	0.3	P=800mW.
50%	3.2	3.3	3.1	2.6	3.3	2.5	1.0	1.5	V_{CB}=20V.
75%	3.6	3.8	4.2	3.0	3.7	3.1	2.7	2.8	T_A=25°C.
90%	5.1	4.5	20.0	3.7	4.7	3.5	3.4	3.5	
95%	5.1	4.5	20.0	3.7	4.7	3.5	3.4	3.5	
Max	5.1	4.5	20.0	3.7	4.7	3.5	3.4	3.5	
Min	0.4	0.9	0.5	0.5	0.1	0.1	<0.1	0.3	
5%	0.4	0.9	0.5	0.5	0.1	0.1	<0.1	0.3	
10%	0.5	1.1	0.6	0.6	0.2	0.3	0.2	0.4	
25%	0.8	1.6	1.2	1.0	0.5	0.6	0.5	1.0	P=700mW.
50%	1.3	2.1	1.7	1.5	1.3	1.3	1.0	1.2	V_{CB}=20V.
75%	2.6	3.2	3.0	2.7	2.8	6.1	10.3	11.3	T_A=25°C.
90%	3.2	363.8	140.1	34.2	38.4	---	408.0	---	
95%	3.3	891.6	140.1	79.7	90.8	---	---	---	
Max	3.3	891.6	140.1	79.7	90.8	---	---	---	
Min	0.5	0.8	1.2	0.4	0.1	0.1	<0.1	0.1	
5%	0.5	0.9	1.5	0.5	0.3	0.2	<0.1	0.6	
10%	0.7	1.2	1.6	0.7	0.5	0.5	0.3	1.0	
25%	1.0	1.6	1.8	1.3	0.9	1.0	1.0	1.2	P=500mW.
50%	1.8	2.6	2.9	2.3	1.7	1.6	1.5	1.6	V_{CB}=20V.
75%	3.7	4.3	4.2	3.9	3.0	3.6	3.3	3.9	T_A=25°C.
90%	4.3	5.8	5.2	4.5	3.7	4.3	3.7	4.3	
95%	4.8	12.8	9.5	175.7	57.6	23.8	38.1	4.8	
Max	4.9	---	---	---	---	---	---	7.6	
Min	0.5	1.0	0.3	0.3	0.7	0.3	0.4	0.3	
5%	0.5	1.0	0.3	0.3	0.7	0.3	0.4	0.3	
10%	0.5	1.0	0.3	0.3	0.7	0.3	0.4	0.3	
25%	0.8	1.3	0.9	0.7	0.7	0.7	0.8	0.4	P=400mW.
50%	1.5	1.9	1.6	1.3	1.2	1.2	1.3	1.3	V_{CB}=20V.
75%	4.4	4.6	4.0	3.8	3.2	3.5	3.6	3.9	T_A=150°C.
90%	4.8	4.7	4.5	4.0	3.5	3.6	3.7	4.2	
95%	4.8	4.7	4.5	4.0	3.5	3.6	3.7	4.2	
Max	4.8	4.7	4.5	4.0	3.5	3.6	3.7	4.2	

TABLE 75. (CONTINUED).

HRS.	INIT.	168	340	680	1000	1500	2000	3000	
Min	0.6	1.4	1.0	0.8	0.7	0.2	0.5	<0.1	P=200mW. V_{CB}=20V. T_A=150°C.
5%	0.6	1.4	1.0	0.8	0.7	0.2	0.5	<0.1	
10%	0.7	1.4	1.0	0.9	0.8	0.2	0.6	0.5	
25%	1.3	1.7	1.3	1.2	1.0	0.7	1.1	1.0	
50%	2.0	2.5	2.3	2.3	1.7	1.9	2.0	1.6	
75%	3.8	3.8	3.8	3.8	3.0	3.3	3.3	3.4	
90%	4.5	14.9	117.5	66.4	19.5	4.9	149.8	5.8	
95%	4.9	30.1	287.2	159.6	43.1	6.5	368.3	7.8	
Max	4.9	30.1	287.2	159.6	43.1	6.5	368.3	7.8	

TABLE 75 GRAPH.

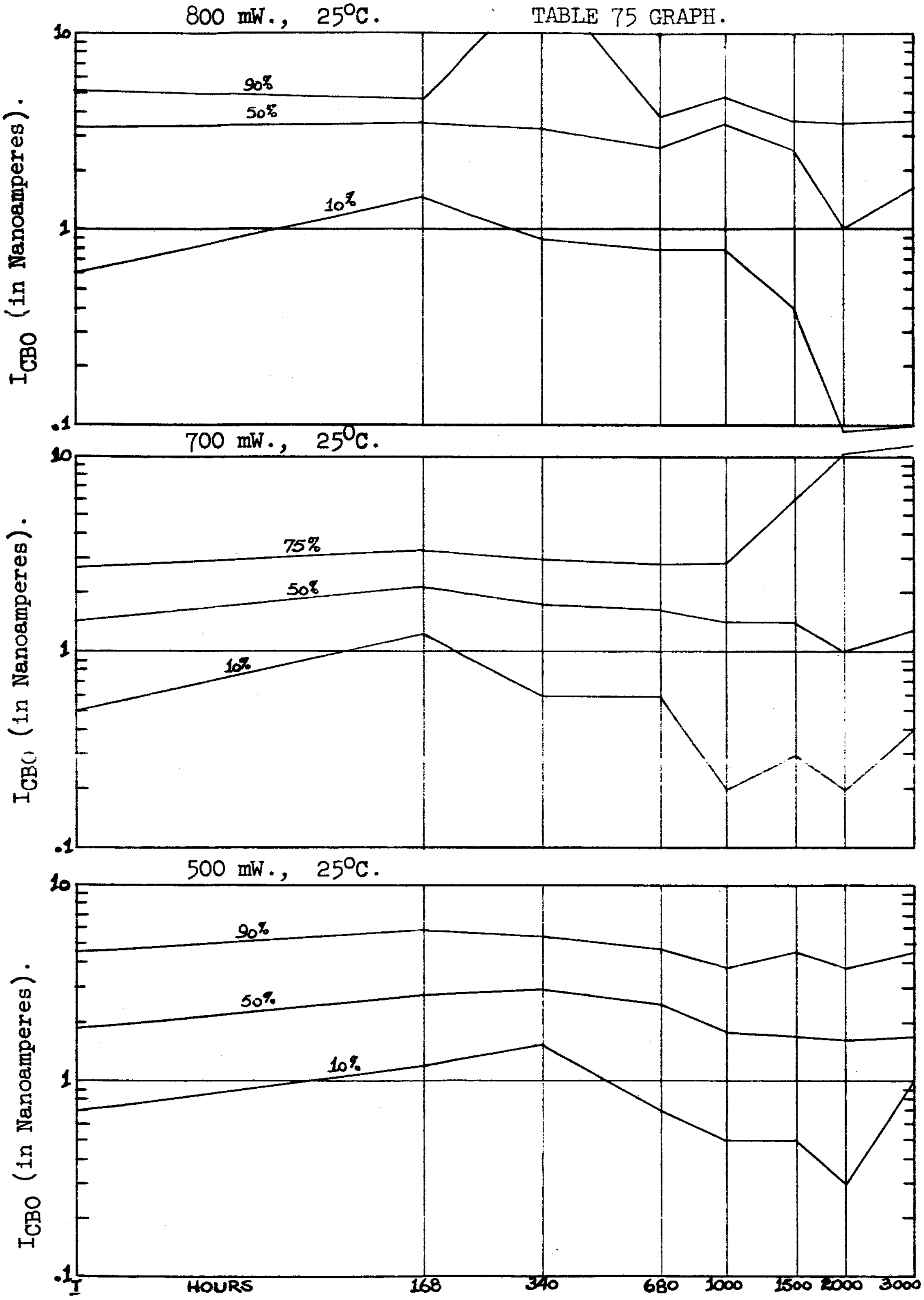

TABLE 75 GRAPH.

400 mW., 150°C.

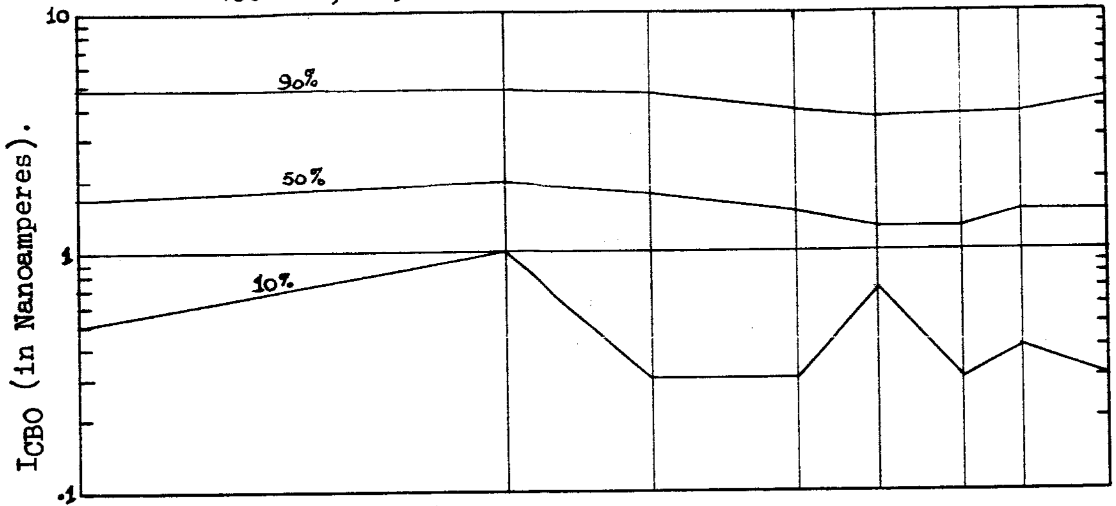

200 mW., 150°C.

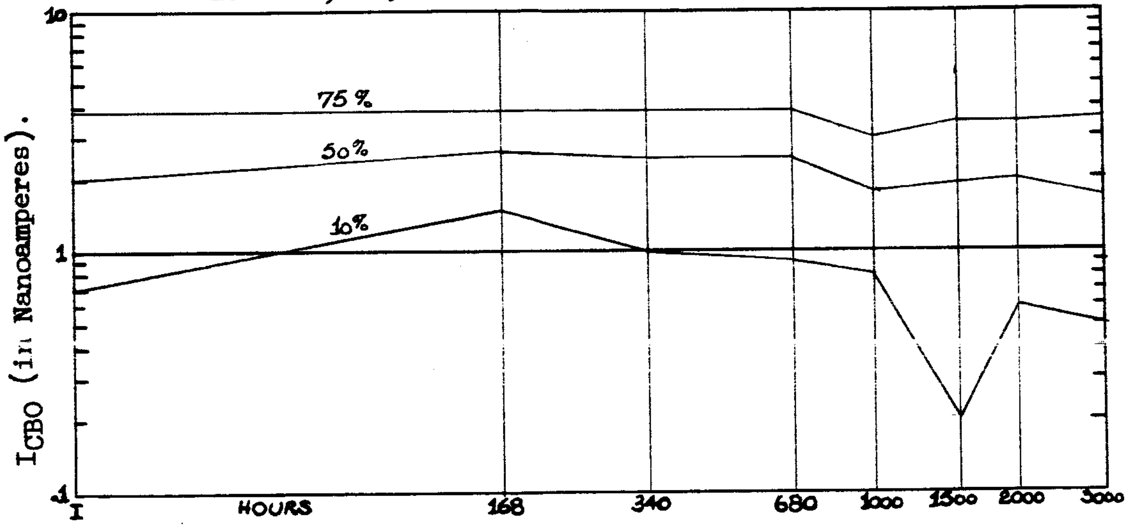

PROCESS C. CENTRIFUGE ONLY SCREEN. TABLE 76.

I_{CBO} DISTRIBUTION CHANGES WITH LIFE TEST.

	I_{CBO} (V_{CB} = 60 V.) (Nanoamperes).								
HRS.	INIT.	168	340	680	1000	1500	2000	3000	
Min	<0.1	0.5	<0.1	<0.1	<0.1	<0.1	0.1	<0.1	
5%	<0.1	0.5	<0.1	<0.1	<0.1	<0.1	0.1	<0.1	
10%	<0.1	0.5	<0.1	<0.1	<0.1	<0.1	0.1	<0.1	
25%	0.2	0.6	0.2	0.3	0.2	<0.1	0.2	4.3	P=800mW.
50%	0.3	1.2	0.6	0.7	1.6	1.4	1.7	27.7	V_{CB}=20V.
75%	0.4	5.8	15.5	19.4	80.4	57.3	53.2	216.7	T_A=25°C.
90%	4.0	60.0	251.1	249.0	254.9	356.6	258.7	936.7	
95%	5.1	65.1	273.0	269.0	272.3	387.9	823.6	---	
Max	5.1	65.1	273.0	269.0	272.3	387.9	823.6	---	
Min	<0.1	0.6	<0.1	<0.1	0.1	0.3	<0.1	0.3	
5%	<0.1	0.6	<0.1	<0.1	0.1	0.3	<0.1	0.3	
10%	<0.1	0.6	<0.1	<0.1	0.1	0.5	<0.1	0.5	
25%	<0.1	0.7	0.1	<0.1	0.2	1.0	<0.1	0.7	P=700mW.
50%	<0.1	0.8	0.2	0.3	0.3	1.3	0.4	1.1	V_{CB}=20V.
75%	0.1	1.2	0.5	2.3	0.8	2.5	2.3	3.8	T_A=25°C.
90%	0.2	2.3	3.2	7.0	7.2	39.1	28.9	409.8	
95%	1.2	30.6	6.9	10.3	9.4	623.7	951.4	972.5	
Max	1.3	32.1	7.1	10.5	9.5	623.7	---	---	
Min	<0.1	0.2	0.8	0.1	<0.1	<0.1	<0.1	0.3	
5%	<0.1	0.3	0.9	0.1	<0.1	<0.1	<0.1	0.3	
10%	<0.1	0.4	0.9	0.2	0.1	<0.1	0.1	0.3	
25%	<0.1	0.5	1.0	0.3	0.3	0.1	0.2	0.5	P=500mW.
50%	<0.1	0.7	1.3	0.5	0.5	0.3	0.3	0.8	V_{CB}=20V.
75%	0.3	1.2	2.2	1.0	0.9	0.7	0.5	1.4	T_A=25°C.
90%	1.8	3.4	5.1	3.2	3.3	2.5	2.9	4.8	
95%	3.4	5.7	7.8	41.5	26.1	3.9	6.6	61.8	
Max	6.3	662.4	13.5	116.0	206.3	11.5	292.7	215.7	
Min	<0.1	0.7	0.2	<0.1	0.2	<0.1	0.5	<0.1	
5%	<0.1	0.7	0.2	<0.1	0.2	<0.1	0.5	<0.1	
10%	<0.1	0.7	0.2	<0.1	0.2	<0.1	0.5	<0.1	
25%	<0.1	0.8	0.3	0.2	0.4	0.1	0.6	0.3	P=400mW.
50%	0.1	1.1	0.8	0.7	3.8	0.7	1.1	2.9	V_{CB}=20V.
75%	0.1	42.8	92.1	102.1	99.2	81.1	8.3	20.2	T_A=150°C.
90%	0.6	740.2	916.7	914.2	917.7	926.4	408.5	903.9	
95%	0.7	813.6	---	---	---	---	408.5	---	
Max	0.7	813.6	---	---	---	---	408.5	---	

TABLE 76. (CONTINUED).

HRS.	INIT.	168	340	680	1000	1500	2000	3000	
Min	<0.1	0.5	<0.1	0.1	0.1	<0.1	<0.1	<0.1	
5%	<0.1	0.5	<0.1	0.1	0.1	<0.1	<0.1	<0.1	
10%	<0.1	0.7	<0.1	0.2	0.1	<0.1	<0.1	<0.1	
25%	<0.1	0.8	0.3	0.3	0.2	0.1	0.1	0.1	P=200mW.
50%	0.2	1.2	0.6	0.5	0.5	0.2	0.2	0.3	V_{CB}=20V.
75%	0.4	1.7	1.7	1.4	3.1	1.2	0.8	0.9	T_A=150°C.
90%	2.3	9.0	8.4	4.8	31.3	3.9	3.8	5.6	
95%	3.4	950.4	950.3	950.2	951.6	6.2	64.7	322.4	
Max	3.4	---	---	---	---	6.3	67.9	339.1	

TABLE 76 GRAPH.

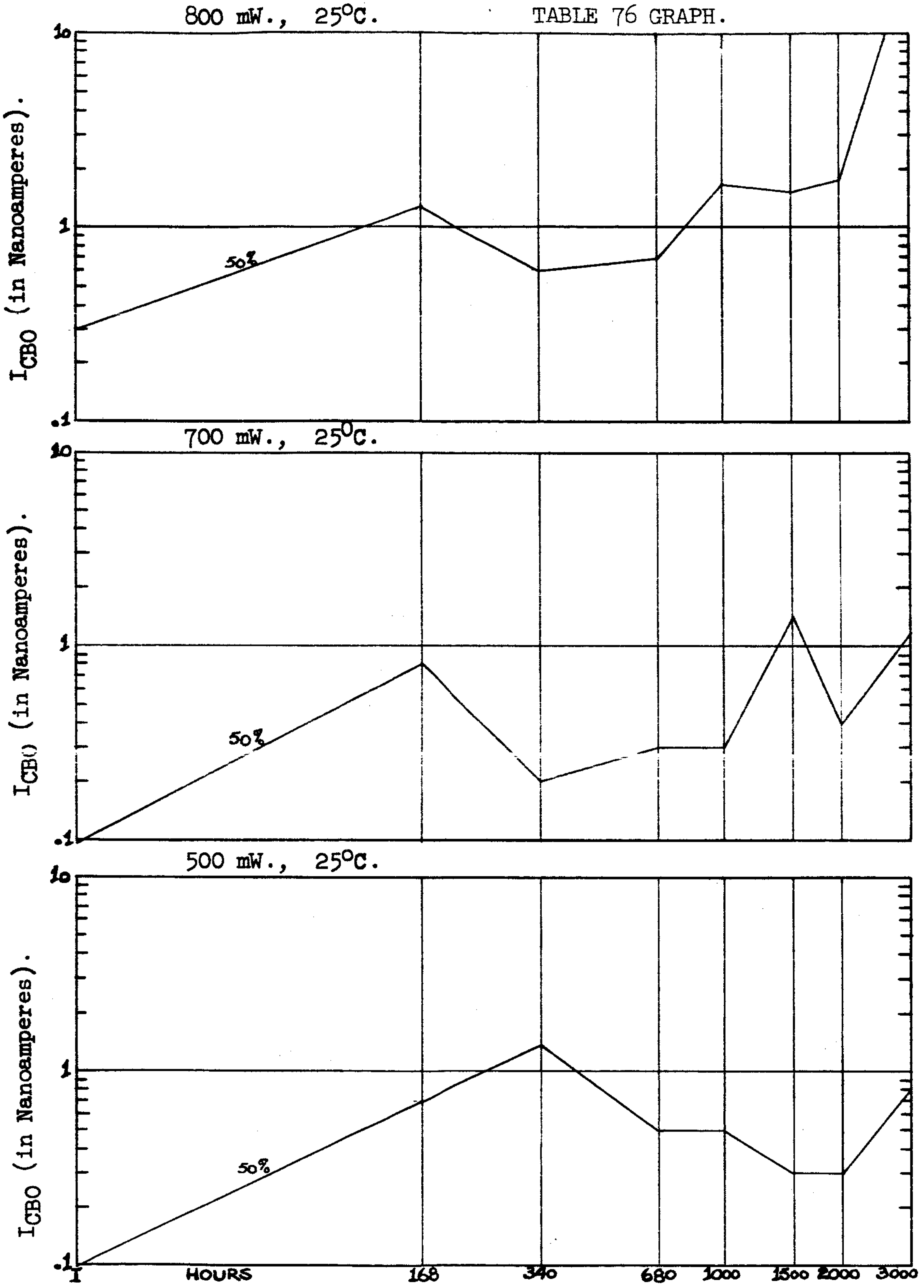

400 mW., 150°C. TABLE 76 GRAPH.

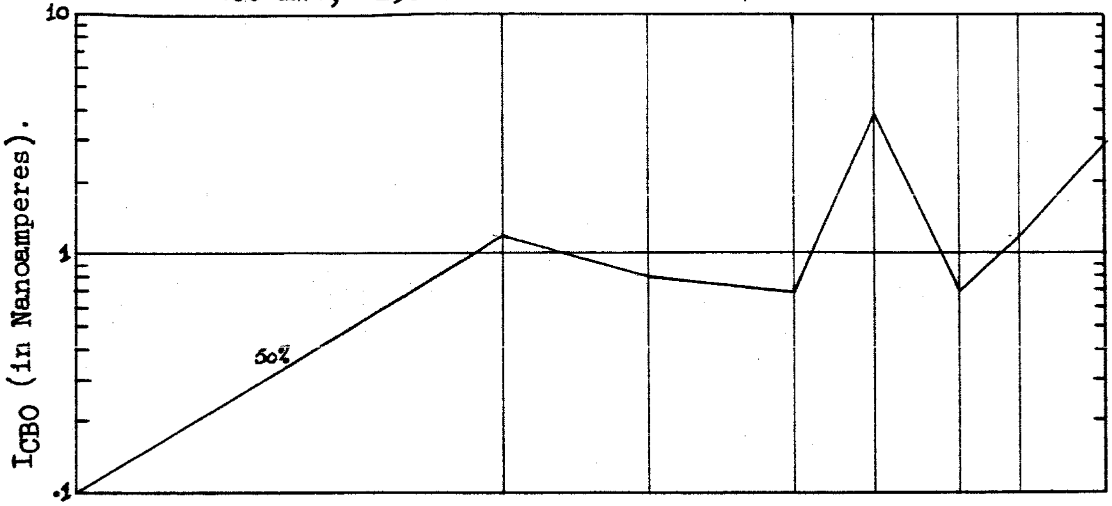

200 mW., 150°C.

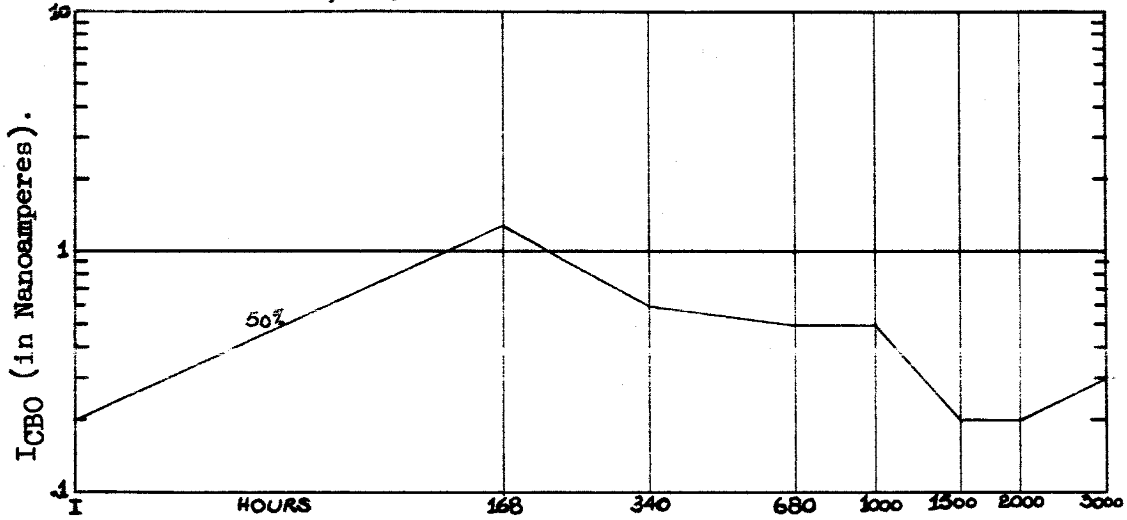

PROCESS A. CENTRIFUGE ONLY SCREEN. TABLE 77.

h_{FE} DISTRIBUTION CHANGES WITH LIFE TEST.

	h_{FE} (I_C = 20 mA., V_{CE} = 5 V.)								
HRS.	INIT.	168	340	680	1000	1500	2000	3000	
Min	62	63	57	62	63	63	80	20	
5%	62	63	57	62	63	63	80	20	
10%	62	63	57	62	63	63	80	20	
25%	76	80	71	79	81	80	81	80	P=800mW.
50%	90	91	77	87	91	91	91	89	V_{CB}=20V.
75%	93	94	86	92	94	93	92	101	T_A=25°C.
90%	101	101	101	99	101	101	99	855	
95%	101	101	101	99	101	101	99	855	
Max	101	101	101	99	101	101	99	855	
Min	49	51	52	51	52	50	20		
5%	49	51	52	51	52	50	20		
10%	57	58	58	56	58	57	41		
25%	71	75	75	73	74	74	68		P=700mW.
50%	77	83	83	81	84	84	83		V_{CB}=20V.
75%	87	93	93	91	92	92	92		T_A=25°C.
90%	92	94	95	92	94	95	94		
95%	94	95	95	94	95	96	95		
Max	94	95	95	94	95	96	95		
Min	59	56	60	58	20	20	20	20	
5%	63	59	60	63	20	20	20	20	
10%	65	65	64	63	34	20	20	20	
25%	70	71	72	70	69	68	70	68	P=500mW.
50%	80	82	82	78	78	80	84	83	V_{CB}=20V.
75%	85	86	86	87	88	89	91	92	T_A=25°C.
90%	91	93	93	94	94	94	98	98	
95%	95	100	100	98	99	99	101	105	
Max	99	106	106	103	101	104	107	116	
Min	69	69	65	61	67	65	68	68	
5%	69	69	65	61	67	65	68	68	
10%	69	69	65	61	67	65	68	68	
25%	72	73	67	63	73	69	73	73	P=400mW.
50%	74	78	72	69	77	77	78	78	V_{CB}=20V.
75%	84	88	80	76	87	82	87	88	T_A=150°C.
90%	85	91	81	77	89	87	89	90	
95%	85	91	81	77	89	87	89	90	
Max	85	91	81	77	89	87	89	90	

TABLE 77. (CONTINUED).

HRS.	INIT.	168	340	680	1000	1500	2000	3000	
Min	66	69	64	20	20	20	47	20	
5%	66	69	64	20	20	20	47	20	
10%	67	69	64	53	52	20	59	39	
25%	73	74	70	71	69	67	71	70	P=200mW.
50%	79	81	80	80	78	76	82	80	V_{CB}=20V.
75%	91	94	85	90	87	86	93	89	T_A=150°C.
90%	96	97	91	97	93	96	97	96	
95%	97	98	91	97	94	96	97	97	
Max	97	98	91	97	94	96	97	97	

TABLE 77 GRAPH.

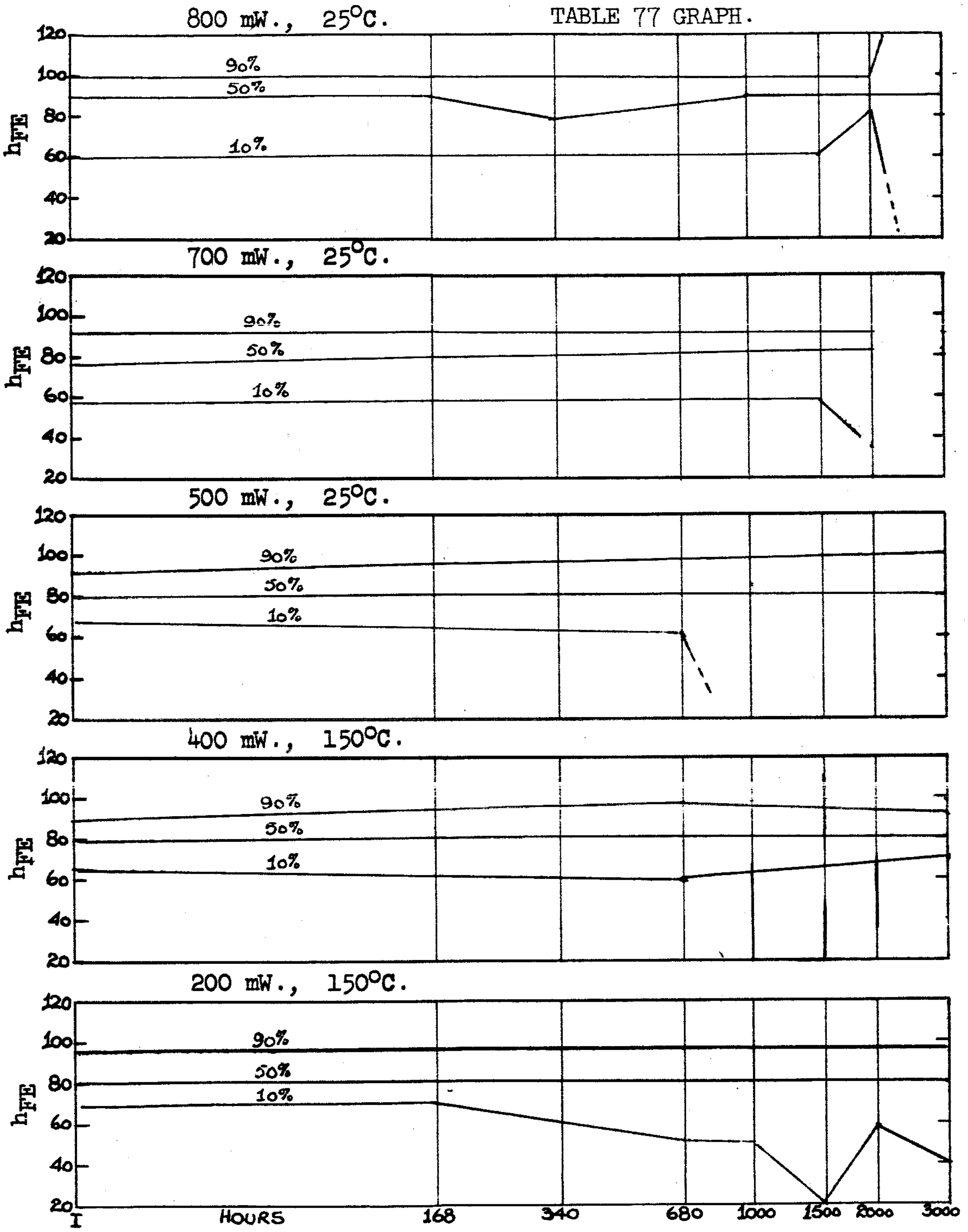

800 mW., 25°C.

700 mW., 25°C.

500 mW., 25°C.

400 mW., 150°C.

200 mW., 150°C.

h_{FE} DISTRIBUTION CHANGES WITH LIFE TEST.

	h_{FE} (I_C = 20 mA., V_{CE} = 5 V.)								
HRS.	INIT.	168	340	680	1000	1500	2000	3000	
Min	82	78	79	77	74	77	20	20	P=800mW. V_{CB}=20V. T_A=25°C.
5%	82	78	79	77	74	77	20	20	
10%	82	78	79	77	74	77	20	20	
25%	82	87	86	88	89	92	20	20	
50%	100	108	103	109	110	114	112	86	
75%	106	117	112	115	116	118	119	118	
90%	107	117	113	117	116	124	131	131	
95%	107	117	113	117	116	124	131	131	
Max	107	117	113	117	116	124	131	131	
Min	76	58	57	61	20	20	20	20	P=700mW. V_{CB}=20V. T_A=25°C.
5%	76	58	57	61	20	20	20	20	
10%	78	68	68	66	20	20	20	24	
25%	86	80	80	78	67	23	20	61	
50%	93	90	91	94	95	95	82	95	
75%	100	98	99	101	99	101	101	105	
90%	106	102	104	109	110	109	109	592	
95%	110	104	106	112	114	114	114	909	
Max	110	104	106	112	114	114	114	909	
Min	69	20	61	62	23	20	20	20	P=500mW. V_{CB}=20V. T_A=25°C.
5%	69	60	68	68	68	25	24	20	
10%	75	74	73	73	70	70	69	69	
25%	85	84	83	85	86	87	86	84	
50%	90	92	91	90	91	93	91	92	
75%	97	99	97	97	95	100	99	101	
90%	99	103	100	100	101	107	105	109	
95%	102	107	108	102	108	110	108	110	
Max	103	110	---	109	108	110	109	111	
Min	83	82	76	77	79	81	81	85	P=400mW. V_{CB}=20V. T_A=150°C.
5%	83	82	76	77	79	81	81	85	
10%	83	82	76	77	79	81	81	85	
25%	84	82	81	77	82	82	86	90	
50%	94	94	93	87	87	92	91	94	
75%	99	98	97	94	100	105	109	114	
90%	103	101	98	100	105	108	113	128	
95%	103	101	98	100	105	108	113	128	
Max	103	101	98	100	105	108	113	128	

TABLE 78. (CONTINUED).

HRS.	INIT.	168	340	680	1000	1500	2000	3000	
Min	69	72	76	77	76	76	79	79	P=200mW. V_{CB}=20V. T_A=150°C.
5%	69	72	76	77	76	76	79	79	
10%	78	79	83	84	82	82	84	84	
25%	87	91	90	93	93	91	94	95	
50%	92	93	94	96	95	94	96	99	
75%	96	96	97	99	96	96	99	100	
90%	98	102	98	101	100	101	103	103	
95%	101	103	98	102	101	102	103	103	
Max	101	103	98	102	101	102	103	103	

TABLE 78 GRAPH.

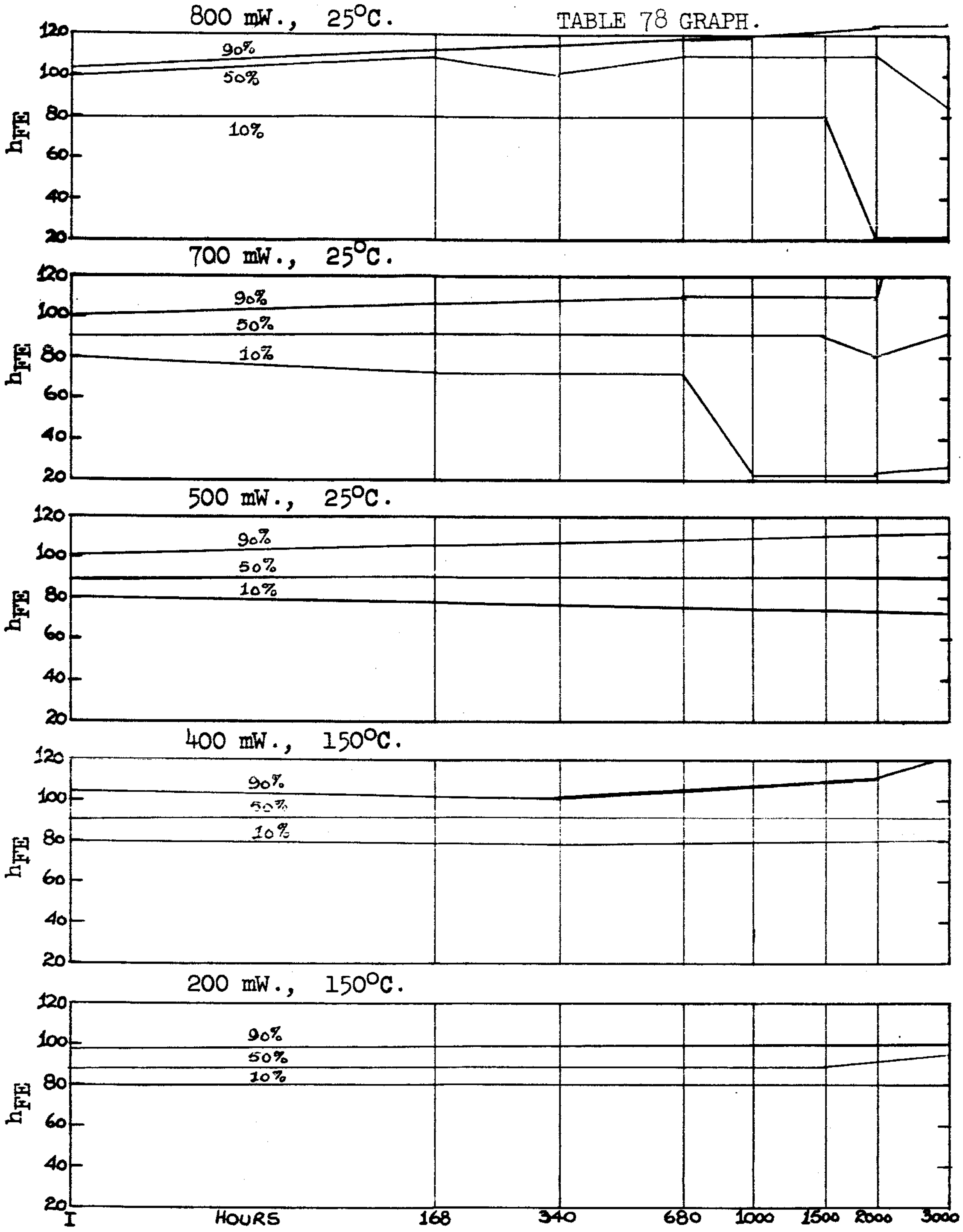

PROCESS C. CENTRIFUGE ONLY SCREEN. TABLE 79.

h_{FE} DISTRIBUTION CHANGES WITH LIFE TEST.

	h_{FE} (I_C = 20 mA., V_{CE} = 5 V.)								
HRS.	INIT.	168	340	680	1000	1500	2000	3000	
Min	49	50	49	50	51	51	42	20	P=800mW. V_{CB}=20V. T_A=25°C.
5%	49	50	49	50	51	51	42	20	
10%	50	50	50	50	51	51	42	20	
25%	61	62	59	62	63	62	48	25	
50%	77	78	73	79	80	78	66	53	
75%	88	88	82	88	89	88	80	80	
90%	106	109	101	110	111	110	104	103	
95%	106	110	101	110	111	110	106	105	
Max	106	110	101	110	111	110	106	105	
Min	48	49	48	48	20	20	20	20	P=700mW. V_{CB}=20V. T_A=25°C.
5%	48	49	48	48	21	20	20	21	
10%	50	51	51	50	49	48	23	48	
25%	58	59	58	59	58	57	57	58	
50%	96	94	89	97	98	93	89	94	
75%	106	106	109	109	110	108	110	109	
90%	122	113	116	122	124	123	121	121	
95%	125	124	125	128	130	128	127	128	
Max	125	124	125	128	130	128	128	128	
Min	48	49	49	49	50	50	49	51	P=500mW. V_{CB}=20V. T_A=25°C.
5%	54	54	52	53	54	54	52	53	
10%	59	59	58	55	59	60	57	59	
25%	70	70	69	68	71	70	69	72	
50%	86	85	82	85	86	87	84	86	
75%	108	106	106	108	109	111	107	110	
90%	124	123	122	121	126	128	123	126	
95%	134	131	126	128	133	135	131	133	
Max	140	141	138	137	139	140	135	139	
Min	54	54	54	52	53	53		10	P=400mW. V_{CB}=20V. T_A=150°C.
5%	54	54	54	52	53	53		20	
10%	55	55	55	52	54	54		23	
25%	71	71	71	63	69	68		54	
50%	96	98	95	83	84	85		67	
75%	101	104	102	90	100	102		98	
90%	114	114	114	97	111	113		112	
95%	115	115	116	98	112	114		113	
Max	115	115	116	98	112	114		113	

TABLE 79. (CONTINUED).

HRS.	INIT.	168	340	680	1000	1500	2000	3000	
Min	51	51	51	20	20	20	20	20	P=200mW. V_{CB}=20V. T_A=150°C.
5%	51	51	51	21	21	21	21	21	
10%	52	53	53	51	49	51	51	51	
25%	63	60	63	59	57	58	58	58	
50%	102	102	103	104	100	95	95	95	
75%	116	116	117	118	115	117	118	118	
90%	124	124	124	127	122	126	126	126	
95%	125	126	125	127	123	128	128	128	
Max	125	126	125	127	123	128	128	129	

800 mW., 25°C. TABLE 79 GRAPH.

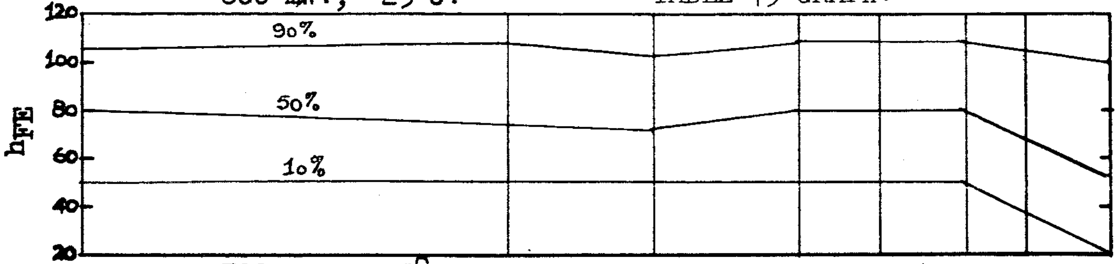

700 mW., 25°C.

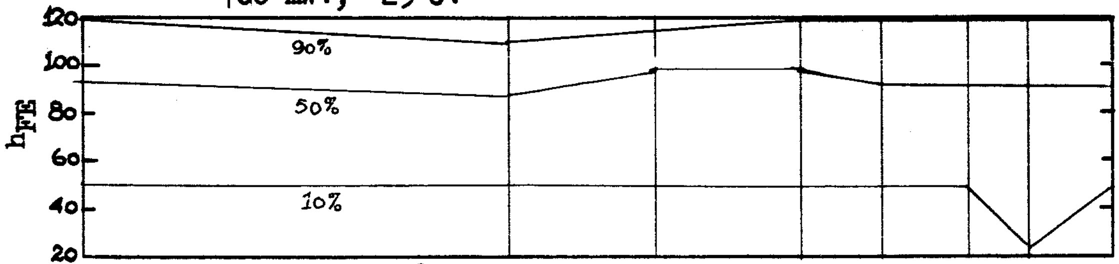

500 mW., 25°C.

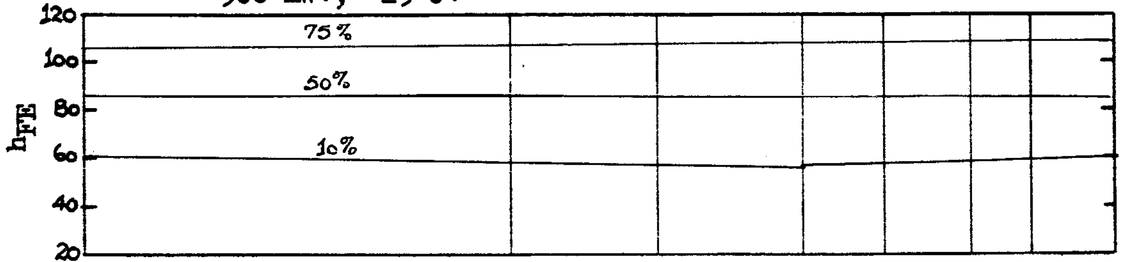

400 mW., 150°C.

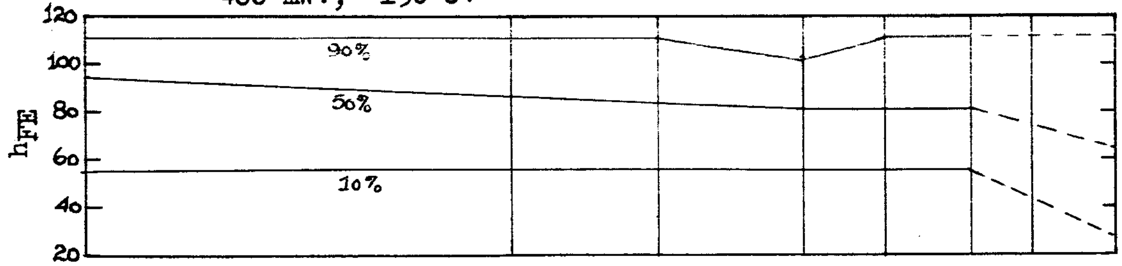

200 mW., 150°C.

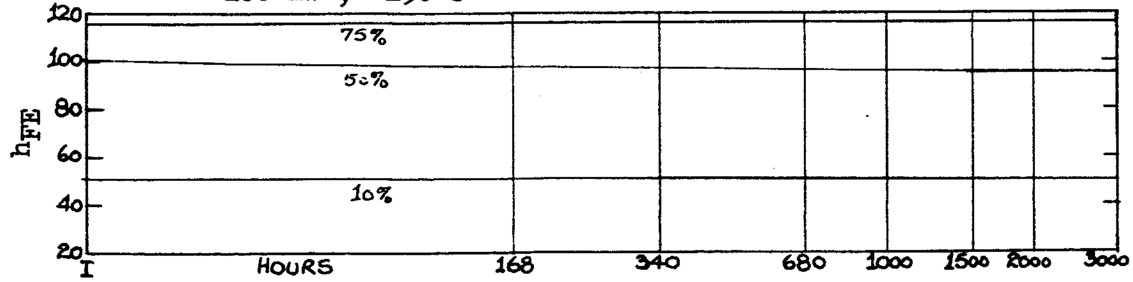

I_{CBO} DISTRIBUTION CHANGES WITH LIFE TEST.

	I_{CBO} (V_{CB} = 60 V.) (Nanoamperes).								
HRS.	INIT.	168	340	680	1000	1500	2000	3000	
Min	0.3	0.6	0.2	<0.1	<0.1	<0.1	<0.1	0.1	P=800mW. V_{CB}=20V. T_A=25°C.
5%	0.3	0.6	0.2	<0.1	<0.1	<0.1	<0.1	0.1	
10%	0.3	0.6	0.2	<0.1	<0.1	<0.1	<0.1	0.1	
25%	0.3	0.7	0.2	0.1	0.2	<0.1	0.5	0.2	
50%	0.4	1.1	0.6	0.3	0.3	0.1	0.7	0.3	
75%	0.7	1.3	0.6	0.6	1.0	0.3	1.5	0.7	
90%	1.1	1.5	1.1	2.0	1.5	0.7	1.5	1.1	
95%	1.1	1.5	1.1	2.0	1.5	0.7	1.5	1.1	
Max	1.1	1.5	1.1	2.0	1.5	0.7	1.5	1.1	
Min	0.3	0.6	0.1	<0.1	<0.1	<0.1	<0.1	0.5	P=700mW. V_{CB}=20V. T_A=25°C.
5%	0.3	0.6	0.1	<0.1	<0.1	<0.1	<0.1	0.5	
10%	0.3	0.7	0.1	0.1	0.1	<0.1	0.1	0.5	
25%	0.3	0.8	0.3	0.4	0.2	<0.1	0.3	0.5	
50%	0.4	0.9	0.4	0.5	0.4	0.2	0.4	0.7	
75%	0.6	1.0	0.7	0.8	0.6	0.5	1.0	1.1	
90%	1.7	2.6	2.7	4.4	4.3	44.0	45.3	56.6	
95%	2.1	3.4	3.5	5.7	5.9	85.5	88.2	110.5	
Max	2.1	3.4	3.5	5.7	5.9	85.5	88.2	110.5	
Min	0.1	<0.1	0.5	0.8	<0.1	<0.1	<0.1	<0.1	P=500mW. V_{CB}=20V. T_A=25°C.
5%	0.1	<0.1	0.6	0.9	<0.1	<0.1	<0.1	<0.1	
10%	0.2	<0.1	0.6	1.0	0.1	<0.1	0.1	<0.1	
25%	0.2	0.3	0.7	1.0	0.2	0.1	0.2	0.2	
50%	0.4	0.5	0.9	1.2	0.3	0.3	0.3	0.4	
75%	0.6	0.6	1.5	1.6	1.0	0.7	1.1	0.8	
90%	1.2	0.7	1.9	2.1	1.6	1.3	1.5	1.4	
95%	1.4	17.8	31.5	42.5	766.0	37.5	43.8	51.5	
Max	1.7	275.2	589.0	809.0	>1 uA	72.4	842.7	---	
Min	0.2	0.7	<0.1	0.3	0.2	<0.1	<0.1	0.2	P=400mW. V_{CB}=20V. T_A=150°C.
5%	0.2	0.7	<0.1	0.3	0.2	<0.1	<0.1	0.2	
10%	0.2	0.7	<0.1	0.3	0.2	<0.1	<0.1	0.2	
25%	0.2	0.9	0.2	0.3	0.2	0.2	0.1	0.2	
50%	0.4	1.2	0.4	0.4	0.4	0.3	0.3	0.4	
75%	0.6	1.4	0.6	0.5	0.5	0.3	0.8	0.7	
90%	0.8	3.0	0.8	1.0	1.4	1.3	1.7	1.7	
95%	0.8	3.0	0.8	1.0	1.4	1.3	1.7	1.7	
Max	0.8	3.0	0.8	1.0	1.4	1.3	1.7	1.7	

TABLE 80. (CONTINUED).

HRS.	INIT.	168	340	680	1000	1500	2000	3000	
Min	<0.1	0.6	0.1	0.2	0.1	<0.1	<0.1	0.1	
5%	<0.1	0.6	0.1	0.2	0.1	<0.1	<0.1	0.1	
10%	0.1	0.6	0.2	0.3	0.1	<0.1	<0.1	0.1	
25%	0.2	0.8	0.4	0.3	0.3	0.2	0.1	0.3	P=200mW.
50%	0.5	1.0	0.5	0.6	0.5	0.3	0.3	0.6	V_{CB}=20V.
75%	0.9	1.5	0.8	0.8	0.9	0.6	0.5	0.9	T_A=150°C.
90%	1.5	1.9	1.4	1.7	3.8	1.3	1.1	2.0	
95%	1.7	2.1	1.7	2.0	6.2	1.6	1.4	2.0	
Max	1.7	2.1	1.7	2.0	6.2	1.6	1.4	2.0	

800 mW., 25°C. TABLE 80 GRAPH.

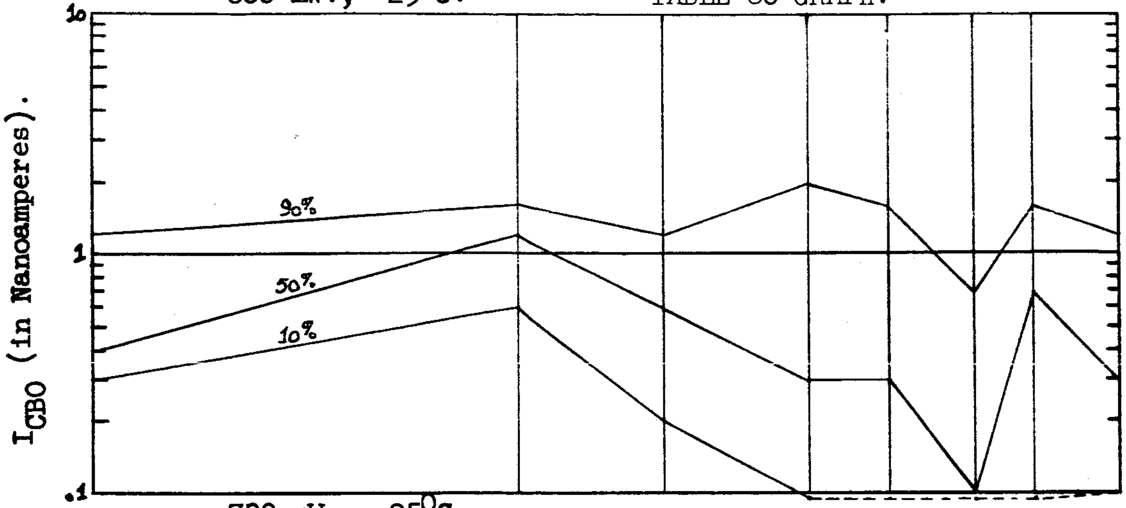

700 mW., 25°C.

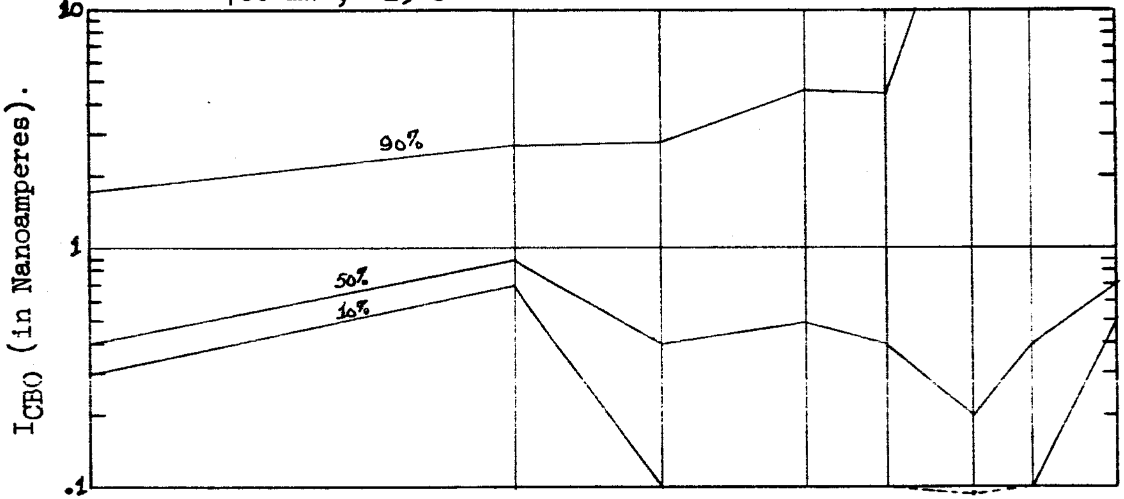

500 mW., 25°C.

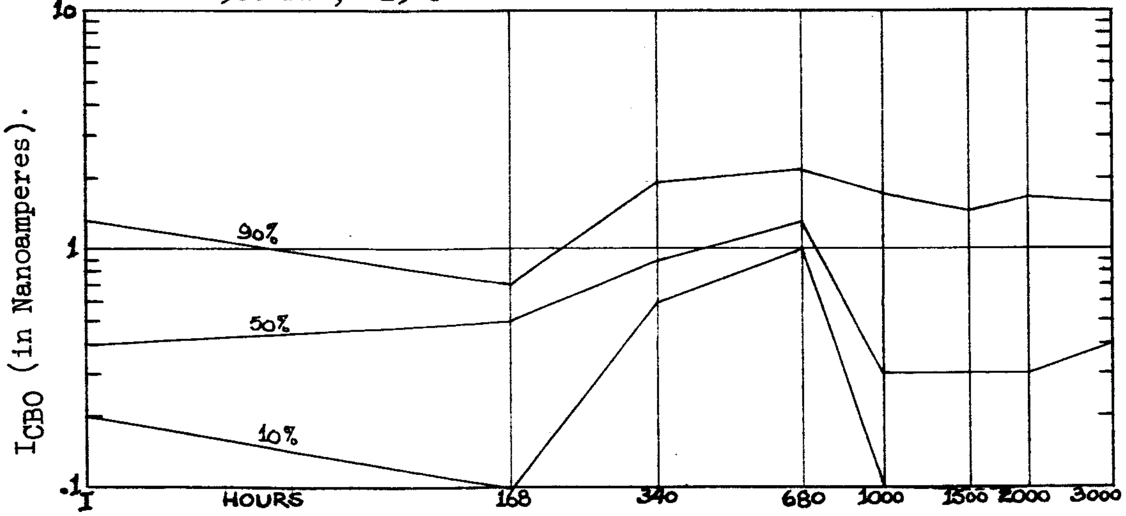

TABLE 80 GRAPH.

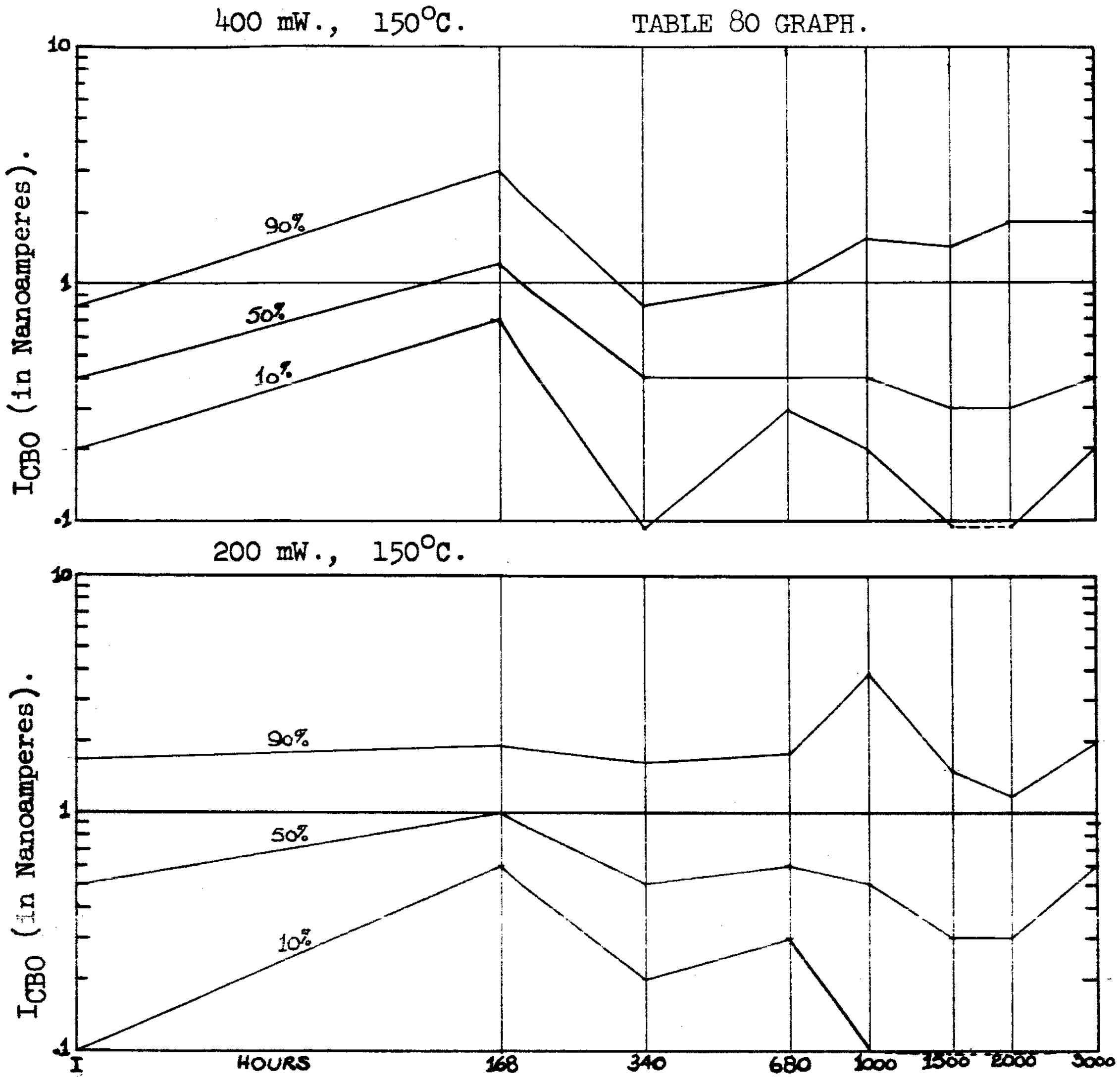

400 mW., 150°C.

200 mW., 150°C.

PROCESS B. CONTROL LOT. TABLE 81.

I_{CBO} DISTRIBUTION CHANGES WITH LIFE TEST.

	I_{CBO} (V_{CB} = 60 V.) (Nanoamperes).								
HRS.	INIT.	168	340	680	1000	1500	2000	3000	
Min	0.7	1.0	1.8	<0.1	0.1	0.3	<0.1	0.7	
5%	0.7	1.0	1.8	<0.1	0.1	0.3	<0.1	0.7	
10%	0.7	1.0	1.8	<0.1	0.1	0.3	<0.1	0.7	
25%	0.9	1.9	2.7	0.4	0.7	0.3	<0.1	0.8	P=800mW.
50%	2.6	3.3	3.5	2.4	1.9	0.8	1.5	1.3	V_{CB}=20V.
75%	3.9	3.7	3.9	2.9	3.4	3.1	3.0	8.1	T_A=25°C.
90%	4.0	3.8	4.1	3.0	3.5	93.5	55.0	10.3	
95%	4.0	3.8	4.1	3.0	3.5	93.5	55.0	10.3	
Max	4.0	3.8	4.1	3.0	3.5	93.5	55.0	10.3	
Min	0.4	1.4	0.8	0.3	1.0	0.3	0.3	1.0	
5%	0.4	1.4	0.8	0.3	1.0	0.3	0.3	1.0	
10%	0.5	1.4	0.8	0.7	1.0	0.4	0.4	1.1	
25%	1.4	2.1	1.6	1.4	1.3	0.6	0.7	2.0	P=700mW.
50%	3.0	4.1	3.4	3.0	3.7	3.2	2.7	3.5	V_{CB}=20V.
75%	3.8	4.5	3.7	3.3	3.8	3.6	3.1	3.9	T_A=25°C.
90%	4.9	6.9	4.9	4.3	610.0	6.4	3.3	4.5	
95%	5.4	9.1	5.9	4.8	700.0	6.8	3.3	4.7	
Max	5.4	9.1	5.9	4.8	700.0	6.8	3.3	4.7	
Min	0.2	0.4	1.3	0.2	0.3	0.1	<0.1	0.1	
5%	0.4	0.4	1.4	0.6	0.5	0.4	0.1	0.4	
10%	0.7	0.5	1.6	0.8	0.7	0.5	0.4	0.5	
25%	1.0	1.2	1.8	1.0	1.0	0.8	0.7	1.2	P=500mW.
50%	1.5	1.8	2.3	1.6	1.5	1.3	1.3	1.6	V_{CB}=20V.
75%	3.1	4.0	3.9	3.6	3.6	3.3	3.4	3.6	T_A=25°C.
90%	4.4	6.1	6.5	5.0	4.7	4.0	4.3	4.4	
95%	5.0	110.1	124.5	105.3	108.4	104.5	104.2	5.8	
Max	5.6	---	---	---	---	---	---	10.1	
Min	0.2	0.9	0.3	0.4	0.2	<0.1	0.3	0.8	
5%	0.2	0.9	0.3	0.4	0.2	<0.1	0.3	0.8	
10%	0.2	0.9	0.3	0.4	0.2	<0.1	0.3	0.8	
25%	0.6	1.3	0.7	0.7	0.6	0.5	0.6	0.9	P=400mW.
50%	1.1	2.0	1.4	1.3	1.2	1.0	1.2	3.9	V_{CB}=20V.
75%	3.7	4.2	3.6	3.6	3.4	3.1	4.0	---	T_A=150°C.
90%	4.3	5.0	4.2	4.3	3.6	3.4	---	---	
95%	4.3	5.0	4.2	4.3	3.6	3.4	---	---	
Max	4.3	5.0	4.2	4.3	3.6	3.4	---	---	

TABLE 81. (CONTINUED).

HRS.	INIT.	168	340	680	1000	1500	2000	3000	
Min	0.3	0.9	0.5	0.6	0.4	0.4	1.1	0.4	P=200mW. V_{CB}=20V. T_A=150°C.
5%	0.3	0.9	0.5	0.6	0.4	0.4	1.1	0.4	
10%	0.4	1.1	0.7	0.6	0.5	0.5	1.2	0.5	
25%	1.0	1.4	1.2	1.1	1.0	0.9	1.7	1.0	
50%	1.2	1.9	1.9	1.8	1.7	1.6	2.5	2.1	
75%	2.4	3.4	3.4	3.3	2.9	3.2	3.8	3.6	
90%	3.5	4.2	6.2	5.6	4.4	3.9	5.4	13.6	
95%	3.8	4.5	8.2	7.0	4.6	4.1	6.3	15.7	
Max	3.8	4.5	8.2	7.0	4.6	4.1	6.3	15.7	

TABLE 81 GRAPH.

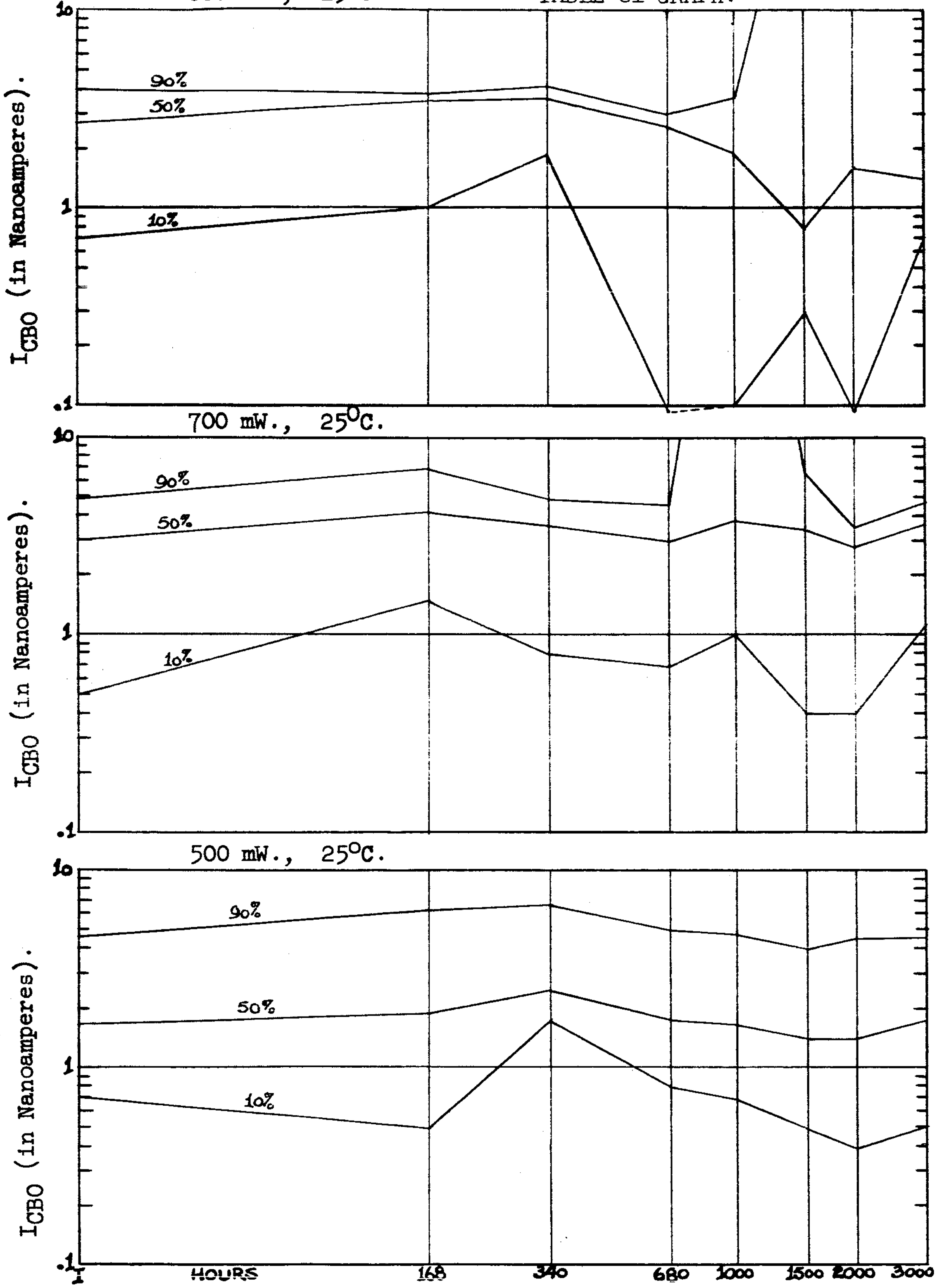

800 mW., 25°C.

700 mW., 25°C.

500 mW., 25°C.

TABLE 81 GRAPH.

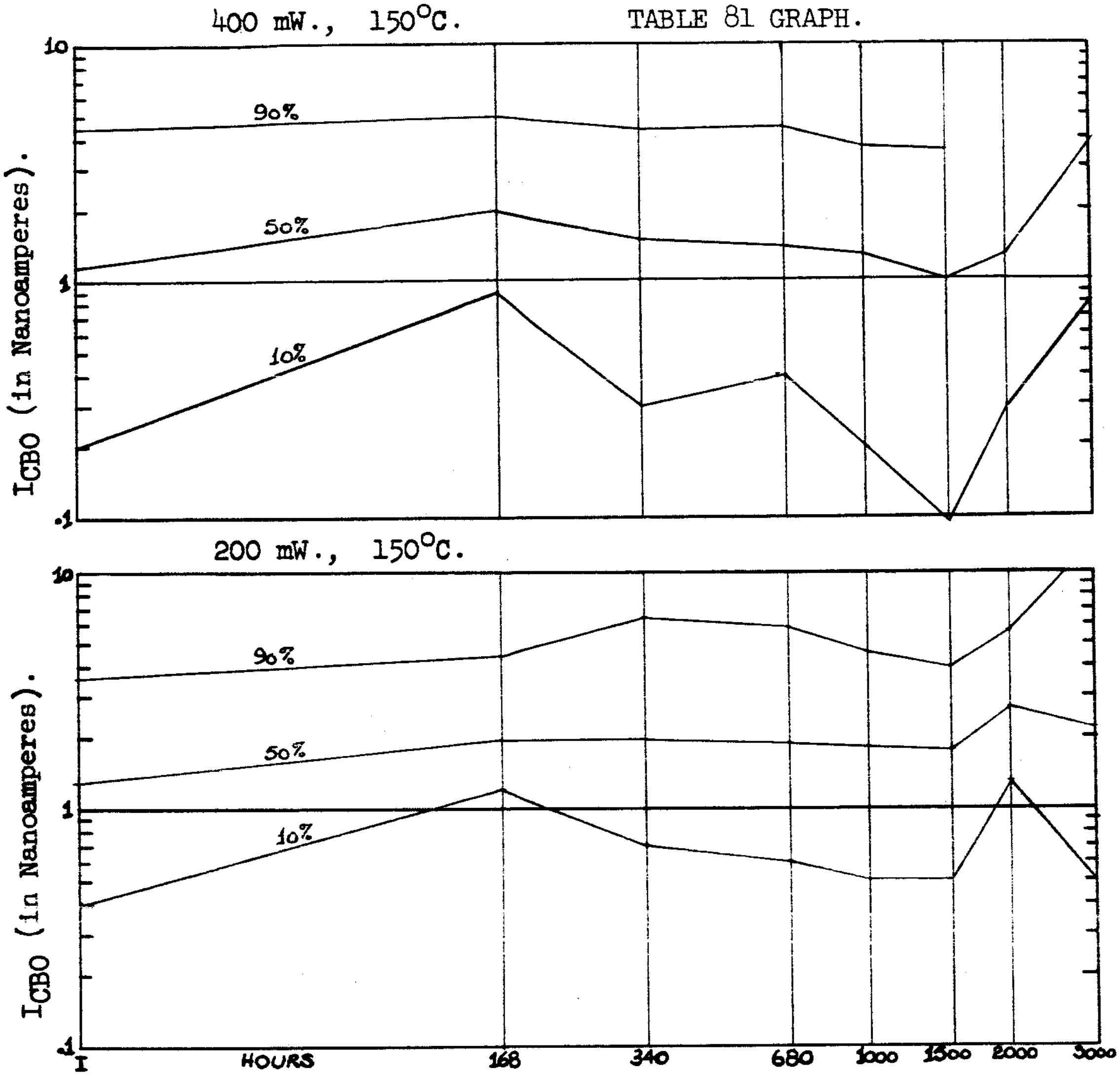

PROCESS C. CONTROL LOT. TABLE 82.

I_{CBO} DISTRIBUTION CHANGES WITH LIFE TEST.

	I_{CBO} (V_{CB} = 60 V.) (Nanoamperes).								
HRS.	INIT.	168	340	680	1000	1500	2000	3000	
Min	<0.1	0.6	0.1	0.1	0.1	<0.1	<0.1	<0.1	P=800mW. V_{CB}=20V. T_A=25°C.
5%	<0.1	0.6	0.1	0.1	0.1	<0.1	<0.1	<0.1	
10%	<0.1	0.6	0.1	0.1	0.1	<0.1	<0.1	<0.1	
25%	<0.1	0.7	0.2	0.2	0.2	<0.1	0.1	0.2	
50%	0.1	1.0	0.2	0.4	0.4	0.2	1.6	4.9	
75%	0.3	1.5	0.3	0.6	0.6	1.7	43.9	147.1	
90%	0.4	3.5	900.0	1.8	1.8	3.3	912.4	926.4	
95%	0.4	3.7	---	1.9	1.9	3.4	---	---	
Max	0.4	3.7	---	1.9	1.9	3.4	---	---	
Min	<0.1	0.4	<0.1	<0.1	<0.1	<0.1	<0.1	<0.1	P=700mW. V_{CB}=20V. T_A=25°C.
5%	<0.1	0.4	<0.1	<0.1	<0.1	<0.1	<0.1	<0.1	
10%	<0.1	0.6	<0.1	<0.1	<0.1	<0.1	<0.1	0.1	
25%	<0.1	0.7	<0.1	<0.1	0.1	<0.1	0.3	0.2	
50%	<0.1	0.9	0.3	0.4	0.6	0.4	2.5	4.0	
75%	0.2	1.7	1.3	2.2	2.5	2.4	67.6	345.0	
90%	0.5	20.2	174.4	96.4	120.2	81.3	918.7	---	
95%	1.2	950.9	610.8	955.2	956.5	648.1	---	---	
Max	1.2	---	632.8	---	---	677.7	---	---	
Min	<0.1	0.4	0.2	<0.1	<0.1	<0.1	<0.1	0.2	P=500mW. V_{CB}=20V. T_A=25°C.
5%	<0.1	0.5	0.8	<0.1	0.1	<0.1	<0.1	0.3	
10%	<0.1	0.5	1.0	0.1	0.1	<0.1	<0.1	0.3	
25%	<0.1	0.7	1.0	0.3	0.3	0.1	0.1	0.5	
50%	0.1	0.9	1.3	0.5	0.6	0.2	0.4	0.8	
75%	0.4	1.7	1.7	1.2	1.3	1.0	1.3	2.0	
90%	0.6	3.4	4.3	3.2	3.4	2.5	2.9	4.1	
95%	1.1	107.4	208.2	213.7	219.1	244.4	252.3	50.9	
Max	1.2	---	---	---	---	---	---	133.1	
Min	<0.1	0.6	0.2	<0.1	0.1	<0.1	0.5	0.1	P=400mW. V_{CB}=20V. T_A=150°C.
5%	<0.1	0.6	0.2	<0.1	0.1	<0.1	0.5	0.1	
10%	<0.1	0.6	0.2	<0.1	0.1	<0.1	0.5	0.1	
25%	<0.1	0.8	0.4	0.2	0.2	0.1	0.7	0.3	
50%	0.3	1.0	0.5	0.3	0.6	0.2	1.0	3.7	
75%	0.4	253.2	16.8	12.8	8.9	3.1	1.2	97.2	
90%	1.0	---	906.3	904.1	902.0	281.1	12.8	919.5	
95%	1.0	---	---	---	---	311.5	12.8	---	
Max	1.0	---	---	---	---	311.5	12.8	---	

TABLE 82. (CONTINUED).

HRS.	INIT.	168	340	680	1000	1500	2000	3000	
Min	<0.1	0.4	0.1	<0.1	<0.1	<0.1	<0.1	<0.1	
5%	<0.1	0.4	0.1	<0.1	<0.1	<0.1	<0.1	<0.1	
10%	<0.1	0.5	0.1	0.1	<0.1	<0.1	<0.1	<0.1	
25%	<0.1	0.6	0.3	0.2	0.2	<0.1	0.1	0.1	P=200mW.
50%	0.2	0.9	0.5	0.5	0.5	0.3	0.5	0.3	V_{CB}=20V.
75%	0.6	1.5	1.5	1.8	161.1	1.0	1.3	1.4	T_A=150°C.
90%	1.9	23.1	2.9	4.4	---	2.2	3.0	5.1	
95%	5.8	70.0	526.1	---	---	---	---	---	
Max	5.8	70.0	526.1	---	---	---	---	---	

TABLE 82 GRAPH.

800 mW., 25°C.

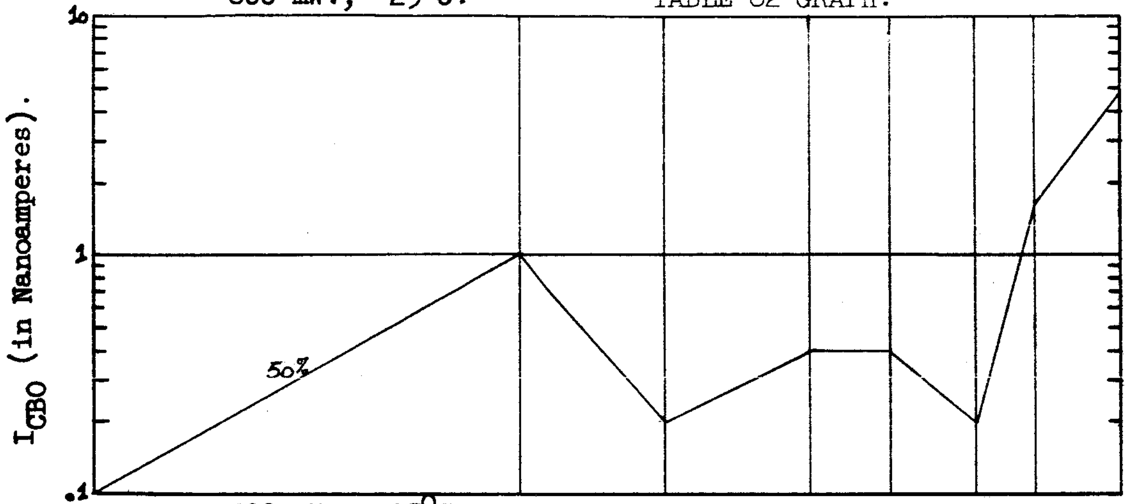

700 mW., 25°C.

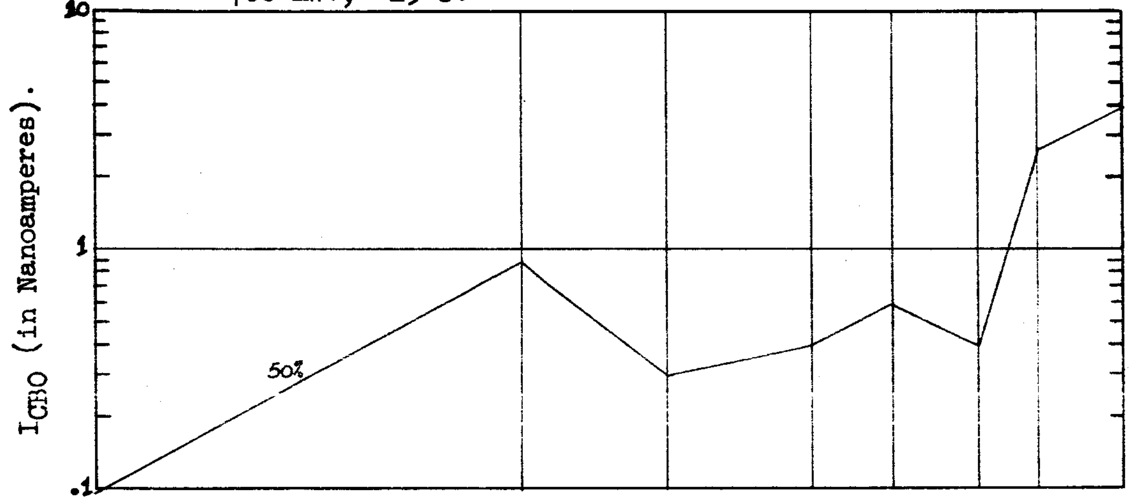

500 mW., 25°C.

400 mW., 150°C. TABLE 82 GRAPH.

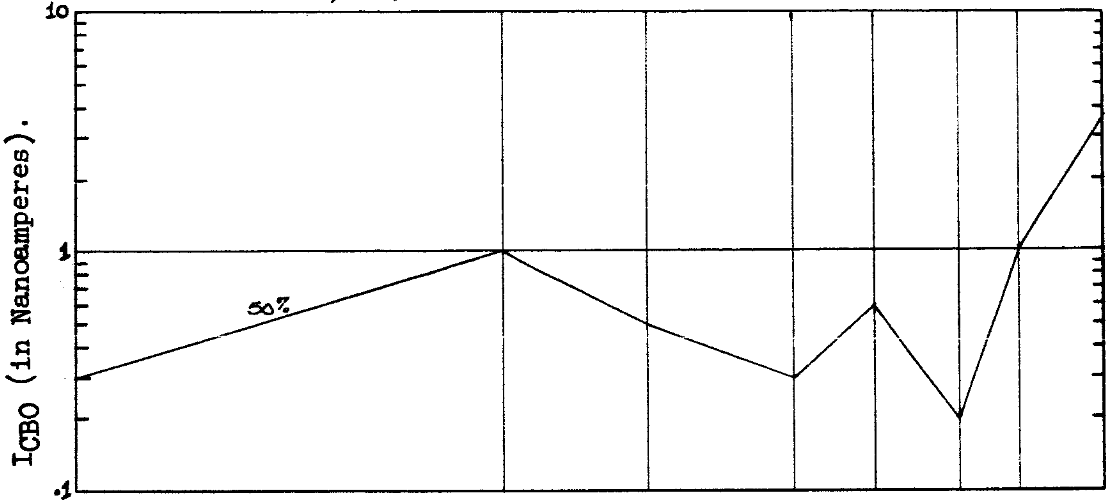

200 mW., 150°C.

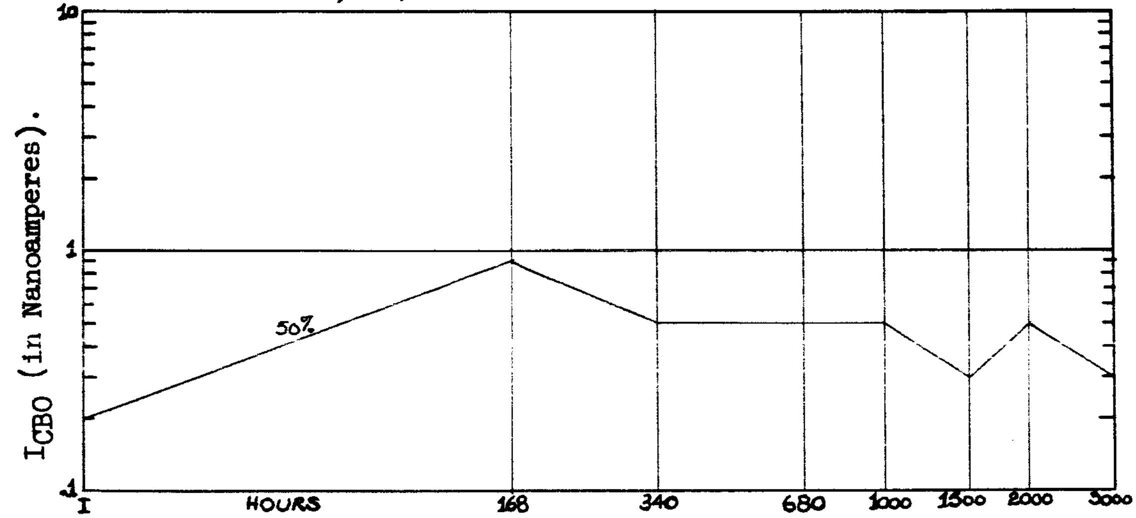

PROCESS A. CONTROL LOT. TABLE 83.

h_{FE} DISTRIBUTION CHANGES WITH LIFE TEST.

	h_{FE} (I_C = 20 mA., V_{CE} = 5 V.)								
HRS.	INIT.	168	340	680	1000	1500	2000	3000	
Min	74	74	68	73	75	73	20	20	P=800mW. V_{CB}=20V. T_A=25°C.
5%	74	74	68	73	75	73	20	20	
10%	74	74	68	73	75	73	20	20	
25%	74	74	68	74	75	75	72	72	
50%	78	79	70	80	81	80	81	80	
75%	84	87	78	86	87	82	87	86	
90%	85	87	79	87	88	83	87	87	
95%	85	87	79	87	88	83	87	87	
Max	85	87	79	87	88	83	87	87	
Min	65	66	67	66	66	66	65		P=700mW. V_{CB}=20V. T_A=25°C.
5%	65	66	67	66	66	66	65		
10%	66	66	67	67	67	67	66		
25%	67	69	69	69	68	68	67		
50%	81	80	86	85	81	87	85		
75%	88	89	90	89	89	89	89		
90%	89	92	92	91	91	93	93		
95%	90	92	93	92	92	93	93		
Max	90	92	93	92	92	93	93		
Min	49	48	50	49	20	20	20	20	P=500mW. V_{CB}=20V. T_A=25°C.
5%	59	62	63	60	20	20	20	20	
10%	67	65	69	63	20	20	20	20	
25%	72	71	75	70	65	65	66	64	
50%	83	85	83	81	75	76	79	78	
75%	89	91	93	86	86	87	90	88	
90%	93	96	99	91	94	95	97	93	
95%	98	98	99	92	97	97	99	96	
Max	100	101	102	96	101	100	105	100	
Min	56	57	56	54	55	56	57	22	P=400mW. V_{CB}=20V. T_A=150°C.
5%	56	57	56	54	55	56	57	22	
10%	56	57	56	54	55	56	57	22	
25%	63	63	63	60	61	62	63	56	
50%	77	82	84	78	79	81	82	73	
75%	81	85	85	80	82	83	84	91	
90%	91	92	91	87	89	91	91	541	
95%	91	92	91	87	89	91	91	541	
Max	91	92	91	87	89	91	91	541	

TABLE 83. (CONTINUED).

HRS.	INIT.	168	340	680	1000	1500	2000	3000	
Min	57	59	56	59	57	59	58	59	
5%	57	59	56	59	57	59	58	59	
10%	63	64	61	64	63	64	63	64	
25%	74	76	72	76	74	76	74	76	P=200mW.
50%	78	83	77	83	81	83	83	83	V_{CB}=20V.
75%	83	88	87	87	86	87	87	87	T_A=150°C.
90%	96	92	89	91	90	91	460	92	
95%	99	94	89	94	92	94	829	94	
Max	99	94	89	94	92	94	829	94	

TABLE 83 GRAPH.

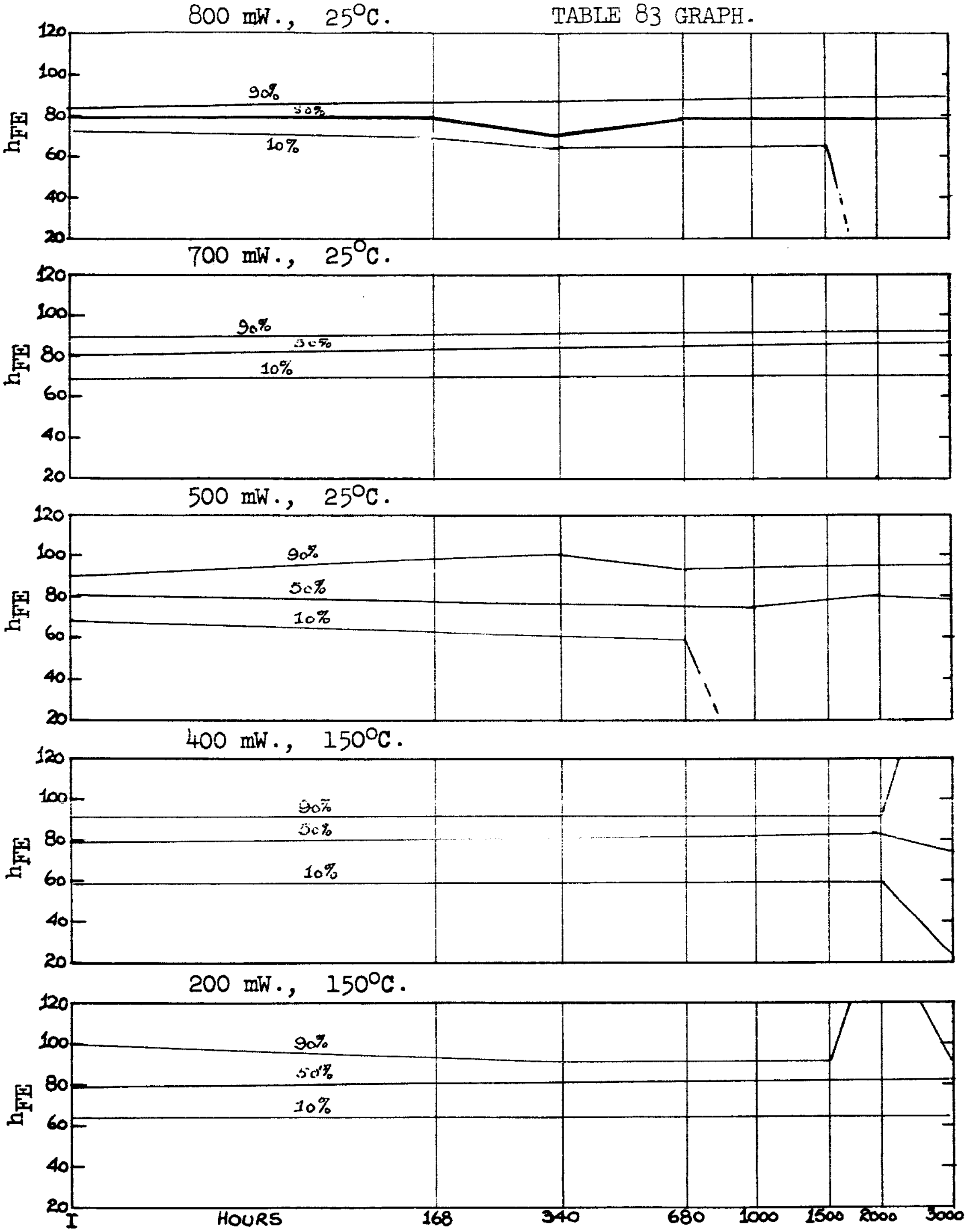

PROCESS B. CONTROL LOT. TABLE 84.

h_{FE} DISTRIBUTION CHANGES WITH LIFE TEST.

	h_{FE} (I_C = 20 mA., V_{CE} = 5 V.)								
HRS.	INIT.	168	340	680	1000	1500	2000	3000	
Min	69	71	20	20	20	20	20	90	P=800mW. V_{CB}=20V. T_A=25°C
5%	69	71	20	20	20	20	20	90	
10%	69	71	20	20	20	20	20	90	
25%	76	81	70	71	71	20	20	95	
50%	85	87	89	90	91	93	91	110	
75%	95	101	102	106	107	112	110	117	
90%	100	104	106	107	108	115	116	120	
95%	100	104	106	107	108	115	116	120	
Max	100	104	106	107	108	115	116	120	
Min	64	65	63	64	66	20	20	50	P=700mW. V_{CB}=20V. T_A=25°C.
5%	64	65	63	64	66	20	20	50	
10%	65	68	68	69	70	44	20	57	
25%	77	77	76	76	77	75	65	79	
50%	89	88	89	86	87	89	88	95	
75%	94	101	102	102	102	108	112	114	
90%	101	110	112	112	111	114	120	128	
95%	105	111	114	115	113	115	124	128	
Max	105	111	114	115	113	115	124	128	
Min	61	61	20	25	25	20	20		P=500mW. V_{CB}=20V. T_A=25°C.
5%	64	64	56	56	56	57	57		
10%	76	75	72	71	71	71	71		
25%	83	84	81	83	82	83	83		
50%	89	93	88	93	90	93	92		
75%	100	102	98	102	101	103	102		
90%	101	106	101	107	105	106	107		
95%	103	110	109	110	107	110	110		
Max	105	113	110	114	111	114	113		
Min	61	60	61	19	20	20	20	20	P=400mW. V_{CB}=20V. T_A=150°C.
5%	61	60	61	19	20	20	20	20	
10%	61	60	61	19	20	20	20	20	
25%	92	90	89	59	60	61	162	62	
50%	103	96	101	98	102	104	267	105	
75%	105	100	104	102	104	109	281	107	
90%	111	103	110	105	108	---	297	111	
95%	111	103	110	105	108	---	297	111	
Max	111	103	110	105	108	---	297	111	

TABLE 84. (CONTINUED).

HRS.	INIT.	168	340	680	1000	1500	2000	3000	
Min	57	56	55	55	54	54	55	54	
5%	57	56	55	55	54	54	55	54	
10%	60	58	59	59	58	58	59	58	
25%	78	78	76	78	75	75	77	79	P=200mW.
50%	92	90	89	90	88	88	90	91	V_{CB}=20V.
75%	97	94	95	96	95	93	97	98	T_A=150°C.
90%	106	102	104	105	104	104	105	107	
95%	108	107	104	106	104	104	105	109	
Max	108	107	104	106	104	104	105	109	

TABLE 84 GRAPH.

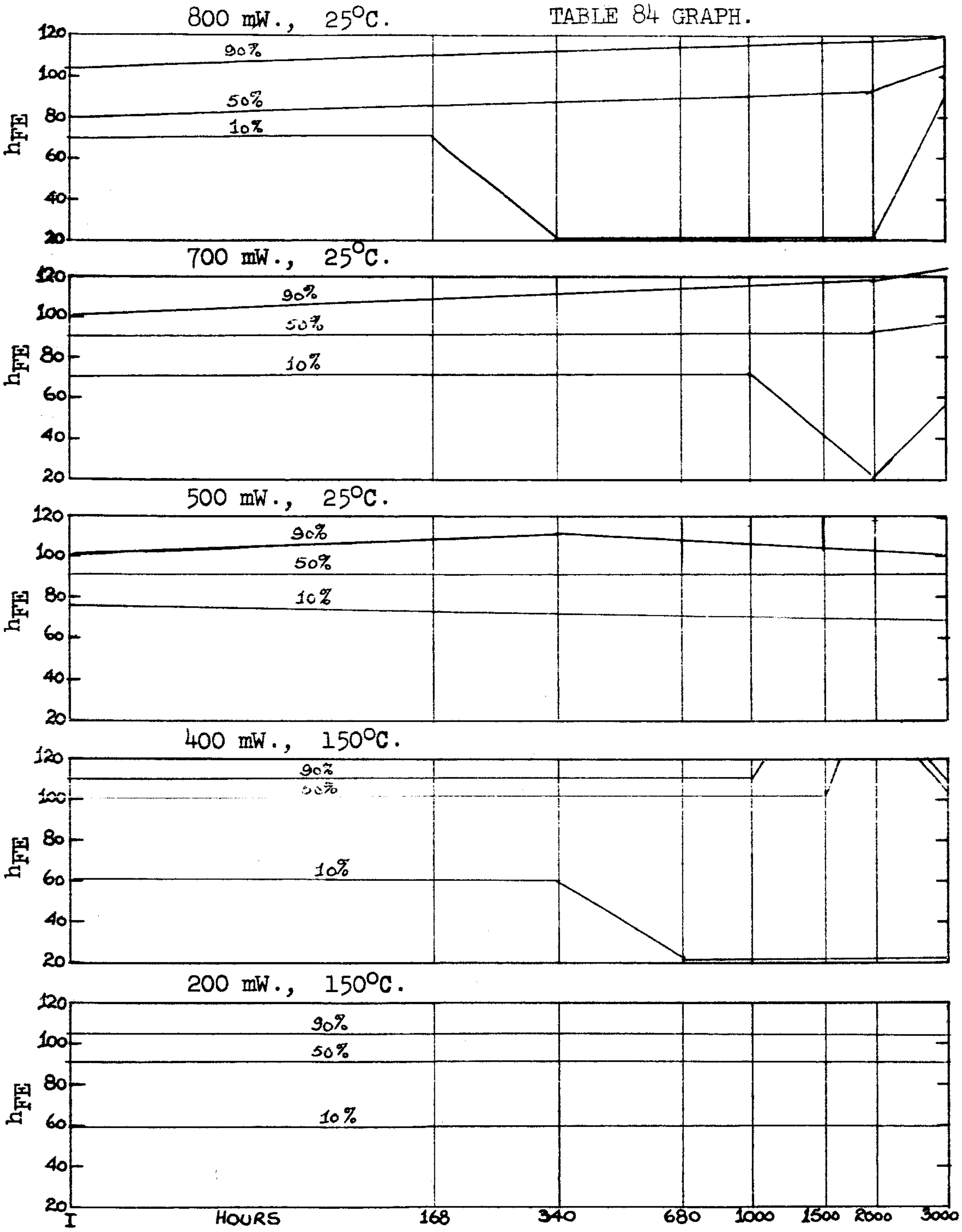

PROCESS C. CONTROL LOT. TABLE 85.

h_{FE} DISTRIBUTION CHANGES WITH LIFE TEST.

	h_{FE} (I_C = 20 mA., V_{CE} = 5 V.)								
HRS.	INIT.	168	340	680	1000	1500	2000	3000	
Min	51	53	43	49	51	52	48	24	P=800mW. V_{CB}=20V. T_A=25°C.
5%	51	53	43	49	51	52	48	24	
10%	52	54	43	50	51	52	49	25	
25%	65	65	54	64	65	66	67	46	
50%	89	91	61	89	89	83	91	76	
75%	120	118	88	106	108	109	111	111	
90%	131	133	95	118	119	119	119	120	
95%	131	134	96	119	120	120	119	121	
Max	131	134	96	119	120	120	119	121	
Min	36	49	48	48	20	20			P=700mW. V_{CB}=20V. T_A=25°C.
5%	36	49	49	49	20	21			
10%	48	58	58	58	28	49			
25%	64	67	65	69	66	58			
50%	84	85	84	87	88	97			
75%	91	92	100	95	104	111			
90%	118	119	115	121	123	127			
95%	126	123	122	126	128	130			
Max	126	123	122	126	128	130			
Min	52	53	20	53	54	53	53	20	P=500mW. V_{CB}=20V. T_A=25°C.
5%	56	57	55	57	58	57	57	56	
10%	60	63	60	63	64	63	64	61	
25%	68	71	70	68	71	70	70	71	
50%	79	87	80	82	85	82	82	78	
75%	102	100	95	101	102	101	101	101	
90%	119	115	111	116	118	117	116	116	
95%	126	126	128	126	128	127	127	121	
Max	140	141	---	139	142	140	141	142	
Min	41	49	40	32	32	33	33	20	P=400mW. V_{CB}=20V. T_A=150°C.
5%	41	49	40	32	32	33	33	20	
10%	42	50	41	33	33	34	33	21	
25%	63	65	56	50	50	49	46	39	
50%	81	82	77	77	80	82	87	74	
75%	111	113	106	101	110	113	109	98	
90%	129	130	124	120	127	130	132	116	
95%	131	131	126	122	128	131	132	117	
Max	131	131	126	122	128	131	132	117	

TABLE 85. (CONTINUED).

HRS.	INIT.	168	340	680	1000	1500	2000	3000	
Min	35	54	54	52	53	55	54	55	P=200mW. V_{CB}=20V. T_A=150°C.
5%	35	54	54	52	53	55	54	55	
10%	54	54	55	52	54	55	55	56	
25%	58	60	60	57	59	60	60	61	
50%	80	80	79	76	77	74	78	79	
75%	104	107	104	104	107	110	111	113	
90%	120	116	114	110	119	122	121	142	
95%	120	121	120	114	126	132	135	159	
Max	120	121	120	114	126	132	135	159	

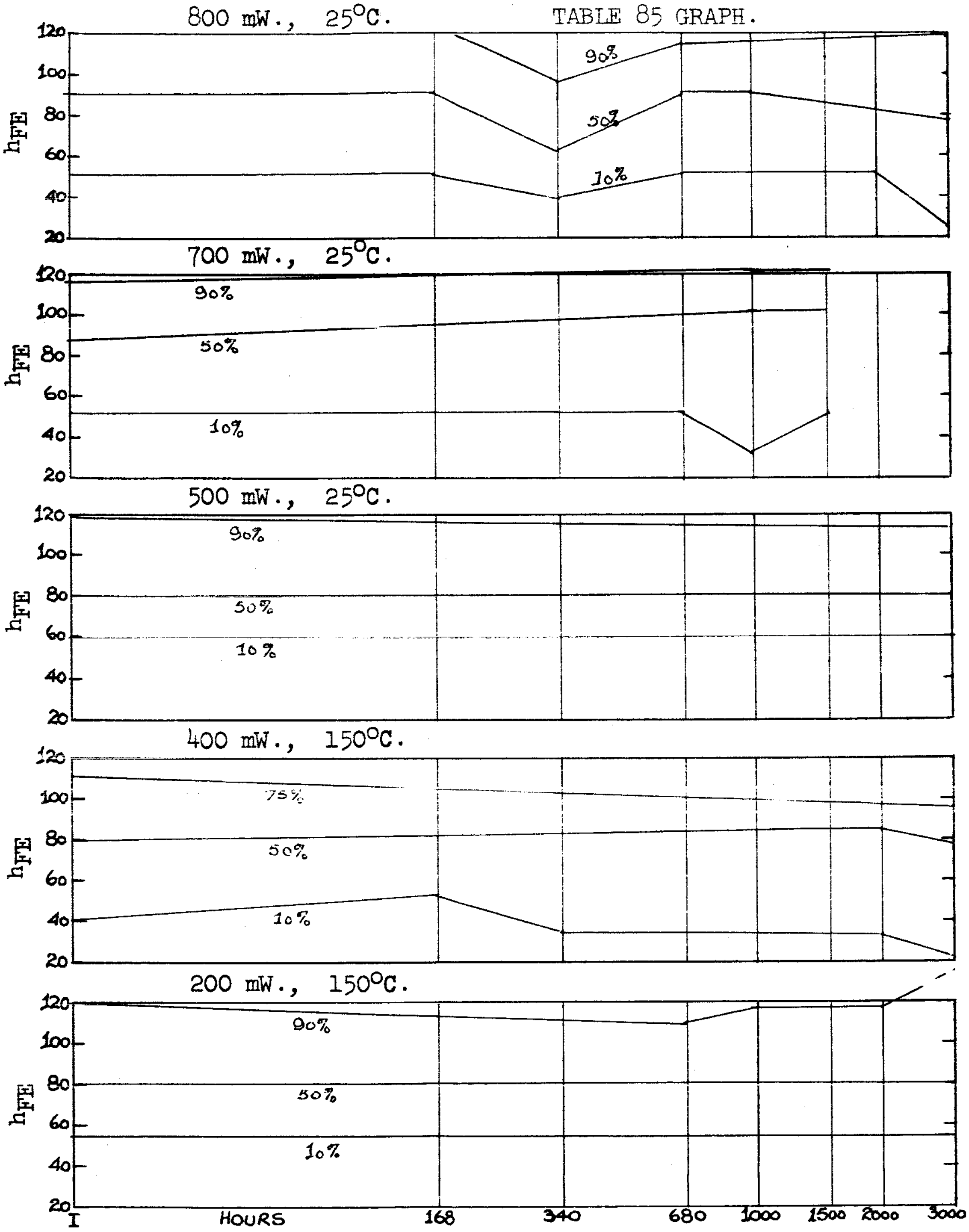

TABLE 85 GRAPH.

TABLE 86. SCREEN, BURN-IN AND LIFE TEST YIELDS.

		HIGH STRESS SCREEN				MODERATE STRESS SCREEN				CENTRIFUGE SCREEN				CONTROL LOT			
		PROCESS				PROCESS				PROCESS				PROCESS			
		A	B	C	COMBINED	A	B	C	COMBINED	A	B	C	COMBINED	A	B	C	COMBINED
STARTING QUANTITY		161	154	56	371	167	165	192	524	85	85	111	281	80	77	115	272
GOOD AFTER ELECTRICAL SCREEN		155	143	28	326	163	156	163	482	85	84	111	280	80	77	115	272
STRESS	1	20	0	0	20	1	1	4	6	0	1	9	10	0	0	3	3
SCREEN	2	5	10	3	18	0	4	23	27	0	1	8	9	0	1	5	6
RESPONSE	3	1	4	6	11	0	1	12	13	0	1	3	4	0	0	1	1
BY CATEGORY	4	4	9	11	24	0	4	17	21	0	1	0	1	0	0	4	4
GOOD AFTER STRESS SCREEN		125	120	8	253	162	146	107	415	85	80	91	256	80	76	102	258
BURN-IN	1	0	0	1	1	0	0	1	1	1	1	1	3	1	0	0	1
SCREEN	2	1	15	0	16	1	6	5	12	0	2	6	8	0	2	7	9
RESPONSE	3	0	3	1	4	0	1	4	5	0	1	1	2	0	1	6	7
BY CATEGORY	4	0	4	0	4	0	2	2	4	0	8	9	17	1	3	8	12
GOOD AFTER BURN-IN		124	98	6	228	161	137	95	393	84	68	74	226	78	70	81	229
LIFE	1	0	0	0	0	0	0	0	0	0	0	0	0	0	0	0	0
TEST	2	4	8	2	14	2	3	6	11	2	3	5	10	1	5	4	10
RESPONSE	3	1	1	1	3	0	0	5	5	0	1	3	4	0	0	5	5
BY CATEGORY	4	5	11	1	17	4	7	11	22	6	5	5	16	6	3	2	11
GOOD AFTER LIFE TEST		114	78	2	194	155	127	73	355	76	59	61	196	71	62	70	203

TABLE 87

TEST MATRIX CELL NUMBER ASSIGNMENT

PROCESS	STRESS SCREEN TYPE	SCREEN CELL NUMBER	Life Test Cell Numbers (V_{CB} = 20V)				
			P = 800mW T_A = 25°C	P = 700mW T_A = 25°C	P = 500mW T_A = 25°C	P = 400mW T_A = 150°C	P = 200mW T_A = 150°C
A	High	404-101	419-201	419-202	419-203	419-204	419-205
A	Moderate	-102	-206	-207	-208	-209	-210
A	Centrifuge	-103	-211	-212	-213	-214	-215
A	None	-104	-216	-217	-218	-219	-220
B	High	404-105	419-221	419-222	419-223	419-224	419-225
B	Moderate	-106	-226	-227	-228	-229	-230
B	Centrifuge	-107	-231	-232	-233	-234	-235
B	None	-108	-236	-237	-238	-239	-240
C	High	404-109	419-241	419-242	419-243	---	---
C	Moderate	-110	-244	-245	-246	419-247	419-248
C	Centrifuge	-111	-249	-250	-251	-252	-253
C	None	-112	-254	-255	-256	-257	-258

TABLE 88

TRUNCATION SCREENING - UNSCREENED FAILURES

UNIT NUMBERS	I_{CBO}	I_{EBO}	BV_{CEO}	h_{FE}	$V_{CE(SAT)}$	$V_{BE(SAT)}$	I_{NO}	I_{N1}	I_{N2}	I_{N3}	FAIL
201-1	65	85	54	62	44	60	35	55	45	65	I_{CBO}
-7	85	35	19	12	75	50	80	70	85	95	BV_{CEO}
204-3	35	40	91	35	69	55	80	90	75	45	$V_{CE(SAT)}$
-4	30	70	45	79	62	60	55	35	40	50	I_{CBO}
206-14	91	50	9	67	66	30	30	30	65	65	h_{FE}
209-12	45	75	78	97	50	75	80	65	50	50	h_{FE}
211-1	45	70	95	3	93	45	5	25	8	35	h_{FE}
216-1	60	50	62	33	66	94	50	40	30	50	h_{FE}
228-28	35	15	58	23	70	60	50	50	70	60	h_{FE}
-5	65	64	55	6	94	60	85	80	85	97	I_{EBO}
226-2	93	40	43	93	45	16	0	50	30	15	h_{FE}
-10	90	25	53	83	81	25	30	35	35	30	h_{FE}
229-14	100	15	3	97	20	4	10	15	10	15	h_{FE}
231-1	60	76	9	73	85	50	45	50	50	50	h_{FE}
-2	76	35	50	53	45	15	25	15	10	5	h_{FE}
232-5	50	55	97	17	70	75	90	85	65	90	I_{CBO}
233-21	56	50	30	87	79	56	75	50	95	50	h_{FE}
236-1	63	60	63	13	45	25	76	65	75	55	h_{FE}
239-1	83	15	9	73	25	30	10	10	10	5	I_{CBO}

Note: Tabulated values are the percentiles of the parameter distribution.

TABLE 89

FAILURES REMOVED BY THE TRUNCATION SCREENING OF INITIAL PARAMETERS

UNIT NUMBERS	I_{CBO}	I_{EBO}	BV_{CEO}	h_{FE}	$V_{CE(SAT)}$	$V_{BE(SAT)}$	I_{NO}	I_{N1}	I_{N2}	I_{N3}
201-8			8	98			10	3		5
202-12		98		2	10					
204-14			92		92			93		
205-27		98	94			95				
218-13				100			8			
221-4		93								
221-2		94					97		91	90
221-11		93						91		90
221-10						5				
221-5				97		10	5		5	
222-1		91	6	3			93	98	96	96
222-4									5	
222-9							90	10		
222-13					10					
222-14			93	0						
222-15		97			6		90			
223-12										
223-8										
223-5		98	9			92				
223-34										
223-36				8		91				
223-50										
223-3										
226-1		96	96		93					
226-4		98		3						
227-6		97								90
227-21										
228-65						91				
229-5.			97							

TABLE 89 (CONTINUED)

FAILURES REMOVED BY THE TRUNCATION SCREENING OF INITIAL PARAMETERS

UNIT NUMBERS	I_{CBO}	I_{EBO}	BV_{CEO}	h_{FE}	$V_{CE(SAT)}$	$V_{BE(SAT)}$	I_{NO}	I_{N1}	I_{N2}	I_{N3}
231-6										
232-2		100								
232-4							97	95	97	97
232-12					4					
232-7						0				
233-8			97		90	96				
233-1						9	10		0	
233-6		90								

Note: Tabulated values are the percentiles of the parameter distribution.

TABLE 90

TRUNCATION SCREENING APPLIED TO ALL FAILURES CONSIDERED FREE FROM STRESS DAMAGE

UNIT NUMBERS	I_{CBO}	I_{EBO}	BV_{CEO}	h_{FE}	$V_{CE(SAT)}$	$V_{BE(SAT)}$	I_{NO}	I_{N1}	I_{N2}	I_{N3}
206-14				100			8			
209-12				97						
211-1			95	3	93		5		8	
216-1					94					
226-2	93			93			0			
226-10	90									
226-1		96	96		93					
226-4		98		3						
227-6		97								90
227-21										
229-5			97							
229-14	100		3	97		4	10		10	
231-1			9							
231-6										
231-2									10	5
232-5			97							
232-2		100								
232-4							97	95	97	97
232-12					4					
232-7						0				
236-1										
239-1			9				10	10	10	5
245-6							96			90
245-21			9	100	4					
245-23										
245-25				3			90			
245-26										

Note: Tabulated values are the percentiles of the parameter distribution.

TABLE 90 (CONTINUED)

UNIT NUMBERS	I_{CBO}	I_{EBO}	BV_{CEO}	h_{FE}	$V_{CE(SAT)}$	$V_{BE(SAT)}$	I_{NO}	I_{N1}	I_{N2}	I_{N3}
245-5										
245-14					99	96	93	97		95
245-17						4	7	5	7	
245-22										
248-15					97		10		3	
248-28					97			10		3
248-1					10					
248-22			92							
248-11								10		
248-23										
248-14				4						
250-19			97	94	95					
250-10										
250-11										
250-15								95		
253-9			93							
253-11										
255-10										
255-16										
255-8										
255-13										
255-3			9							
255-9				0			93		90	94
258-12										

Note: Tabulated values are the percentiles of the parameter distribution.

TABLE 91

TRUNCATION SCREENING SUMMARY

PROCESS		A			B			C			COMB		
NUMBER IN LOT		258			254			216			728		
FAILURE TYPE		I_{CBO}	h_{FE}	COMB	I_{CBO}	h_{FE}	COMB	I_{CBO}	h_{FE}	COMB	I_{CBO}	h_{FE}	COMB
NUMBER FAILED		3	6	9	11	13	24	45	6	51	59	25	84
Failures which could be eliminated by screening to:	h_{FE} - 95th Percentile	0	3	3	1	2	3	2	0	2	3	5	8
	h_{FE} - 5th Percentile	0	2	2	1	0	1	0	2	2	1	4	5
	100Kc Noise High Limit	1	0	1	3	0	3	4	1	5	8	1	9
	100 Cycle Noise High Limit	0	0	0	4	1	5	4	1	5	8	2	10
	100Kc I_N - 95th Percentile	1	0	1	2	0	2	2	0	2	5	0	5

TRANSISTOR FAILURE ANALYSIS FLOW CHART.

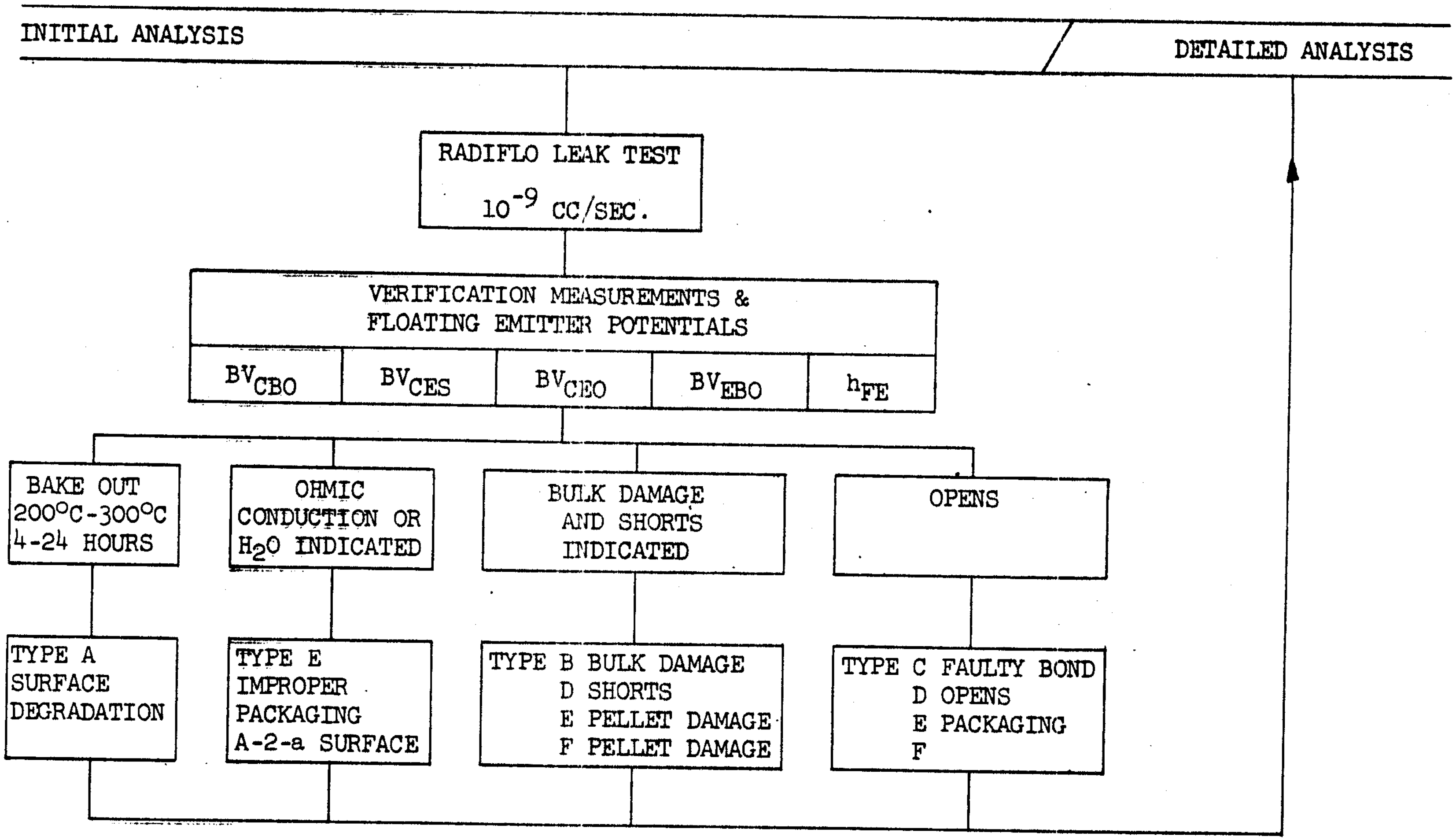

TRANSISTOR FAILURE ANALYSIS FLOW CHART.

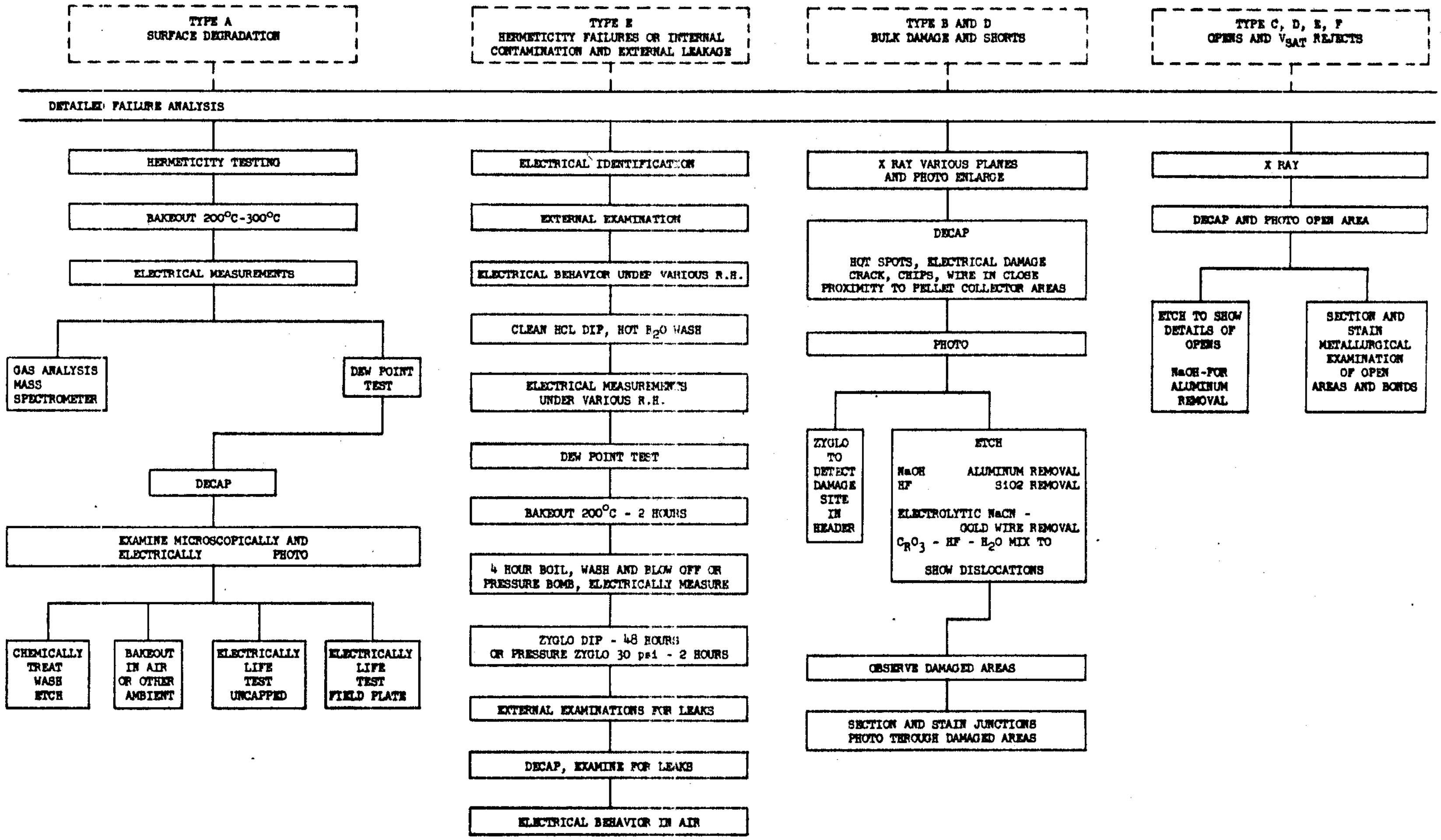

FIGURE 3

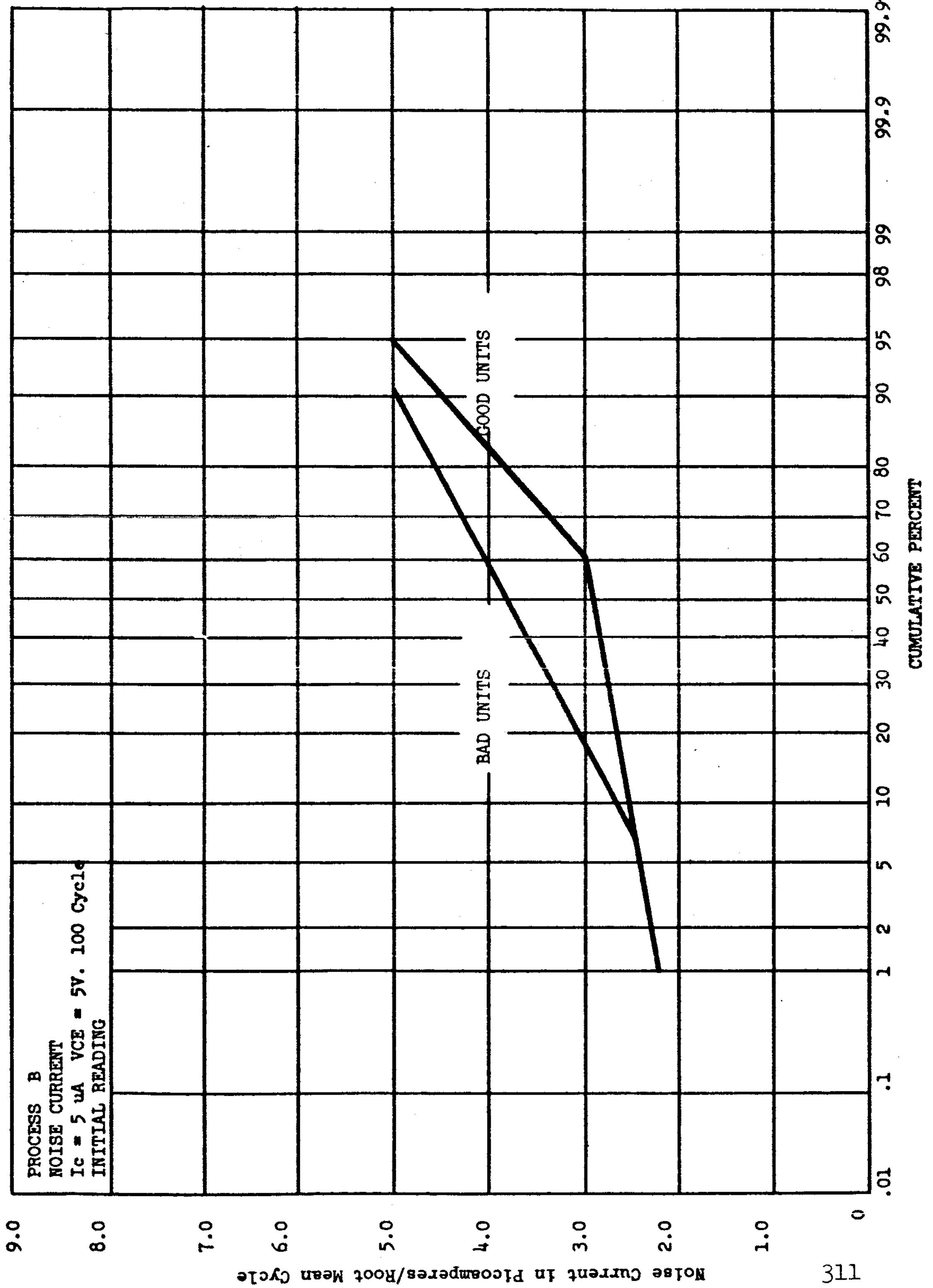
PROCESS B
NOISE CURRENT
Ic = 5 uA VCE = 5V. 100 Cycle
INITIAL READING
GOOD UNITS
BAD UNITS
CUMULATIVE PERCENT
.01
.1
1
2
5
10
20
30
40
50
60
70
80
90
95
98
99
99.9
99.99
Noise Current in Picoamperes/Root Mean Cycle
0
1.0
2.0
3.0
4.0
5.0
6.0
7.0
8.0
9.0

FIGURE 4

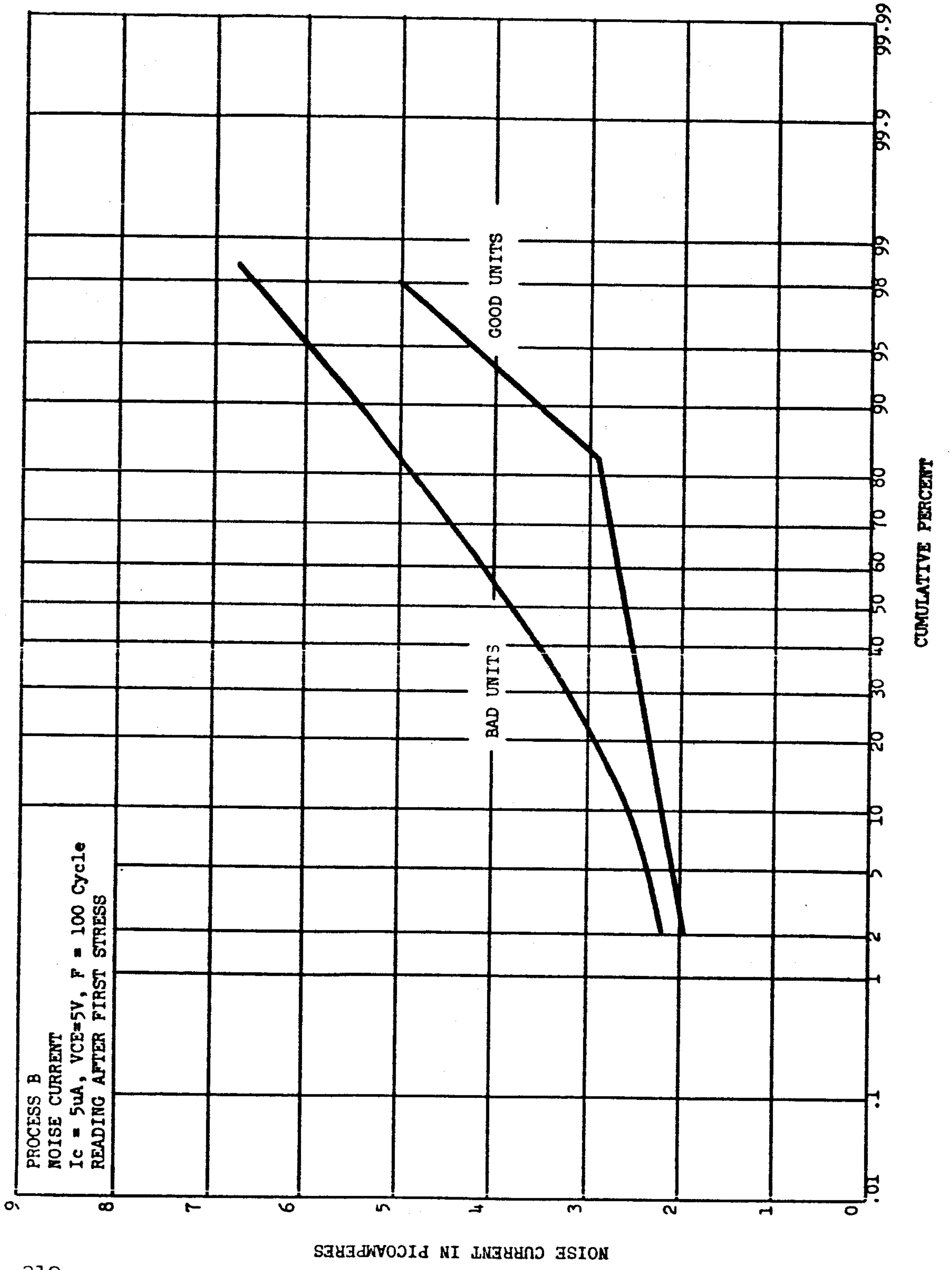
PROCESS B
NOISE CURRENT
Ic = 5uA, VCE=5V, F = 100 Cycle
READING AFTER FIRST STRESS
GOOD UNITS
BAD UNITS
0
1
2
3
4
5
6
7
8
9
NOISE CURRENT IN PICOAMPERES
.01
.1
1
2
5
10
20
30
40
50
60
70
80
90
95
98
99
99.9
99.99
CUMULATIVE PERCENT

FIGURE 5

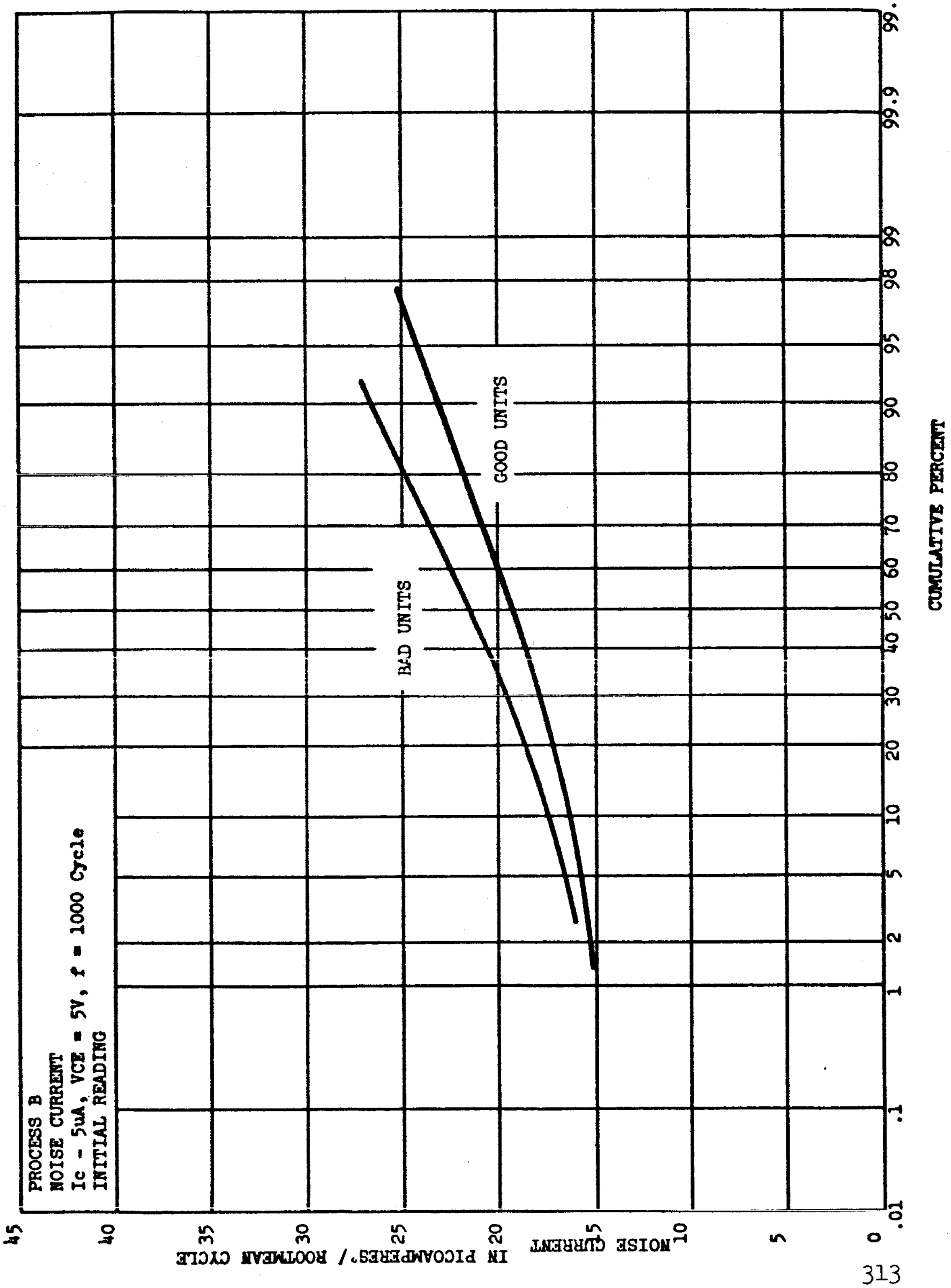
PROCESS B
NOISE CURRENT
Ic - 5uA, VCE = 5V, f = 1000 Cycle
INITIAL READING
GOOD UNITS
BAD UNITS
CUMULATIVE PERCENT
.01
.1
1
2
5
10
20
30
40
50
60
70
80
90
95
98
99
99.9
99.99
NOISE CURRENT IN PICOAMPERES/ ROOTMEAN CYCLE
0
5
10
15
20
25
30
35
40
45

CUMULATIVE DISTRIBUTION COMBINED LOT CONSISTING OF ALL FAILURES FOUND IN PROCESS A, PROCESS B AND PROCESS C.

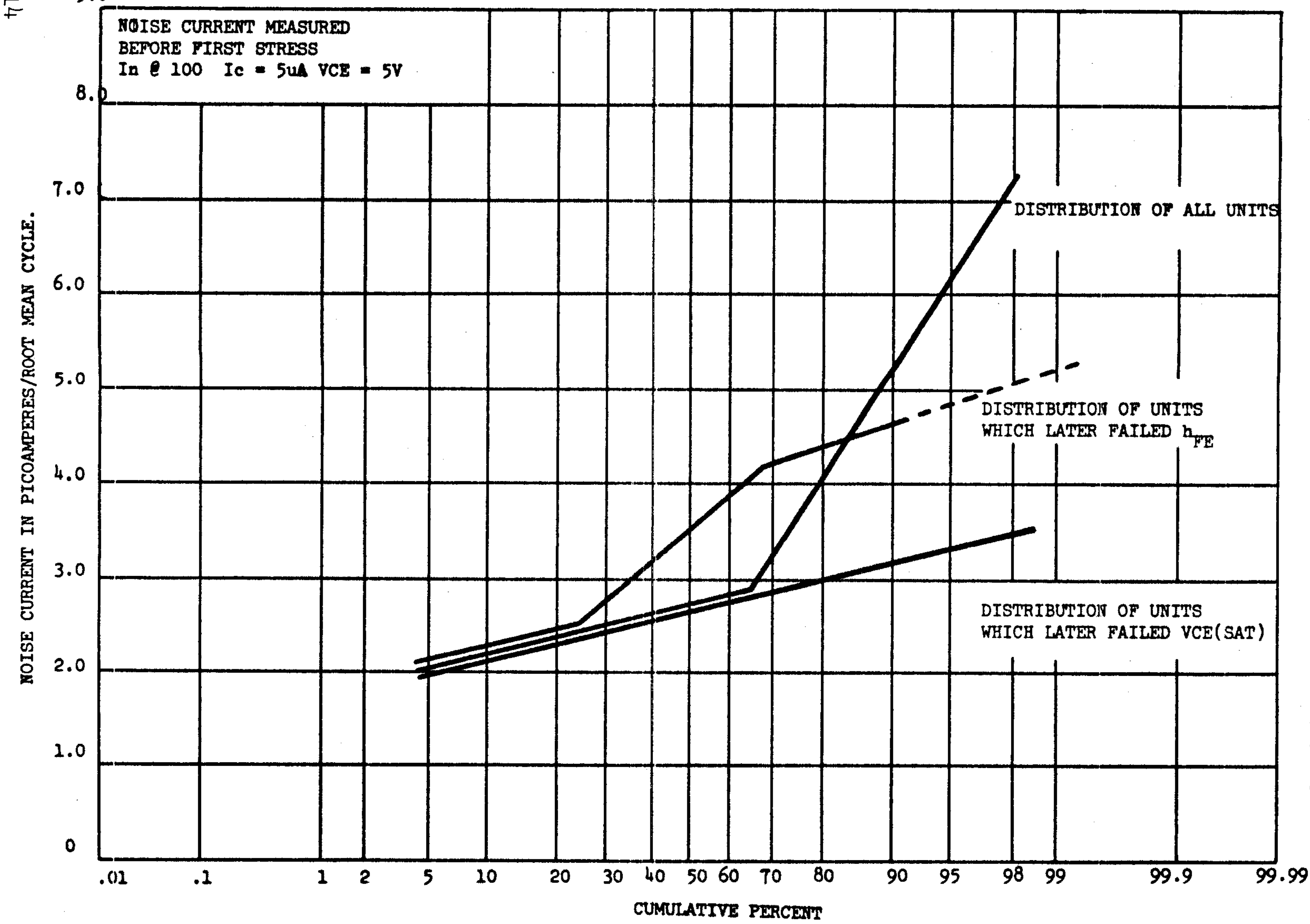

FIGURE 6

CUMMULATIVE DISTRIBUTION OF ALL UNITS AND FOR UNITS WHICH LATER DEGRADED IN hFE & VCE(SAT)

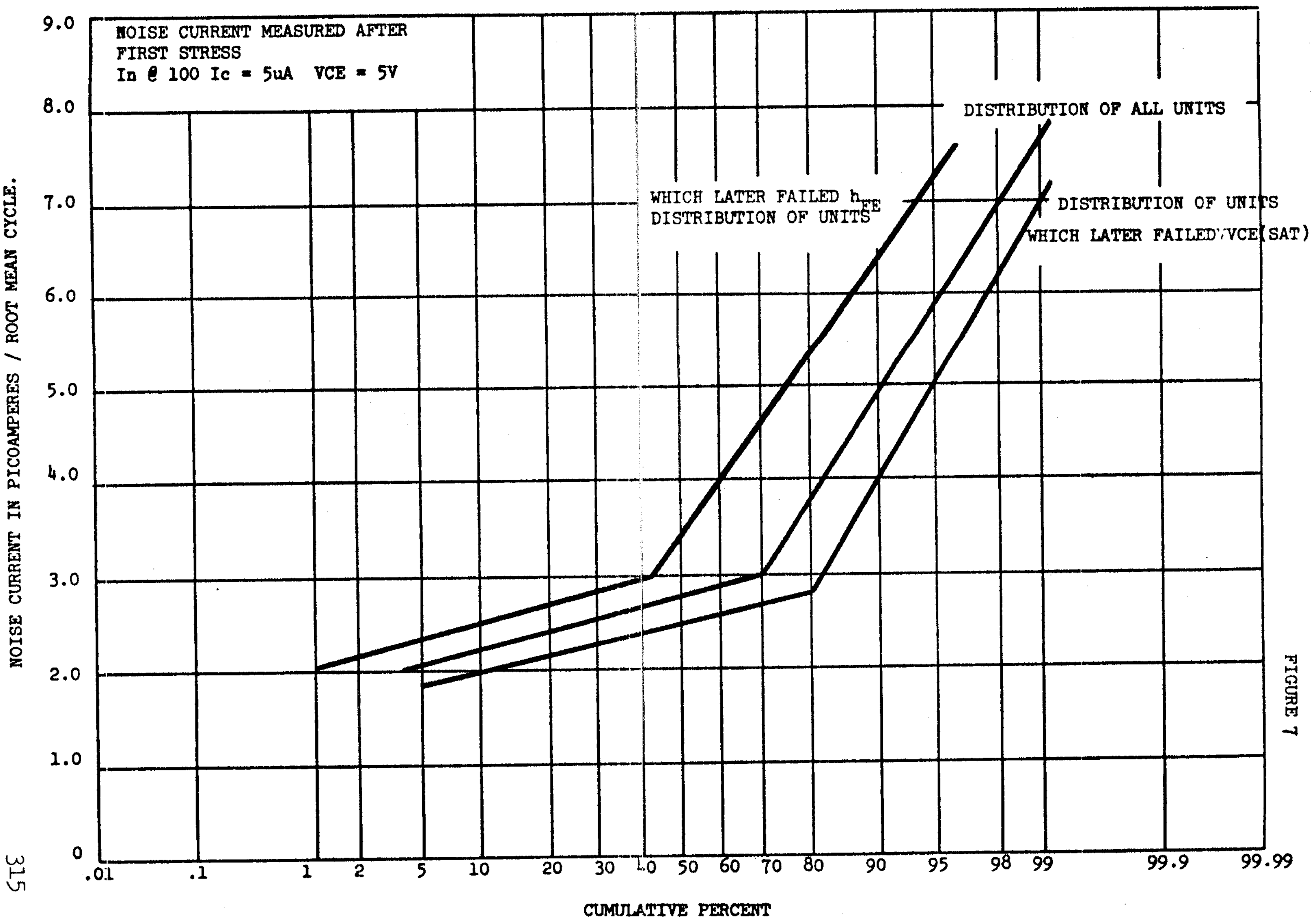

FIGURE 7

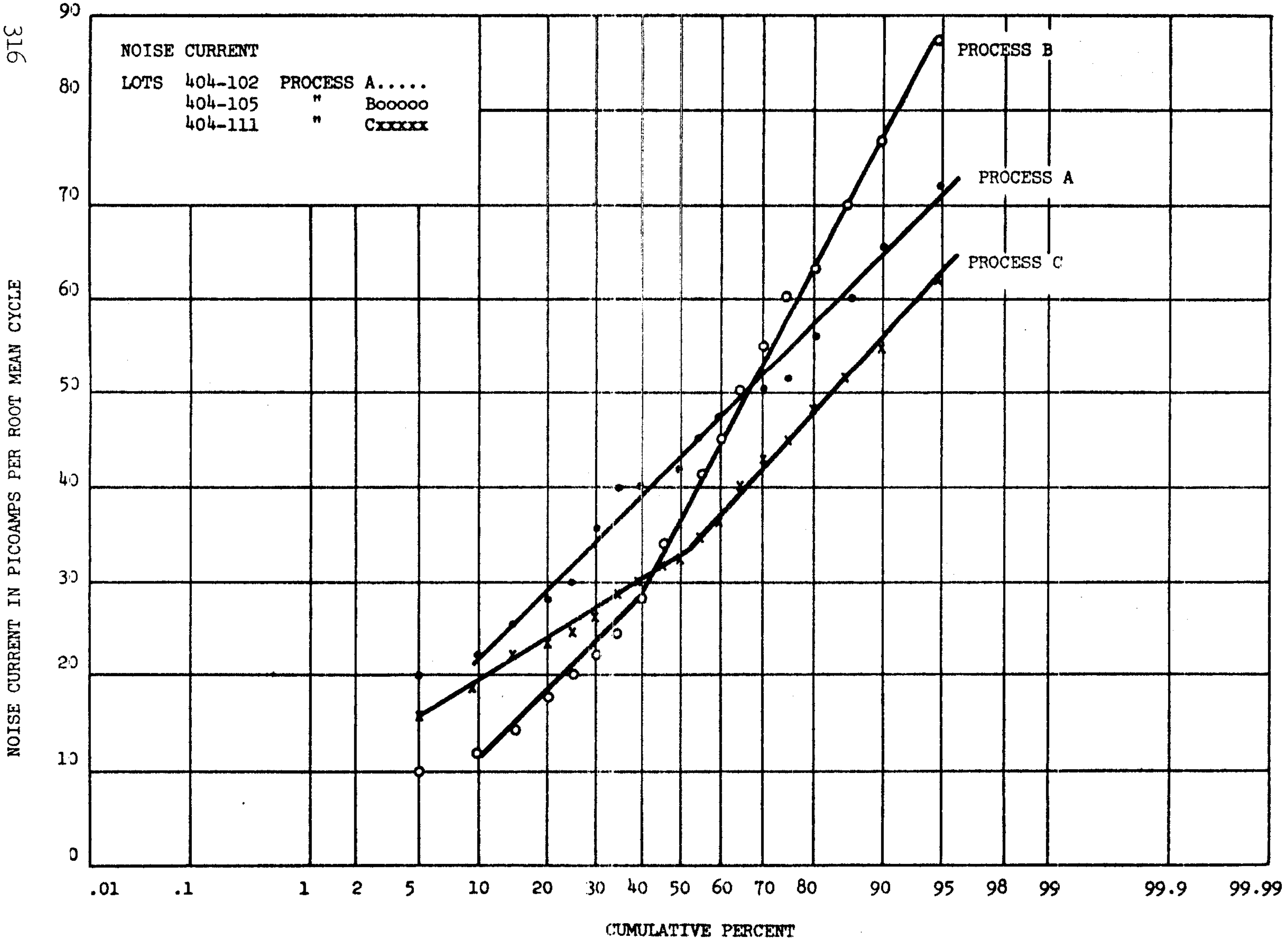
NOISE CURRENT
LOTS 404-102 PROCESS A.....
404-105 " Booooo
404-111 " Cxxxxx
PROCESS B
PROCESS A
PROCESS C
NOISE CURRENT IN PICOAMPS PER ROOT MEAN CYCLE
90
80
70
60
50
40
30
20
10
0
.01
.1
1
2
5
10
20
30
40
50
60
70
80
90
95
98
99
99.9
99.99
CUMULATIVE PERCENT

FIGURE 8 .

Bibliography -

(1) Van der Ziel, A., Fluctuation Phenemenon in Semiconductors London, Butterworth, 1959 pp 46-63

(2) Williams, N. H. and Thatcher, E. W., Phys. Rev., 40(1932) 121

(3) Christenson, C. S. and Pearson, G. L., Bell System Tech., Jan. 15 (936) 197

(4) Baker, D., J. Appl. Phys., 25 (1954) 922

(5) Firle, T. and Winston, H., Appl. Phys., 26 (1955) 716 259

(6) Rohm, B. V. and Templeton, I. M., Proc. Phys. Sec. Land, B66 (1953)

(7) Champlin, K. S., J. Appl. Phys., 50 (1959)

(8) Chenette, E. R., Measurement of the Correlation between Flicker Noise Sources in Transistors, Proc. I.R.E. 46, June 1958.

(9) Van der Ziel, A., Study of Noise in Semiconductor Devices, Signal Corps Contract DA 36-039 Sc-85374, University of Minnesota. Final Report page 25.

(10) Rose, D., J. Phys. Rev., 105 (1957) 413

(11) Chenette, E. R. and Van der Ziel, A., Accurate Noise Measurements on Transistors, IRE Transactions PGED-9, 123 (Mar 1962)

(12) Plumb, J. L. and Chenette, E. R., Flicker Noise in Junction Transistors, IRE Trans. PGED 10, Sept. 1963.

(13) Pearson, G. L., Montgomery, H. C. and Feldman, W. L., Jour. Appl. Physics, 27 (1956) 91.

(14) Brophy, J. J., J. Appl. Phys., 27 (1956) 1383

(15) Brophy, J. J., J. Appl. Phys., 106 (1957) 675

(16) Bess, L., J. Appl. Phys., 25 (1954) 1377

(17) Brophy, J. J., Phys. Rev., 106 (1957) 675

Bibliography Cont. -

(18) McWhorter, A. L., 1/f noise and Related Effects in Germanium, M.I.T. Lincoln Laboratory Report No. 80-May 1955.

(19) Bevington, J. R. & Ingle, L. V., Non-Destructive Reliability Screening of Electronic Parts, Technical Documentary Report No. RADC-TDR-64-311, Rome Air Development Center

(20) Phillips, A. B., Transistor Engineering, McGraw-Hill Book Co., Inc., 1962, pg. 210.

(21) Colteryahn and Kersey, Failure Mechanisms and Kinetics of Intermetallic Formation, Wescon Paper, August 1965.

(22) Deal and Sklar, Thermal Oxidation of Heavily Doped Silicon, J. Electrochem. Soc., Vol. 112, April 1965.

(23) Bernstein, L., Gold Alloying to Germanium, Silicon, and Aluminum-Silicon Eutectics, Semiconductor Products, August 1961, pg. 37.